

**SYNTHESIS OF NOVEL ARCHITECTURES FROM TRIAZINYL
HYDRAZINE AND VARIOUS CARBONYL COMPOUNDS**

by

VISHAL RAJAT SHARMA

Bachelor of Science, 2010
Southern Methodist University
Dallas, Texas

Master of Chemistry, 2014
Texas Woman's University
Denton, Texas

Submitted to the Graduate Faculty of
Science and Engineering College
Texas Christian University
in partial fulfillment of the requirements
for the degree of
Doctor of Philosophy
December 2019


SYNTHESIS OF NOVEL ARCHITECTURES FROM TRIAZINYL
HYDRAZINE AND VARIOUS CARBONYL COMPOUNDS

by

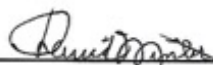
Vishal Rajat Sharma

Dissertation approved:

 SIMANEK
Major Professor

 MONTU H P

 J. ANESKO





For the College of Science and Engineering

Acknowledgements

I would like to express my sincere gratitude to my advisor Dr. Eric Simanek, for his support, inspiration, patience, guidance, and assistance through my graduate studies at Texas Christian University. I would like to thank my committee members, Dr. Benjamin Janesko, Dr. David Minter, and Dr. Jean-Luc Montchamp. I am thankful to Dr. Janesko for all the computational work in my projects. I am also thankful to Dr. Minter for helping with NMR spectra. I am specially thankful to Dr. Montchamp for his support and invaluable feedback. I also appreciate the support from faculties, staffs, and students in chemistry department.

I would also like to thank my family especially my mother (Pushpa Devi), wife (Reena Devi), and siblings (Poonam Sharma, Karuna Sharma, and Ravi Kumar) for their constant support. I would also like to thank my uncle (Kashmir Masih) and aunt (Nirmal Masih) for providing the opportunity to come to the United States of America.

Table of Contents

Acknowledgements.....	ii
List of figures.....	x
List of schemes.....	xiv
List of tables.....	xx
List of mechanisms.....	xxi
List of charts.....	xxii
List of abbreviations.....	xxiii
Chapter 1. Introduction to imine chemistry.....	1
1.1 Introduction and history of imine chemistry.....	1
1.2 Mechanism of imine formation.....	4
1.3 Mechanism of imine hydrolysis.....	7
1.4 Imine as starting material in organic reactions.....	8
1.5 Biological relevance.....	9
1.5.1 Antimalarial activity.....	10
1.5.2 Antibacterial activity.....	11
1.5.3 Antifungal activity.....	12
1.5.4 Antiviral activity.....	13
1.6 Triazinyl hydrazines.....	14

Chapter 2. The effect of pH on the hydrolysis rates of triazinyl hydrazones with different groups at N2.....	20
2.1 Introduction and previous work.....	20
2.2 Results and discussions.....	21
2.2.1 Synthesis of triazinyl hydrazine 1	21
2.2.2 Synthesis of <i>N</i> -phenyl triazinyl hydrazine 2	22
2.2.3 Synthesis of <i>N</i> -methyl triazinyl hydrazine 3	23
2.2.4 Synthesis of hydrazones.....	24
2.2.5 Hydrolysis studies.....	31
2.2.6 Effect of N2 substituents on hydrazone stability to hydrolysis.....	37
2.3 Conclusion.....	40
2.4 Experimental section.....	41
2.4.1 Materials and methods.....	41
2.4.2 Synthesis of intermediate 2.1	41
2.4.3 Synthesis of intermediate 2.2	42
2.4.4 Synthesis of triazinyl hydrazine 1	43
2.4.5 Synthesis of intermediate 2.3	43
2.4.6 Synthesis of intermediate 2.4	44
2.4.7 Synthesis of intermediate 2.5	45
2.4.8 Synthesis of triazinyl hydrazine 2	46
2.4.9 Synthesis of intermediate 2.6	46
2.4.10 Synthesis of intermediate 2.7	47
2.4.11 Synthesis of triazine hydrazine 3	48

2.4.12 Synthesis of 1a	48
2.4.13 Synthesis of 1b	49
2.4.14 Synthesis of 1c	50
2.4.15 Synthesis of 1d	50
2.4.16 Synthesis of 2a	51
2.4.17 Synthesis of 2b	52
2.4.18 Synthesis of 2c	53
2.4.19 Synthesis of 2d	53
2.4.20 Synthesis of 3a	54
2.4.21 Synthesis of 3b	55
2.4.22 Synthesis of 3c	55
2.4.23 Synthesis of 3d	56
Chapter 3. A hydrogen bond and strong electron withdrawing group help in the formation of stable cyclic hemiaminals	58
3.1 Introduction and history of hemiaminal.....	59
3.2 Biological relevance.....	67
3.3 Our work on hemiaminal	72
3.4 Results and discussions.....	73
3.4.1 Synthetic route of aromatic hydrazine 2	73
3.4.2 General reaction conditions for the synthesis of hemiaminals and pyrazoles	73
3.4.3 Nomenclature.....	74
3.4.4 Distinguishing fingerprints for characterization of.....	75
3.4.5 Hemiaminals or pyrazole products	78

3.4.6 Reactions of phenylhydrazine, 1 , with diketones (a-d) yield primarily pyrazoles ...	79
3.4.7 Reactions of triazinyl hydrazine, 2 , with diketones (a-d).....	81
3.4.8 Reactions of 2-hydrazinylpyridine, 3 , with diketones (a-d).....	83
3.4.9 Reactions of 4-hydrazino-2,6-dimethylpyrimidine, 4 , with diketones (a-d).....	84
3.4.10 A summary of hemiaminal stability and hydrogen bond.....	85
3.4.11 Computational studies.....	86
3.4.12 Design criteria for the preparation of stable hemiaminals.....	88
3.5 Conclusion	89
3.6 Experimental procedures	90
3.6.1 Synthesis of P-1a	90
3.6.2 Synthesis of P-1b	91
3.6.3 Synthesis of H-1c and P-1c'	92
3.6.4 Synthesis of P-1c	93
3.6.5 Synthesis of H-1d and P-1d	93
3.6.6 Synthesis of hydrazine 2	94
3.6.7 Synthesis of H-2a and P-2a	95
3.6.8 Synthesis of P-2a	96
3.6.9 Synthesis H-2b	97
3.6.10 Synthesis of P-2b	98
3.6.11 Synthesis of H-2c	98
3.6.12 Synthesis of P-2c	99
3.6.13 Synthesis of H-2d	100
3.6.14 Synthesis of H-2d and P-2d	101

3.6.15 Synthesis of P-3a	101
3.6.16 Synthesis of H-3b	102
3.6.17 Synthesis of P-3b	103
3.6.18 Synthesis of H-3c and P-3c'	104
3.6.19 Synthesis of P-3c	105
3.6.20 Synthesis of H-3d	105
3.6.21 Synthesis of H-3d and P-3d	107
3.6.22 Synthesis of P-4a	108
3.6.23 Synthesis of H-4b	108
3.6.24 Synthesis of P-4b	109
3.6.25 Synthesis of H-4c	110
3.6.26 Synthesis of P-4c	111
3.6.27 Synthesis of H-4d	111
3.6.28 Synthesis of H-4d and P-4d	112
Chapter 4. Efficient synthesis of macrocycles of sizes ranging 22 to 28	114
4.1 Introduction of macrocycles	114
4.2 Synthetic methodologies of macrocycles.....	116
4.3 Previous work	118
4.4 Results and discussions.....	120
4.4.1 Nomenclature.....	120
4.4.2 General synthetic routes.....	120
4.4.3 Synthesis of macrocycles.....	122
4.4.4 Solid state structures	124

4.4.5 One dimensional ^1H NMR of macrocycles.....	127
4.4.6 One dimensional ^{13}C NMR of macrocycles.....	131
4.4.7 two dimensional ^1H COSY and NOESY.....	134
4.4.8 Assessing the purity of macrocycles with HPLC	138
4.4.9 HPLC studies of heterodimers.....	139
4.4.10 Solubility of macrocycles	143
4.5 Conclusion	144
4.6 Experimental procedure	145
4.6.1 Synthesis of compound 4.12	145
4.6.2 Synthesis of compound 4.13	146
4.6.3 Synthesis of compound 4.14	146
4.6.4 Synthesis of compound 4.15	147
4.6.5 Synthesis of compound 4.16	148
4.6.6 Synthesis of compound 4.17	149
4.6.7 Synthesis of compound 4.18	149
4.6.8 Synthesis of compound 4.19	150
4.6.9 Synthesis of compound 4.20	151
4.6.10 Synthesis of monomer M1	151
4.6.11 Synthesis of monomer M2	152
4.6.12 Synthesis of monomer M3	153
4.6.13 Synthesis of monomer M4	154
4.6.14 Synthesis of monomer M5	155
4.6.15 Synthesis of monomer M6	156

4.6.16 Synthesis of monomer M7	157
4.6.17 Synthesis of macrocycle 1•1	157
4.6.18 Synthesis of macrocycle 2•2	158
4.6.19 Synthesis of macrocycle 3•3	159
4.6.20 Synthesis of macrocycle 4•4	160
4.6.21 Synthesis of macrocycle 5•5	161
4.6.22 Synthesis of macrocycle 6•6	161
4.6.23 Synthesis of macrocycle 7•7	162
4.6.24 Synthesis of model compound 8	163
4.6.25 Synthesis of macrocycles 1•1, 1•2, and 2•2	163
4.6.26 Synthesis of macrocycles 3•3, 3•5, and 5•5	164
4.6.27 Synthesis of macrocycles 1•1, 1•4, and 4•4	164
4.6.28 Synthesis of macrocycles 1•1, 1•6, and 6•6	164
4.6.29 Synthesis of macrocycles 1•1, 1•5, and 5•5	165
4.6.30 Synthesis of macrocycles 2•2, 2•6, and 6•6	165
4.6.31 Synthesis of mixture of 14-21 macrocycles.....	165
Chapter 5. Conclusions and future work.....	166
References:.....	169
Vita	
Abstract	

List of Figures

Figure 1.1 General structures and categories of imines	1
Figure 1.2 Possible four transition states. General acid and general acid-general base catalysis...	5
Figure 1.3 Antimalarial Schiff bases.....	10
Figure 1.4 Series of 5-chlorosalicylaldehyde and primary amine derivatives as potential antimicrobial compounds.....	12
Figure 1.5 Antifungal Schiff bases	13
Figure 1.6 Antiviral Schiff bases	14
Figure 1.7 Chemotherapeutic agents with hydrazone functionalities with carrier	16
Figure 1.8 Various triazinyl hydrazone derivatives of barbiturates.....	18
Figure 1.9 Triazinyl hydrazones made during the purification of water	18
Figure 1.10 1,2,4-Triazinyl hydrazones as anticonvulsant	19
Figure 2.1 ¹ H NMR of 1b in CDCl ₃	27
Figure 2.2 ¹³ C NMR of 1b in CDCl ₃	27
Figure 2.3 ¹ H NMR of 1c in CDCl ₃	29
Figure 2.4 ¹ H NMR of 2b in CDCl ₃	30
Figure 2.5 ¹ H NMR of 2c in CDCl ₃	30
Figure 2.6 ¹ H NMR of 3c in CDCl ₃	31
Figure 2.7 HPLC percent hydrolysis of all the hydrazones at pH 4.0	33
Figure 2.8 Time-dependent hydrolysis profile of hydrazone 3a	34

Figure 2.9 Change in percent concentration of 3a at pH 4.0	35
Figure 2.10 Pseudo first-order kinetics of 3a at pH 4.0.....	35
Figure 2.11 Computed proton affinity of hydrazones relative to 1a	38
Figure 2.12 Computed geometry of protonated 2b has proton H-bond by the OH group.....	39
Figure 3.1 A metal-organic framework with amino-functionalized links	59
Figure 3.2 Examples of Hemiaminals.....	71
Figure 3.3 Representation of different regioisomers of hemiaminals and pyrazoles.....	74
Figure 3.4 ¹ H NMR of H-3b in CDCl ₃	76
Figure 3.5 ¹ H NMR of P-3b in CDCl ₃	76
Figure 3.6 ¹³ C NMR of H-3b in CDCl ₃	77
Figure 3.7 ¹³ C NMR of P-3b in CDCl ₃	77
Figure 3.8 Crystal structure of hemiaminal H-1c	81
Figure 3.9 Crystal structure of hemiaminal H-2c	83
Figure 3.10 Crystal structure of hemiaminal H-3c	84
Figure 3.11 Crystal structure of hemiaminal H-4c	85
Figure 3.12 Hemiaminal stability relative to H-1a	87
Figure 3.13 Calculated energies of OH- -N bond for selected hemiaminals.....	88
Figure 4.1 Structures of common macrolides	114
Figure 4.2 Different variants of nisin.....	115
Figure 4.3 Structures of chemotherapeutic and immunosuppressant agents	116

Figure 4.4 EM profiles vs. ring size for different cyclization reactions	117
Figure 4.5 Structure of homodimers and heterodimer synthesized	119
Figure 4.6 Morphology of bigger macrocycles: x-ray structures of 4•4 and 6•6	125
Figure 4.7 Morphology of smaller macrocycles: x-ray structures of 1•1 , 2•2 and 3•3	126
Figure 4.8 Structure of model compound 8	127
Figure 4.9 ¹ H NMR of 6•6 in DMSO- <i>d</i> ₆	129
Figure 4.10 ¹ H NMR of 4•4 in DMSO- <i>d</i> ₆	130
Figure 4.11 ¹ H NMR of 7•7 in DMSO- <i>d</i> ₆	130
Figure 4.12 ¹³ C NMR of M2 in CDCl ₃	132
Figure 4.13 ¹³ C NMR of 2•2 in CD ₃ OD.....	133
Figure 4.14 Possible rotational isomers of macrocycles.....	135
Figure 4.15 ¹ H COSY of 4•4 in DMSO- <i>d</i> ₆	136
Figure 4.16 ¹ H NOESY of 4•4 in DMSO- <i>d</i> ₆	136
Figure 4.17 HPLC chromatograms of 1•1 , 2•2 , 3•3 , and 5•5	138
Figure 4.18 HPLC chromatograms of 4•4 and 6•6	139
Figure 4.19 HPLC chromatograms of 1•1 , 1•2 , and 2•2	140
Figure 4.20 Mass spectrum of mixture of 1•1 , 1•2 , and 2•2	140
Figure 4.21 HPLC chromatograms of 3•3 , 3•5 , and 5•5	141
Figure 4.22 LC-MS of a mixture of possible 21 macrocycles.....	142

Figure 5.1 General structure of triazinyl hydrazones synthesized.....	166
Figure 5.2 General structure of stable hemiaminals synthesized.....	167
Figure 5.3 General structure of macrocycles synthesized.....	168

List of Schemes

Scheme 1.1 General scheme of imine formation.....	1
Scheme 1.2 Oxidative synthesis of imines from alcohols and amines.....	3
Scheme 1.3 Various methods of forming imines	3
Scheme 1.4 Reactions of olefins and tertiary alcohols with hydrazoic acid	4
Scheme 1.5 Rate determining steps under acidic and neutral conditions.....	5
Scheme 1.6 Second order attack of semicarbazide and protonated p-nitrobenzaldehyde.....	6
Scheme 1.7 Major resonance structure of hydrazone conjugates.....	8
Scheme 1.8 Application of Schiff bases in organic synthesis	9
Scheme 1.9 Ease of substitution of triazine ring	17
Scheme 2.1 Synthesis of triazinyl hydrazine hydrogen chloride salt 1	22
Scheme 2.2 Synthesis of N-phenyl-tert-butyl carbazate 2.3	22
Scheme 2.3 Synthesis of N-phenyl triazinyl hydrazine hydrogen chloride salt 2	23
Scheme 2.4 Synthesis of N-methyl triazinyl hydrazine hydrogen chloride salt 3	24
Scheme 2.5 Hydrolysis of hydrazone.....	32
Scheme 2.6 Synthesis of compound 2.1	41
Scheme 2.7 Synthesis of compound 2.2	42
Scheme 2.8 Synthesis of triazinyl hydrazine 1	43
Scheme 2.9 Synthesis of intermediate 2.3	43
Scheme 2.10 Synthesis of intermediate 2.4	44
Scheme 2.11 Synthesis of intermediate 2.5	45

Scheme 2.12 Synthesis of triazinyl hydrazine 2	46
Scheme 2.13 Synthesis of intermediate 2.6	46
Scheme 2.14 Synthesis of intermediate 2.7	47
Scheme 2.15 Synthesis of triazine hydrazine 3	48
Scheme 2.16 Synthesis of 1a	48
Scheme 2.17 Synthesis of 1b	49
Scheme 2.18 Synthesis of 1c	50
Scheme 2.19 Synthesis of 1d	50
Scheme 2.20 Synthesis of 2a	51
Scheme 2.21 Synthesis of 2b	52
Scheme 2.22 Synthesis of 2c	53
Scheme 2.23 Synthesis of 2d	54
Scheme 2.24 Synthesis of 3a	54
Scheme 2.25 Synthesis of 3b	55
Scheme 2.26 Synthesis of 3c	55
Scheme 2.27 Synthesis of 3d	56
Scheme 3.1 Solvent free reactions to create hemiaminals	60
Scheme 3.2 First stable hemiaminal obtained at room temperature.....	61
Scheme 3.3 Hemiaminal and Schiff base synthesis from 4-amino-1,2,4-triazole and nitro-substituted benzaldehyde	61
Scheme 3.4 Reaction of various diketones and hydrazines to yield hemiaminals	62
Scheme 3.5 Synthesis of both hemiaminal and pyrazole derivative at low temperature	63
Scheme 3.6 Synthesis of hemiaminal at from various hydrazines at high temperature	63
Scheme 3.7 Synthesis of stable hemiaminals and their dehydration by using DAST.....	63

Scheme 3.8 Solvent-free synthesis of hemiaminals by using microwave irradiation	64
Scheme 3.9 Solvent-free synthesis of hemiaminals and pyrazoles at high temperatures	64
Scheme 3.10 Selective synthesis of pyrazole regioisomer by using silica.....	65
Scheme 3.11 Synthesis of both regioisomers of pyrazole derivatives	65
Scheme 3.12 Selective synthesis of pyrazole derivatives by using different solvents	66
Scheme 3.13 Selective synthesis of pyrazole regioisomers in different solvents	67
Scheme 3.14 Synthesis of hemiaminal derivative from ynone and 2-hydrazinopyridine.....	67
Scheme 3.15 Synthesis of various hemiaminals in ethanol or diethyl ether	68
Scheme 3.16 Synthesis of various combination of hemiaminal and pyrazole derivatives.....	68
Scheme 3.17 Condensation reaction of 2-hydrazino-4,6-dimethylpyrimidine and diketones	69
Scheme 3.18 Synthesis of hemiaminals from amino guanidine and 4-alkoxy-1,1,1-trihalo-3-alken-2-ones.....	70
Scheme 3.19 Synthesis of hemiaminal from aliphatic hydrazine.....	70
Scheme 3.20 Synthesis scheme of triazinyl hydrazine 2	73
Scheme 3.21 Illustration of an isodesmic reaction for H-1b	87
Scheme 3.22 Synthesis of P-1a	90
Scheme 3.23 Synthesis of P-1b	91
Scheme 3.24 Synthesis of H-1c and P-1c'	92
Scheme 3.25 Synthesis of P-1c	93
Scheme 3.26 Synthesis of H-1d and P-1d	93
Scheme 3.27 Synthesis of hydrazine 2	94
Scheme 3.28 Synthesis of H-2a and P-2a	95
Scheme 3.29 Synthesis of P-2a	96
Scheme 3.30 Synthesis H-2b	97

Scheme 3.31 Synthesis of P-2b	98
Scheme 3.32 Synthesis of H-2c	98
Scheme 3.33 Synthesis of P-2c	99
Scheme 3.34 Synthesis of H-2d	100
Scheme 3.35 Synthesis of H-2d and P-2d	101
Scheme 3.36 Synthesis of P-3a	101
Scheme 3.37 Synthesis of H-3b	102
Scheme 3.38 Synthesis of P-3b	103
Scheme 3.39 Synthesis of H-3c and P-3c'	104
Scheme 3.40 Synthesis of P-3c	105
Scheme 3.41 Synthesis of H-3d	105
Scheme 3.42 Synthesis of H-3d and P-3d	107
Scheme 3.43 Synthesis of P-4a	108
Scheme 3.44 Synthesis of H-4b	108
Scheme 3.45 Synthesis of P-4b	109
Scheme 3.46 Synthesis of H-4c	110
Scheme 3.47 Synthesis of P-4c	111
Scheme 3.48 Synthesis of H-4d	111
Scheme 3.49 Synthesis of H-4d and P-4d	112
Scheme 4.1 Self-assembly of two monomer units	119
Scheme 4.2 Synthesis of 4.13	120
Scheme 4.3 Synthesis of 4.15	121
Scheme 4.4 General synthesis of monomers M1 , M2 , and M4 from 4.13	121
Scheme 4.5 General synthetic scheme of six macrocycles	122

Scheme 4.6 General synthesis reaction of model compound 8	134
Scheme 4.7 Synthesis of compound 4.12	145
Scheme 4.8 Synthesis of compound 4.13	146
Scheme 4.9 Synthesis of compound 4.14	146
Scheme 4.10 Synthesis of compound 4.15	147
Scheme 4.11 Synthesis of compound 4.16	148
Scheme 4.12 Synthesis of compound 4.17	149
Scheme 4.13 Synthesis of compound 4.18	149
Scheme 4.14 Synthesis of compound 4.19	150
Scheme 4.15 Synthesis of compound 4.20	151
Scheme 4.16 Synthesis of monomer M1	151
Scheme 4.17 Synthesis of monomer M2	152
Scheme 4.18 Synthesis of monomer M3	153
Scheme 4.19 Synthesis of monomer M4	154
Scheme 4.20 Synthesis of monomer M5	155
Scheme 4.21 Synthesis of monomer M6	156
Scheme 4.22 Synthesis of monomer M7	157
Scheme 4.23 Synthesis of macrocycle 1•1	157
Scheme 4.24 Synthesis of macrocycle 2•2	158
Scheme 4.25 Synthesis of macrocycle 3•3	159
Scheme 4.26 Synthesis of macrocycle 4•4	160
Scheme 4.27 Synthesis of macrocycle 5•5	161
Scheme 4.28 Synthesis of macrocycle 6•6	161

Scheme 4.29 Synthesis of macrocycle 7•7	162
Scheme 4.30 Synthesis of model compound 8	163
Scheme 4.31 Synthesis of macrocycles 1•1, 1•2, and 2•2	163

List of Tables

Table 2.1 Summary of hydrazones synthesized from a and d	25
Table 2.2 Summary of hydrazones synthesized from b and c	26
Table 2.3 List of hydrazones hydrolyzed using HPLC	33
Table 2.4 Half-lives and rate constants of hydrazones.....	36
Table 3.1 Summary of all the hemiaminals and pyrazole derivatives synthesized.....	79
Table 3.2 Hydrogen bond characteristics.....	86
Table 4.1 Summary of monomers synthesized by using 4.13 and 4.15	122
Table 4.2 List of homodimers synthesized.....	123
Table 4.3 Selected ¹ H NMR data of macrocycles	128
Table 4.4 Selected ¹³ C NMR data of macrocycles.....	131
Table 4.5 Comparison of solution state and expected solid state nOe signals.....	137
Table 4.6 Products observed based on HPLC after mixing equal moles of monomers.....	141
Table 4.7 LC-MS molar mass of mixture of possible 21 products	143
Table 4.8 Solubility of macrocycles in H ₂ O, CH ₃ OH, and CH ₂ Cl ₂	144

List of Mechanisms

Mechanism 1.1 Mechanism of hydrolysis of imine.....	7
Mechanism 1.2 Hydrolysis of hydrazones and oximes under acidic conditions	14
Mechanism 2.1 Proposed mechanism of acid catalyzed hydrolysis of hydrazones	37

List of Charts

Chart 2.1 List of triazinyl hydrazines and carbonyl compounds used.....	21
Chart 3.1 List of aromatic hydrazines used	72
Chart 3.2 List of diketones used	72
Chart 4.1 Various acetal linkers and amino acids used	120

List of Abbreviations

α	Alpha
β	Beta
δ	Chemical shift
J	Coupling constant
AIDS	Acquired immunodeficiency syndrome
BOC	<i>tert</i> -butyloxycarbonyl
COSY	Correlation spectroscopy
DAST	Diethylaminosulfur trifluoride
DCM	Dichloromethane
DIPEA	<i>N,N</i> -diisopropylethylamine
DFT	Density function theory
DMF	<i>N,N</i> -dimethyl formamide
DMSO	Dimethylsulfoxide
EDC.HCl	<i>N</i> -ethyl- <i>N'</i> -(3-dimethylaminopropyl)carbodiimide hydrochloride
EtOH	Ethanol
FDA	Food and drug administration
FTIR	Fourier-transform infrared spectroscopy
Gl. AcOH	Glacial acetic acid
HFIP	1,1,1,3,3,3-hexafluoro-2-propanol
HIV	Human immunodeficiency virus
HOBT	Hydroxybenzotriazole
HPLC	High performance liquid chromatography

LC-MS	Liquid chromatography-mass spectrometry
MHz	Megahertz
MeOH	Methanol
MOF	Metal organic frameworks
NMR	Nuclear magnetic resonance
NOESY	Nuclear overhauser effect spectroscopy
$t_{1/2}$	Half-life
TEA	Triethylamine
TFA	Trifluoroacetic acid
TFE	Trifluoroethanol
THF	Tetrahydrofuran
TLC	Thin layer chromatography
<i>p</i> -TSA	<i>para</i> -toluenesulfonic acid

Chapter 1: Introduction to imine chemistry

1.1 Introduction and history of imine chemistry

The imine functional group is characterized by the presence of a double bond (Figure 1.1) between the carbon and nitrogen atoms. Substituent groups, R_1 and R_2 , on the carbon atom may be alkyl, aromatic, heteroaryl, or a hydrogen atom. Substituents on the nitrogen atom, R_3 , may be alkyl, aryl, heteroaryl, hydrogen, nitrogen, oxygen, or a metal (usually Si, Al, B, Sn).¹⁻⁸

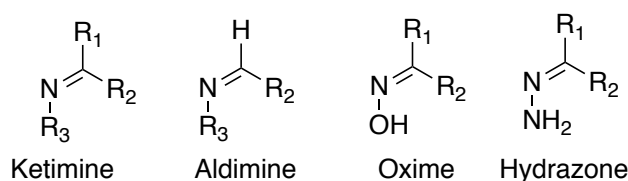
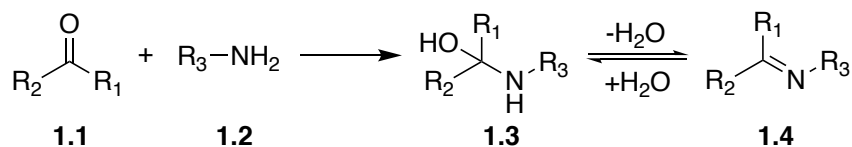


Figure 1.1. General structures and categories of imines.

Based on the substituents of the carbon atom, imines are sub-categorized as ketimines ($R_1 = R_2 =$ alkyl, aryl) or aldimines (R_1 or $R_2 = H$). When heteroatoms appear on the nitrogen atom, oximes ($R_3 = OH$ or OR) and hydrazones ($R_3 = NH_2$ or NR_2) result. Ketimines and aldimines are called Schiff bases when R_3 is not hydrogen to honor professor Hugo Schiff who reported them in 1864.¹ Schiff's original method for preparing imines involved the condensation reaction between an aldehyde or a ketone with primary amine.^{1,5,9-11} The process involves the elimination of one molecule of water (Scheme 1.1).

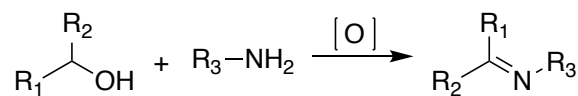


Scheme 1.1. General scheme of imine formation. R_1 and R_2 can be H-atom, alkyl, aryl, and aromatic groups. R_3 can be H-atom, alkyl, and aryl groups.

Reaction between **1.1** and **1.2** leads to the formation of a relatively unstable tetrahedral intermediate (**1.3**) called a hemiaminal or carbinolamine. The reversible removal of a water molecule forms the imine. Removing water from the reaction mixture speeds up the formation of

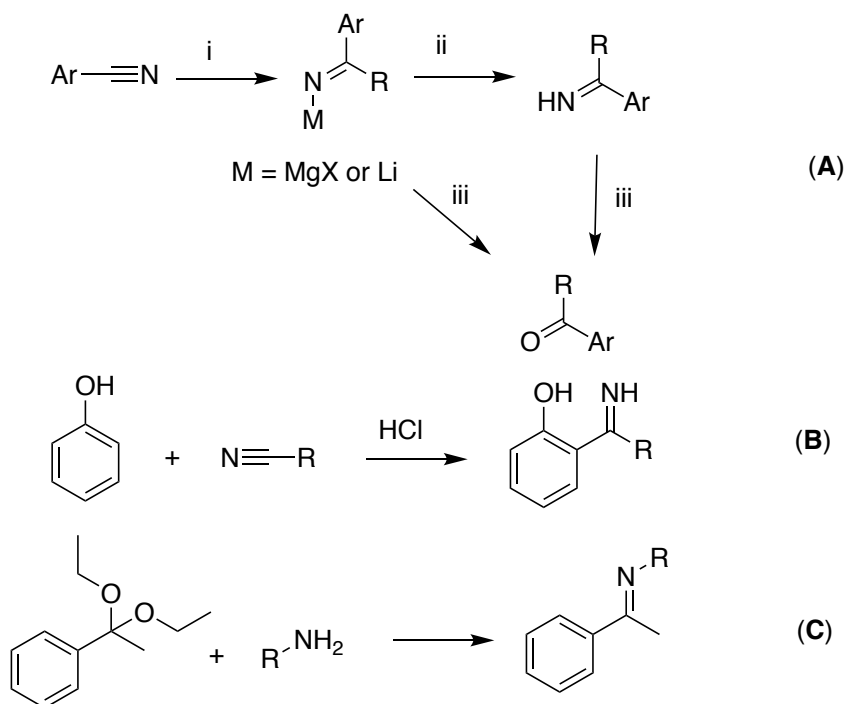
imines and also avoids the reverse reaction from **1.4** to **1.3**. Schiff used a Dean-Stark trap for azeotropic distillation of water whenever the boiling point of the aldehyde or ketone and amine used was higher than water. Since then, the use of dehydrating agents such as MgSO₄, molecular sieves, or tetramethyl orthosilicate have been reported.¹²⁻¹⁴ The reactions have been found to be accelerated by the presence of a small amount of acid. The use of H₂SO₄, HCl, acidic resins, or Lewis acids such as ZnCl₂, TiCl₄, SnCl₄ etc. have been reported.¹⁵⁻²¹ The efficiency of these methods is actually dependent on the use of a highly electrophilic carbonyl group and strongly nucleophilic amine.¹⁸

In addition to the original method developed by Schiff, still the most commonly used, many other methods have been developed for the preparation of imines. Aldehydes and ketones are generally obtained from the oxidation of primary and secondary alcohols, respectively. Hence, a straightforward method for the synthesis of imines has been developed from amines and alcohols (Scheme 1.2) through a tandem oxidation process.²³⁻²⁹ This process entails the oxidation of alcohol to aldehyde or ketone which is trapped in situ by a nucleophile to make a variety of useful synthetic compounds including imines. Alcohols with aromatic groups can be converted to imines in excellent yields by using manganese octahedral sieves (K-OMS-2).²⁷ Yields are inferior when aliphatic alcohols were used. Aliphatic alcohols can be converted to imines in quantitative yields by using Pd/ZrO₂ in KOH at 30 °C.²⁸ The synthesis of imines has been carried out using a polymer with incarcerated gold and palladium alloy nanoparticles and molecular oxygen as oxidizing agent.²⁶



Scheme 1.2. Oxidative synthesis of imines from alcohols and amines. R₁, R₂, and R₃ may be H, alkyl, or aryl groups.

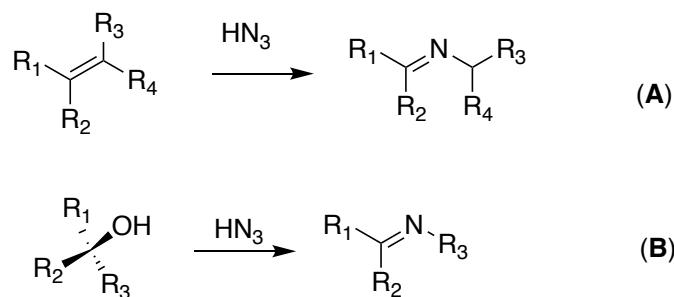
Imines can also be prepared by the reaction of Grignard or organolithium reagents with an aryl cyanide (Scheme 1.3 (A)) under acidic conditions.³⁰⁻³² In addition, phenols and aromatic ethers can also react with alkyl and aryl cyanides (scheme 1.3 (B)) to make imines in the presence of acid catalyst.³³⁻³⁵ Imines can also be synthesized by reacting aryl ketone diethyl ketals with arylamines and alkylamines (Scheme 1.3 (C)).³⁶⁻³⁷



Scheme 1.3. Various methods of forming imines. A) Addition of organometallic reagents to cyanides. i) RMgX or RLi; ii) HCl, -15 °C then NH₄OH; iii) hydrolysis. B) Synthesis of ketimines from phenols and nitriles. C) Synthesis of ketimines from ketals and amines.

In addition, alkenes and tertiary alcohols (Scheme 1.4) can be converted to ketimines by reacting with hydrazoic acid in sulfuric acid.³⁸ Furthermore, amino acids can be converted to imines with

sodium hypochlorite. This reaction involves the formation of the chloramine intermediate followed by the elimination of carbon dioxide and sodium chloride.³⁹



Scheme 1.4. Reaction of olefins (A) and tertiary alcohols (B) with hydrazoic acid.

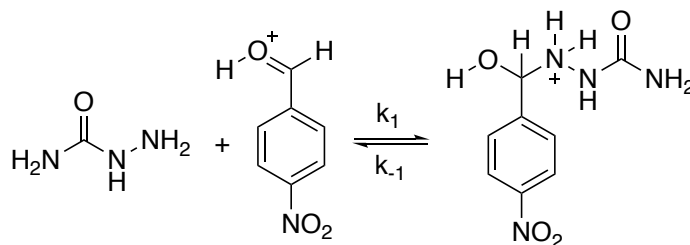
Furthermore, in the past decade, a number of new techniques have been developed to synthesize imines including solid-state synthesis, K-10/microwave irradiation, water suspension medium, solvent free-microwave irradiation and silica-ultrasound irradiation.⁴⁰⁻⁴⁸ Among them microwave irradiation is extensively used due to its simplicity, reaction rates, greater selectivity, and high efficiency.⁴⁸

1.2 Mechanism of imine formation

Imine formations are usually done under slightly acidic or neutral conditions. Mechanistically, the addition of an amine to a carbonyl group of an aldehyde or ketone proceeds through the formation of a short lived tetrahedral intermediate **1.7** (Scheme 1.5) called a hemiaminal. Cordes and Jencks extensively studied the mechanism of formation of imines at 25 °C by using semicarbazone with substituted benzaldehydes and concluded that nucleophilic attack at the carbonyl carbon takes place without protonating the oxygen atom.⁴⁹⁻⁵⁹ Instead, nucleophilic attack of semicarbazone on to the carbonyl carbon along with proton transfer takes place in a single step. Under acidic conditions (Mechanism 1.1 (A)) nucleophilic attack of semicarbazone becomes

Transition states **1.11** and **1.12** evolve from specific acid-general base catalysis and are mechanistically different from transition states **1.9** and **1.10**. In **1.11**, nucleophilic attack on the carbonyl carbon is aided by both the pre-equilibrium protonation of carbonyl oxygen atom and by conversion of the amine into an amide ion by partial removal of a proton. In **1.12**, proton removal occurs after a pre-equilibrium formation of the protonated addition product derived from nucleophilic addition to the carbonyl.

To explore these mechanism, Jencks calculated the second-order rate constant, k_1 , for the attack of semicarbazide on the conjugate acid of *p*-nitrobenzaldehyde (Scheme 1.5). It was found to be larger than the rate constant of diffusion-controlled reaction of aqueous solution. As a result, Jencks concluded that general acid catalysis of the attack of semi-carbazide on the benzaldehyde involves true general acid catalysis with proton transfer concerted with attack of nucleophilic reagent (**1.9**). Jencks ruled out the possibilities of forming other transition states **1.10**, **1.11**, and **1.12** on the basis of rate constants.



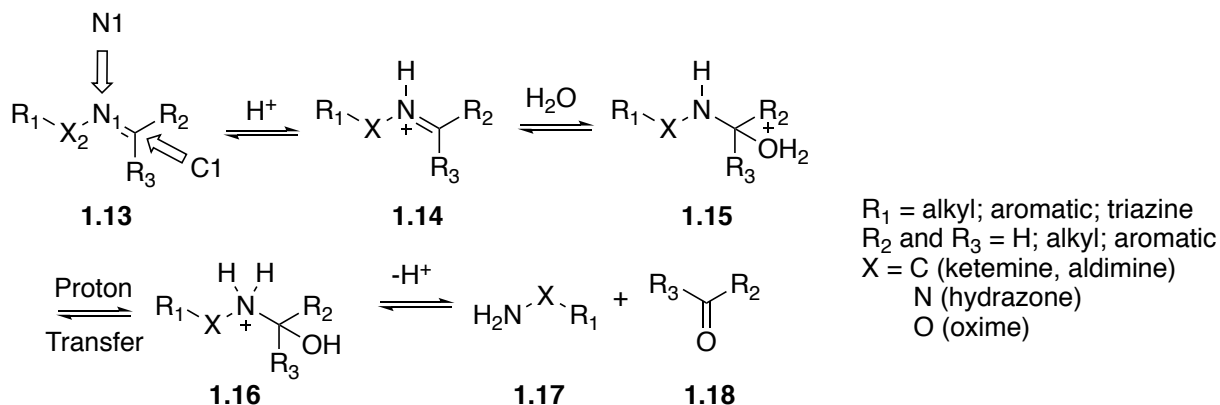
Scheme 1.6. Second order attack of semicarbazide and protonated *p*-nitrobenzaldehyde.

In summary, N-C bond formation in the transition state accompanies some movement of the hydrogen atom toward oxygen atom. The complete transfer of proton to oxygen is believed to be very fast after the formation of N-C bond followed by diffusion-controlled separation of the products. The reactions occur via a pre-equilibrium proton transfer and do not involve proton transfer in the transition state. They were found to be more rapid in D_2O than H_2O due to increased

basicity. This observation indicates that proton-catalyzed reaction involves general rather than specific acid catalysis.

1.3 Mechanism of imine hydrolysis

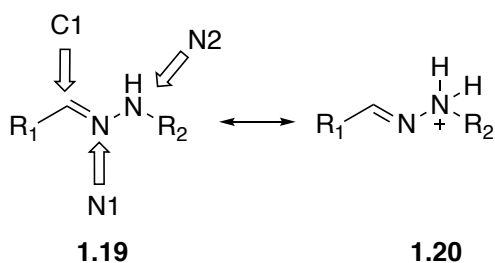
Imine hydrolysis is relatively fast in aqueous acidic conditions or in the presence of Lewis acid catalysts and slower under neutral or basic conditions. The mechanism involves the protonation of nitrogen atom (N1) of C=N under acidic conditions making C1 more electrophilic (Mechanism 1.1) to yield **1.14**. Nucleophilic attack of water on the carbon, C1, of the C=N group forms tetrahedral intermediate **1.15**. A thermodynamically favorable proton transfer takes place from protonated oxygen atom (pKa \approx -2.2) to N1 (pKa \approx 10) making it a good leaving group in intermediate **1.16**. The lone pair on the oxygen atom creates a double bond while pushing out amine **1.17** in a concerted step and eventually forms a carbonyl compound **1.18** after losing H⁺.⁶⁰



Mechanism 1.1. Mechanism of hydrolysis of imine.

Imines used in prodrugs can be slowly hydrolyzed in the blood (slightly basic) or inside the cells (slightly acidic) in order to release the active drug. Hydrolysis can be halted either by keeping imines away from the water or maintaining basic conditions. One of the ways to increase the stability of imines is by having long hydrophobic side chains or groups on the carbon or nitrogen atoms.

Stability of the imines can also be increased by incorporating oxygen (oximes) or nitrogen (hydrazones) atoms adjacent to the nitrogen atom of the $-N=C$ bond. Oximes have a general structure of $RO-N=CR_1R_2$. A $NR-N=CR_1R_2$ group is called a hydrazone. Hydrazones and oximes are more stable toward hydrolysis than regular imines. Raines and Kalia reasoned the greater stability of hydrazones and oximes was due to the ability of N or O atoms to resist the protonation of the nitrogen atom of $C=N$ group and as a result decreases the electrophilicity of the carbon atom of the imine group.⁶¹⁻⁶² However, they found that oximes are relatively more stable than hydrazones. Protonation of the second nitrogen atom (N2) (Scheme 1.7 (1.20)) in case of hydrazones resists the hydrolysis.



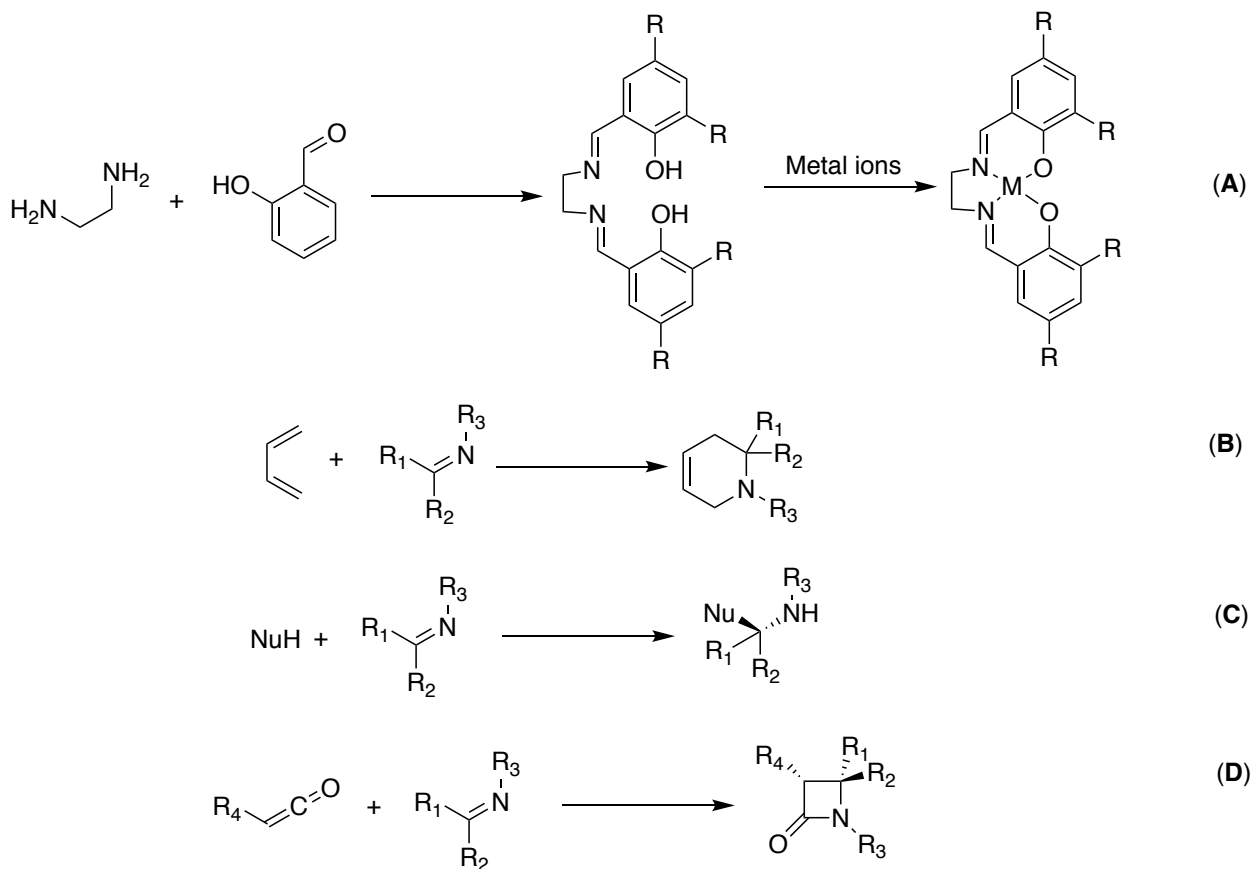
Scheme 1.7. Major resonance structures of hydrazone conjugates.

1.4 Imines as starting material in organic reactions

Imines and Schiff bases are used in as starting material and intermediates in organic synthesis. In an oversimplification,⁶³⁻⁷⁶ there are four different types of reactions in which Schiff bases are used (Scheme 1.8 (A-D)). Reaction of *ortho*-hydroxybenzaldehyde with ethylene diamine forms a bis-imine tetradentate ligand. The ligand is used to make coordination compounds with various metal cations (Co^{2+} , Mn^{2+} , Cr^{2+} etc.) also called salen complexes (Scheme 1.8 (A)).

Imines can be used as non-symmetrical dienophiles in Diels-Alder reactions (Scheme 1.8 (B)) to furnish nitrogen containing heterocycles. In addition, the Staudinger reaction of imines with ketenes (Scheme 1.8 (D)) yields biologically important beta-lactam rings present in many

antibiotics such as penicillin. Electronegativity difference between carbon and nitrogen makes imines behave similar to carbonyl groups of ketones and aldehydes. As a result, imine functional groups undergo nucleophilic addition reactions with organometallic reagents or hydrides to form tetrahedral products (Scheme 1.8 (C)). In addition, imines are used as intermediates in organic chemistry, pigments and dyes, catalysts, and also as polymer stabilizers.⁷⁷



Scheme 1.8. Application of Schiff bases in organic synthesis. A) Chiral salen metal complex synthesis; B) Hetero Diels-Alder reaction; C) Addition reactions; D) Staudinger reaction with ketenes.

1.5 Biological relevance

Schiff bases are also found to have biological activities including anti-inflammatory, antibacterial, anti-fungal, anti-proliferative, and antipyretic properties.⁷⁷⁻⁷⁸ In addition, imines are also present in various natural, semi-synthetic, and synthetic compounds and have been

demonstrated to be essential for their biological activities.⁷⁹⁻⁸¹ Below are some of the examples of the biological active Schiff bases.

1.5.1 Antimalarial activity

Malaria is currently found in more than 100 countries. About 500 million people worldwide are afflicted by this disease, of whom 1-3 million die annually.⁸² Researchers around the globe are always in search of new drugs, vaccines, and insecticides to prevent and treat malaria.⁸³ Schiff bases have been shown to be biologically active against some of the species of *Plasmodium*. Ancistrocladidine (Figure 1.3 (1.21)), a natural product produced from the families of *Ancistrocladaceae* and *Dioncophyllaceae*, has an imine scaffold in the molecule.⁷⁸ The imine group has been shown to be significant in conferring the antimalarial activity against *P. falciparum*. The minimum inhibitory concentrations (MIC) of ancistrocladidine necessary to completely abolish *P. falciparum* K1 and 3D7 growth were 0.3 and 1.9 $\mu\text{g/mL}$, respectively.⁷⁸ In addition, commercially synthesized 5-nitroisoquinoline derivatives (Figure 1.3 (1.22)) that contain an imine have also found to be effective antimalarial agents and showed IC_{50} of 0.7 $\mu\text{g/mL}$ against *P. falciparum*.⁸³

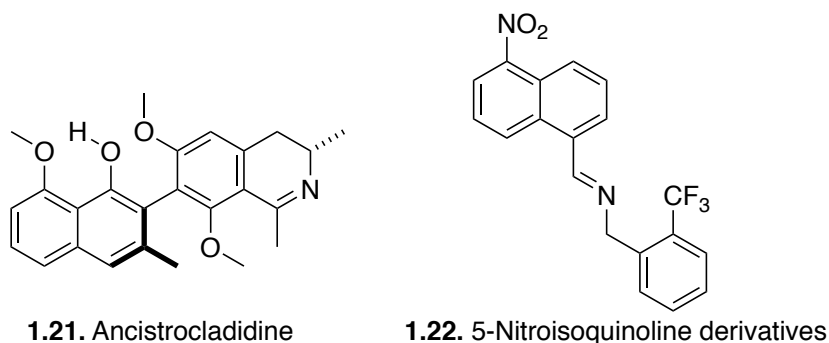


Figure 1.3. Antimalarial Schiff bases.

1.5.2 Antibacterial activity

Antibiotics either kill bacteria or inhibit their growth and multiplication. However, bacteria develop resistance toward antibiotics making them ineffective. There is always a need for new and more effective antibiotics.⁸⁴⁻⁸⁷ Schiff's bases have been identified as promising antimicrobial agents. A series of Schiff bases (Figure 1.4) with promising antimicrobial activity have been synthesized from the condensation of 5-chlorosalicylaldehyde and primary amines.⁸⁸ *Pseudomonas fluorescens*, *Escherichia coli*, and *Staphylococcus aureus* were some of most sensitive strains to these compounds.⁸⁷ *Pseudomonas fluorescens* was most sensitive to compounds **1.24** to **1.33** with MIC values ranging from 2.5-5.2 µg/mL. The MIC value for the reference drug kanamycin against the same bacterial strain was 3.9 µg/mL.⁸⁷ Panneerselvam et al. also described the synthesis of eleven morpholine-derived imines that have also shown antimicrobial activity.⁸⁸ *Staphylococcus aureus* and *Micrococcus luteus* were the bacteria most sensitive to the morpholine-derived Schiff bases with MIC 20 µg/mL and 32 µg/mL, respectively.⁸⁸

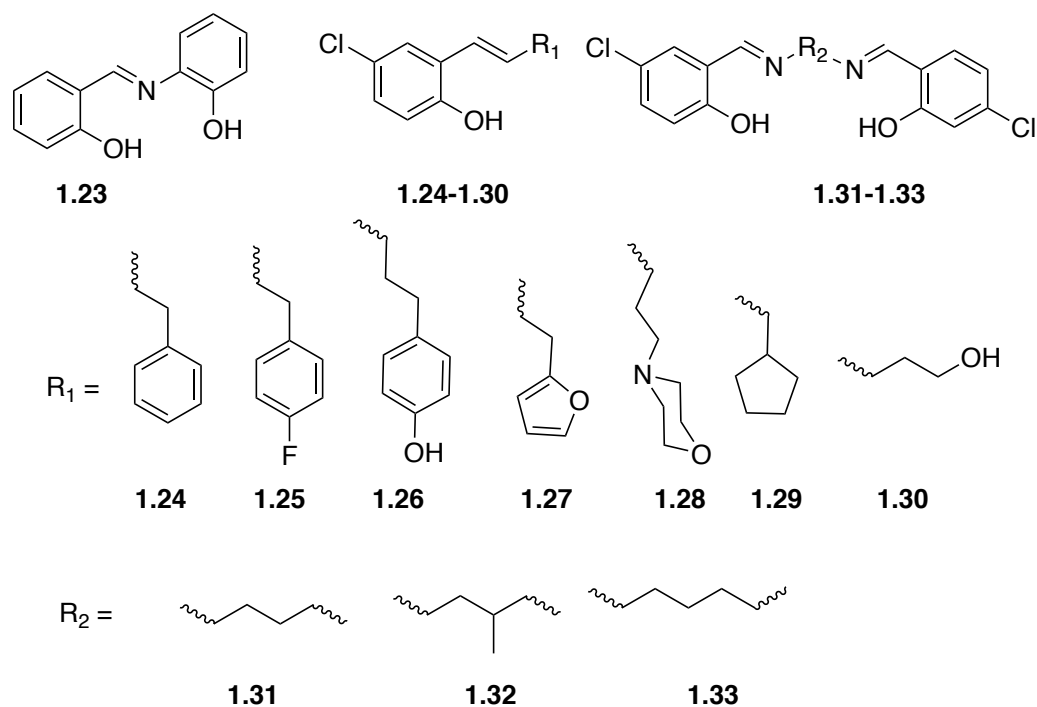


Figure 1.4. Series of 5-chlorosalicylaldehyde and primary amines derivatives as potential antimicrobial compounds.

1.5.3 Antifungal activity

Fungal infection is usually more frequent in elderly patients after major surgery, during immunosuppressive therapy, with acquired immunodeficiency syndrome, during cancer treatment or solid-organ transplant.⁸⁹⁻⁹¹ Schiff's bases of chitosan (Figure 1.5) have shown antifungal activities against *Botrytis cinerea* and *Colletotrichum lagenarium*.⁹¹ They inhibited the growth of *Botrytis cinerea* and *Colletotrichum lagenarium* by 26-33% and 35-38% when used at 1000 ppm, respectively.⁹¹ In addition, imines with 2,4-dichloro-5-fluorophenyl moieties (Figure 1.5) inhibit the growth of fungi of clinical interest such as *Aspergillus fumigatus*, *Aspergillus flavus*, *Trichophyton ment-agrophytes* and *Penicillin marneffei*.⁹² The MIC values of these compounds were in the range of 6.3-12.5 $\mu\text{g/mL}$, indicating that they are as potent as the reference fluconazole.⁹² Piperonyl derived imine compounds have been found active against some fungi even at micromolar concentration.⁹³ These compounds inhibited the growth of *Trichophyton*

rubrum and *Epidermophyton floccosum* with the MIC value of 820-980 μM and 200-930 μM , respectively.⁹³

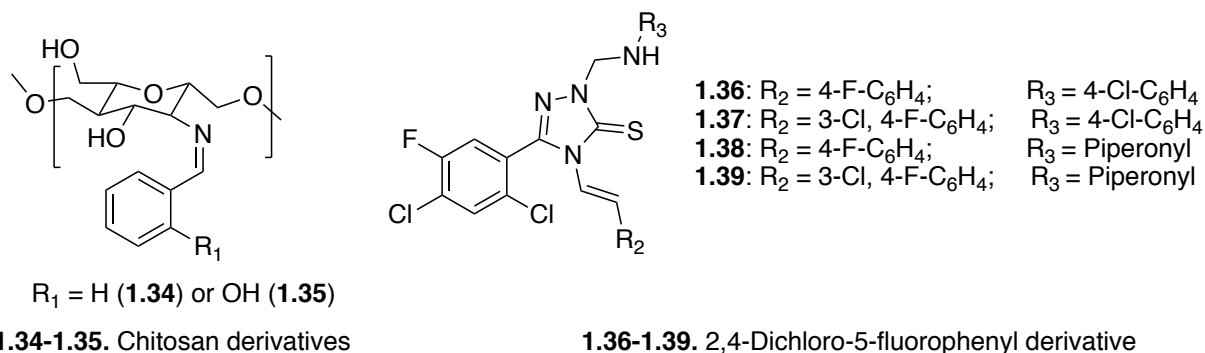


Figure 1.5. Antifungal Schiff bases.

1.5.4 Antiviral activity

Vaccines have helped eradicate many diseases resulting from the viral pathogens smallpox, polio, and rubella. However, viral diseases such as hepatitis C, HIV virus, and other immunodeficiency illnesses require antiviral agents.⁹⁴ There are many therapeutic options for the viral infections, however the need for new and more effective drugs is always there. Schiff bases derived from 1-amino-3-hydroxyguanidine tosylate have been a good platform to design new antiviral agents.⁹⁴ Sriram and colleagues reported the synthesis and antiviral activity of the abacavir-derived Schiff bases (Figure 1.6) which can be used as abacavir prodrugs.⁹⁵ Abacavir inhibits the activity of reverse transcriptase and used to treat human immunodeficiency virus (HIV) and acquired immunodeficiency syndrome (AIDS). The effective concentration of these derivatives necessary to achieve 50% protection of human leukemic cells against the cytopathic effect of HIV-1 was lower than 6 μM .⁹⁵

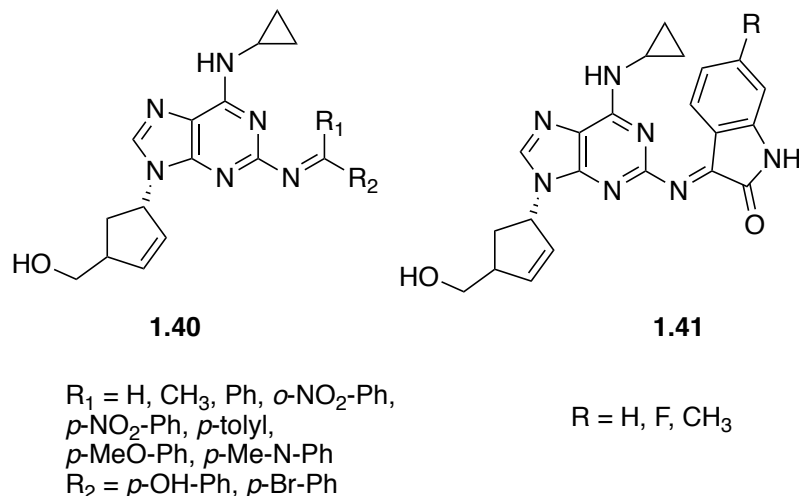
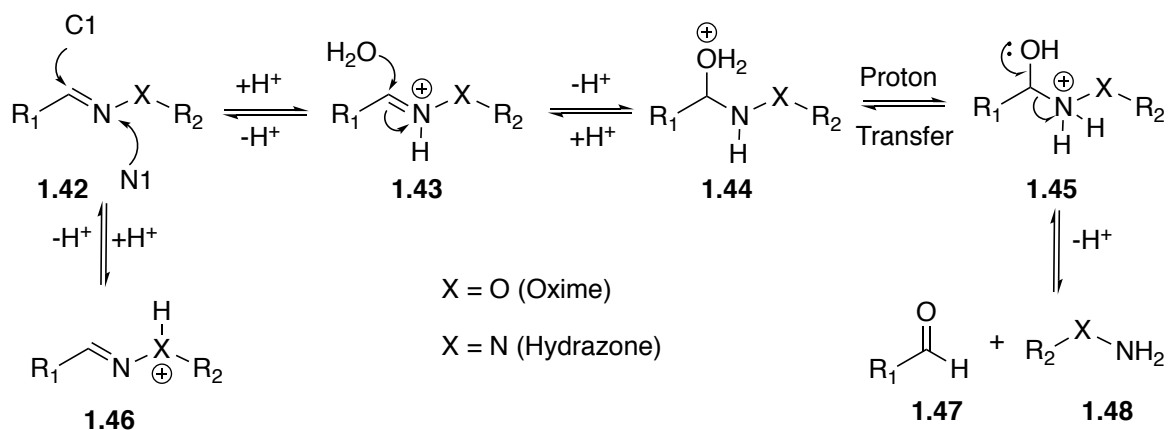


Figure 1.6. Antiviral Schiff bases.

1.6 Triazinyl hydrazines

Two subcategories of imine functional groups, hydrazones and oximes, have been extensively studied. Among those, acid-labile property can be utilized to control hydrolysis rates under different pH conditions. As described earlier, regular imines hydrolyze under acidic or neutral conditions faster than oximes ($X = \text{O}$) and hydrazones ($X = \text{N}$). However, the hydrolysis of hydrazones has been found to be 100 to 1000 times faster than oximes.⁶⁰ The electronegativity of the oxygen atom in the oxime reduces the electron density on the nitrogen atom making it less likely to get protonated than in the case of hydrazones.⁶⁰ The protonated N1 relatively enhances the electrophilicity of C1 making it more susceptible to nucleophilic attack by water and results in hydrolysis.



Mechanism 1.2. Hydrolysis of hydrazones and oximes under acidic conditions.

Hence, the pH-sensitive nature of hydrazones has allowed their use in various fields from materials science to medical science. Poor water solubility can reduce the likelihood that a molecule can be used as an oral drug.⁹⁶ In such situations, labile functional groups can carry the active drug in the form of prodrugs, inactive compounds that carries the actual drugs, and release it at the site of injury or illness by either chemical or enzymatic actions.⁹⁶⁻⁹⁸ An ideal prodrug should be soluble in water and plasma, relatively non-toxic, induce minimum irritation along the digestive tract, have the ability to travel through the blood stream without breaking down and able to release the active drug at the site of injury.⁹⁹⁻¹⁰⁰ Labile groups such as esters, ethers, acetals, oximes, hydrazones, and acetyls have been used to control the release of drugs.¹⁰¹⁻¹⁰⁸ The carbon-nitrogen double bond in the case of hydrazones has been found to be fairly stable at neutral pH. However, the same functional group hydrolyzes relatively quickly in acidic medium such as the environments afforded by lysosomes and hypoxic, cancerous tumors.¹⁰⁹ Two prodrugs with hydrazone functional groups carrying anti-cancer drugs, now-abandoned due to cost, are mylotarg¹¹⁰ and kadcylla.¹¹¹ Drugs including doxorubicin,¹¹²⁻¹¹³ (Figure 1.7) calicheamicin,¹¹⁴ paclitaxel,¹¹⁵⁻¹¹⁶ docetaxel,¹¹⁷ mitomycin C,¹¹⁸ dexamethasone,¹¹⁹ and cisplatin¹²⁰ have been conjugated to nanocarriers using hydrazones. Hydrazones have also been used in creating dynamic

combinatorial libraries and as reagents in organic synthesis.¹²¹⁻¹²² Interestingly, hydrazone chemistry has also been used to anchor aldehydes and ketones in colognes.¹²³ In addition, hydrazones have been used in molecular switches, metallo-assemblies, and sensors.¹²⁴ Finally, hydrazones based on coupling methods have been used in medical biotechnology to attach drugs to target antibodies.¹²⁵⁻¹²⁸

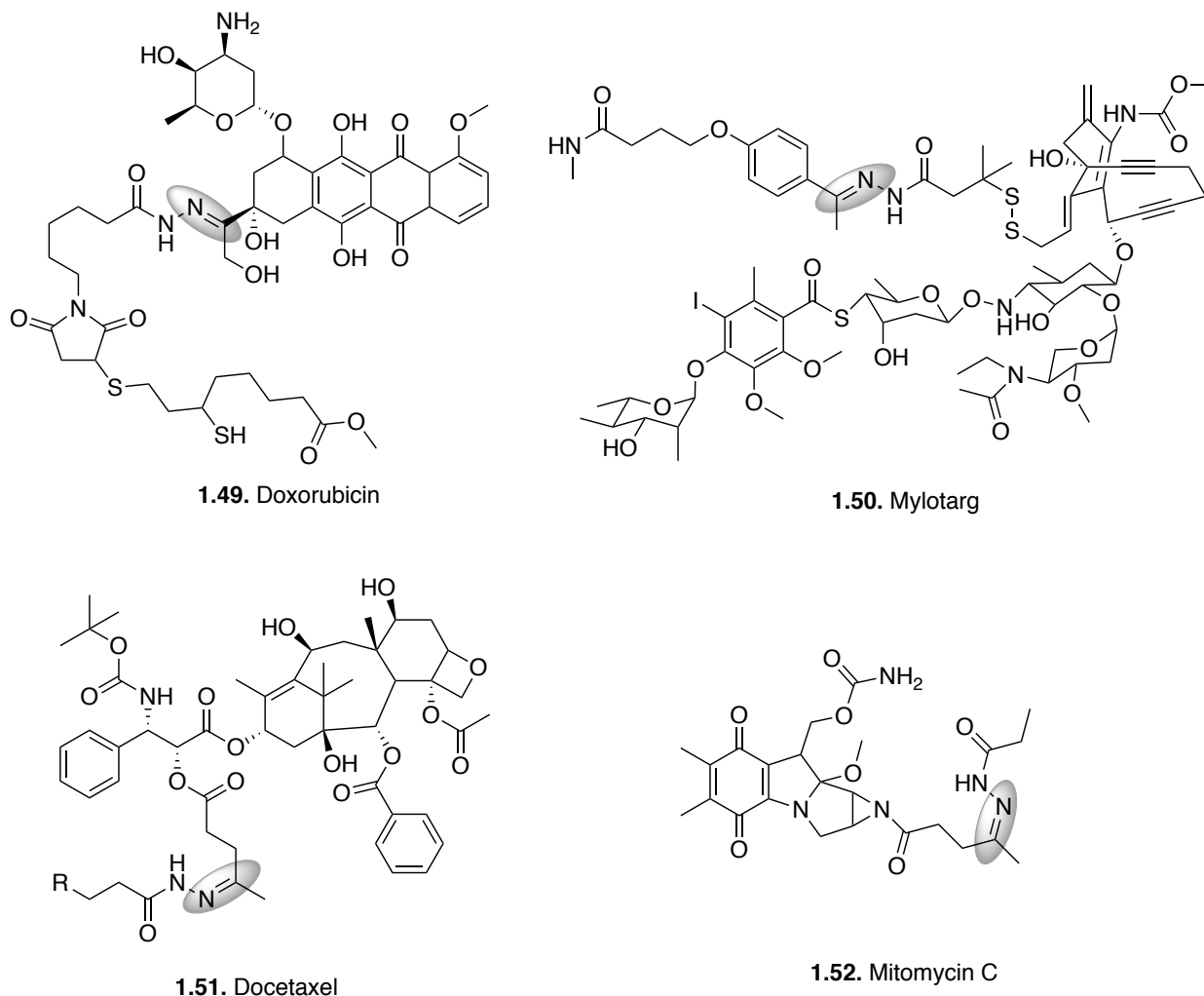


Figure 1.7. Chemotherapeutic agents with hydrazone functionalities with carrier.

The Simanek laboratory's longstanding interest in triazine chemistry led us to explore the stability of hydrazones made by the condensation of various triazinyl hydrazines with aldehydes and ketones. The starting material cyanuric chloride is used to create triazinyl hydrazines. It

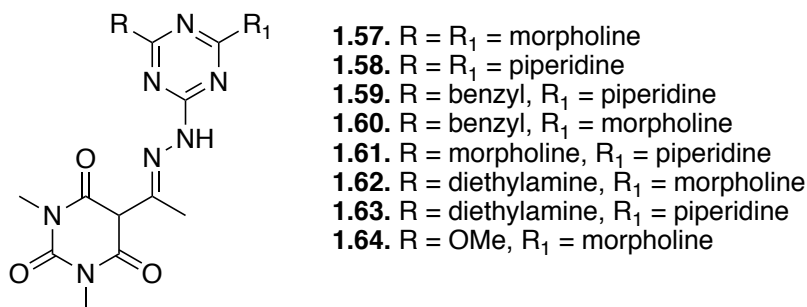


Figure 1.8. Various triazinyl hydrazone derivatives of barbiturates.

Triazine based hydrazines have been developed and applied for the titration of aldehydes in water. The carbonyl compounds, especially short chain aldehydes are some of the most common pollutants in the liquid samples. Triazinyl hydrazines compounds react with these carbonyl to afford hydrazones at high yields. Reverse phase liquid chromatography with binary gradients of acetonitrile and water is used to separate the triazinyl hydrazine and carbonyl compounds. UV-vis spectroscopy as well as fluorescence detection can be used to quantify the hydrazones.¹³²

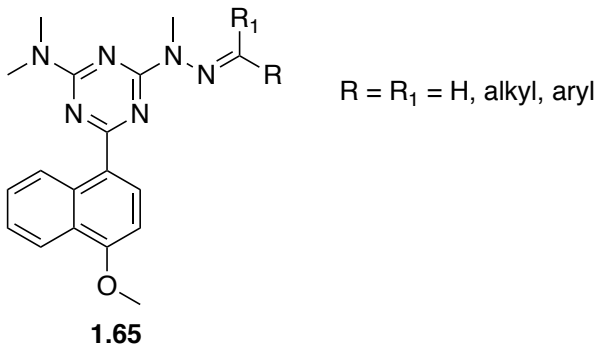


Figure 1.9. Triazinyl hydrazones made during the analysis of water.

Amir et. al used 1,2,4-triazinyl hydrazine to create hydrazones in the development of various anticonvulsant agents with effective dose varied from 30 mg/Kg to 300 mg/Kg.¹³³

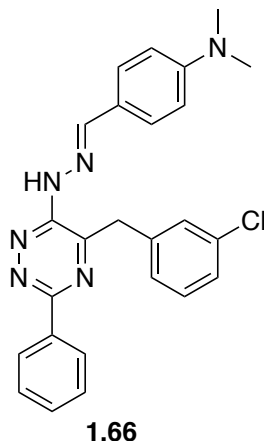


Figure 1.10. 1,2,4-Triazinyl hydrazones as anticonvulsant agents.

Previously, our research group compared the hydrolysis rates between acyl-hydrazones and triazinyl hydrazones made by condensation of various aldehydes and ketones with respective hydrazines.¹²¹ Triazinyl hydrazones are observed to be more stable at acidic pH than acyl hydrazones.¹²¹ Hydrolysis studies were limited to only one type of triazinyl hydrazine and monocarbonyl compounds of ketones and aldehyde. We continued the previous work by synthesizing and studying the hydrolysis rates of various triazinyl hydrazones occupying different alkyl groups at the nitrogen atom vicinal to triazine ring described in the chapter 2. During the synthesis of hydrazones with diketones, we also made some stable hemiaminals under acidic conditions that have been isolated only under neutral conditions and steered us to studied the effect of H-bonds and strong electron withdrawing groups to their stability described in the chapter 3. Finally, we used substituted triazine rings to make macrocycles of ring sizes 22-28 by spontaneous condensation of amine and aldehyde groups in the presence of strong acid and will be discussed in chapter 4.

Chapter 2: The effect of pH on the hydrolysis rates of triazinyl hydrazones with different groups at N₂

2.1 Introduction and previous work

A change in pH is one of the most studied triggers for the release of a drug from a formulation. There are significant changes in the pH across tissues in the body from stomach to gastrointestinal track to blood stream. Some cellular compartments have considerable differences in pH than other compartments. As examples, the pH values of the cytosol, Golgi apparatus, endosomes, and lysosomes are 7.4, 6.4, 5.5-6.0, and 4.5-5.0 respectively.¹³⁴ In addition, tumor cells over-produce lactic acid due to their high metabolic activities and as a result, the pH of cancerous tissues is lowered to pH 6.5-7.0 from pH 7.4.¹³⁵

In general, the rate of hydrolysis of hydrazones has been found to increase with decreasing pH. Previously our group compared the hydrolysis of acetyl hydrazones with triazinyl hydrazones and found that at low pH triazinyl hydrazones are more stable than acyl hydrazones.¹²¹ During these preliminary studies, 1,3-diketones were not examined as they can form stable pyrazole rings following a second dehydration event.

One way to avoid the formation of pyrazole rings is by replacing H-atom of nitrogen (N₂) with a methyl (-CH₃) or phenyl (-C₆H₅) group (Chart 2.1). Not only the pyrazole formation prevented, but the hydrolysis rate might be tuned due to the inductive and resonance effect communicated by these groups.

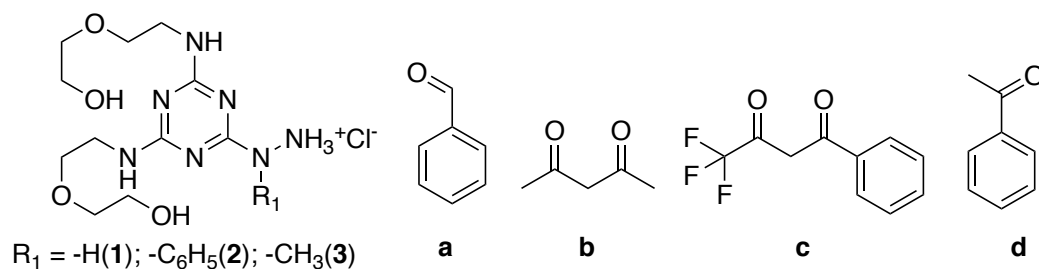


Chart 2.1. List of triazinyl hydrazines and carbonyl compounds used.

In this chapter, the synthesis of twelve hydrazones from the condensation of three different triazinyl hydrazines hydrochloride salts, **1-3**, and aldehydes or ketones, **a-d**, (Chart 2.1) is described. Hydrazones formed from triazinyl hydrazine **1** with aldehyde **a** will be referred to as hydrazone **1a** and so on. Hydrolysis rates are studied using HPLC under different pH conditions (4.0, 5.0, and 7.0). A ten equivalent excess formaldehyde was used to trap the released hydrazine.

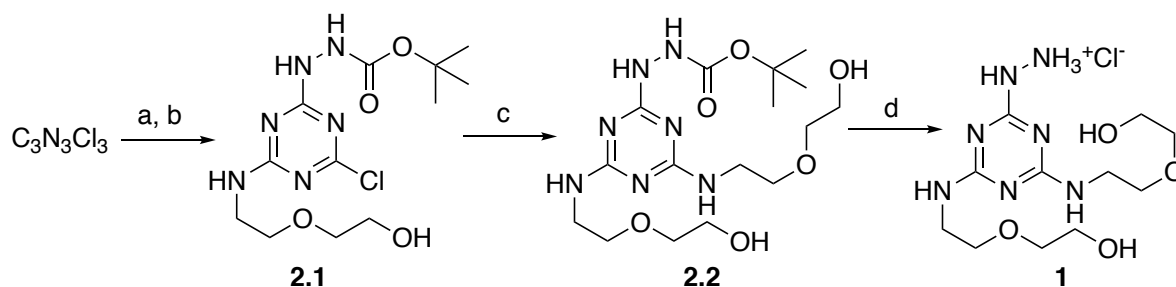
2.2 Results and discussions

Triazinyl hydrazines **1**, **2**, and **3** with -H, -C₆H₅, and CH₃ at N₂ respectively were synthesized by adapting three schemes each with slightly different steps. In each synthetic method, two chlorine atoms of starting material cyanuric chloride were replaced by 2-(2-aminoethoxy)-ethanol substituents to enhance the solubility of the final product in water. The intermediates and final products were characterized by mass and NMR-spectroscopy.

2.2.1 General synthetic route of triazinyl hydrazine hydrogen chloride salt **1**

The most successful synthetic strategy to synthesize triazinyl hydrazine hydrogen chloride salt as **1** (Scheme 2.1) involved three steps with an overall yield of 65% with the formation of two intermediate compounds **2.1** and **2.2**. Sequential additions of *tert*-butyl carbazate at low temperature to the mixture of cyanuric chloride and *N,N*-diisopropylethylamine (DIPEA) followed by the addition of 2-(2-aminoethoxy)-ethanol at room temperature yields compound **2.1**.

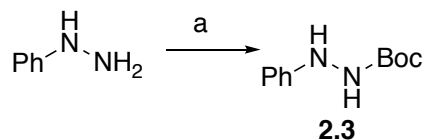
Compound **2.1** was characterized by the presence of a singlet at 1.49 ppm (9H) of *tert*-butyl group and a multiplet between 3.50-3.78 ppm (8H) of 2-(2-aminoethoxy)-ethanol group. Introduction of 2-(2-aminoethoxy)-ethanol in the first step resulted in the desired product along with un-identified impurities which could not be separated by chromatography. The substitution of the third chlorine atom by 2-(2-aminoethoxy)-ethanol was done using microwave irradiations at 95 °C to afford compound **2.2**. Finally, the deprotection of *tert*-butyl carbamate group with 4M HCl to afforded triazinyl hydrazine hydrochloride salt **1**. Detailed description of synthetic procedure is provided in experimental section.



Scheme 2.1. Synthesis of triazinyl hydrazine hydrogen chloride salt **1**. Reagents and conditions: (a) *tert*-butyl carbamate, THF, DIPEA, 0 °C, 1 h. (b) 1 equiv. 2-(2-aminoethoxy)-ethanol, THF, DIPEA, rt, 12 h, 88%. (c) 1 equiv. 2-(2-aminoethoxy)-ethanol, dioxane, Cs₂CO₃, microwave irradiation, 95 °C, 1 h, 74%. (d) 4M HCl, CH₂Cl₂, rt, 12 h, 99%.

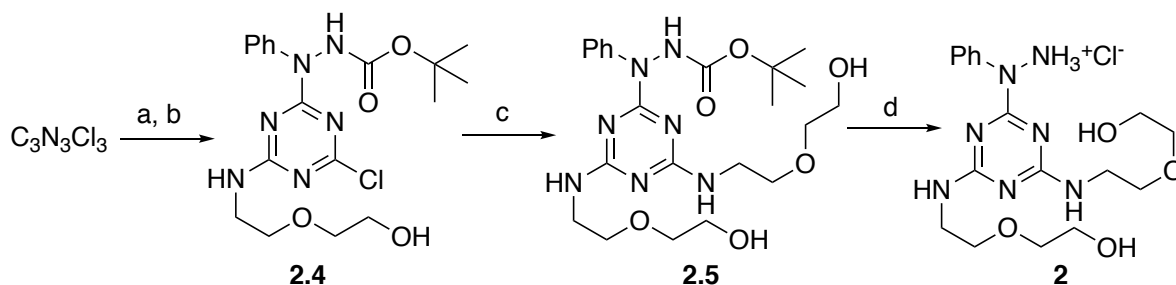
2.2.2 General synthetic route of *N*-phenyl triazinyl hydrazine hydrogen chloride salt **2**

N-Phenyl-*tert*-butyl carbamate, **2.3**, was prepared by refluxing phenyl hydrazine in THF with di-*tert*-butyl carbonate for three hours in the presence of triethyl amine (Scheme 2.2).



Scheme 2.2. Synthesis of *N*-phenyl-*tert*-butyl carbamate a) Di-*tert*-butyl carbonate, THF, reflux, 3 h, 61%.

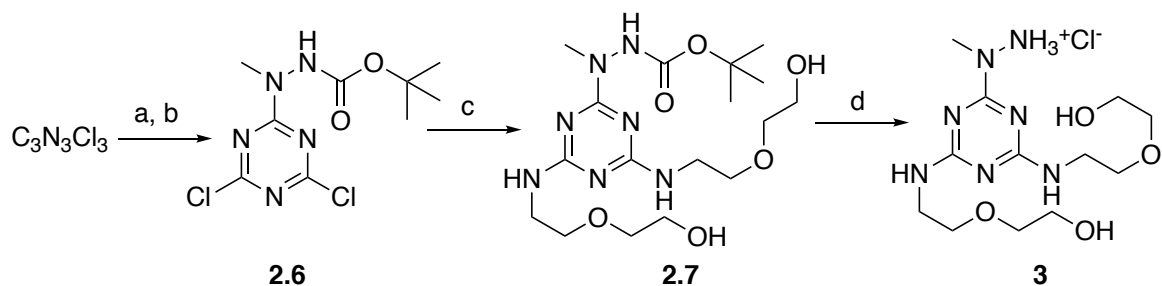
The synthesis of triazinyl hydrazine **2** involved similar steps (Scheme 2.3) as the synthesis of triazinyl hydrazine **1** with an overall yield of 23%.



Scheme 2.3. Synthesis of *N*-phenyl triazinyl hydrazine hydrogen chloride salt **2**. Reagents and conditions: (a) Compound **2.3**, THF, DIPEA, 0 °C, 1 h. (b) 1 equiv. 2-(2-aminoethoxy)-ethanol, THF, DIPEA, rt, 12 h, 58%. (c) 1 equiv. 2-(2-aminoethoxy)-ethanol, dioxane, Cs₂CO₃, microwave irradiation, 95 °C, 1 h, 69%. (d) 4M HCl, CH₂Cl₂, rt, 12 h, 99%.

2.2.3 General synthetic route of *N*-methyl triazinyl hydrazine hydrogen chloride salt **3**

The synthesis of hydrazine **3** relied on the synthesis of dichlorotriazine intermediate **2.6**. Methyl iodide was used to alkylate at N2 in the presence of DIPEA. While DIPEA also reacted with methyl iodide to make the methylated DIPEA salt, resulted in low yield of **2.6**. However, obtained **2.6** was sufficient to continue the next steps. A singlet at 3.35 ppm (3H) suggested the formation of compound **2.6**. The other two chlorine atoms are substituted by 2-(2-aminoethoxy)-ethanol in one container at elevated temperature followed by the deprotection with 4M HCl yielded **3** with an overall percent yield of 24% (Scheme 2.4).



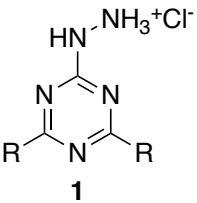
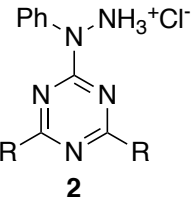
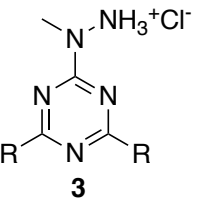
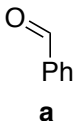
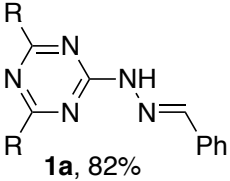
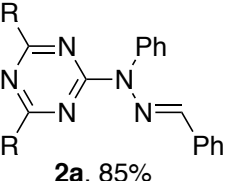
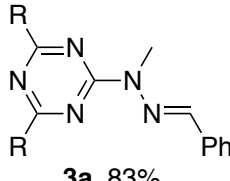
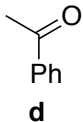
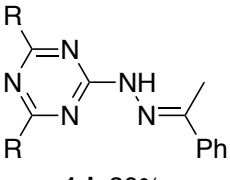
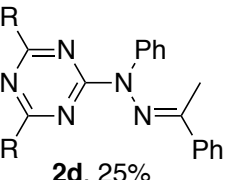
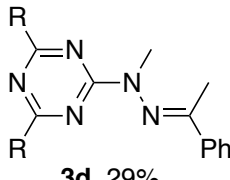
Scheme 2.4. Synthesis of *N*-methyl triazinyl hydrazine hydrogen chloride salt **3**. Reagents and conditions: (a) *tert*-butyl carbazate, THF, DIPEA, 0°C, 1 h. (b) Methyl iodide, DIPEA, RT, 12 h. 28% (c) 2 equiv. 2-(2-aminoethoxy)-ethanol, Cs₂CO₃, dioxane, 95°C, microwave, 1h. 88% (d) 4M HCl, CH₂Cl₂, RT, 12 h. 97%

2.2.4 Synthesis of hydrazones

Condensation of carbonyl **a-d** was most efficiently accomplished by reacting excess of each one with each triazinyl hydrazine hydrogen chloride, **1-3**, in anhydrous methanol at room temperature for 12 hours. General purification steps included removing the excess solvent under vacuum, dissolving the residue in dichloromethane, and column chromatography using either silica or alumina.

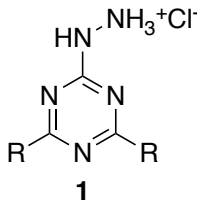
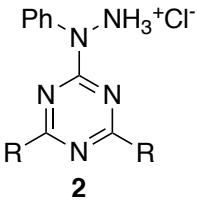
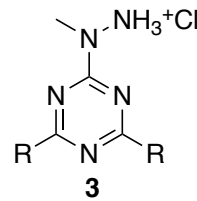
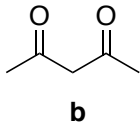
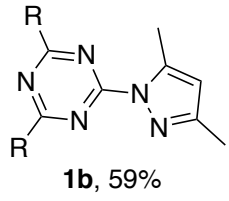
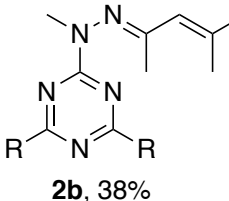
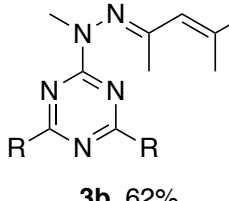
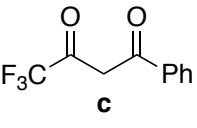
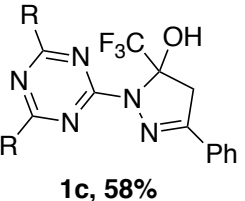
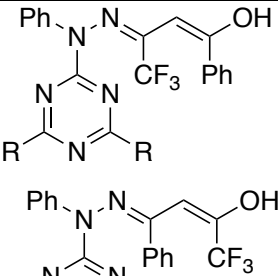
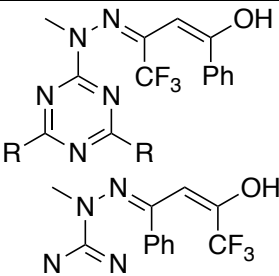
The reaction of benzaldehyde **a** and acetophenone **d** with triazinyl hydrazines (**1-3**) yields regular hydrazones. The summary of these hydrazones is provided in Table 2.1.

Table 2.1. Summary of hydrazones synthesized from **a** and **d**. R = -NH(CH₂CH₂O)₂H. Solvent: CH₃OH/CH₃CN. Conditions: 12 hours at room temperature.

Hydrazines Carbonyls	 <p style="text-align: center;">1</p>	 <p style="text-align: center;">2</p>	 <p style="text-align: center;">3</p>
 <p style="text-align: center;">a</p>	 <p style="text-align: center;">1a, 82%</p>	 <p style="text-align: center;">2a, 85%</p>	 <p style="text-align: center;">3a, 83%</p>
 <p style="text-align: center;">d</p>	 <p style="text-align: center;">1d, 30%</p>	 <p style="text-align: center;">2d, 25%</p>	 <p style="text-align: center;">3d, 29%</p>

The reactions of triazinyl hydrazines (**1-3**) with diketones **b** and **c** yielded interesting hydrazone products. Obtained products ranges from the pyrazole and hemiaminal rings to open chain hydrazones containing enol functional group. The summary of various hydrazones made from the reaction of triazinyl hydrazine **1-3** with diketones **b** and **c** is provided in Table 2.2.

Table 2.2. Summary of hydrazones synthesized from **b** and **c**.

Hydrazines	 1	 2	 3	
Carbonyls	 b	 1b , 59%	 2b , 38%	 3b , 62%
	 c	 1c , 58%	 2c , 50%	 3c , 62%, 4.3:1

R = -NH(CH₂CH₂O)₂H. Solvent: CH₃OH/CH₃CN. Conditions: 12 hours at room temperature.

Reaction of **1** with **b** results in the formation of pyrazole derivative after second dehydration event. The ¹H and ¹³C NMR suggest the formation of aromatic pyrazole derivative. A characteristic singlet at 5.98 ppm corresponds to the only aromatic proton of the pyrazole ring (Figure 2.1).

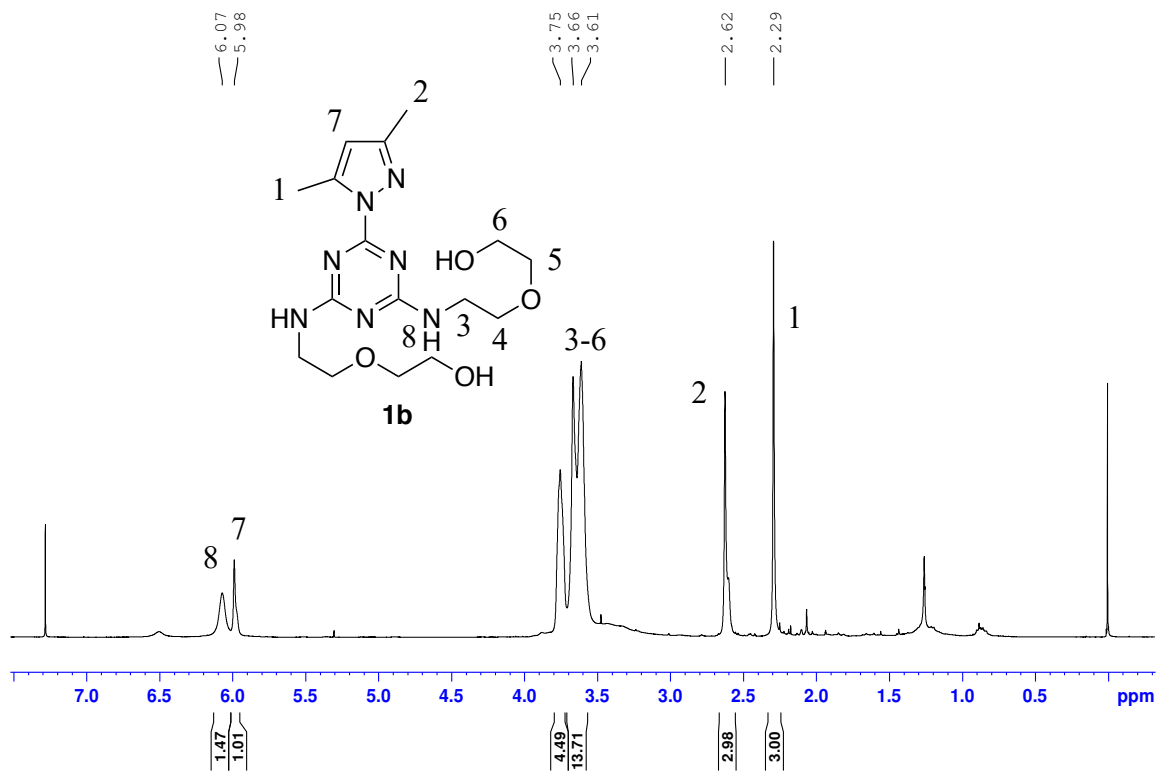


Figure 2.1. ^1H NMR of **1b** in CDCl_3 .

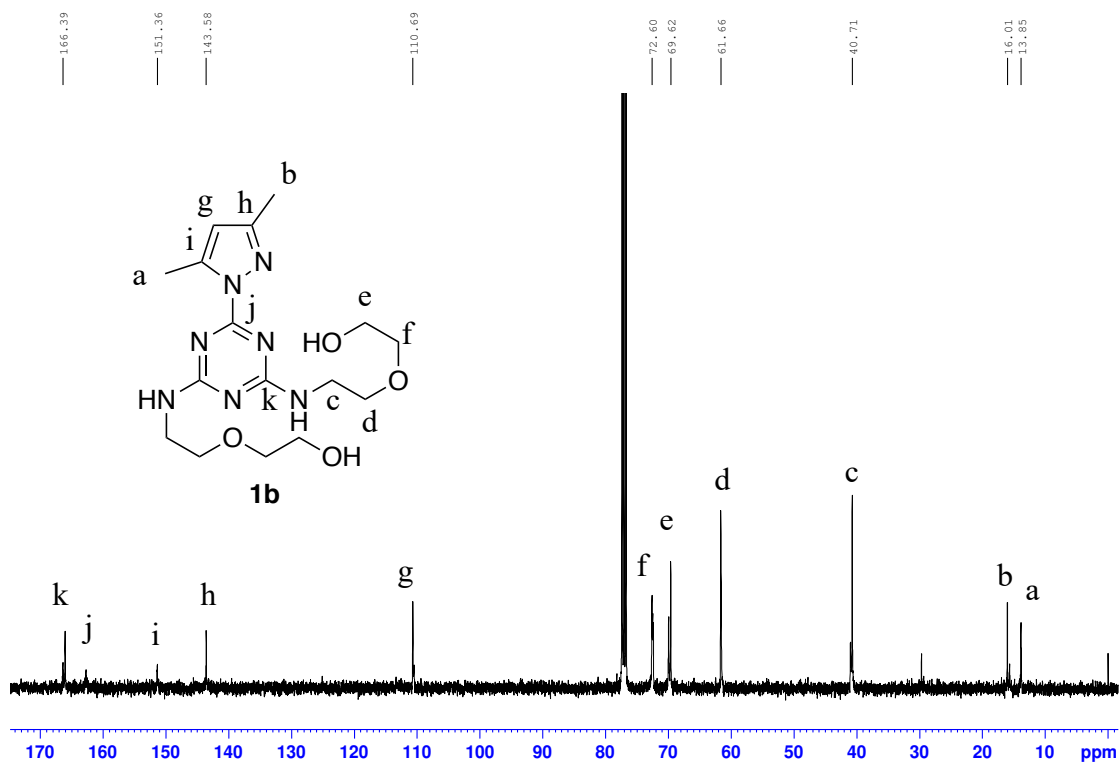


Figure 2.2. ^{13}C NMR of **1b** in CDCl_3 .

The ^{13}C NMR of **1b** (Figure 2.2) also indicates the formation of pyrazole ring. The hydrazone carbon (C=N), unsaturated carbon atom of the pyrazole ring, and carbon atom attached to nitrogen (C-N) of pyrazole ring appear at 110.7, 143.6, and 151.4 respectively.

Diketone **c** (1,1,1-trifluoro-4-phenyl-2,4-butanone) is non-symmetrical. Its condensation with **1** can result in the formation of two regioisomers depending on the site of formation of hydrazone bond with respect to carbonyl group. If carbonyl group next to phenyl makes hydrazone bond, **1c** results. On the other hand, if the carbonyl next to CF_3 group makes hydrazone bond, **1c'** results. Surprisingly hydrazone **1c** did not make the pyrazole ring. Mass spectrum of the product was 18 a.m.u. unit higher than the pyrazole derivatives. It suggested that second dehydration step did not take place and indicated the formation of five membered hemiaminal ring.

The ^1H and ^{13}C NMR corroborate the formation of five membered hemiaminal ring. A singlet at 7.37 ppm is the hydroxyl proton (Figure 2.3). The unsaturated proton of the pyrazole ring was observed at 5.99 ppm in **1b**. An enol proton would appear much further downfield. In addition, the signal between 3.62-3.75 integrated to more than 16 protons and suggested the signal of methylene group of hemiaminal ring was hidden in there. Formation of the hemiaminal was totally unexpected as hemiaminals had been obtained only under neutral conditions previously. The ^1H -NMR also indicated the formation of only one regioisomer but was not enough to identify the particular regioisomer made. As a result, need to grow the crystal structure became crucial in order to determine particular regioisomer that was made. A crystal structure would also support the hypothesis that H-bond formation is responsible for the signal at 8.93 ppm. However, presence of polar groups on the triazine ring made it difficult to grow the crystal structures. As a result, we decided to explore this hemiaminal chemistry by using a rigid morpholine on the triazine ring.

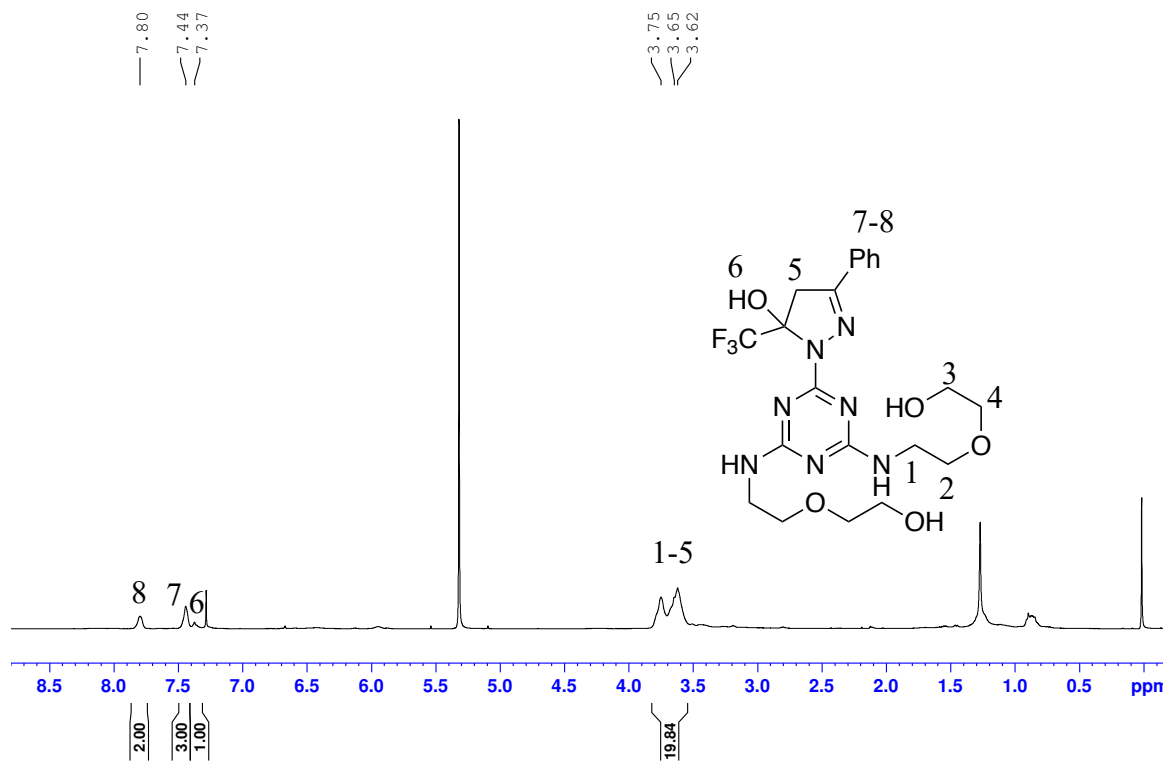


Figure 2.3. $^1\text{H-NMR}$ of **1c** in CDCl_3 .

The reaction of **2** with **b** forms hydrazone compound that contains enol functional group. The chromatographic purifications were done using alumina column instead of silica due to instability of the hydrazone. The characteristic signal at 11.93 ppm corresponds to the enol proton (Figure 2.4). In addition, a signal at 196.9 ppm in the ^{13}C NMR corresponds to the enol carbon atom.

The reaction of **2** with **c** can form two different open chain enol regioisomers depending on the position of carbonyl that makes the hydrazone bond. However, the ^1H NMR suggests the formation of one regioisomer as the signal at 12.27 ppm suggests one enol proton (Figure 2.5)

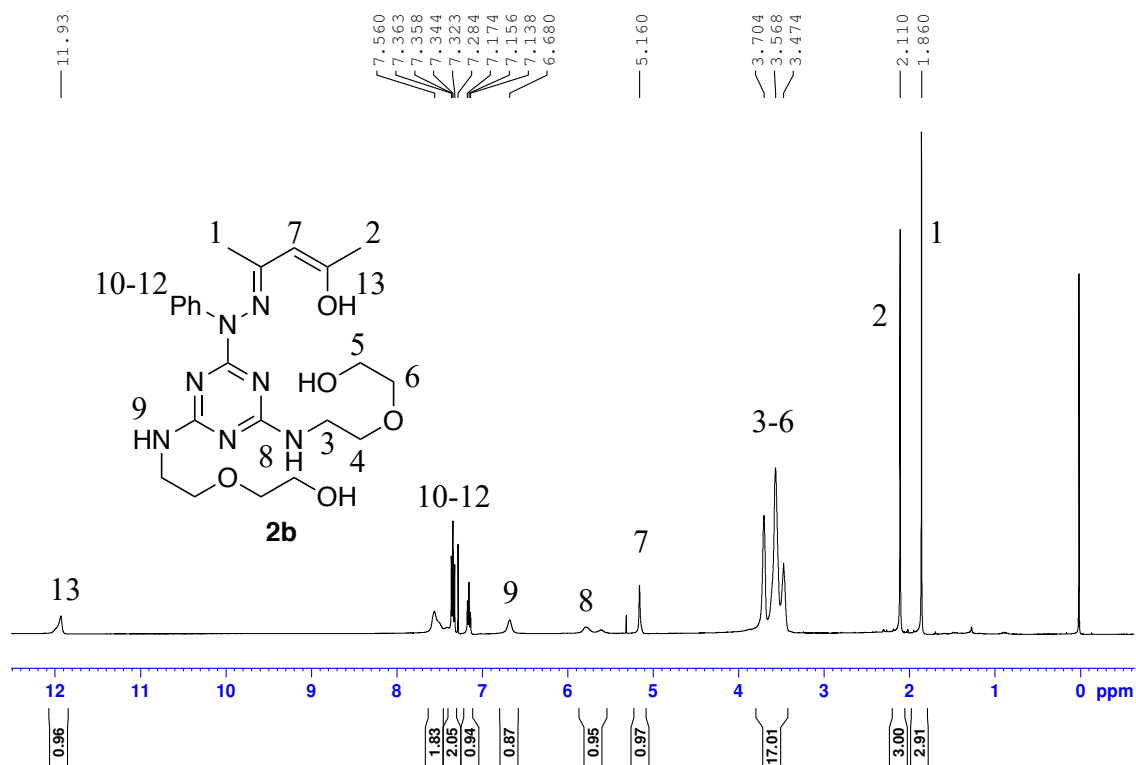


Figure 2.4. $^1\text{H-NMR}$ of **2b** in CDCl_3 .

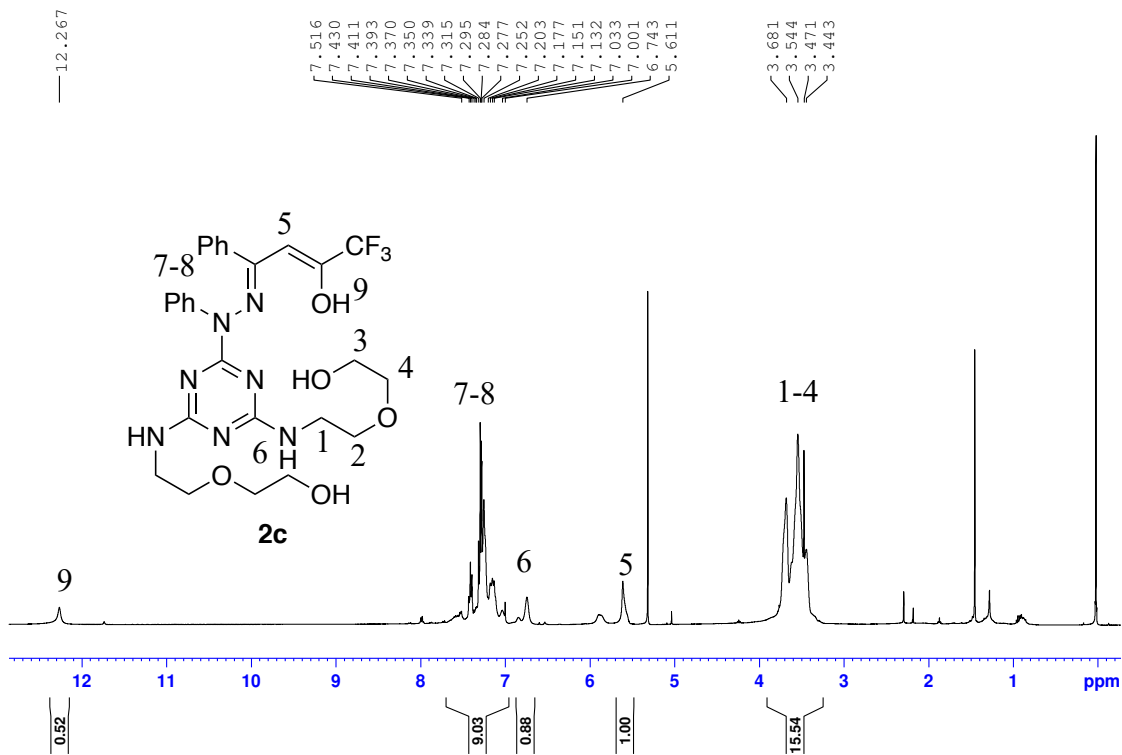


Figure 2.5. $^1\text{H-NMR}$ of **2c** in CDCl_3 .

The reaction of **3** with **b** makes open chain hydrazone with enol functional group similar to **2b**. The reaction of **3** with **c** makes both regioisomers were made in the ratio of 4.28:1 as indicated by the presence of two signals 11.83 ppm and 11.29 ppm correspond to two enol protons (Figure 2.6).

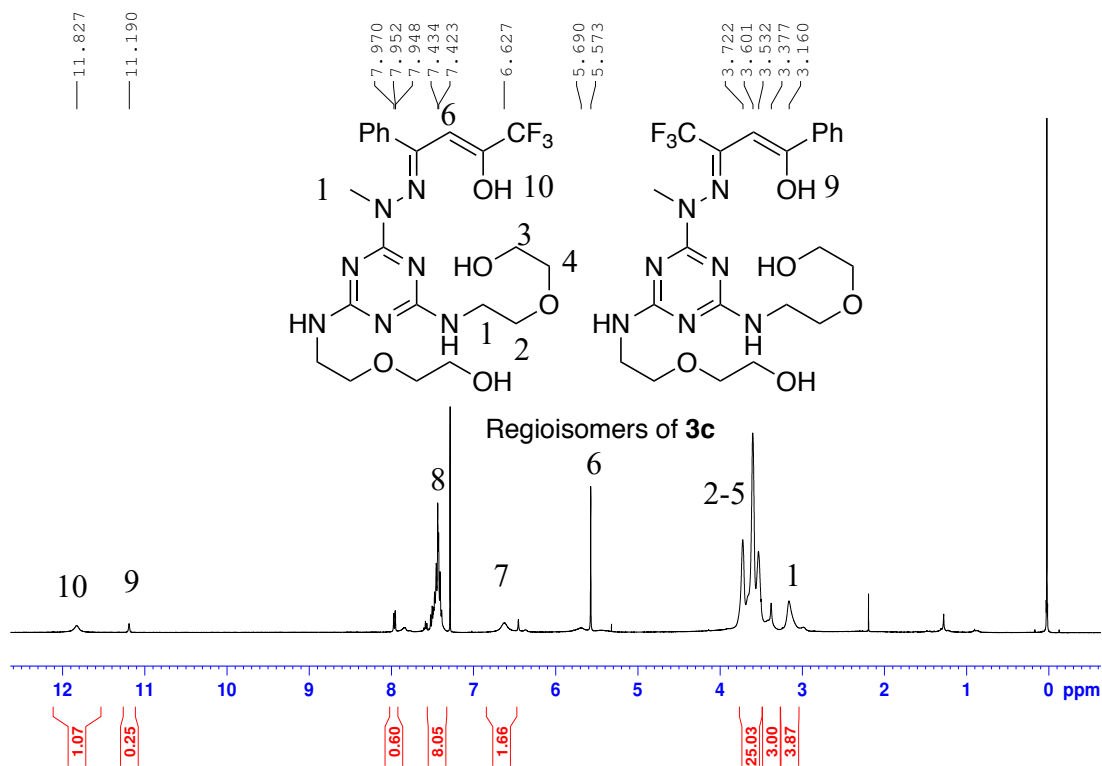
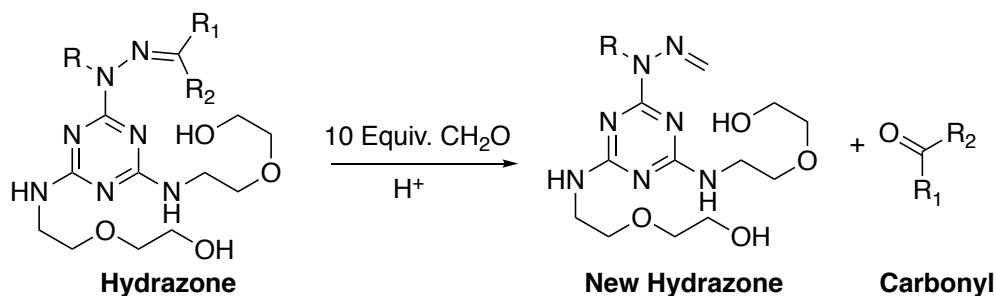


Figure 2.6. ¹H-NMR of **3c** in CDCl₃.

2.2.5 Hydrolysis studies

Hydrolysis rates were measured by high performance liquid chromatography (HPLC) using an established competitive exchange reaction relying on the presence of a 10-fold excess of formaldehyde. Upon hydrolysis, triazinyl hydrazine makes a new hydrazone with formaldehyde and release the carbonyl compound (Scheme 2.5). The change in the concentrations can be followed by HPLC.



Scheme 2.5. Hydrolysis of hydrazones.

Hydrazones **1b** and **1c** do not hydrolyze based on HPLC and mass spectrometry studies. Hydrazone **1b** made a stable pyrazole ring. Hydrazone **1c**, unexpectedly, made a five membered hemiaminal ring and was found to be stable to hydrolysis. Hydrazones **2b**, **2d**, **3b**, and **3d** were relatively unstable and did not survive the HPLC column. As a result, their half-lives were estimated by collecting mass spectra after every 10 minutes. As an example, the molar mass of **3b** is 413.3 amu. Figure 2.8 shows the mass spectrum of hydrazone **3b**. Hydrazone **3b** hydrolyses within ten minutes once placed in buffer solution of pH 4.0. The released hydrazine is trapped with formaldehyde. The line at 414.32 corresponds to the hydrazone **3b**. The triazinyl hydrazine **3** has a molar mass of 332.26 a.m.u. After 10 minutes, mass spectrum shows no peak at 414.32 a.m.u. Instead, a new peak at 344.42 a.m.u. dominates which represents the new hydrazone formed after the condensation reaction of **3** and formaldehyde.

The hydrolysis of all other hydrazones were studied by recording a HPLC chromatogram every 60 minutes. In general, the concentration of the hydrazone decreased over time and measured by integrating the area underneath the curve. The concentration of new hydrazone formed from formaldehyde and released carbonyl was increased. The hydrolysis rate of hydrazones **1a**, **2a**, **3a**, **1d**, **2c**, and **3c** (Table 2.3) was measured using HPLC. A percent decrease of all the hydrazone is

plotted with respect to time as shown in Figure 2.7. Hydrazones **1b** and **1c** did not hydrolyze.

Hydrazones **2b**, **2c**, **3b**, and **3d** hydrolyzed too quickly and as a result are not shown in Figure 2.7.

Table 2.3. List of hydrazones hydrolyzed using HPLC. R = -NH(CH₂CH₂O)₂H.

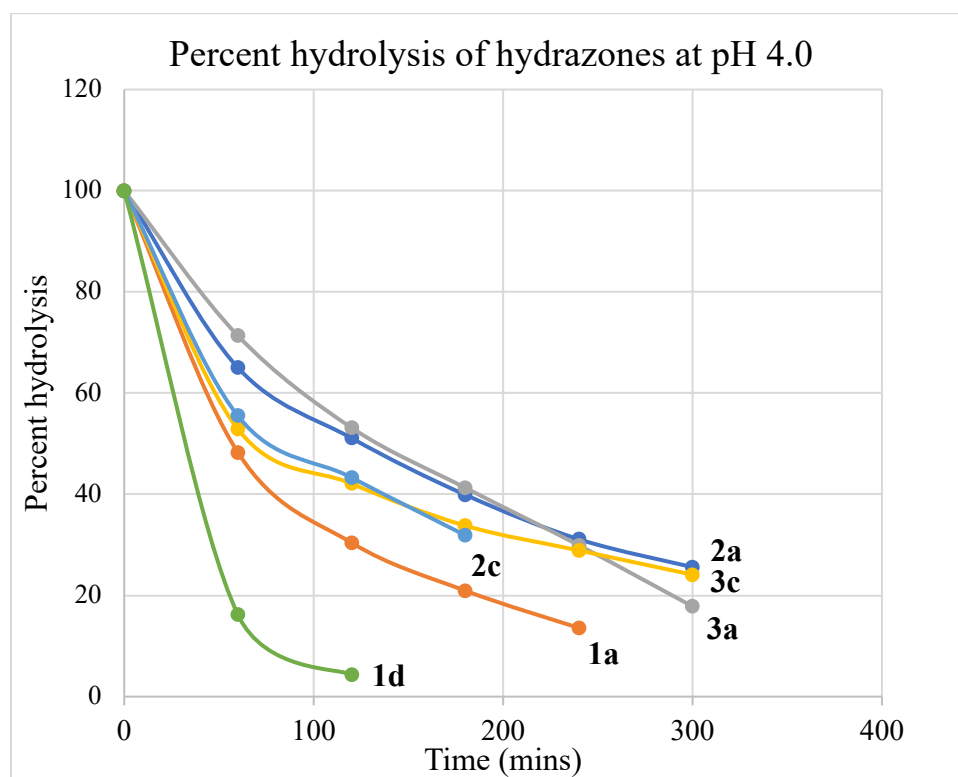
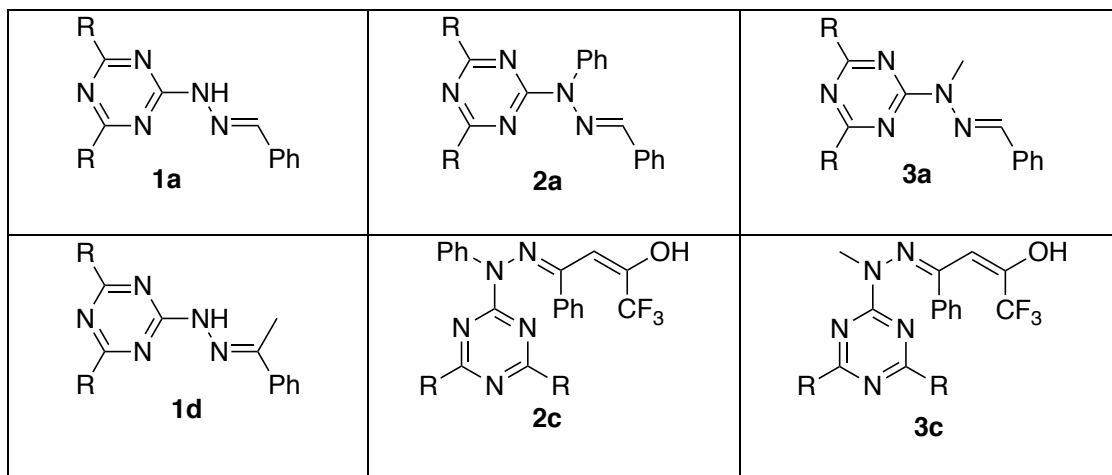


Figure 2.7. HPLC percent hydrolysis of all the hydrazones at pH 4.0.

As an example, the hydrolysis of **3a** is shown as a function of time in Figure 2.8. Hydrazone **3a** was eluted with a retention time of 2.9 min. The formaldehyde-trapped hydrazone and benzaldehyde eluted at retention times of 2.4 and 6.4 minutes respectively. The relative area under the peak at 2.9 decreased while those of peaks at 2.3 and 6.4 minutes were increased. The decrease in the percent concentration of **3a** was observed to be exponential and was plotted as shown in Figure 2.9. In addition, pseudo-first order kinetics plot (Figure 2.10) was also made ($\ln[\mathbf{3a}]$ and time (minutes)) to calculate the pseudo-first order rate constant and half-life of **3a**. The rate constant and half-lives of hydrolysis of all the hydrazones are shown in Table 2.4.

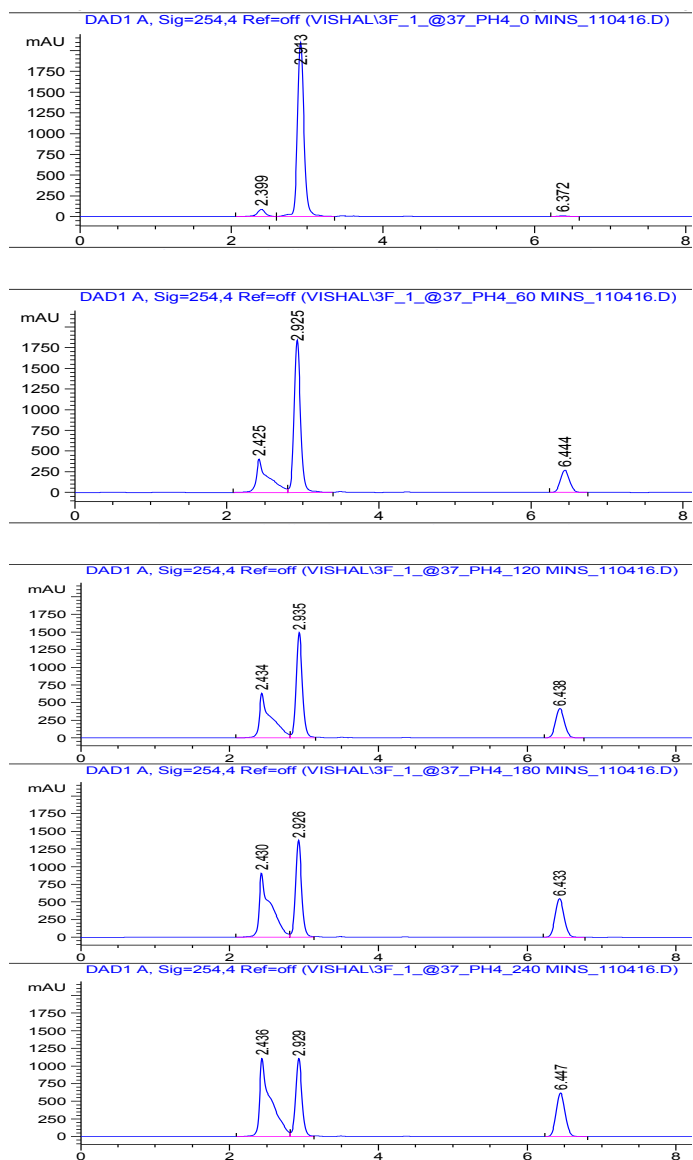


Figure 2.8. Time-dependent hydrolysis profile of hydrazone **3a** at pH 4.0. The peaks at 2.4, 2.9, and 6.4 correspond to formaldehyde-trapped hydrazone, **3a**, and benzaldehyde, respectively.

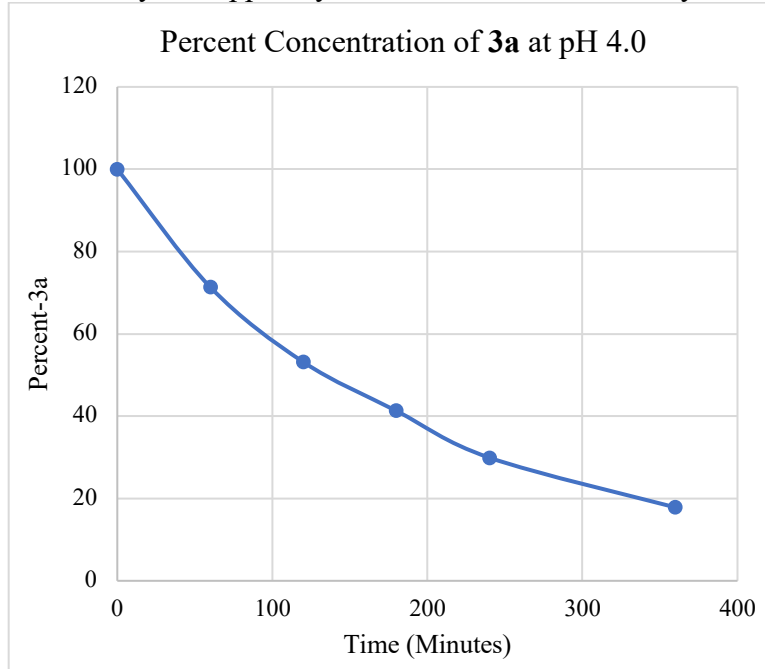


Figure 2.9. Change in percent concentration of **3a** at pH 4.0.

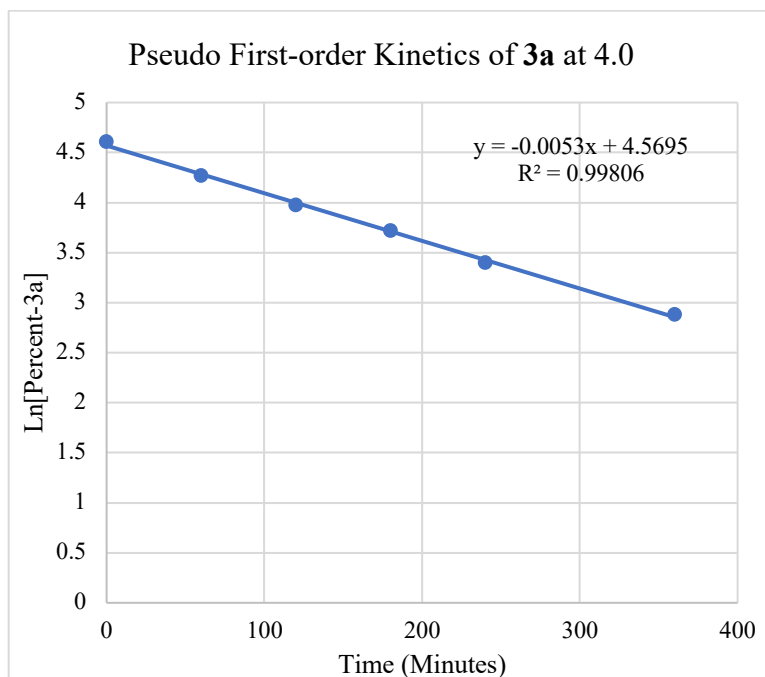
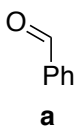
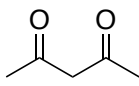
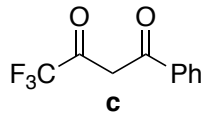
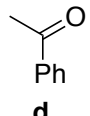


Figure 2.10. Pseudo first-order kinetics of **3a** at pH 4.0.

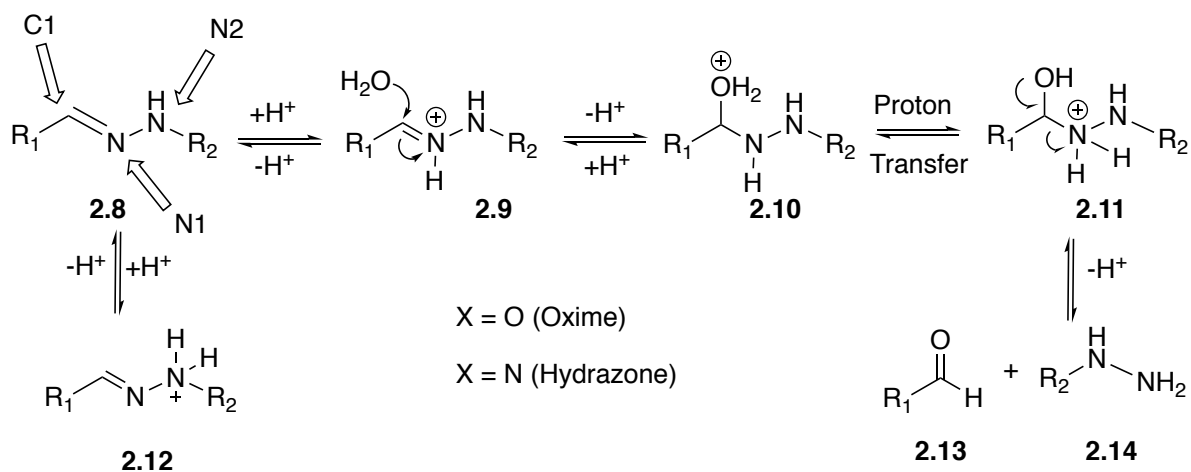
Hydrazones **2c** and **3c** showed multiple peaks indicating the formation of unknown side products upon hydrolysis. The mass spectrum of one of the side products was determined to be 18 a.m.u. less than that of starting hydrazone. Loss of water is not easily explained. Similarly, hydrolysis studies of all hydrazones were performed to measure the half-lives and rate constant at pH 4.0, 5.0 and 7.0. The calculated half-lives and rate constants are summarized in Table 2.4. All other percent hydrolysis and pseudo first-order kinetics graphs are provided in the supplementary information.

Table 2.4. Half-lives and rate constants of hydrazones.

Hydrazones (<i>N</i> -subs.)	Carbonyl compounds	Half-life $t_{1/2}$ (mins) ± 10			Rate Constant 10^{-3} (mins $^{-1}$) ± 1.0		
		pH 4	pH 5	pH 7	pH 4	pH 5	pH 7
1a (H)	 a	82	86	3500	8.5	8.1	0.2
2a (Ph)		144	210	3500	4.8	3.3	0.2
3a (Me)		131	224	3465	5.3	3.1	0.2
1b (H)	 b	-	-	-	-	-	-
2b (Ph)		<20	<20	<20	NA	NA	NA
3b (Me)		<10	<10	<10	NA	NA	NA
1c (H)	 c	-	-	-	-	-	-
2c (Ph)		113	147	115	6.1	4.7	6.0
3c (Me)		99	177	151	7.0	3.9	7.3
1d (H)	 d	28	47	1386	24.9	14.9	0.5
2d (Ph)		<10	<20	<90	NA	NA	NA
3d (Me)		<10	<10	<90	NA	NA	NA

2.2.6 Effect of N2 substituents on hydrazone stability to hydrolysis

Hydrolysis of hydrazones involves (Mechanism 2.1) protonation of imine nitrogen (N₁) to yield **2.9**. The next step is the nucleophilic addition of a water molecule to the carbon (C₁) atom of imine to yields carbinolamine intermediate **2.10**. Proton transfer to N₁ from C₁ gives **2.11** and eventually leads to C–N bond cleavage to form the carbonyl compound **2.13** and the hydrazine **2.14**. Hydrolysis of hydrazones mechanism is consistent with imine hydrolysis observed in acid conditions.^{10,11}



Mechanism 2.1. Proposed mechanism of acid catalyzed hydrolysis of hydrazones (R = acetyl or triaziny)

Based on the mechanism, hydrolysis can be enhanced if the proton affinity of N₁ is increased. By having an electron donating group at N₂, the electron density at N₁ can be increased and consequently, will be more susceptible to accept the proton. The opposite would be true if there was an electron withdrawing group at N₂.

The alkylation of N₂ has a significant effect on the hydrolysis rate of hydrazones derived from benzaldehyde and acetophenone. The main outliers are the proton affinity values of **2a** and **3a**. Hydrazone **1a** (N-H) is found to be less stable than hydrazones **2a** (N-Ph) and **3a** (N-CH₃). However, based on the proton affinity values (Figure 2.11) **1a** should be more stable than **2a** and

3a. Experimentally, the stability of **2a** and **3a** appear to be similar. Higher proton affinity of **3a** agrees with the electron donating nature of methyl (N-CH₃). However, the electron withdrawing nature of phenyl via inductive and resonance effects should have decreased proton affinity. A possible explanation of phenyl for not behaving as electron withdrawing via resonance is the out of plane position of phenyl with respect to the lone pair of nitrogen. To further validate the experiment results, a different solvent system can be used to create acidic pH solution. The concentration of aliquots used to run HPLC can be increased to see the effect of ionic strength.

The hydrolytic stability of hydrazone **1d** is greater than hydrazones **2d** and **3d**. The experimental findings agree with the computed proton affinity (Figure 2.11). The proton affinity of **2d** and **3d** is greater than the proton affinity of **1d**. The presence of alkyl group on the N2 appears to increase the hydrolysis rate.

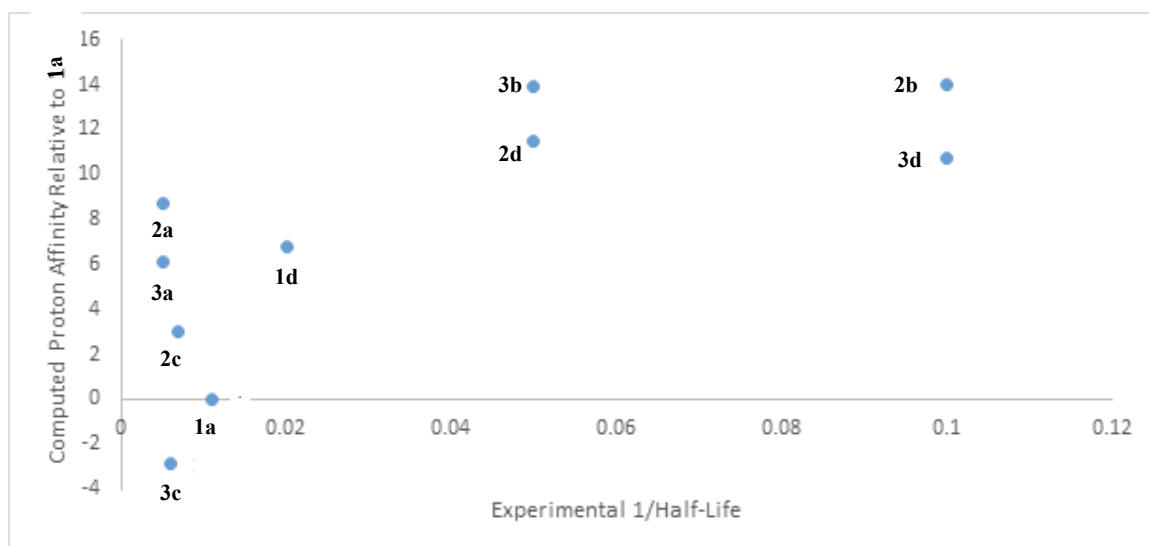


Figure 2.11. Computed proton affinity relative to **1a**.

Hydrazone **2b** and **3b** contain an enol functional group as opposed to **1b** which is a pyrazole ring. The proton affinity values of hydrazones **2b** and **3b** are 13.9 and 14.0 respectively and as a result hydrolyzed quickly in acidic conditions. Hydrazones **2b** and **3b** has the largest proton

affinities as intramolecular H-bond donor is also acting as intramolecular H-bond acceptor providing extra stability to the protonated form (Figure 2.12).

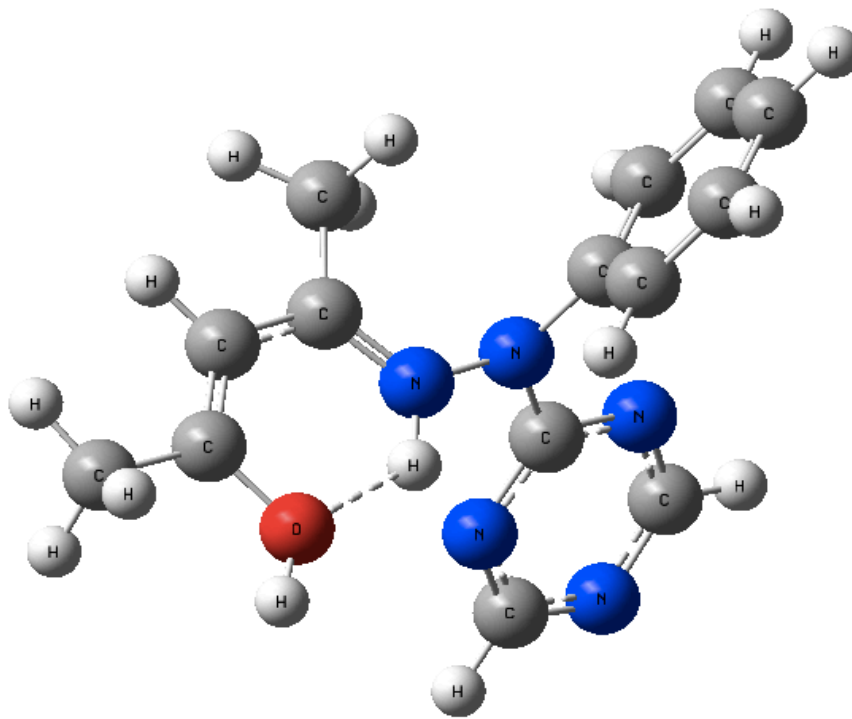


Figure 2.12. Computed geometry of protonated **2b** has proton hydrogen-bonded by the OH group.

The presence of phenyl and strong electron withdrawing group in the diketone, **c**, appears to stabilize the hydrazone (**2c** and **3c**). Similar to hydrazones **2b** and **3b**, hydrazones **2c** and **3c** contain the enol group. However, the proton affinity of **2c** and **3c** is lower than the proton affinities of **2b** and **3b**. The effect of intramolecular H-bond is not prominent in hydrazones **2c** and **3c** compare to **2b** and **3b**. The presence of the electron withdrawing groups on the diketones seems to play a role in stabilizing the hydrazone. In addition, the change in pH does not appear to make any difference in the hydrolysis rate of **2c** and **3c**. As an example, the half-lives of **2c** at pH of 4.0 and 7.0 are calculated to be 113 and 115 minutes, respectively. Similarly, half-lives of **3c** at pH of 4.0 and 7.0 are calculated to be 99 and 151 minutes, respectively.

2.3 Conclusion

Previously, it was found that triazinyl hydrazones showed increased stability to hydrolysis at pH <5 compared to a corresponding acetyl hydrazone, which showed greater stability to hydrolysis at pH >5. While this model is can be used in drug delivery by bonding an active drug through an acid labile hydrazone bond, it would fail if the active drug contains 1,3-diketone group. The use of diketones makes stable pyrazole or hemiaminal ring. The presence of an alkyl group on the N2 precludes the formation of pyrazole or hemiaminal ring. In this project, the presence of methyl and phenyl group results in the formation of hydrazones with enol functional group.

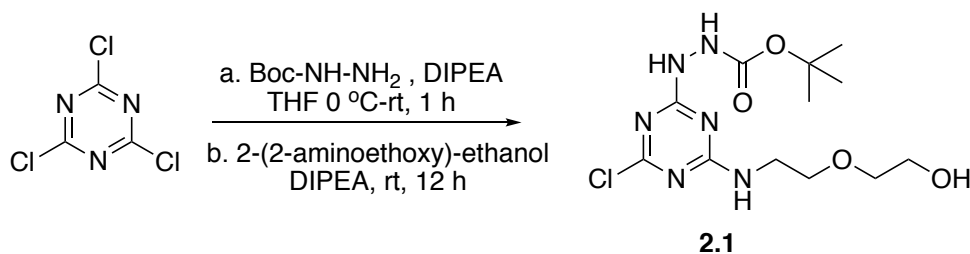
The presence of methyl or phenyl at N2 also increases the hydrolysis rate of regular hydrazones. The increase in experimental hydrolysis rate of **2d** and **3d** compare to **1d** is in agreement with the calculated proton affinities. We see a general experimental and computational stability of hydrazones formed from hydrazines 1>2~3 except the series **a**-hydrazones.

2.4 Experimental Section

2.4.1 Materials and methods

All solvents used were of ACS reagent grade and were used without further purification. All chemicals were purchased from Sigma Aldrich, Chemimpex, Acros etc. and used without further purification. NMR spectra were recorded on a Bruker Ascend 400 MHz spectrometer in CDCl₃, D₂O, and *d*₆-DMSO. All the HPLC data were collected using an Agilent technologies 1260 Infinity system. All ESI spectral data were carried out by an Agilent technology 6224 TOF MS system.

2.4.2 Synthesis of compound 2.1

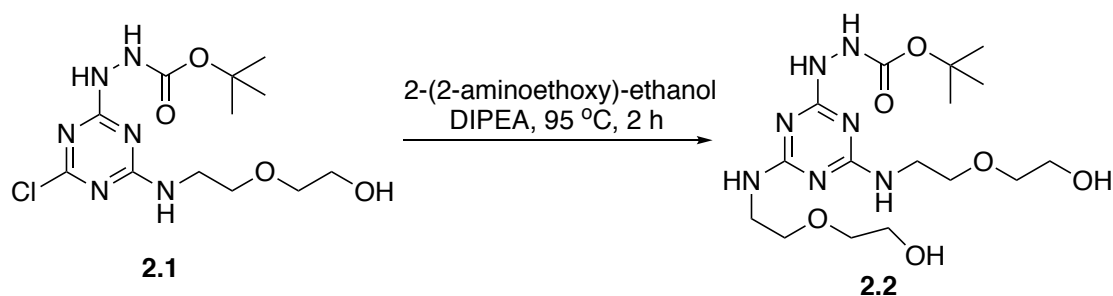


Scheme 2.6. Preparation of monochlorotriazine intermediate 2.1.

Cyanuric chloride (10.06 g, 54.7 mmol) was dissolved in 100 ml THF in a round bottom flask equipped with stirring bar and purged with argon. *Tert*-butyl carbazate (7.22 g, 54.2 mmol) and DIPEA (7.00 g, 54.3 mmol) dissolved in 25 ml THF were added to the flask dropwise at 0 °C. Produced solution was brought to room temperature slowly and stirred for 1 hour. The reaction progress was monitored by TLC. Then, 2-(2-aminoethoxy)-ethanol (5.78 g, 55.0 mmol) and DIPEA (7.00 g, 54.3 mmol) were added to the flask. Resulting reaction mixture was left to stir at room temperature for 12 hours. The excess solvent was removed under vacuum, residues were

dissolved in 40 ml DCM (x2), washed with 20 ml water, dried over Na₂SO₄, and concentrated under vacuum. Crude product was then purified by column chromatography using DCM: MeOH (25:1) to afford intermediate **2.1** (16.80 g, 88%) as white solid. ¹H NMR (400 MHz, CDCl₃) δ 3.70-3.56 (8H, m), 1.50 (9H, s). ¹³C NMR (400 MHz, CDCl₃) δ 168.4, 167.6, 166.0, 156.7, 80.5, 72.0, 68.9, 60.8, 40.3, 27.3. MS (ESI-TOF) calculated for C₁₂H₂₁ClN₆O₄: 348.13; Found 349.14.

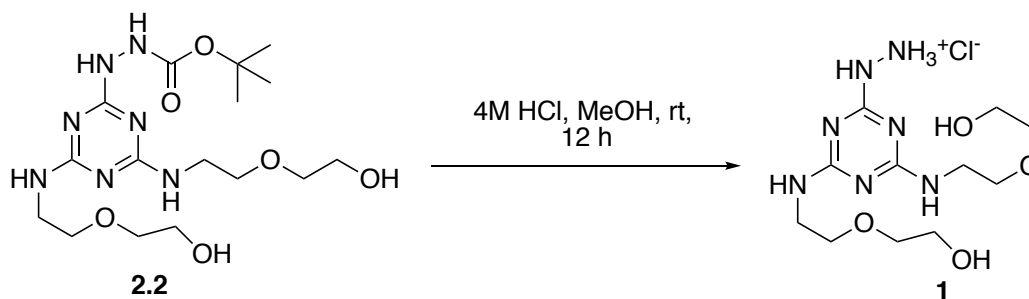
2.4.3 Synthesis of Intermediate 2.2



Scheme 2.7. Preparation of trisubstituted triazine intermediate **2.2**.

Intermediate **2.1** (5.00 g, 14.3 mmol) was dissolved in 10 ml dioxane in a microwave test tube equipped with stirring bar. Cs₂CO₃ (5.13 g, 13.9 mmol) and 2-(2-aminoethoxy)-ethanol (2.25 g, 21.4 mmol) were added to the test tube. Produced solution was stirred in the microwave at 95 °C for 1 hour. Cs₂CO₃ was filtered out, dioxane was removed under vacuum, residue was dissolved in 20 ml DCM (x2), washed with 10 ml water, dried over Na₂SO₄, and concentrated under vacuum. The crude product was then purified by column chromatography using DCM: MeOH (15:1) to afford **2.2** (4.40 g, 74%) as white solid. ¹H NMR (400 MHz, CDCl₃) δ 3.74-3.62 (16H, m), 1.47 (9H, s). MS (ESI-TOF) calculated for C₁₆H₃₁N₇O₆: 417.23; found 418.24.

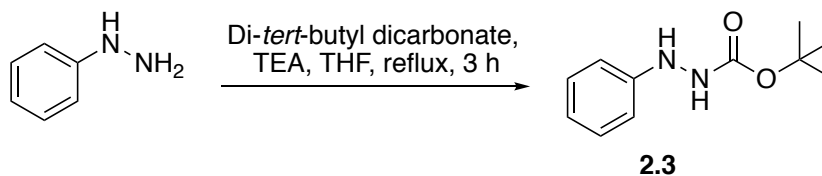
2.4.4 Synthesis of triazinyl hydrazine hydrochloride salt, **1**



Scheme 2.8. Deprotection of trisubstituted triazine intermediate **2.2** to make **1**.

Intermediate **2.2** (4.3 g, 10.3 mmol) was dissolved in a mixture of 6 ml methanol and 3 ml 4M HCl in a round bottom flask equipped with stirring bar. Resulting solution was left to stir at room temperature for 12 hours. The excess solvent was removed under vacuum and dried to recover **1** (3.6 g, 99%) as white solid. ¹H NMR (400 MHz, CD₃OD) δ 5.07 (2H, bs), 3.71-3.61 (16H, m). ¹³C NMR (400 MHz, CD₃OD) δ 163.8, 163.5, 72.1, 68.4, 60.8, 40.9. MS (ESI-TOF) calculated for C₁₁H₂₄N₇O₄: 317.18; found 318.19.

2.4.5 Synthesis of *N*-Phenyl-*tert*-butylcarbazate, **2.3**

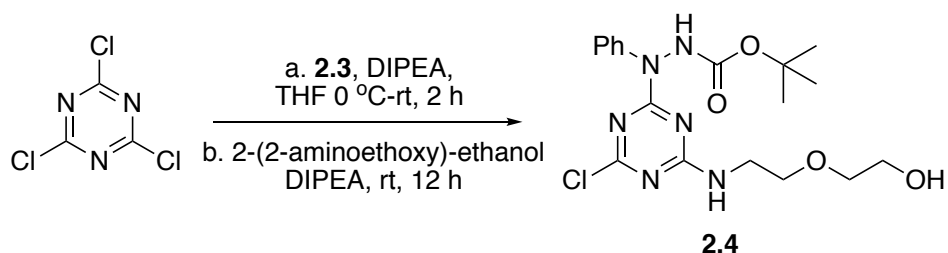


Scheme 2.9. Protection of phenyl hydrazine, synthesis of **2.3**.

Phenylhydrazine (5.0 g, 46.2 mmol) was dissolved in 30 ml THF in a small flask equipped with stirring bar. Triethylamine (5.15 g, 51.0 mmol) and di-*tert*-butyl dicarbonate (11.13 g, 51.1 mmol) were added to the flask. Produced solution was refluxed for 3 hours. Excess solvent was

removed and residue was dissolved in 20 ml DCM. Reaction mixture was extracted with 10 ml H₂O and collected in 20 ml DCM (x2). Organic layer was dried over Na₂SO₄ and concentrated under vacuum. The crude product was then purified by column chromatography using 60:1 DCM:Methanol to afford **2.3** (5.58 g, 58%). ¹H NMR (400 MHz, CDCl₃) δ 7.27-7.23 (2H, dd), 6.92-6.89 (1H, dd), 6.84-6.82 (2H, dd), 6.51 (1H, bs), 5.83 (1H, bs), 1.49 (9H, s). ¹³C NMR (400 MHz, CDCl₃) δ 156.3, 148.4, 129.2, 120.8, 113.0, 81.2, 28.3. MS (ESI-TOF) calculated for C₁₁H₁₆N₂O₂: 208.12; found 209.16.

2.4.6 Synthesis of intermediate **2.4**

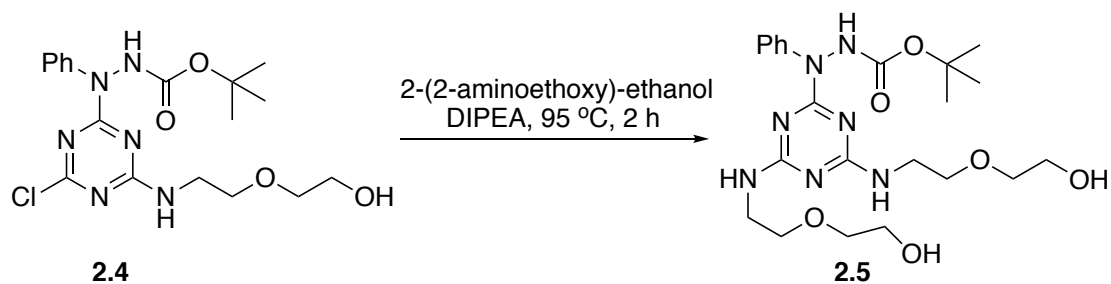


Scheme 2.10. Preparation of monochlorotriazine intermediate **2.4**.

Cyanuric chloride (4.30 g, 23.4 mmol) was dissolved in 60 ml THF in a flask equipped with stirring bar. Intermediate **2.3** (4.8 g, 23.1 mmol) and DIPEA (4.5 g, 34.5 mmol) were dissolved in 20 ml THF and added dropwise to flask at 0 °C. Produced solution was brought to the room temperature slowly and stirred for 2 hours. The reaction progress was monitored using TLC. 2-(2-aminoethoxy)-ethanol (2.7 g, 25.7 mmol) was then added to the reaction mixture and stirred at room temperature for 12 hours. Excess solvent was removed under vacuum and residue was dissolved in 25 ml DCM. The solution was extracted with 20 ml H₂O and product was recovered in 25 ml DCM (x2). Organic layer was dried over Na₂SO₄ and concentrated under vacuum. Crude product was then purified by column chromatography using DCM:Methanol (20:1) to afford **2.4** (5.7 g, 58%) as white solid. ¹H NMR (400 MHz, CDCl₃) δ 7.47-7.42 (2H, dd), 7.36-7.28 (2H, dd),

7.23-7.19 (1H, dd), 6.91 (1H, bs), 3.68-3.51 (8H, m), 1.48 (9H, s). ^{13}C NMR (400 MHz, CDCl_3) δ 170.7, 169.6, 165.7, 155.9, 141.8, 128.5, 126.5, 125.3, 81.9, 72.3, 69.1, 61.4, 40.5, 28.2. MS (ESI-TOF) calculated for $\text{C}_{18}\text{H}_{25}\text{ClN}_6\text{O}_4$: 424.16; found 425.25.

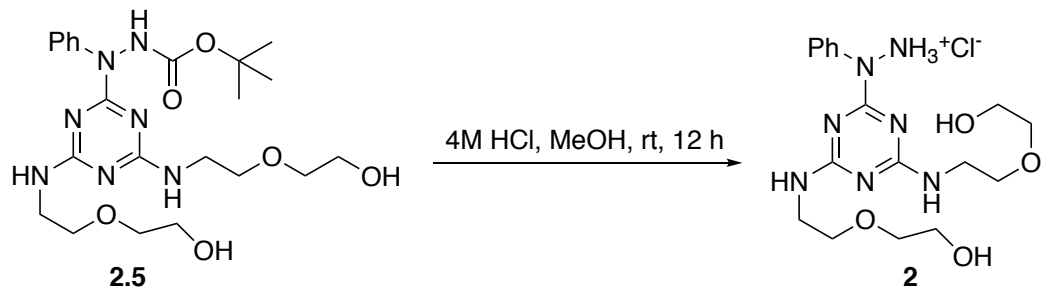
2.4.7 Synthesis of intermediate 2.5



Scheme 2.11. Preparation of trisubstituted triazine intermediate 2.5.

Intermediate **2.4** (1.5 g, 3.55 mmol) was dissolved in 6 ml dioxane in a microwave test tube equipped with stirring bar. 2-(2-aminoethoxy)-ethanol (0.700 g, 6.7 mmol) and Cs_2CO_3 (2.0 g, 6.1 mmol) were added to the test tube. Produced mixture was stirred at 95 °C in the microwave for one hour. Solution was filtered and dioxane was removed under reduced pressure. The residue was dissolved in 20 ml DCM, washed with 10 ml water, dried over Na_2SO_4 , and concentrated under reduced pressure. Crude product was purified by column chromatography using DCM:Methanol (15:1) to afford **2.5** (1.3 g, 69%) as white solid. ^1H NMR (400 MHz, CDCl_3) δ 7.53 (2H, s), 7.33 (2H, dd), 7.17 (1H, dd), 3.71-3.52 (16H, m), 1.50 (9H, s). ^{13}C NMR (400 MHz, CDCl_3) δ 165.9, 156.3, 142.6, 128.0, 125.2, 81.1, 72.6, 70.1, 61.3, 40.3, 28.3. MS (ESI-TOF) calculated for $\text{C}_{21}\text{H}_{28}\text{N}_7\text{O}_5$: 493.26; found 494.22.

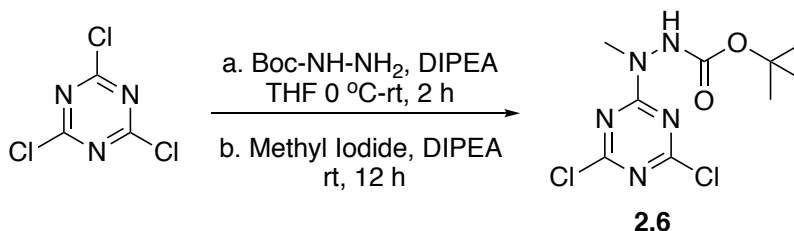
2.4.8 Synthesis of triazinyl hydrazine 2



Scheme 2.12. Deprotection of trisubstituted triazine intermediate **2.5** to form **2**.

Intermediate **2.5** (1.00 g, 2.03 mmol) was dissolved in a mixture of 4 ml methanol and 2 ml 4 M HCl in a small flask. Reaction mixture was left to stir overnight at room temperature. The excess HCl was removed under vacuum and dried under pressure to recover 0.86 g (99%) of compound **2**. ^1H NMR (400 MHz, CDCl_3) δ 7.38-7.64 (5H, m), 3.56-3.63 (16H, m). ^{13}C NMR (400 MHz, CDCl_3) δ 129.7, 127.3, 125.9, 71.5, 68.6, 60.4, 40.3. MS (ESI-TOF) calculated for $\text{C}_{21}\text{H}_{28}\text{N}_7\text{O}_5$: 393.21; found 394.28.

2.4.9 Synthesis of intermediate 2.6

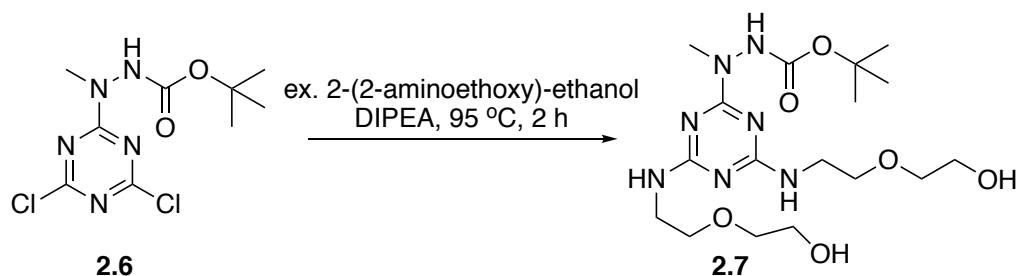


Scheme 2.13. Synthesis of dichlorotriazine intermediate **2.6**.

Cyanuric chloride (10.06 g, 55 mmol) was dissolved in 100 ml THF in a flask equipped with stirring bar. *Tert*-butyl carbazate (7.2 g, 55 mmol) and DIPEA (7.0 g, 55 mmol) were dissolved in 30 ml THF and added dropwise to flask at 0 °C. The reaction mixture was warmed to room temperature slowly and stirred for two hours. Methyl iodide (9.91 g, 70.2 mmol) and DIPEA

(7.0 g, 53 mmol) were added to the solution. Produced solution was left to stir at room temperature for 12 hours. Excess solvent was removed under vacuum, residue was dissolved in 30 ml DCM (x2), washed with 10 ml water, dried over Na₂SO₄, and concentrated under vacuum. The crude product was further purified by column chromatography using 30:1 DCM:MeOH to recover **2.6** (3.0 g, 19%) as white solid. ¹H NMR (400 MHz, CDCl₃) δ 6.78 (1H, s), 3.48 (3H, s), 1.52 (9H, s). ¹³C NMR (400 MHz, CDCl₃) δ 171.0, 170.6, 167.2, 154.6, 82.8, 38.8, 28.1. MS (ESI-TOF) calculated for C₉H₁₃Cl₂N₅O₂: 293.04; found 294.04.

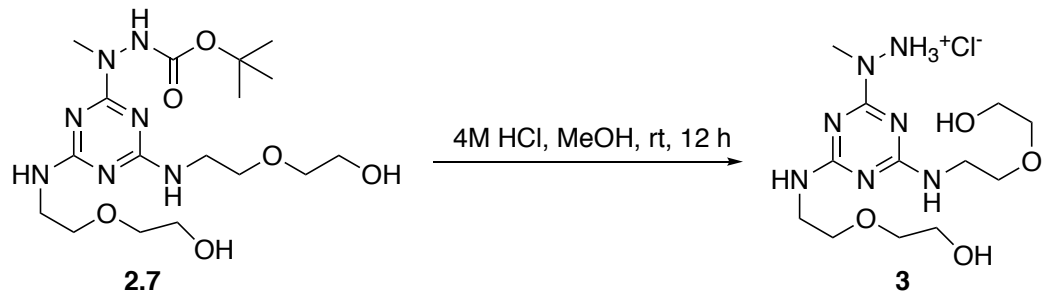
2.4.10 Synthesis of intermediate 2.7



Scheme 2.14. Synthesis of trisubstituted triazine intermediate **2.7**.

Intermediate **2.6** (0.89 g, 3.2 mmol) was dissolved in 5 ml dioxane in a microwave test tube equipped with stirring bar. To this, 2-(2-aminoethoxy)ethanol (0.67 g, 6.4 mmol) and Cs₂CO₃ (2.1 g, 6.2 mmol) were added. The reaction mixture was stirred at 95 °C in the microwave for one hour. Solution was filtered to remove traces of Cs₂CO₃. Solvent was removed under vacuum and residue was dissolved in 20 ml DCM. The solution was washed with 10 ml brine, dried over Na₂SO₄, and concentrated under vacuum. The crude product was purified by column chromatography using 25:1 DCM:MeOH to recover **2.7** (1.21 g, 88%) as white solid. ¹H NMR (400 MHz, CDCl₃) δ 3.72-3.58 (16H, m), 3.31 (3H, s), 1.47 (9H, s). ¹³C NMR (400 MHz, CDCl₃) δ 166.9, 80.9, 72.7, 70.2, 61.4, 40.4, 37.6, 28.3. MS (ESI-TOF) calculated for C₁₇H₃₃N₇O₆: 431.25; found 432.26

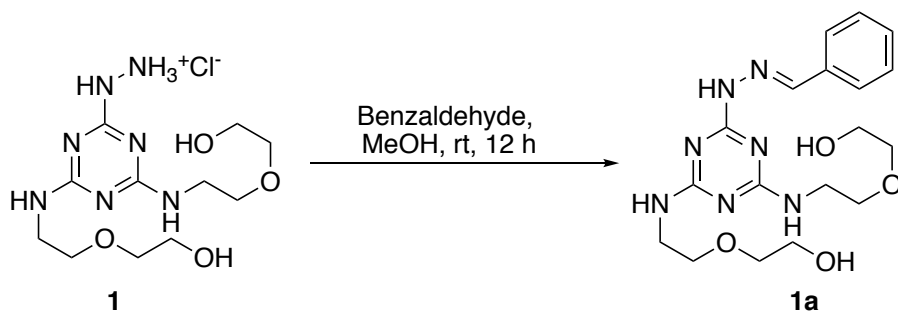
2.4.11 Synthesis of triazinyl hydrazine 3



Scheme 2.15. Deprotection of trisubstituted triazine intermediate **2.7** to make **3**.

Intermediate **2.7** (1.1 g, 2.6 mmol) was dissolved in 5 ml DCM in a small flask and 3 ml of concentrated HCl was added. Produced solution was left to stir at room temperature for 12 hours. Excess solvent was removed under reduced pressure to afford **3** (0.93 g, 97%) as white solid. ^1H NMR (400 MHz, D_2O) δ 3.65-3.56 (16H, m), 3.23 (3H, s). ^{13}C NMR (400 MHz, D_2O) δ 162.6, 155.5, 71.6, 68.3, 60.4, 40.4, 35.1. MS (ESI-TOF) calculated for $\text{C}_{12}\text{H}_{25}\text{N}_7\text{O}_4$: 331.21; found 332.20.

2.4.12 Synthesis of 1a

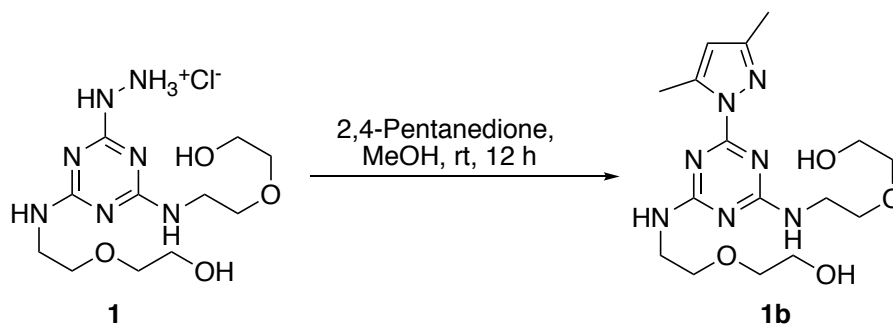


Scheme 2.16. Preparation of hydrazone **1a**.

In a small flask, 140 mg (0.40 mmol) of **1** and 110 mg (1.0 mmol) of benzaldehyde were dissolved in 4 ml of anhydrous along with 2 mg of molecular sieves were added. Produced solution was left to stir at room temperature for 12 hours. The reaction solution was filtered, methanol was

removed under vacuum and crude product was purified by column chromatography using DCM:MeOH (25:1) to recover **1a** (132 mg, 82%) as white solid. ^1H NMR (400 MHz, CDCl_3) δ 7.85 (1H, s), 7.71 (2H, dd), 7.36 (3H, m), 3.77-3.64 (16H, m). ^{13}C NMR (400 MHz, CDCl_3) δ 164.7, 145.9, 134.0, 129.9, 128.4, 127.2, 72.1, 69.0, 60.9, 40.5. MS (ESI-TOF) calculated for $\text{C}_{18}\text{H}_{27}\text{N}_7\text{O}_4$: 405.21; found 406.28

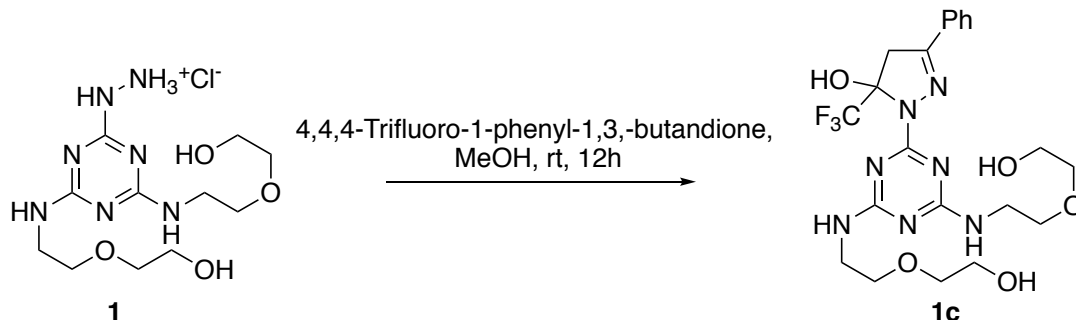
2.4.13 Synthesis of **1b**



Scheme 2.17. Preparation of hydrazone **1b**.

Triazinyl hydrazine **2** (20 mg, 0.057 mmol) and 2,4-pentandione (9mg, 0.089 mmol) were dissolved in 2 ml of anhydrous methanol in a small flask equipped with stirring bar. To the flask, 1 mg of molecular sieves were added. Produced solution was left to stir at room temperature for 12 hours. The reaction solution was filtered, methanol was removed under vacuum, and crude product was the purified by column chromatography using DCM:MeOH (25:1) to afford **1b** (12.8 mg, 59%) as white solid. ^1H NMR (400 MHz, CDCl_3) δ 6.07 (2H, bs), 5.99 (1H, s), 3.76-3.61 (16H, m), 2.63 (3H, s), 2.29 (3H, s). ^{13}C NMR (400 MHz, CDCl_3) δ 166.4, 151.4, 143.6, 110.7, 72.6, 69.6, 61.7, 40.7, 16.0, 13.8. MS (ESI-TOF) calculated for $\text{C}_{16}\text{H}_{27}\text{N}_7\text{O}_4$: 381.21; found 382.23

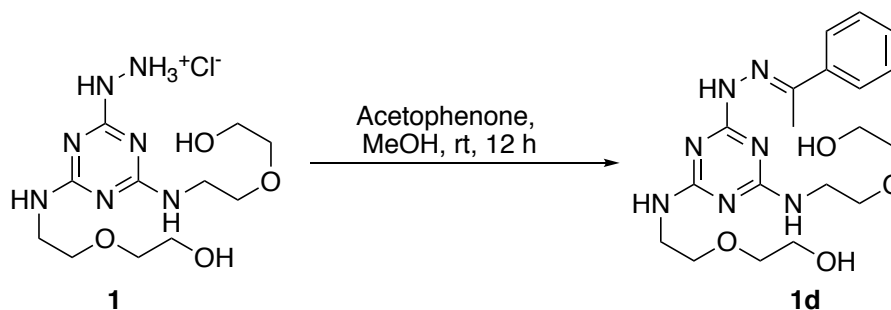
2.4.14 Synthesis of 1c



Scheme 2.18. Preparation of hydrazone **1c**.

Triazinyl hydrazine **1** (100 mg, 0.28 mmol) and 4,4,4-trifluoro-1-phenyl-1,3-butanedione (120 mg, 0.56 mmol) was dissolved in 3 ml of anhydrous methanol in a small flask equipped with stirring bar. To this, 3 mg of molecular sieves were added. Produced solution was stirred at 40 °C for 12 hours. Reaction mixture was filtered, methanol was removed under vacuum and the crude product was further purified by column chromatography using DCM:MeOH (25:1) to recover **1c** (84 mg, 58%) as white solid. ¹H NMR (400 MHz, CDCl₃) δ 8.93 (1H, s), 7.99 (1H, s), 7.79 (1H, dd), 7.53-7.37 (4H, m), 3.82-3.64 (16H, m). ¹³C NMR (400 MHz, CDCl₃) δ 164.7, 145.9, 134.0, 129.9, 128.1, 127.2, 72.1, 69.0, 60.9, 53.5, 40.5. MS (ESI-TOF) calculated for C₂₁H₂₈ F₃N₇O₅: 515.21; found 516.22

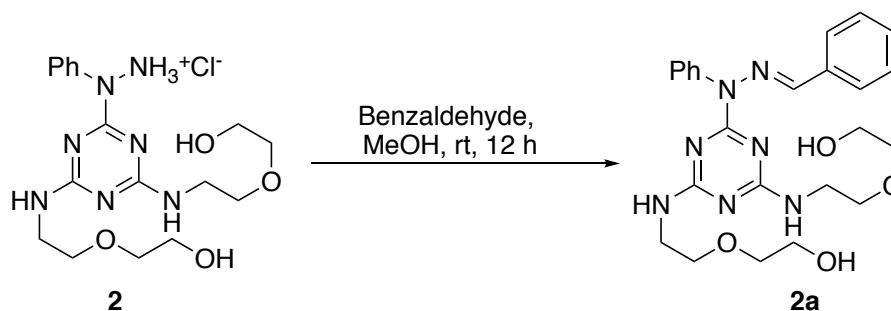
2.4.15 Synthesis of 1d



Scheme 2.19. Preparation of hydrazone **1d**.

Triazinyl hydrazine **1** (150 mg, 0.42 mmol) and acetophenone (101 mg, 0.84 mmol) were dissolved in 4 ml anhydrous methanol in a small flask equipped with stirring bar. To this, 4 mg of dry molecular sieves were added. Resulting reaction mixture was left to stir at room temperature for 12 hours. Solution was filtered, methanol was removed under vacuum, and crude product was purified by aluminum column chromatography using DCM:MeOH (9:1) to afford 52 mg (30%) of **1d** as white solid. ^1H NMR (400 MHz, CDCl_3) δ 7.80 (2H, dd), 7.36-7.38 (3H, m), 3.62-3.75 (16H, m), 2.27 (3H, s). ^{13}C NMR (400 MHz, CDCl_3) δ 165.9, 138.9, 129.6, 128.3, 126.4, 72.7, 70.1, 61.5, 40.5, 13.0. MS (ESI-TOF) calculated for $\text{C}_{19}\text{H}_{29}\text{N}_4\text{O}_7$: 419.23; found 420.32.

2.4.16 Synthesis of **2a**

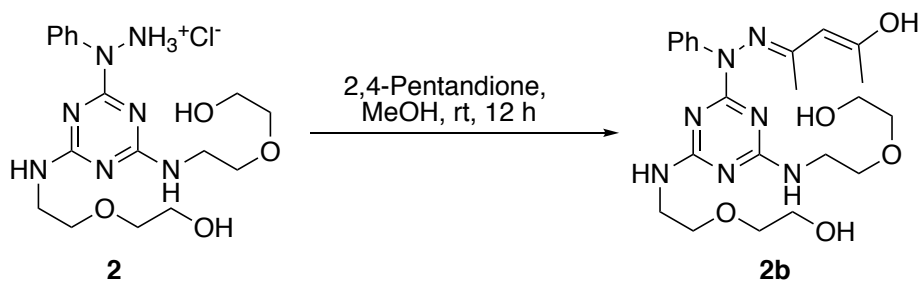


Scheme 2.20. Preparation of hydrazone **2a**.

Triazinyl hydrazine **2** (75 mg, 0.17 mmol) and benzaldehyde (55 mg, 0.52 mmol) were dissolved in 2 ml of anhydrous methanol in a small flask equipped with stirring bar. To this, 2 mg of dry molecular sieves were added and reaction mixture was left to stir at room temperature for 12 hours. The solvent was removed under vacuum and crude product was purified by column chromatography using DCM:Methanol (10:1) to afford **2a** (72 mg, 85%) as white solid. ^1H NMR (400 MHz, CDCl_3) δ 7.52 (2H, dd), 7.47 (2H, s), 7.45 (1H, s), 7.37-7.31 (4H, m), 7.25 (2H, dd), 3.70-3.56 (16H, m). ^{13}C NMR (400 MHz, CDCl_3) δ 165.9, 142.3, 138.7, 134.6, 129.8, 129.4,

128.5, 127.4, 72.4, 69.8, 61.6, 40.5. MS (ESI-TOF) calculated for C₂₄H₃₁N₇O₄: 481.24; found 482.34

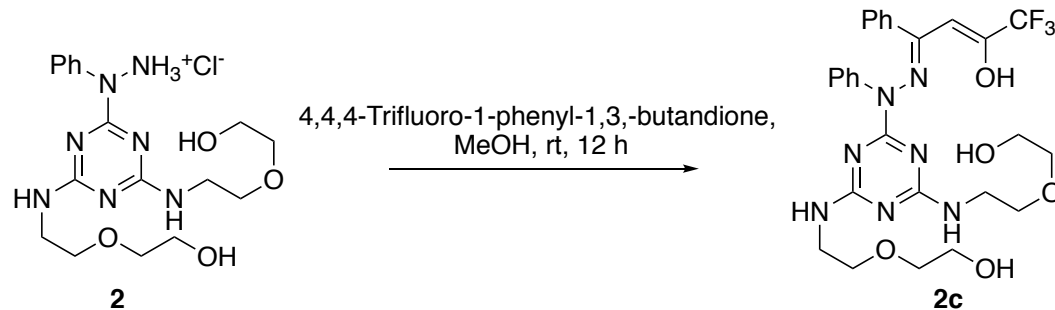
2.4.17 Synthesis of **2b**



Scheme 2.21. Preparation of hydrazone **2b**.

Triazinyl hydrazine **2** (75 mg, 0.17 mmol) and 2,4-Pentandione (37.5 mg, 0.38 mmol) were dissolved in 2 ml of anhydrous methanol in a small flask. After adding 2 mg of molecular sieves, reaction mixture was left to stir at room temperature for 12 hours. Solution was filtered, excess methanol was removed under reduced pressure, and crude product was purified by column chromatography using DCM:Methanol (10:1) to afford **2b** (30 mg, 36%) as white solid. ¹H NMR (400 MHz, CDCl₃) δ 11.93 (1H, s), 7.56 (2H, s), 7.34-7.28 (2H, dd), 7.17-7.13 (1H, dd), 6.68 (1H, bs), 5.16 (1H, s), 3.70-3.47 (16H, m), 2.11 (3H, s), 1.86 (3H, s). ¹³C NMR (400 MHz, CDCl₃) δ 196.9, 166.2, 165.9, 142.6, 128.2, 124.9, 123.6, 96.7, 72.8, 70.1, 61.4, 40.6, 29.2, 18.2. MS (ESI-TOF) calculated for C₂₂H₃₃N₇O₅: 474.25; found 476.34

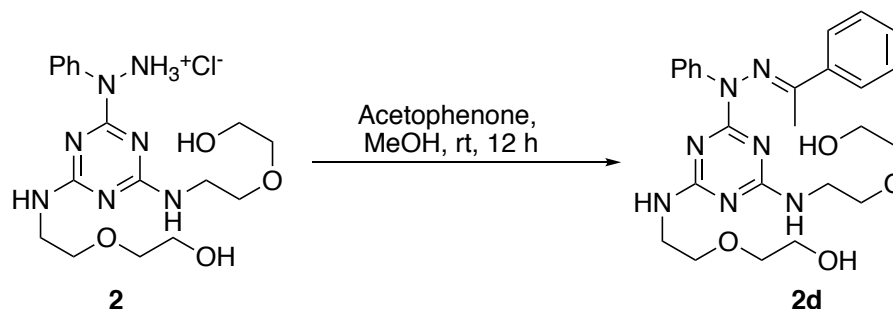
2.4.18 Synthesis of 2c



Scheme 2.22. Preparation of hydrazone **2c**.

Triazinyl hydrazine **2** (100 mg, 0.23 mmol) and 1,1,1-Trifluoro-4-phenyl-1,3-butanedione (150 mg, 0.70 mmol) were dissolved in 2 ml of anhydrous methanol in a small flask. After adding 2 mg of molecular sieves, resulting solution was left to stir at room temperature for 12 hours. The solvent was removed under reduced pressure and crude product was purified by column chromatography using DCM:Methanol (10:1) to afford **2c** (60 mg, 50%) as white solid. ^1H NMR (400 MHz, CDCl_3) δ 7.27-7.23 (2H, dd), 6.92-6.89 (1H, dd), 6.84-6.82 (2H, dd), 6.51 (1H, bs), 5.83 (1H, bs), 1.49 (9H, s). ^{13}C NMR (400 MHz, CDCl_3) δ 156.3, 148.4, 129.2, 120.8, 113.0, 81.2, 28.3. MS (ESI-TOF) calculated for $\text{C}_{21}\text{H}_{28}\text{N}_7\text{O}_5$: 515.21; found 516.22

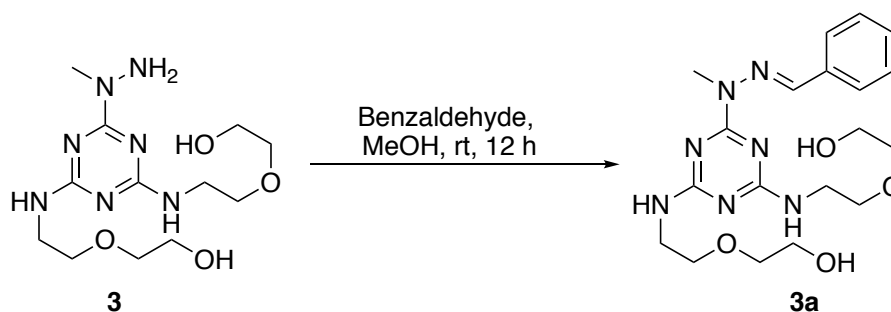
2.4.19 Synthesis of 2d



Scheme 2.23. Preparation of hydrazone **2d**.

Triazinyl hydrazine **2** (100 mg, 0.23 mmol) and acetophenone (61 mg, 0.51 mmol) were dissolved in 3 ml of anhydrous methanol. To this, 3 mg of molecular sieves were added and Produced solution was left to stir at room temperature for 12 hours. The solvent was removed under reduced pressure and crude product was purified by column chromatography using DCM:Methanol (10:1) to afford **2d** (29 mg, 25%) as white solid. ¹H NMR (400 MHz, CDCl₃) δ 7.91 (2H, dd), 7.48-7.44 (5H, m), 7.37-7.28 (2H, m), 7.19 (1H, dd), 3.68-3.54 (21H, m), 2.27 (3H, s). MS (ESI-TOF) calculated for C₂₁H₂₈N₇O₅: 495.42; found 496.55.

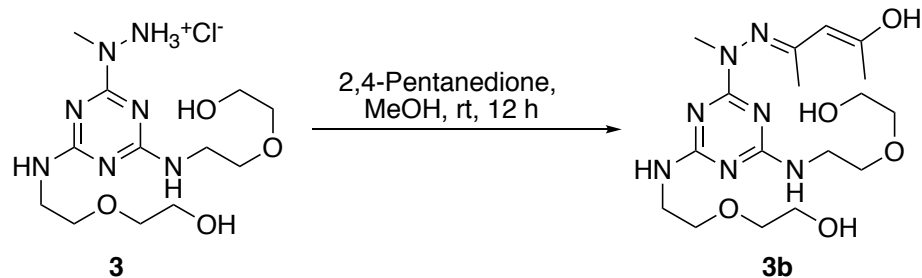
2.4.20 Synthesis of **3a**



Scheme 2.24. Preparation of hydrazone **3a**.

Triazinyl hydrazine **3** (68 mg, 0.18 mmol) and benzaldehyde (39 mg, 0.36 mmol) were dissolved in 2 ml anhydrous methanol in a small flask. After adding 2 mg of dry molecular sieves, produced solution was left to stir at room temperature for 12 hours. Methanol was removed under reduced pressure and crude product was purified by column chromatography using DCM:MeOH (25:1) to recover **3a** (63 mg, 83%) as white solid. ¹H NMR (400 MHz, CDCl₃) δ 8.80-7.78 (3H, m), 7.41-7.34 (3H, m), 3.77-3.62 (19H, m). ¹³C NMR (400 MHz, CDCl₃) δ 166.2, 165.0, 139.0, 135.5, 129.1, 128.6, 127.2, 72.5, 70.0, 61.6, 40.6, 30.3. MS (ESI-TOF) calculated for C₁₉H₂₉N₇O₄: 419.23; found: 420.29.

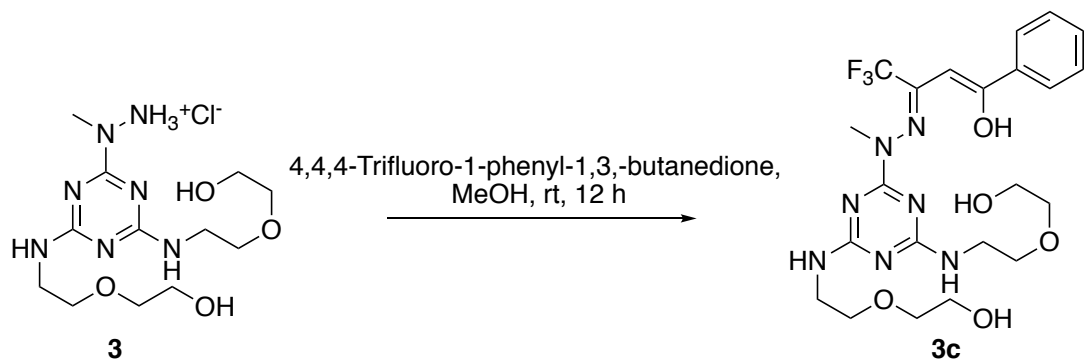
2.4.21 Synthesis of 3b



Scheme 2.25. Preparation of hydrazone **3b**.

Compound **3** (30 mg, 0.08 mmol) and 2,4-pentanedione (18 mg, 0.18 mmol) were dissolved in 2 ml anhydrous methanol in a small flask. After adding 1 mg of molecular sieves, the reaction mixture was left to stir at room temperature for 12 hours. Methanol was removed under reduced pressure and crude product was purified by alumina column chromatography using DCM:MeOH (25:1) to recover **3b** (21 mg, 62%) as white solid. ^1H NMR (400 MHz, CDCl_3) δ 11.46 (1H, s), 5.11 (1H, s), 3.73-3.54 (16H, m), 3.33 (3H, s), 2.09 (3H, s), 1.87 (3H, s). ^{13}C NMR (400 MHz, CDCl_3) δ 196.6, 167.3, 165.9, 165.1, 95.9, 72.7, 70.1, 61.5, 40.5, 38.3, 29.1, 17.8. MS (ESI-TOF) calculated for $\text{C}_{17}\text{H}_{31}\text{N}_7\text{O}_5$: 413.24; found: 414.33

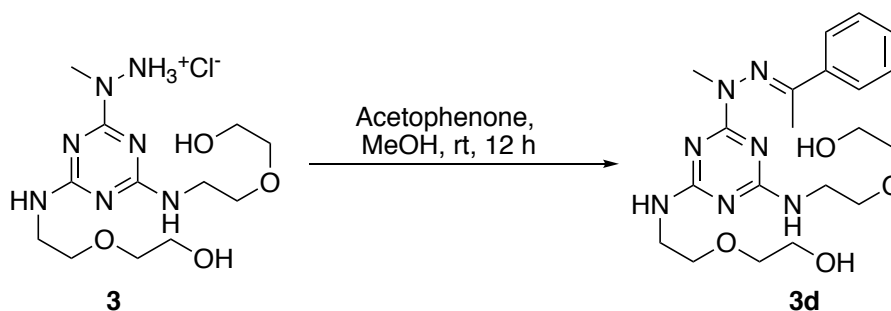
2.4.22 Synthesis of 3c



Scheme 2.26. Preparation of hydrazone **3c**.

Compound **3** (30 mg, 0.08 mmol) and 4,4,4-trifluoro-1-phenyl-1,3-butanedione (39 mg, 0.18 mmol) were dissolved in 3 ml anhydrous methanol. After adding 1 mg of dry molecular sieves, produced solution was left to stir at overnight. Solution was filtered, excess solvent was removed under vacuum, and crude product was purified by column chromatography using DCM:MeOH (25:1) to recover **3c** (23 mg, 62%) as white solid. ¹H NMR (400 MHz, CDCl₃) δ 11.82 (1H, s), 7.43 (5H, s), 5.69 (1H, s), 3.72-3.37 (1H, m), 3.16 (3H, s). ¹³C NMR (400 MHz, CDCl₃) δ 191.2, 167.3, 166.0, 165.6, 133.1, 130.7, 128.5, 127.6, 112.6-121.6 (q), 90.2, 72.6, 69.8, 61.4, 40.52, 38.4. MS (ESI-TOF) calculated for C₂₂H₃₀F₃N₇O₅: 529.23; found: 530.23

2.4.23 Synthesis of **3d**



Scheme 2.27. Preparation of hydrazone **3d**.

Compound **3** (125 mg, 0.34 mmol) and acetophenone (81 mg, 0.68 mmol) were dissolved in 3 ml anhydrous methanol in a small round bottom flask equipped with stirring bar. After adding 3 mg of dry molecular sieves, produced solution was left to stir at room temperature for 12 hours. Excess solvent was removed under reduced pressure and crude product was purified by alumina column chromatography using DCM:MeOH (15:1) to afford **3d** (42 mg, 29%) as white solid. ¹H NMR (400 MHz, CDCl₃) δ 7.87-7.89 (2H, dd), 7.43-7.45 (3H, m), 3.56-3.69 (16H, m), 3.41 (3H, s), 2.26 (3H, s). ¹³C NMR (400 MHz, CDCl₃) δ 172.0, 164.9, 164.4, 137.7, 133.1, 130.4, 128.4,

127.1, 72.7, 70.1, 61.5, 40.4, 37.3, 17.5. MS (ESI-TOF) calculated for $C_{22}H_{30}F_3N_7O_5$: 433.23;
found: 434.27

Chapter 3: A hydrogen bond and strong electron withdrawing group help in the formation of stable cyclic hemiaminals

3.1 Introduction and history of hemiaminal

The accepted mechanism of the addition of an amine nucleophile to a carbonyl group proceeds through the formation of a short-lived tetrahedral intermediate called a hemiaminal or carbinolamine. Some hemiaminals have been obtained, isolated, and/or characterized using very sophisticated methods, i.e. polarography,¹³⁶ FTIR liquid cell spectroscopy,¹³⁷ or low temperature NMR spectroscopy.¹³⁸

The ¹H NMR measurements taken within 2 minutes of mixing a cavitand made of anthracene dialdehyde and various amines shows the short lived intermediates.¹³⁹⁻¹⁴⁰ The hydroxyl peak of hemiaminal observed in the ¹H-NMR disappeared gradually as dehydration of hemiaminal results in the formation of imine. In addition, density functional (DFT) calculations confirmed that the stability of the hemiaminals in the cavitand is in part due to the formation of H-bonds.¹⁴¹

Kawamichi et al. captured hemiaminals inside the pore of a coordination network during post-synthetic modifications of porous metal-organic frameworks (MOFs).¹⁴² A crystal structure of a MOF with a short-lived hemiaminal trapped inside was taken at low temperature, 215 K. The hemiaminal converted to the imine as the temperature was increased to 270 K.¹⁴³ Morris et al. used solid-state ¹⁵N NMR measurements and showed that a zirconium containing metal-organic framework with amino-functionalized links is composed of a mixture of hemiaminals, the thermodynamic product (aziridine), and the protonated amine salt with an approximate ratio of 5:2:3, respectively.¹⁴³

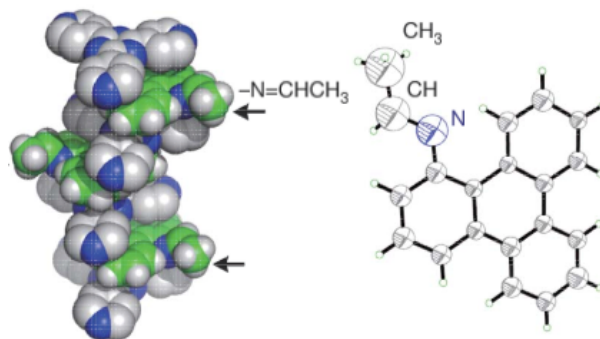
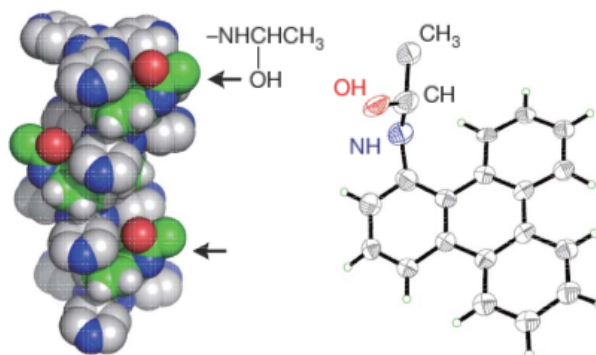
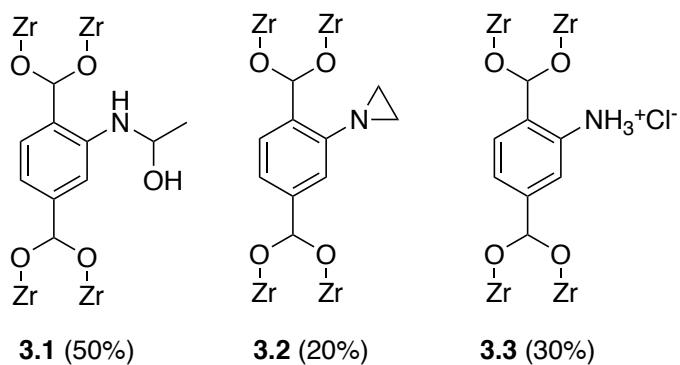
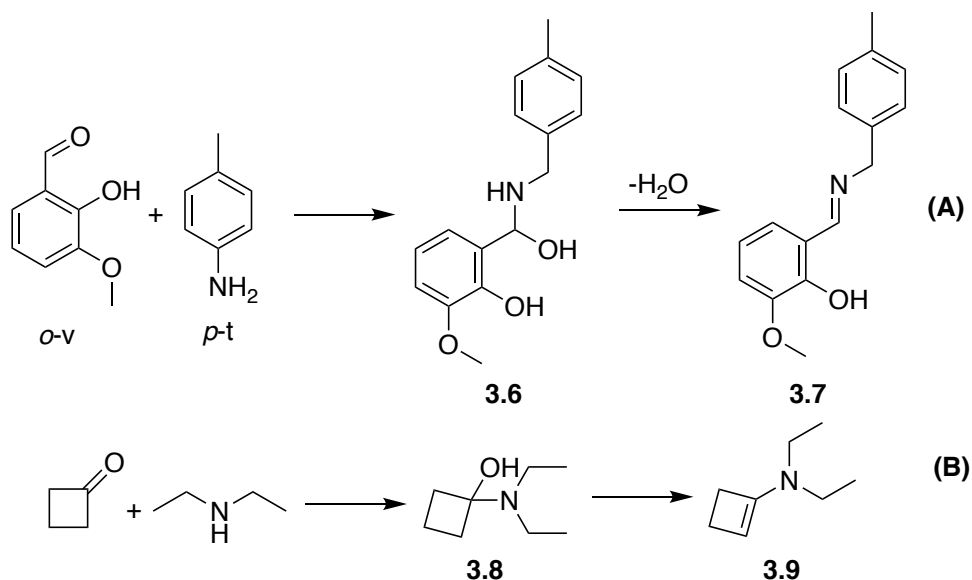


Figure 3.1. A metal-organic framework with amino-functionalized links. 3.1) hemiaminal product. 3.2) aziridine product. 3.3) protonated amine salt. 3.4) X-ray crystal structure of hemiaminal intermediate at 215K. 3.5) X-ray crystal structure of imine. ^{Adapted from ref. 143}

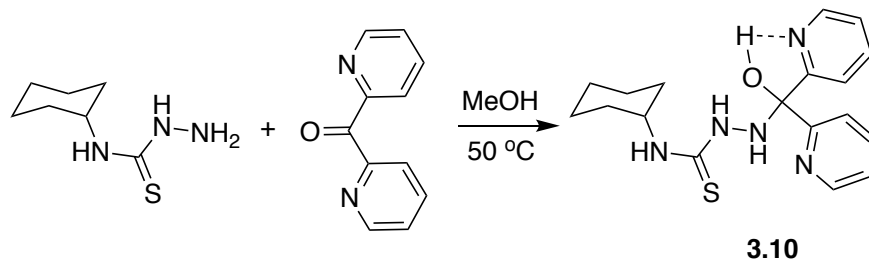
In addition, Dolotko studied the mechanically-induced, solvent-free reaction between *o*-vanillin and *p*-toluidine (Scheme 3.1) that formed a liquid eutectic upon grinding while below 263 K.¹⁴⁴ The ¹H NMR of **3.6** taken at low temperature shows the presence of hydroxyl group of *o*-vanillin at 10.0 ppm, the amine of *p*-toluidine at 8.5 ppm, the C-H of final product imine at 11.0

ppm, and the hydroxyl of hemiaminal at 13.8 ppm. The hydroxyl peak of hemiaminal at 13.8 ppm appeared between 50-64 seconds from the insertion and indicated their short life.¹⁴⁴ Furthermore, Yufit and Howard obtained a crystal structure of the hemiaminal **3.8** formed from the reaction between diethylamine and cyclobutanone at 210 K.¹⁴⁵ At room temperature, no hemiaminal intermediate was observed. This observation suggests that dehydration is slower than the hemiaminal rate formation.¹⁴⁵



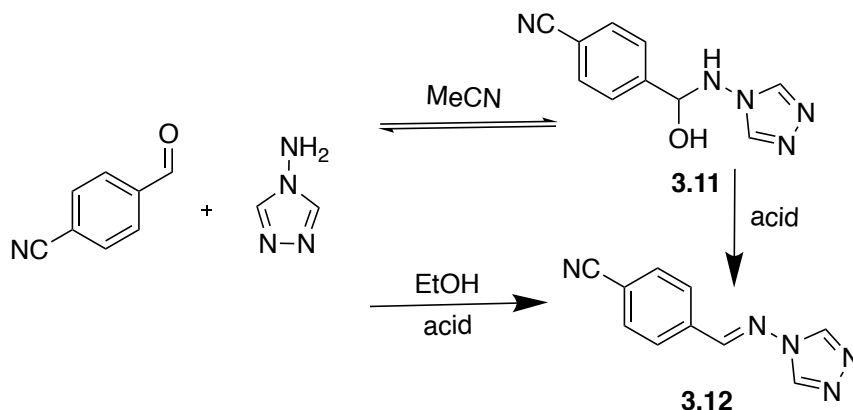
Scheme 3.1. Solvent-free reactions to create hemiaminals A) *o*-Vanillin and *p*-toluidine forms hemiaminal (I) formed only at low temperature. B) Reaction of cyclobutanone and diethylamine makes hemiaminal (III) at low temperature.

Stable hemiaminal obtained at relatively high temperature and characterized by $^1\text{H-NMR}$ spectroscopy and x-ray crystallography, was the result of the reaction between the 4-cyclohexyl-3-thiosemicarbazide and di-2-pyridyl ketone.¹⁴⁶ In this case, the crystal structure and $^1\text{H-NMR}$ of hemiaminal **3.10** confirmed the presence of intramolecular H-bond between the OH of the hemiaminal and the nitrogen atom of pyridyl ring.¹⁴⁶



Scheme 3.2. First stable hemiaminal obtained at room temperature.

Stable hemiaminals from 4-amino-1,2,4-triazole and nitro-substituted benzaldehyde (Scheme 3.3) were obtained under neutral conditions.¹⁴⁷ The stability of these compounds was attributed to both electron-withdrawing groups on the phenyl ring and the presence of an electron-rich 1,2,4-triazole ring. Seven stable hemiaminals were made and characterized by NMR spectroscopy and crystal structures of five of them were obtained.¹⁴⁷ Consistent with Sayer and Jencks discovery, hemiaminal formation equilibrium constants increase with the presence of electron-withdrawing groups on the benzaldehyde.¹⁴⁸ The presence of intramolecular hydrogen bonds have been observed in some the crystal structures of hemiaminals.

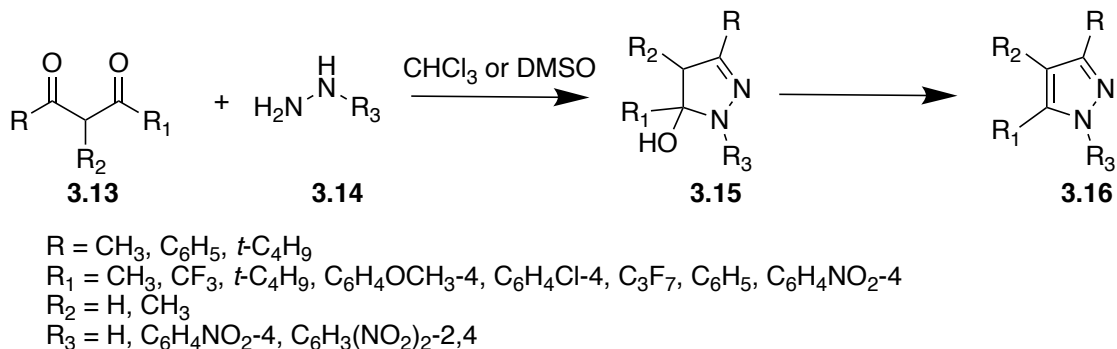


Scheme 3.3. Hemiaminal and Schiff base synthesis from 4-amino-1,2,4-triazole and nitro-substituted benzaldehyde.

Kweicien et. al ruled out the importance of H-bonds.¹⁴⁹ Stable hemiaminals can be obtained when 2-aminopyrimidine and nitrobenzaldehyde derivatives are reacted. The molecular stability of the hemiaminals results from the presence of strong electron withdrawing groups on both the

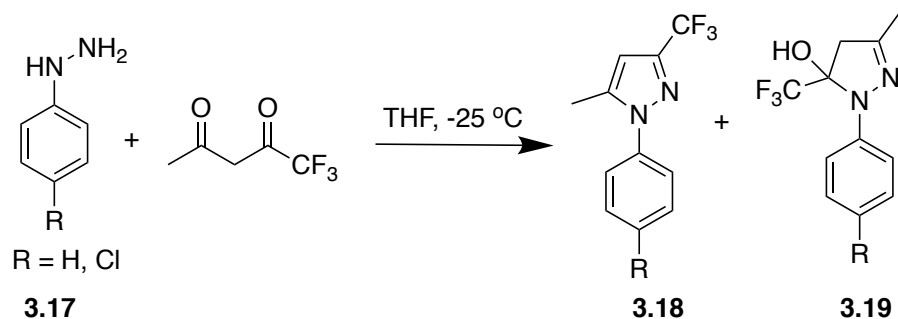
phenyl and pyrimidine ring. According to them, strong electron withdrawing nitro group enhances the stability of hemiaminal and extra intramolecular interactions are not required.

Synthesis of several stable cyclic hemiaminals have been reported. Zelenin et. al isolated the cyclic hemiaminals by reacting hydrazines with dicarbonyl compounds under neutral conditions in CHCl_3 and DMSO as solvents.¹⁵⁰ They suggested the presence of strong electron withdrawing group on the dicarbonyl compound is crucial to make cyclic stable hemiaminal. Zelenin used combination of various groups ranging from electron donating alkyl groups to electron withdrawing groups such as fluoroalkyl and nitrobenzene. They suggested the formation of stable hemiaminal **3.15** required the presence of fluoroalkyl substituent as R_1 . Other R_1 substituents failed to make respective hemiaminal derivatives **3.15** but instead pyrazole derivatives **3.16** were made.



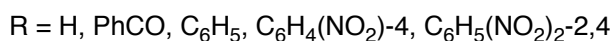
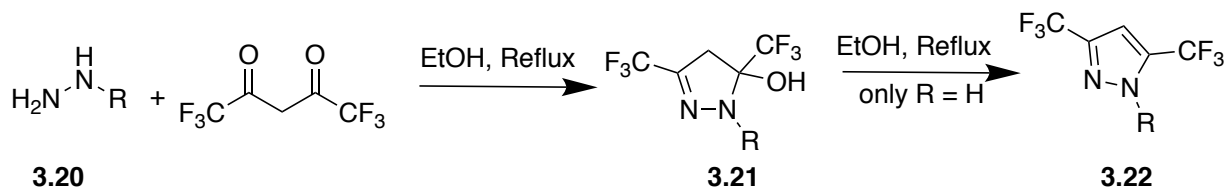
Scheme 3.4. Reaction of various diketones and hydrazines to yield hemiaminals.

Lyga et. al isolated pyrazole **3.18** and hemiaminal **3.19** derivatives when reacting arylhydrazines **3.17** with trifluoromethyl- β -diketones in THF at -25°C in the ratio of 5 to 1, respectively.¹⁵¹



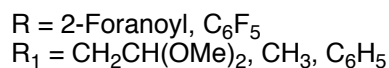
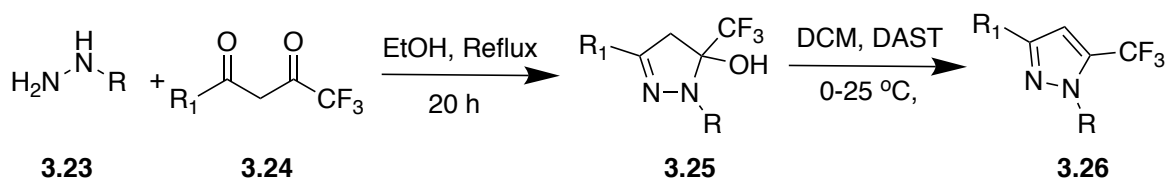
Scheme 3.5. Synthesis of both hemiaminal and pyrazole derivative at low temperature.

Threadgill et. al used various hydrazines, **3.20**, and 1,1,1,5,5,5-hexafluoropentan-2,4-diones in ethanol under refluxing conditions to create hemiaminal derivatives, **3.21**. Along with the presence of electron withdrawing groups, an aromatic group on the hydrazine was crucial to make hemiaminal.¹⁵² The reaction of hydrazine with diketones yielded pyrazole derivative, **3.22**.¹⁵²



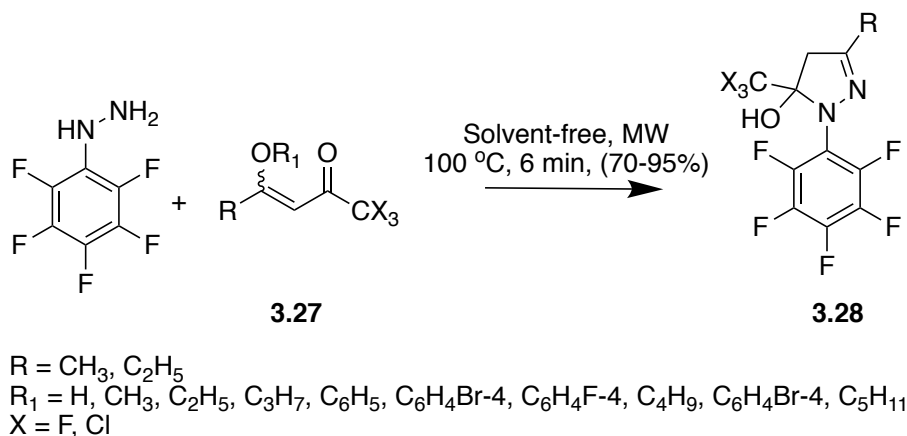
Scheme 3.6. Synthesis of hemiaminal at from various hydrazines at high temperature.

Bonacorso et. al designed an efficient method (Scheme 3.7) with mild conditions to dehydrate the cyclic hemiaminals prepared from **3.23** and **3.24**. They used diethylaminosulfur trifluoride (DAST), a known fluorinating agent, for the dehydration of hemiaminal at low to room temperature.¹⁵³



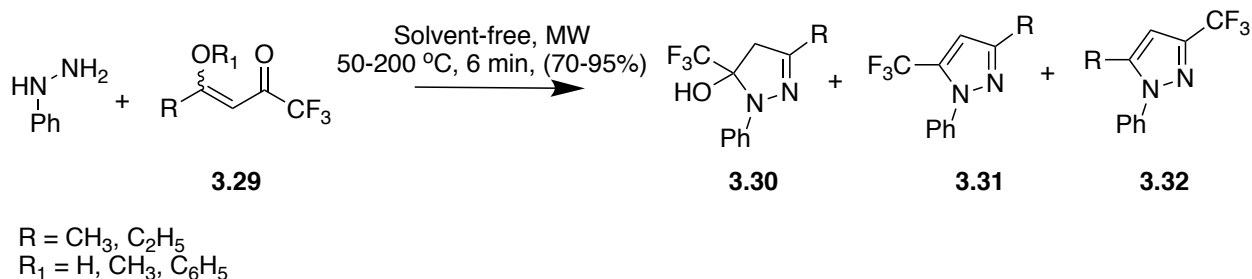
Scheme 3.7. Synthesis of stable hemiaminals and their dehydration by using DAST.

Martins et. al synthesized hemiaminals under microwave irradiation at 100 °C in solvent free conditions (Scheme 3.8). They synthesized various hemiaminals from cyclocondensation reaction of pentafluorophenyl hydrazine and 4-alkoxy-1,1,1-trihalo-3-alken-2-ones.¹⁵⁴



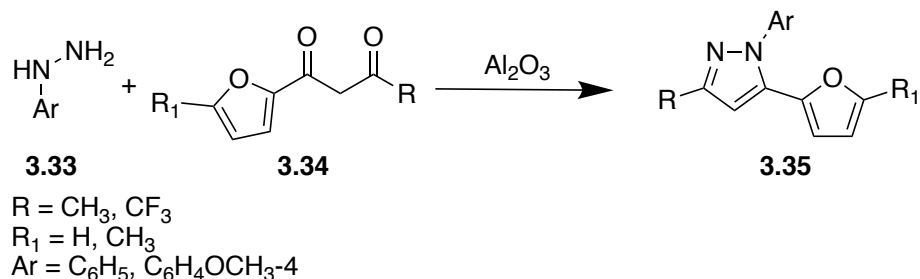
Scheme 3.8. Solvent-free synthesis of hemiaminals by using microwave irradiation.

In addition, the solvent-free reaction of phenyl hydrazine and various 4-alkoxy-1,1,1-trihalo-3-alken-2-ones in microwave at higher temperature resulted in the formation of pyrazole derivatives instead of hemiaminal derivatives (Scheme 3.9). At 50 °C, hemiaminal derivative **3.30** was observed all the cases. At 100 °C a mixture of hemiaminal **3.30** and pyrazole **3.31** derivatives were observed in various ratio with pyrazole derivatives being the major product. At 150 °C and higher, other regioisomer of pyrazole derivative **3.32** was also made along with **3.31**.¹⁵⁵



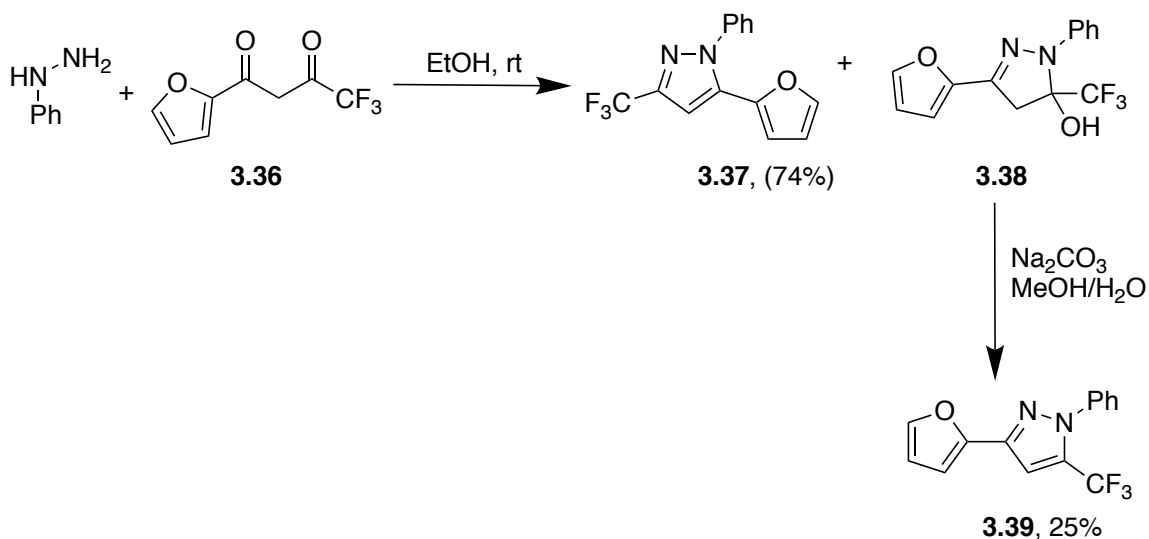
Scheme 3.9. Solvent-free synthesis of hemiaminal and pyrazole derivatives at high temperatures.

Weinheim et. al selectively made one regioisomer of pyrazole in solvent-free conditions by mixing arylhydrazines and 1,3-diketones in the presence of alumina with yields ranging from 63-88%.¹⁵⁶



Scheme 3.10. Selective synthesis of pyrazole regioisomer by using silica.

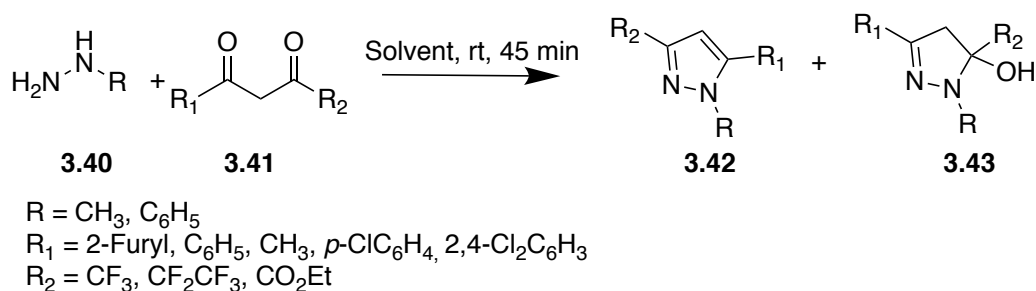
The reaction of **3.36** with phenylhydrazine in ethanol gave pyrazole regioisomers **3.37** and hemiaminal **3.38**. The reaction of **3.38** with sodium carbonate in methanol yielded other regioisomer of pyrazole **3.39**.¹⁵⁶



Scheme 3.11. Synthesis of both regioisomers of pyrazole derivatives.

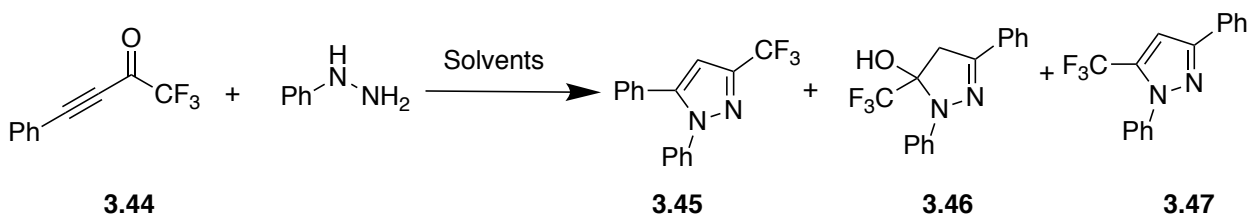
Villanova et. al studied the reaction of *N*-methyl and *N*-phenylhydrazine with 1,3-dicarbonyl derivatives in ethanol, trifluoroethanol (TFE), and 1,1,1,3,3,3-hexafluoro-2-propanol (HFIP). The use of ethanol provided a mixture hemiaminal, **3.43**, and pyrazole, **3.42**, derivatives (Scheme 3.12). However, they reported that the use of TFE and HFIP improved the regioselectivity

of the pyrazole derivatives, **3.42**. When HFIP was used as solvent, the ratio of pyrazole **3.42** to hemiaminal **3.43** derivative varied ranging from 80:1 to be 99:1. The conversion of hemiaminals **3.43** to their respective pyrazole derivatives was accomplished by refluxing them in aqueous HCl solution.^{8, 157}



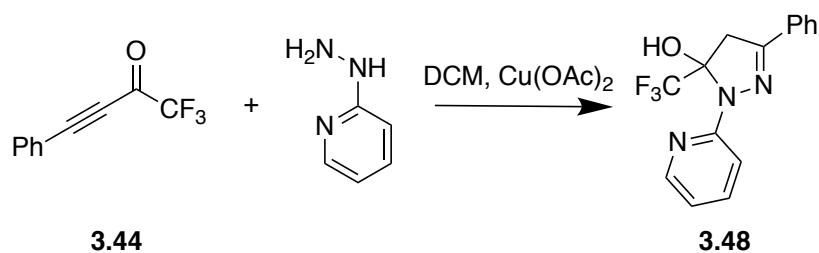
Scheme 3.12. Selective synthesis of pyrazole derivatives by using different solvents.

Min-Tsang Hsieh et. al performed [3+2] cyclocondensation of trifluoromethyl- α , β -ynones with hydrazines. The product distribution depended on the reaction conditions. Their reaction in DMSO made one type of pyrazole regioisomers. However, other pyrazole regioisomers were made when DCM and various catalysts $\text{Cu}(\text{OAc})_2$ were used. As an example, the reaction of phenylhydrazine with **3.44** gives three products under different conditions. As a summary, pyrazole **3.45** was the major product with yield ranges from 70-98% when refluxed in DCM in the presence of catalysts such as AuCl , AgOTf , AgNO_3 , CuI , CuCl_2 , CuSO_4 , $\text{Cu}(\text{OAc})_2$, $\text{Pd}(\text{OAc})_2$, ZnI_2 , or FeCl_3 . In the absence of catalyst, all three products **3.45**, **3.46**, and **3.47** were obtained when refluxed in THF, dioxane, or DMF. Only pyrazole regioisomers **3.45** and **3.47** were reported when refluxed in ethanol. The use of phenylhydrazine hydrogen chloride salt resulted in the inferior yields. The reaction conditions (DCM, 2.0 mol% $\text{Cu}(\text{OAc})_2$, reflux) were considered to be optimal and was used as a general procedure.¹⁵⁸



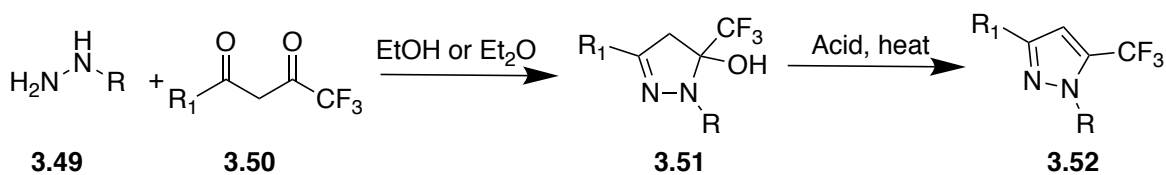
Scheme 3.13. Selective synthesis of pyrazole regioisomers in different solvents.

The reaction of **3.44** with 2-hydrazinopyridine in DCM and 2 mol% $\text{Cu}(\text{OAc})_2$ yielded hemiaminal **3.48** with 90% yield (Scheme 3.14).¹⁵⁸

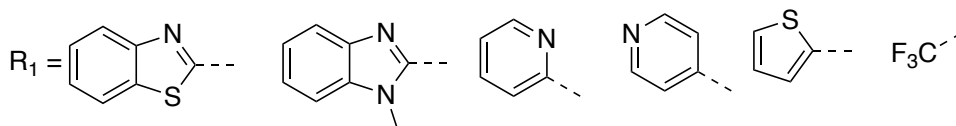


Scheme 3.14. Synthesis of hemiaminal derivative from ynone and 2-hydrazinopyridine.

Singh et. al synthesized numerous cyclic hemiaminals by using various hydrazines and diketones shown in Scheme 3.15. The reaction conditions involved the use of ethanol or diethyl ether to yield **3.51**. The dehydration of **3.51** to yield **3.52** derivatives was done by refluxing them in ethanol and various acids such as acetic acid, conc. HCl, and conc. H_2SO_4 .¹⁵⁹ According to them, the second dehydration step is slower in the presence of $-\text{CF}_3$ group resulting in stable hemiaminals.

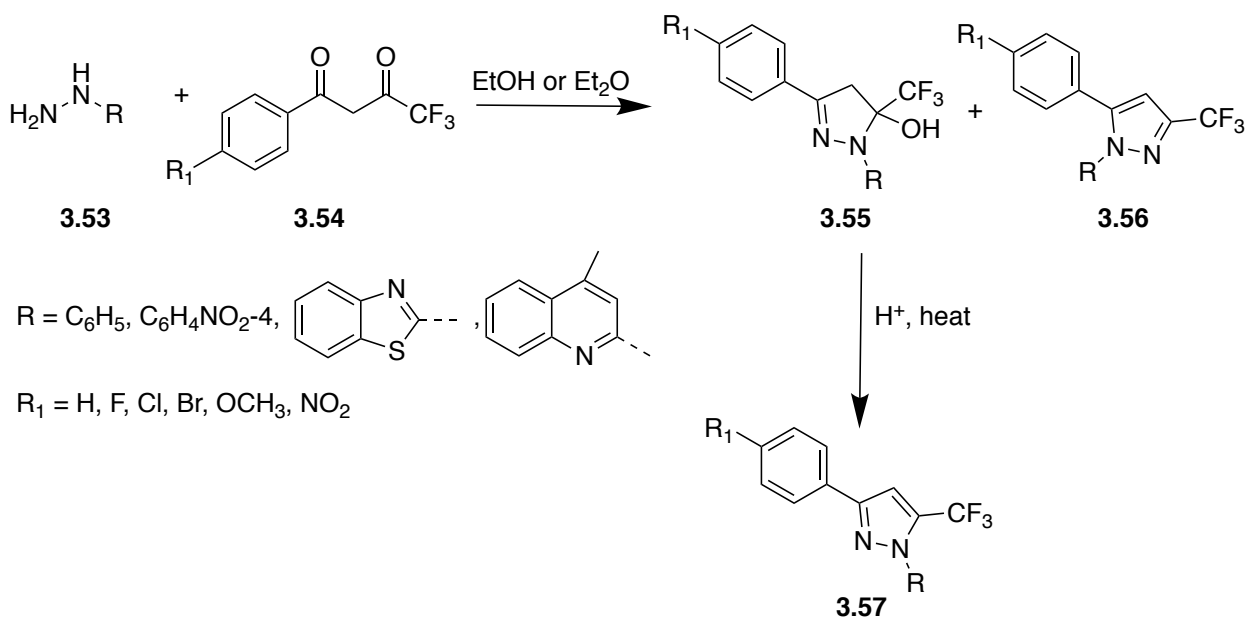


R = H, C₆H₄NO₂-4, C₆F₅



Scheme 3.15. Synthesis of various hemiaminals in ethanol or diethyl ether.

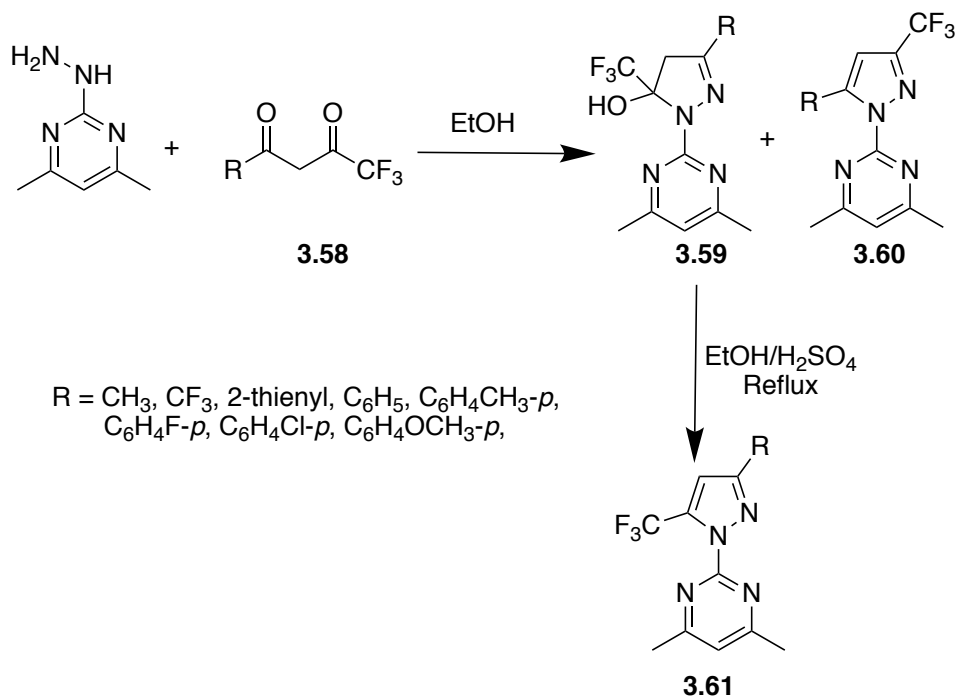
In another set of experiments, Singh et. al created numerous hemiaminals by using various aromatic hydrazines and diketones (Scheme 3.16). They enforced the importance of strong electron withdrawing groups in the formation of stable hemiaminal.¹⁶⁰



Scheme 3.16. Synthesis of various combination of hemiaminal and pyrazole derivatives.

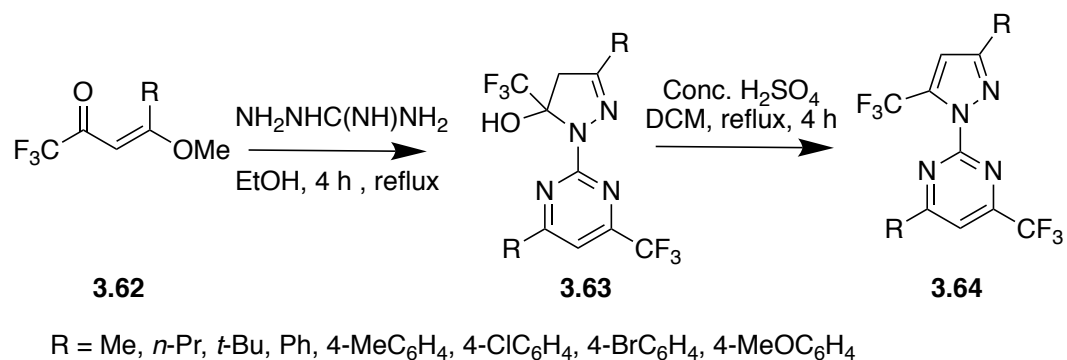
Aggarwal et. al used 2-hydrazino-4,6-dimethylpyrimidine and various diketones to create numerous hemiaminals (Scheme 3.17). Reaction of hydrazine with **3.58** (R = CH₃, CF₃, 2-thienyl) in ethanol yielded exclusively **3.59** derivatives. Reaction of hydrazine with **3.58** (R = C₆H₅, C₆H₄CH₃-*p*, C₆H₄OCH₃-*p*, C₆H₄F-*p*, C₆H₄Cl-*p*) yielded both hemiaminal **3.59** (major product) and

pyrazole **3.60** (minor product) derivatives. Conversion of hemiaminal derivatives **3.59** to pyrazole derivatives was done by refluxing them in ethanol and concentrated H₂SO₄ or aqueous acetic anhydride solution.¹⁶¹



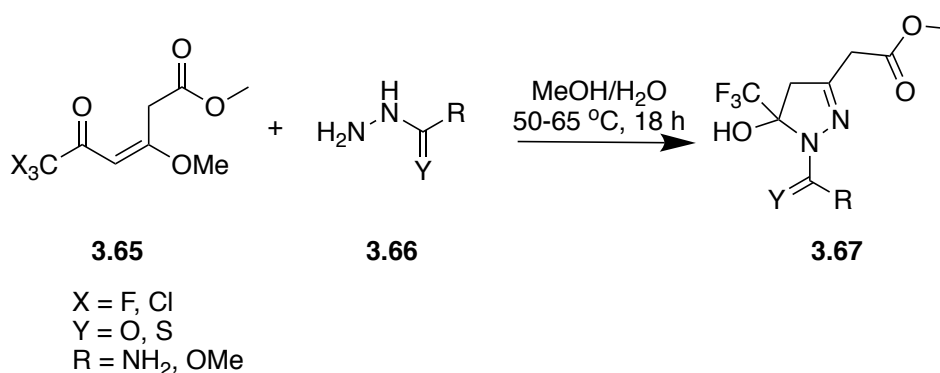
Scheme 3.17. Condensation reaction of 2-hydrazino-4,6-dimethylpyrimidine and diketones.

Bonacorso et. al studied the reactions between 2 mole equivalent of various 4-alkoxy-1,1,1-trihalo-3-alken-2-ones and 1 mole equivalent of amino guanidine bicarbonate in ethanol that yielded cyclic hemiaminal derivatives **3.63** (Scheme 3.18). Concentrated H₂SO₄ in DCM under refluxing conditions were used to convert **3.63** derivatives to pyrazole derivatives **3.64**.¹⁶²



Scheme 3.18. Synthesis of hemiaminals from amino guanidine and 4-alkoxy-1,1,1-trihalo-3-alken-2-ones

Martin et. al synthesized various derivatives of hemiaminal **3.67** by reacting **3.65** derivatives with **3.66** hydrazine derivatives (Scheme 3.19).¹⁶³ The dehydration of hemiaminals **3.67** was achieved in 95% H₂SO₄ at 40 °C after stirring for 4 hours.



Scheme 3.19. Synthesis of hemiaminal from aliphatic hydrazine.

3.2 Biological relevance

Some stable, naturally existing cyclic hemiaminals has also been reported. Mulundocandin **3.70** belongs to an echinocandins class of antifungal lipopeptides.¹⁶⁴⁻¹⁶⁵ Echinocandins possess a reactive hemiaminal group at the ornithine-5-position. They inhibit the synthesis of β -D-glucan which is an essential component of cell wall of fungi and is absent in mammalian cells.¹⁴⁹ Naturally

occurring echinocandins possess a reactive hemiaminal that can undergo ring opening and rearrangement to form linear peptides with diminished biological activity.¹⁶⁶⁻¹⁶⁷ Semisynthetic modifications at ornithine-5-position of mulundocandin were carried out to improve its chemical stability.¹⁶⁸

Two natural products with hemiaminal functional groups have been isolated from neothiobinupharidine family.¹⁶⁹ Isomer 1, 6-dihydroxythiobinupharidine, **3.68** and 2, 6'-dihydroxythiobinupharidine, **3.69** were isolated from the extract of *Nuphar luteum* of Polish origin and possess activities against human pathogenic fungi. Deuterium labeled hemiaminals 3 from 1 and 4 from 2 (Figure 3.3) have been also recovered after reducing the hydroxyl groups of respective neothiobinupharidine by using sodium borodeuteride.¹⁷⁰

Some other hemiaminals are also obtained as fluoroacyl and N-acylpyrrole derivatives.¹⁷¹⁻¹⁷³ In some cases, coordination of metal ions with O or N donor ligands of hemiaminal provide stability.¹⁷⁴

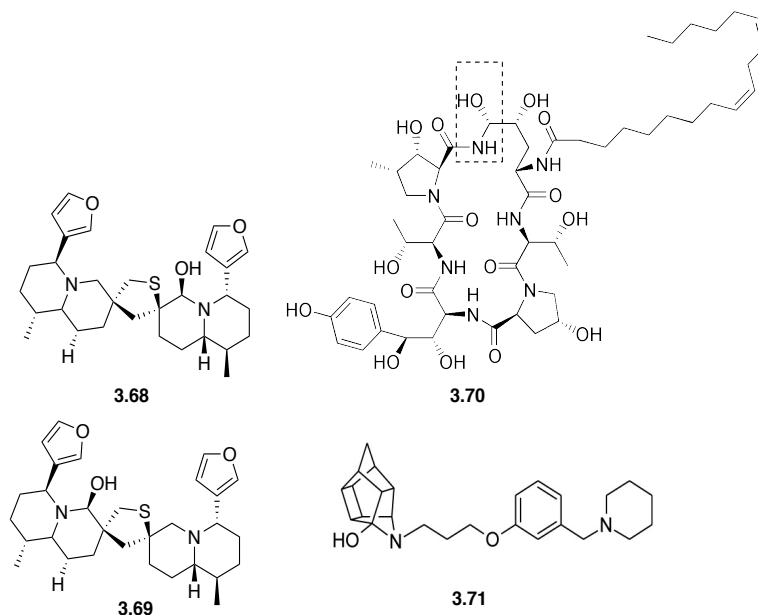


Figure 3.2. Examples of hemiaminals. Natural products, **3.68** and **3.69**, isolated from neothiobinupharidine family. **3.70**) Echinocandins. **3.71**) Chemically synthesized polycyclic cages.

Another interesting and biologically active class of hemiaminals are polycyclic cages. Modified hydrocarbon polycyclic cages **3.71** such as thrishomocubane derivatives¹⁷⁵⁻¹⁸⁰ are known to modulate cocaine-induced effects,¹⁷⁵ inhibition of nitric oxide synthase,¹⁷⁷ and have been shown to improve the blood-brain barrier permeability of some non-steroidal anti-inflammatory drugs.¹⁷⁸

3.3 Our work on hemiaminals

Triazinyl hydrazines and 2-hydrazinopyridine were used to create library of stable hemiaminals. These cyclic hemiaminals that are stable both in the solution (neutral and acidic) and in the solid state using four aromatic hydrazines (**1-4**) and four diketones (**a-d**). Here, some of aromatic hydrazones contains hydrogen bond acceptor (**2-4**) and some diketones contains electron withdrawing groups (**b-d**). The studies focuses on the use of three commercially available aromatic hydrazines (**1,3,4**) phenylhydrazine (**1**), 2-hydrazinylpyridine (**3**),^{152, 157} and 2-hydrazinyl-4,6-dimethylpyrimidine (**4**)¹⁶¹ and one readily synthetically made triazinyl hydrazine (**2**) as shown in Chart 3.1.

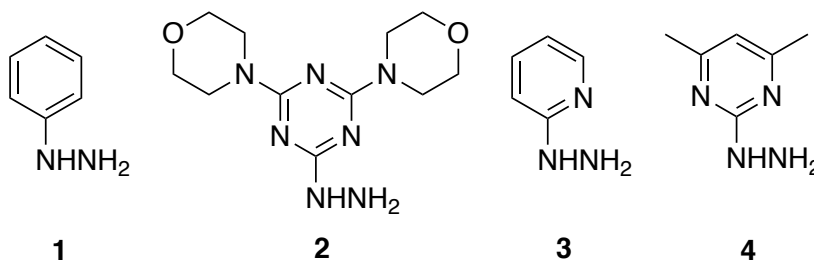


Chart 3.1. List of aromatic hydrazines used.

Four commercially available diketones used in this study are 2,4-pentanedione (**a**), 1,1,1-trifluoro-2,4-pentandione (**b**), 4,4,4-trifluoro-1-phenyl-1,3-butanedione (**c**) and 1,1,1,5,5,5-hexafluoro-2,4-pentanedione (**d**) as shown in Chart 3.2. Diketone **a** has no electron withdrawing group. Other diketones **b**, **c**, and **d** contain at least one electron withdrawing group. The stabilities of the hemiaminals synthesized were examined as a function of temperature and pH.

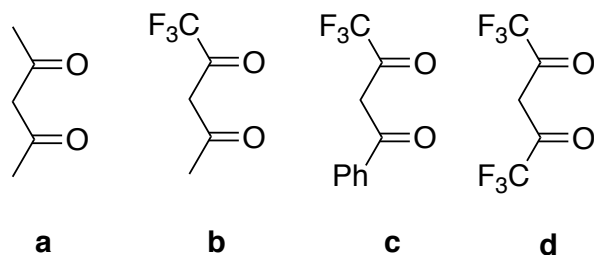
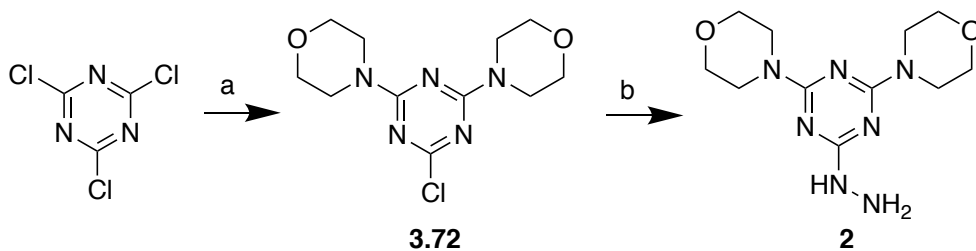


Chart 3.2. List of diketones used.

3.4 Results and Discussions:

3.4.1 Synthesis of aromatic hydrazine **2**

Aromatic hydrazines **1**, **3** and **4** are commercially available. The triazine derivative, **2**, was synthesized in two steps by reacting cyanuric chloride with two equivalents of morpholine at low temperature to yield **3.72** followed by an excess of hydrazine monohydrate at elevated temperature with an overall yield of 87% as shown in Scheme 3.20.



Scheme 3.20. Synthesis scheme of triazinyl hydrazine **2**. a) 2 equiv. morpholine, DIPEA, THF, 0 °C-rt, 12 h, 94%. b) excess hydrazine, DIPEA, dioxane, 95°, 15 mins, 92%.

3.4.2 General reaction conditions for the synthesis of hemiaminals and pyrazoles

The neutral conditions relied on the use of absolute ethanol, methanol, or acetonitrile as a solvent. In some cases, a few drops of acetonitrile were added along with absolute ethanol to improve the solubility. Acidic conditions relied on either neat glacial acetic acid or absolute

ethanol in the presence of catalytic concentrated HCl. To compare the stability of the stable hemiaminals, reactions mixtures were refluxed in glacial acetic acid. Pyrazoles did not form using a catalytic amount of HCl in absolute ethanol at elevated temperature. Both conditions could be described as ‘dehydrating’, presumably favoring pyrazole formation.

3.4.3 Nomenclature

To facilitate discussion, compounds are named to reflect whether a hemiaminal, **H**, or pyrazole, **P**, derivative forms from the respective starting materials. That is, **2** and **a** could yield hemiaminal **H-2a** and/or a pyrazole **P-2a**. Because two of the diketones (**b-c**) are non-symmetrical, two different regioisomers can result. Accordingly, reaction with diketone **b** yields molecules designated with a **b** or **b'**. A similar convention is adopted for **c**. In the cases of **b** and **c** (and not **b'** and **c'**), the CF₃-group is geminal to the hydroxyl group of the hemiaminal. Similar numbering system was adopted for the rest of the **b** and **c**-series hemiaminals and pyrazoles (Figure 3.3).

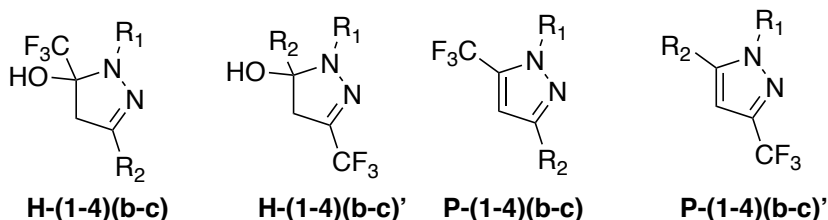


Figure 3.3. Representation of different regioisomers of hemiaminals and pyrazole derivatives. R₁ is the aromatic ring (**2-4**). R₂ is methyl (**b**) and phenyl (**c**).

The numbering system employed for the diketones reflects the relative stability of the resulting hemiaminals (**a**<**b**<**c**<**d**). Compared with **1**, hemiaminals from **2**, **3**, and **4** hydrazines are more stable. The relative stability of hemiaminals derived from **2**, **3**, and **4** and the diketones is not rigorously established in these studies.

3.4.4 Distinguishing fingerprints for characterization

Hemiaminal and pyrazole derivatives are easily distinguished using mass spectrometry and ^1H and ^{13}C NMR. The mass spectroscopy of hemiaminal derivatives is 18 a.m.u. higher than respective pyrazole derivatives. The ^1H NMR of a hemiaminal is different than that of pyrazole by two diagnostic peaks. The methylene protons of the five membered ring of hemiaminal appear as diastereotopic doublets between 2.8-3.8 ppm with a coupling constant of around 18 Hz. In addition, the hydroxyl proton of the hemiaminal appears as a broad singlet at two different position. In some hemiaminals, it appears between 8.0 and 9.0 ppm indicative of a strong hydrogen bond, while in other cases, it appears between 3.0 and 4.0 ppm, indicative of a weak hydrogen bond. The aromatic proton of the pyrazole appears further downfield between 6.0 and 7.3 ppm as expected. As an example, Figure 3.4 shows the ^1H NMR of **H-3b**. The doublet of doublets between 3.13-3.36 ppm correspond to the methylene protons of the five membered hemiaminal ring and singlet at 8.76 ppm corresponds to the hydroxyl proton. The downfield shift suggests a formation of strong hydrogen bond. The signals between 3.13-3.36 ppm and at 8.76 ppm disappears when **H-3b** was converted to **P-3b**. A singlet at 6.69 ppm corresponds to the only aromatic proton of the pyrazole ring (Figure 3.5).

The ^{13}C NMR spectra can also be used to differentiate between hemiaminal and pyrazole (Figure 3.6 and 3.7). The carbon atom of a hemiaminal appears between 90 and 95 ppm as a diagnostic quartet with coupling constant, $^2J_{\text{F-C}}$, between 35 and 40 Hz. In contrast, the same C-atom in pyrazole derivatives appears downfield between 130 and 145 ppm as quartet with same coupling constant between 35 and 40 Hz. As an example, ^{13}C NMR of **H-3b** shows two characteristics signals. A quartet between 92.3-93.3 ppm corresponds to the hemiaminal carbon atom. A signal at 47.9 ppm corresponds to the methylene carbon atom of the five membered hemiaminal ring.

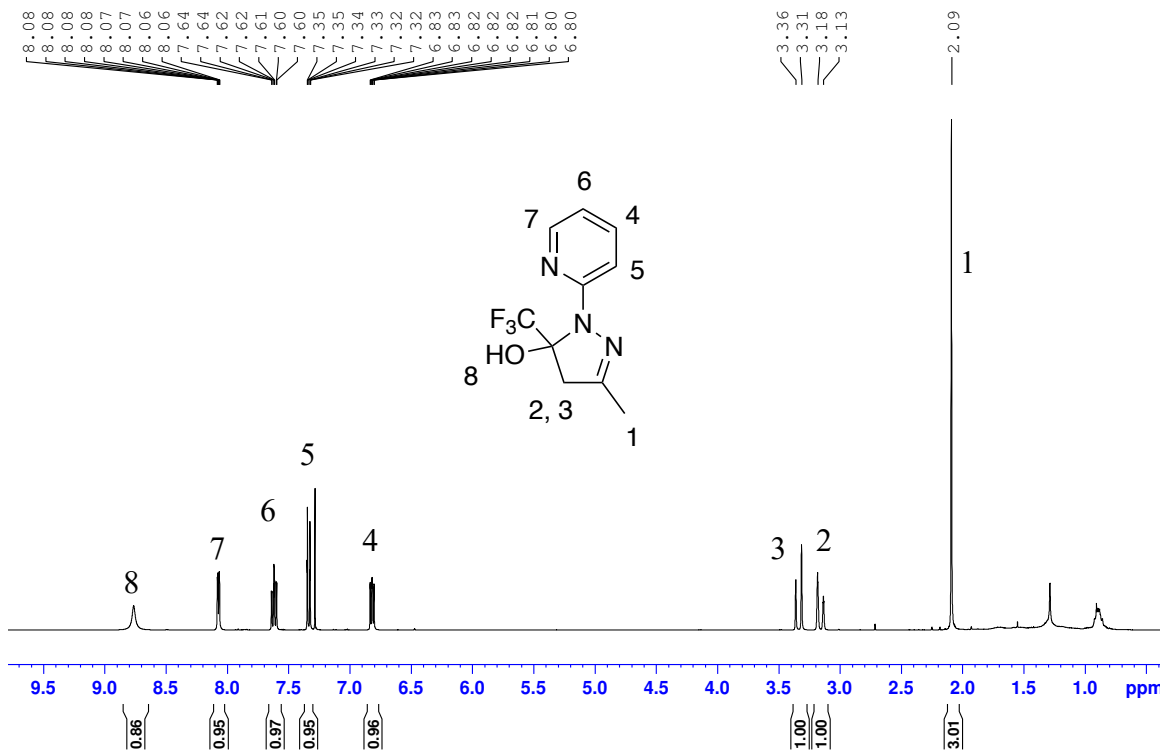


Figure 3.4. ¹H NMR of H-3b in CDCl₃.

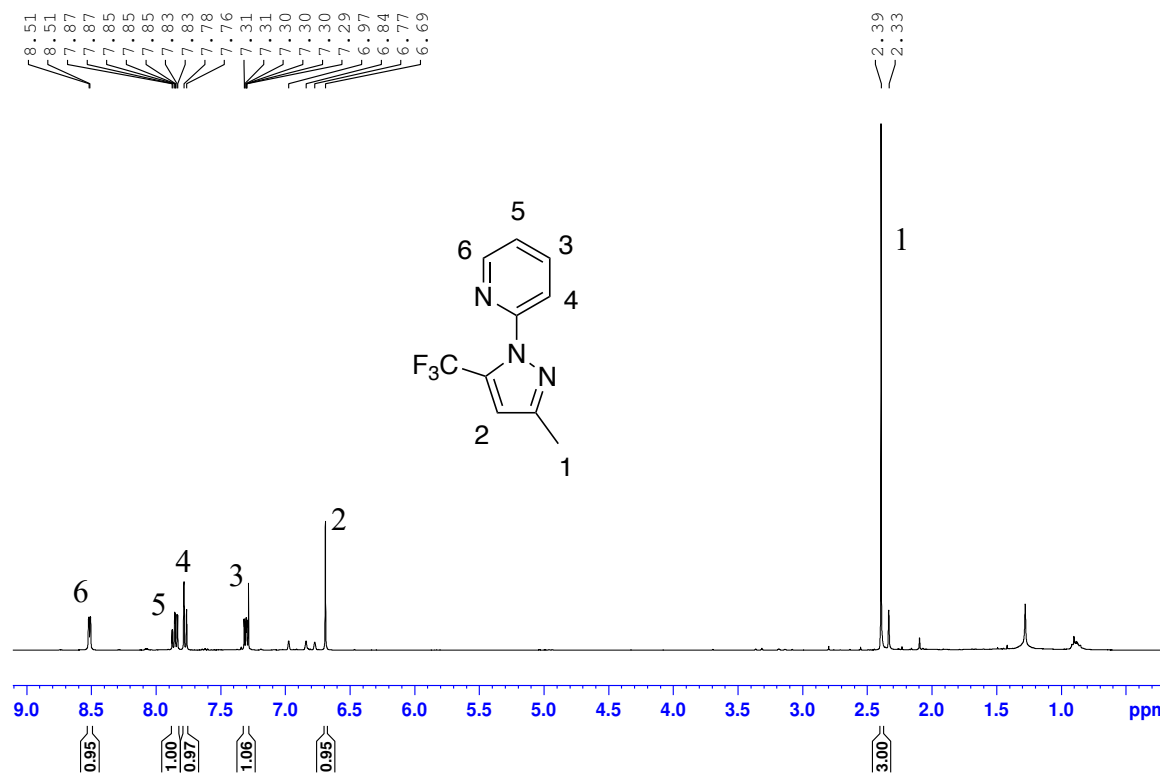


Figure 3.5. ¹H NMR of P-3b in CDCl₃.

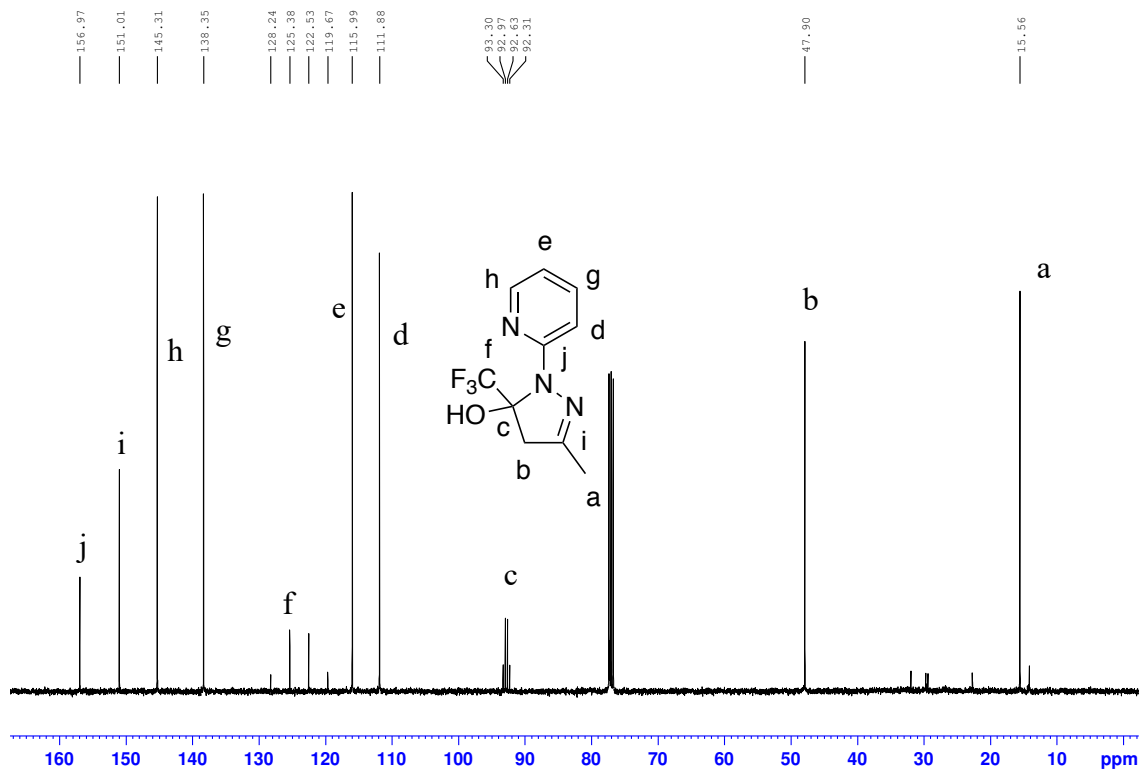


Figure 3.6. ^{13}C NMR of H-3b in CDCl_3 .

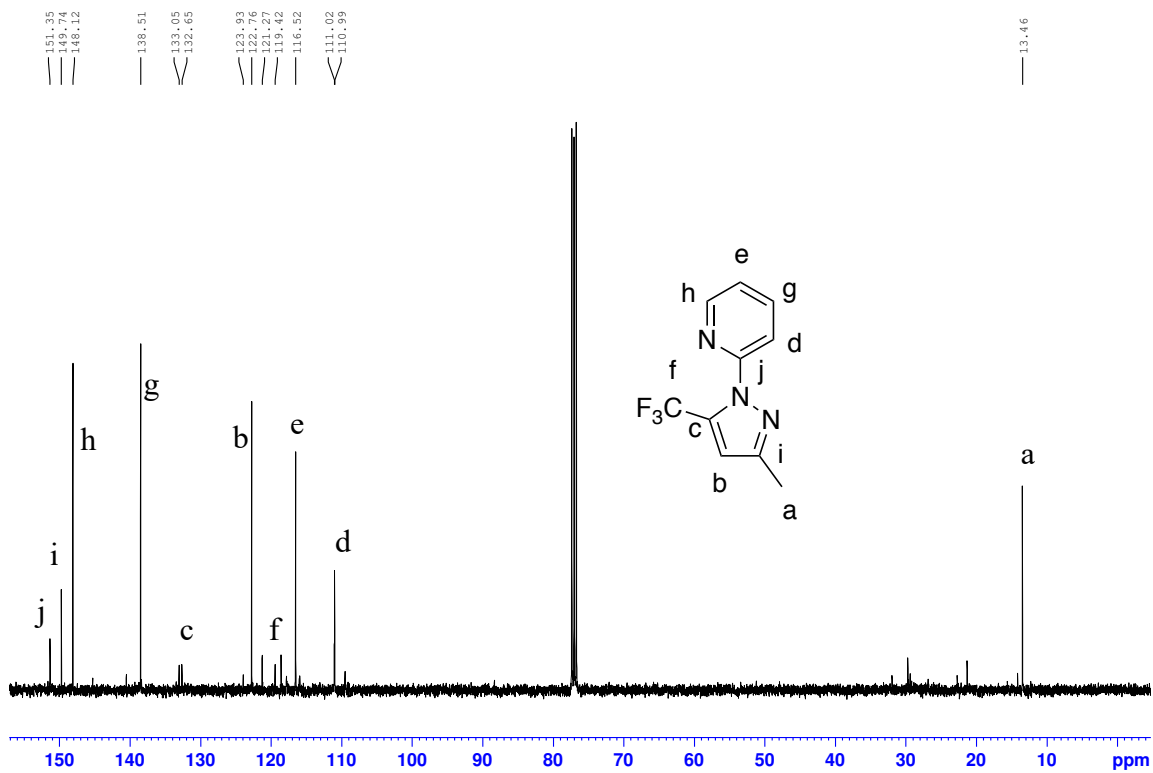


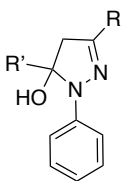
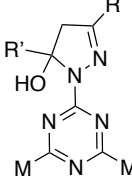
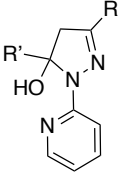
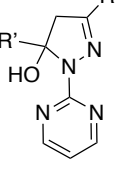
Figure 3.7. ^{13}C NMR of P-3b in CDCl_3 .

The ^{13}C NMR of **P-3b** shows a significant change in the chemical shift among two characteristic signals. The quartet downfield shift between 132.3-133.4 ppm suggests the formation of double bond. A new signal at 123.9 ppm corresponds to the unsaturated carbon atom of the pyrazole ring.

3.4.5 Hemiaminal or pyrazole products

Table 3.1 summarizes the results of our studies wherein a '+' indicates formation of the corresponding product and a '-' indicates that the product was not observed. Quick inspection of the table reveals a host of stable hemiaminals (green) that are stable in neutral solutions indefinitely and in neat glacial acetic acid at room temperature. At higher temperatures as indicated by increasing shades of red—these stable hemiaminals do form the expected pyrazole products in the presence of acid. In some cases, hemiaminals (blue) are observed, but not considered stable (even if isolable as are **H-1c** and **H-1d**) because they dehydrate to the corresponding pyrazole over time at room temperature. Elaboration is provided in the following paragraphs. The notable absence of stable hemiaminals when a CF_3 -group is absent (**a-series**) and when the hydrazine donor does not provide a hydrogen-bond acceptor (products of **1**) underscore the importance of both features as design criteria. Hemiaminals **H-1c**,¹⁵⁷⁻¹⁵⁸ **H-1d**,^{152,157} **H-4b**,¹⁶¹ **H-4c**,¹⁶¹ and **H-4d**¹⁶¹ have been synthesized before and same synthetic approach was adopted in this project. Hemiaminal **H-3c** was also synthesized before by using different synthetic method, however.¹⁵⁸

Table 3.1. Summary of all the hemiaminals and pyrazole derivatives synthesized. ‘+’ Product observed. ‘-’ Product not observed. ‘t’ minor product. ‘Green’ stable hemiaminals. ‘Blue’ unstable hemiaminals. ‘Red’ Observed under acidic condition when heated. ‘H’ hemiaminals. ‘P’ pyrazoles.

		H-1		H-2		H-3		H-4					
													
Conditions:		Neut	Acid	Neut	Acid	Neut	Acid	Neut	Acid				
Product:		H	P	H	P	H	P	H	P				
a	R=R'=Me	-	+	-	+	+	+	-	+	-	+	-	+
b	R=Me; R'=CF ₃	-	+	-	+	+	-	+	-	+	-	+	-
b'	R=CF ₃ ; R'=Me	-	-	-	+	-	-	-	-	-	-	-	-
c	R=Ph; R'=CF ₃	+	-	-	+	+	-	+	-	+	-	+	-
c'	R=CF ₃ ; R'=Me	-	t	-	-	-	-	-	t	-	-	-	-
d	R=R'=CF ₃	+	t	-	+	+	-	+	-	+	-	+	-

3.4.6 Reactions of phenylhydrazine, **1**, with diketones (**a-d**) yield primarily pyrazoles^{152, 157}

Table 3.1 reveals that pyrazoles are the predominant product of condensations of **1** with **a**, **b**, **c**, and **d**. Reaction of **a** with **1** at room temperature under neutral or acidic conditions exclusive yields one pyrazole, **P-1a**. For reactions of **1** and **b**, acidic conditions yield **P-1b**. Under neutral conditions, however, an inseparable mixture of two pyrazoles results. ¹H-NMR spectroscopy reveals regioisomers in 1.7:1 ratio for **P-1b**: **P-1b'**. We conclude that under neutral conditions, attack at either sp² center occurs. Under acidic conditions, we hypothesize (with corroborating DFT calculations) that protonation/activation of the carbonyl distant from the CF₃-group occurs before attack at this carbon.

The first observable hemiaminals come from reactions of **1** with **c** and **d**. Like **b**, **c** is non-symmetrical and offers an electron withdrawing CF₃-group and a phenyl ring. Neutral conditions yield a mixture of the **H-1c** and **P-1c'** which is separable by conventional silica gel chromatography. The product distribution reflects attack of the hydrazine at both sp² carbons. The hemiaminal corresponding to **H-1c'** is not observed, presumably, because the CF₃-group is not positioned to stabilize it, and accordingly, dehydration is facile. **H-1c** is marginally stable, but by extending the reaction time from 12 hours to 30 days, hemiaminal **H-1c** is completely converted to **P-1c**. Hemiaminal **H-1c** was characterized by the presence of two doublets between 3.48-3.74 ppm (¹J = 18.0 Hz) and a hydroxyl proton at 3.18 ppm. The upfield chemical shift and broad shape of the hydroxyl proton signal is not consistent with a strong hydrogen bond. Solid state structure does not show the formation of any hydrogen bond (Figure 3.8). Not surprisingly, the addition of a catalytic amount of HCl converts **H-1c** to its pyrazole derivative **P-1c** at room temperature (indicated with a 'd' in Table 3.1) in less than hours. Under neutral conditions at room temperature, the same reaction (**H-1c** to **P-1c**) requires 4 weeks. Under acidic conditions, reaction of phenylhydrazine **1** and **c** exclusively yields **P-1c**.

For reactions of **1** and **d**, a mixture **H-1d** and **P-1d** is observed. Hemiaminal **H-1d** is found to be more stable than **H-1c** based on the time required for conversion to the respective pyrazole derivative. In a solution of CDCl₃, after 4 weeks, the ratio of **H-1d**: **P-1d** was 6.6:1. Addition of catalytic 1M HCl converted **H-1d** to **P-1d** in 2 hours. This suggests that **H-1d** is more stable than **H-1c** under neutral conditions.

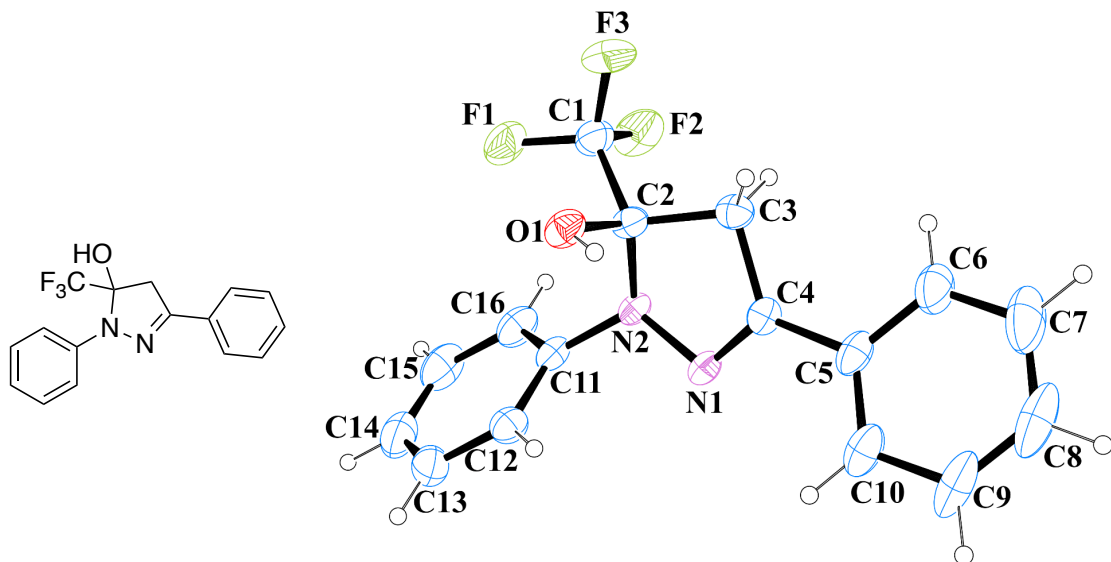


Figure 3.8. Crystal structure of hemiaminal **H-1c**. The thermal ellipsoids are drawn at 30% probability.

3.4.7 Reactions of triazinyldiazine, 2

The addition of a hydrogen-bond acceptor group in **2** leads to the appearance of stable hemiaminals. However, the importance of the CF₃-group is underscored by reactions of **2** with **a**. While **P-2a** is observed under acidic conditions, after 12 hours under neutral conditions an inseparable mixture of **H-2a** and **P-2a** is obtained. The ratio of **P-2a**:**H-2a** is 1.6:1. The ¹H NMR shows five membered methylene protons as doublet of doublets between 2.78-3.09 ppm (¹J_{H-H} = 18.17 Hz) and proton attached to Csp² as singlet at 6.00 ppm evident the formation of both hemiaminal and pyrazole respectively. In addition, a broad singlet at 5.90 ppm suggests the presence of a weak hydrogen bond derived from the OH group and heterocyclic N-acceptor. Hemiaminal **H-2a** can be converted to **P-2a** with time or by the addition of a small amount of HCl. Diketones with a CF₃ group (**b-d**) exclusively yield stable hemiaminals under acidic and neutral conditions at room temperature. Reaction of **2** with **b** under acidic conditions yield a stable

hemiaminal, **H-2b** while isomer **H-2b'** (which is not stabilized by a CF₃-group) is not observed for the reason previously advanced (selective protonation).

The ¹H-NMR of **H-2b** reveals the hydroxyl proton downfield at 8.16 ppm, a value indicative of the formation of a hydrogen bond. This peak disappears upon addition of D₂O. The methylene protons of five-membered ring appear as a doublet of doublets between 3.16-3.33 ppm (¹J_{H-H}=18.9 Hz). In ¹³C-NMR, both fluorinated and hemiaminal carbon atoms couple with the fluorine atoms and appear as a quartet at 119.4-128.1 ppm with coupling constant ¹J_{C-F}=288.1 Hz, and at 91.9-92.9 ppm with coupling constant ²J_{C-F}=33.6 Hz, respectively. One bond and two bond coupling constants of C-F agree with the range of coupling constants ranges in literature.¹⁷⁹

The reaction of **2** with **c** results in hemiaminal **H-2c** as evident from ¹H-NMR, ¹³C-NMR and X-ray crystallography. Again, a strong hydrogen bond is observed from the presence of a hydroxyl proton at 8.21 ppm. The methylene protons of five membered ring appear at 3.59-3.65 ppm as doublet of doublets due to the diastereotopic environments created by the hemiaminal, ²J_{H-H}=18.9 Hz obscured by signals from the morpholine groups. The hemiaminal carbon appeared as a quartet at 91.4-92.4 ppm, ²J_{C-F}=33.6 Hz. The fluorinated carbon appeared as quartet at 119.1-122.1 ppm, ¹J_{C-F}=288.7 Hz. The crystal structure obtained for **H-2c** reveals a hydrogen bond between the triazine and OH of the hemiaminal (Figure 3.9).

Reaction of **2** with **d** under neutral and acidic conditions resulted in the formation of hemiaminal **H-2d**. When **H-2d** was refluxed in glacial acetic acid for about 24 hours, a mixture of **P-2d** and **H-2d** in the ratio of 3.5:1 was obtained. The stability trends of all the hemiaminals of this series increases from **H-2b** < **H-2c** < **H-2d**.

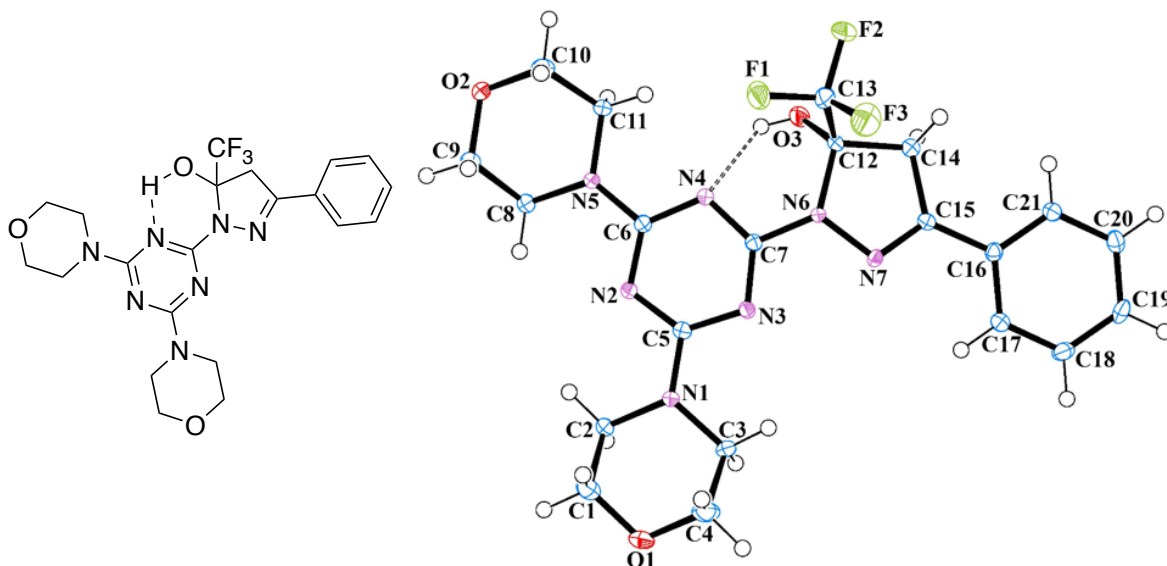


Figure 3.9. Crystal structure of hemiaminal **H-2c** showing a hydrogen-bond implicated in stability. The thermal ellipsoids are drawn at 30% probability.

3.4.8 Reactions of 2-hydrazinylpyridine, **3**.

Like triazinylhydrazine **2**, reactions of **3** yield similar results. **H-3a** was not observed in either neutral or acidic conditions. Hemiaminals **H-3b**, **H-3c**,¹⁵⁸ and **H-3d** were observed under both neutral and acidic condition. Hydrogen bonds between of OH group with the nitrogen atom of the pyridine ring was seen in crystal structures (Figure 3.10) and by $^1\text{H-NMR}$ with a peak for **H-3b**, **H-3c**, and **H-3d** appearing at 8.75, 8.73, and 8.47 ppm, respectively. Similar to series **2** hydrazones, stability of the hemiaminals increase from **H3-b** < **H3-c** < **H3-d**. The stability of hemiaminals was determined by measuring the amount of time hemiaminals took to convert to pyrazole derivative. That is, in refluxing glacial acetic acid, **H-3b** undergoes complete conversion in 2-3 hours while **H-3c** requires 10-12 hours. After refluxing **H-3d** in glacial acetic acid for 20 h, the ratio of **P-3d**:**H-3d** was 2.7:1.

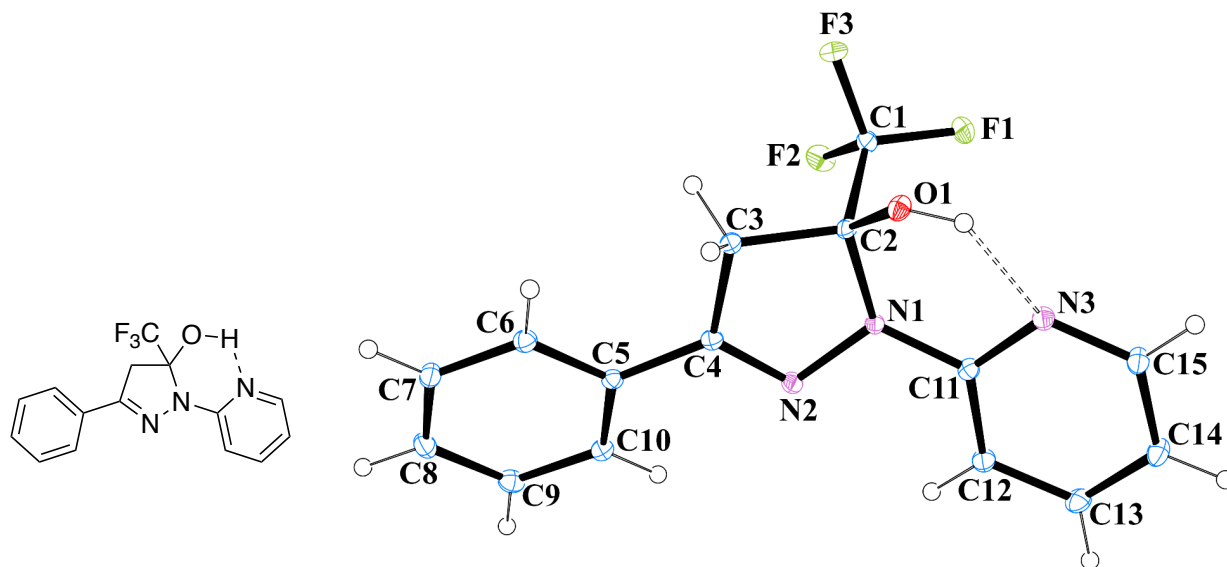


Figure 3.10. Crystal structure of hemiaminal **H-3c** showing a hydrogen-bond implicated in stability. The thermal ellipsoids are drawn at 30% probability.

A bis-hemiaminal along with **H-3d** was observed in the NMR spectrum of crude product made from **3** and **d** under neutral conditions. However, during chromatographic purification, the bis-hemiaminal was converted to hemiaminal **H-3d**. This observation also confirms that dehydration step in the formation of hydrazone is indeed the rate determining step.

3.4.9 Reactions of 4-hydrazino-2,6-dimethylpyrimidine, **4** with diketones¹⁶¹

As with **2** and **3**, a similar product distribution was obtained when 4-hydrazino-2,6-dimethylpyrimidine, **4**, was employed.¹⁶¹ The stabilities of the hemiaminals was **H-4b** ~ **H-4c** < **H-4d**. Pyrazoles were obtained from the first two hemiaminals after refluxing in glacial acetic acid for 12h. Refluxing a solution of **H-4d** in glacial acetic acid for 72 hours yielded a ratio of **H-4d**: **P-4d** of 1:1.8. Hydrogen bonds between of OH group with the nitrogen atom of the pyridine ring were seen in the NMR spectra of **H-4b**, **H-4c**, and **H-4d** at 8.19, 8.48, and 8.16 ppm, respectively.

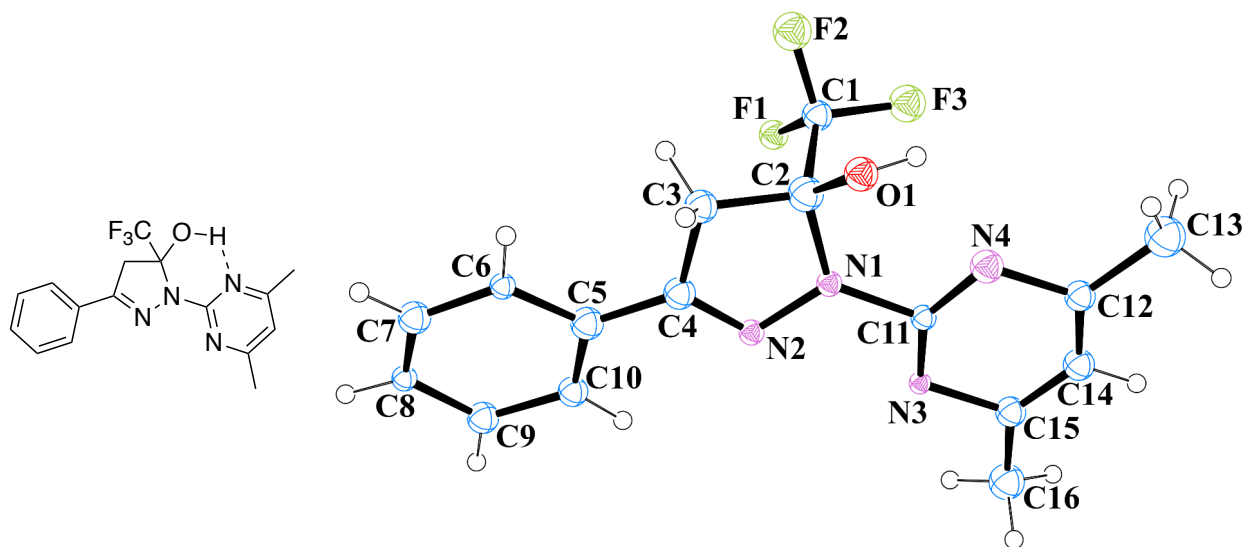


Figure 3.11. Crystal structure of hemiaminal **H-4c**. The thermal ellipsoids are drawn at 30% probability.

3.4.10 A summary of hemiaminal stability and hydrogen bond data.

Data for the hydrogen bonds obtained from crystal structures as well as the stability data for the hemiaminals appears in Table 3.2. Relative stability of hemiaminal was determined by the amount of time taken and conditions they required including the pH conditions and elevated temperature for their conversion to the respective pyrazole derivatives. The data shows a trend for both the hydrazine donor and the 1,3-diketone. In summary, hemiaminal stability increase from those derived $\mathbf{a} < \mathbf{b} < \mathbf{c} < \mathbf{d}$. Using the **d** series, we are led to hypothesize that stability increases with hemiaminals derived from $\mathbf{1} < \mathbf{2} < \mathbf{3} < \mathbf{4}$.

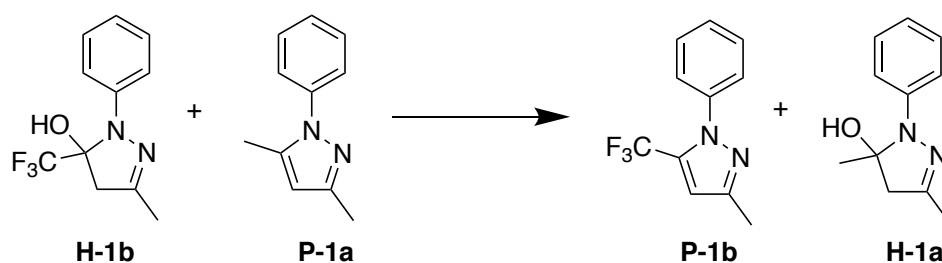
Table 3.2. Hydrogen bond characteristics and conversion of hemiaminals to pyrazole derivatives.

H-#	OH (ppm)	OH--N bond Length	O-H-N bond angle	Conditions	Time	Temp. (°C)	% conversion to pyrazole
1c	3.25	2.17	174	neutral	30 days	25	100
				cat. HCl	2h	25	100
1d	3.48			neutral	30 days	25	87
				cat. HCl	2 h	25	100
2a	5.90				NA		
2b	8.16			gl. AcOH	3	118	100
2c	8.21	2.03	135	gl. AcOH	10	118	100
2d	7.95			gl. AcOH	24	118	85
3b	8.75			gl. AcOH	3	118	100
3c	8.73	1.96	137	gl. AcOH	12	118	100
3d	8.47			gl. AcOH	24	118	73
4b	8.19			gl. AcOH	12	118	100
4c	8.48	2.28	112	gl. AcOH	12	118	100
4d	8.18	1.98	142	gl. AcOH	72	118	65

3.4.11 Computational Studies

For computational studies, the relative stability of the hemiaminals were compared to that of **H-1a** (Figure 3.8). Relative energy difference was measured between the stable hemiaminals such as **H-1b** and reference hemiaminal **H-1a** (Scheme 3.21). Isodesmic reactions were used for all other stable hemiaminals to determine the relative stability. When compared with **1**, hemiaminals from **2**, **3** and **4** exhibit higher stability due to the presence of a hydrogen bond acceptor. For each parent hydrazine, the location of CF₃ groups significantly affected the hemiaminal stability where the regioisomer with CF₃ group not located on hydroxyl carbon shows lower stability (e.g. **H-2b** > **H-2b'**, **H-3c** > **H-3c'** and **H-4b** > **H-4b'** etc.). This factor is more

pronounced for **H-1b'** and **H-1c'** which additionally lack the stability due to the absence of the hydrogen-bond. In addition, the products which does not contains CF₃ group (**H-2a**, **H-3a** and **H-4a**) have lower stability compared to their counterparts which contains CF₃ group. Arshad Mehmood from Dr. Benjamin Janesko group determined the relative stability calculations of all hemiaminals with respect to **H-1a**. Relative stabilities of all hemiaminals from Density function theory (DFT) shown in Figure 3.12 confirm the hypothesis that the presence of both CF₃ group and hydrogen bond acceptors are essential for the stability of hemiaminals.



Scheme 3.21. Illustration of an isodesmic reaction for **H-1b** used to calculate the reaction energy mentioned in Figure 3.12.

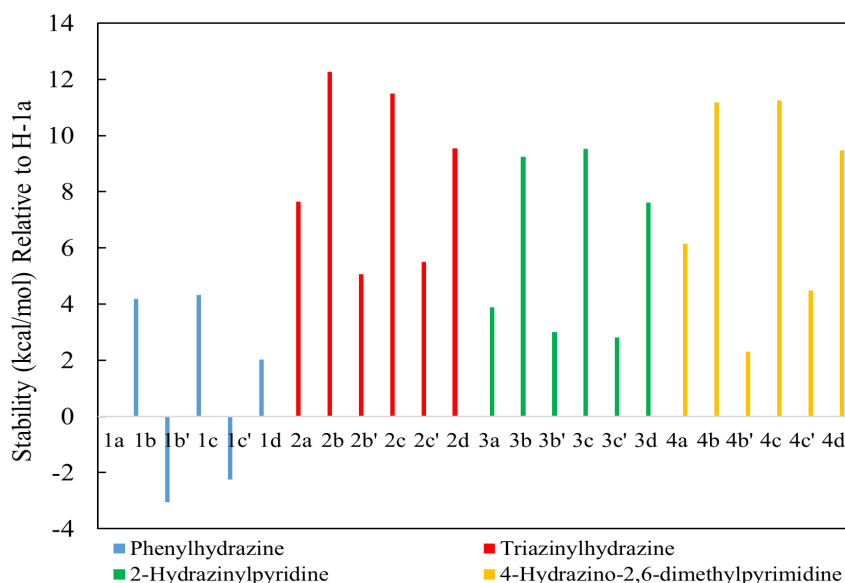


Figure 3.12. Hemiaminal stability relative to **H-1a**. More positive value corresponds to the more stable hemiaminal

Figure 3.13 presents the calculated energy of OH \cdots N hydrogen bond for 5 hemiaminals at M06-2X/6-311++g(2d,2p) level. The hydrogen bonds in hemiaminals obtained from 2,4-

pentanedione (**a**) are ~ 3.5 kcal/mol lower in energy compared to those obtained from other 1,3-diketones, which establishes that fundamental role CF_3 group in stabilizing the hydrogen bond.

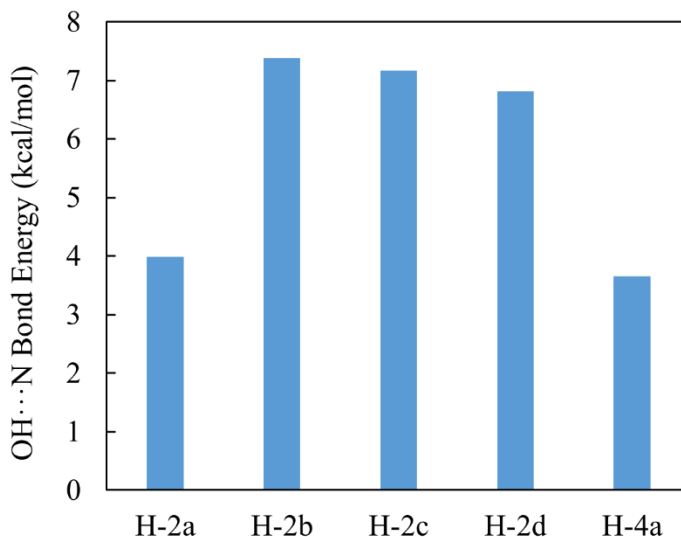


Figure 3.13. Calculated energies of $\text{OH}\cdots\text{N}$ bond for selected hemiaminals.

3.4.12 Design criteria for the preparation of stable hemiaminals.

The studies performed suggest two design criteria for the preparation of stable hemiaminals; a hydrogen bond involving an OH acceptor, and a CF_3 group vicinal to that OH group. The literature provides examples wherein hemiaminal stability is attributed to intramolecular hydrogen bonds in solution as well as intramolecular hydrogen bonds in the solid state. Hydrogen-bonding in our system is observed in the x-ray crystal structures determined wherein the hydroxyl proton forms a hydrogen bond to the nitrogen in the aromatic ring hydrazine donor (pyridine, pyrimidine, or triazine). Table 3.2 summarizes the characteristics of these hydrogen bonds as well as the chemical shifts observed for the OH groups in CDCl_3 . We hypothesize that the downfield chemical shifts reported for the OH in the ^1H NMR are consistent with a similar hydrogen bond forming in solution. Indeed, there are no other hydrogen-bond donors available to assign these shifts to, although the magnitude of the effect that the CF_3 group

has could be considerable. In our studies, resistance to conversion to the pyrazole derivative from the requisite hemiaminal reveals the critical role of the CF₃ group. In the absence of a CF₃ group, conversion to the pyrazole happens rapidly at room temperature. Hemiaminals with a single CF₃ group (derived from **b** or **c**) convert more rapidly to the pyrazole than those with two CF₃ groups (**d**).

3.5 Conclusion

The work described expands the number of examples of stable hemiaminals and reinforces design criteria that have emerged from different reports. The literature shows that hemiaminal formation is favored primarily by neutral conditions as well as apolar aprotic solvents. Here, however, hemiaminals are obtained from reactions in ethanol under acidic conditions. This observation underscores the influence of adopting both a strong electron withdrawing group and a hydrogen bond acceptor as design criteria.

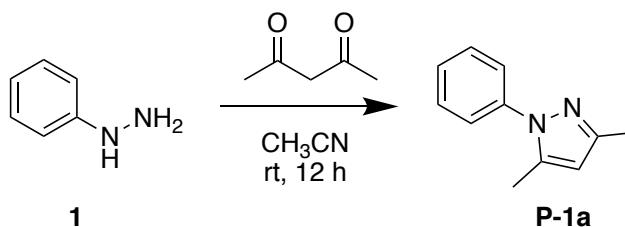
Hemiaminals **H-4b**, **H-4c**, **H-4d**, and **H-3c** have been synthesized before and have been found stable under acidic conditions.^{158, 161} Their conversion to pyrazole required elevated temperature. In addition to the synthesis of some known hemiaminals, new library of stable hemiaminals **H-2b**, **H-2c**, **H-3d**, **H-3b**, and **H-3d** were synthesized and were found to be stable at room temperature in acidic ethanolic solutions (HCl, glacial acetic acid, *p*TSA, and H₂SO₄). Refluxing for three hours hemiaminals in solutions of diisopropylethylamine or pyridine led to no change. A noticeable difference in stability was found between hemiaminals derived from either **1** or **a** which lack a hydrogen-bond acceptor and CF₃ group, respectively. As these hemiaminals were converted to pyrazole derivatives in neutral conditions over the course of time or quickly in acidic conditions even at room temperature. However, the hemiaminals containing hydrogen-bond

acceptor and CF₃ required acid and elevated temperature to convert to respective pyrazole derivatives.

The experimental findings are in agreement with computational data. The hypothesis can be further tested by replacing the nitrogen atom of the rings (**2**, **3**, **4**) by a different hydrogen bond donors atoms such as oxygen and fluorine, and other electronegative non-hydrogen bond donor atoms such as sulfur. It would be interesting to compare the stability of these hemiaminals with already synthesized hemiaminals. Stability at room temperature across a range of pH values as well is in neat glacial acetic acid suggests that these structures might have general utility in a range of applications.

3.6 Experimental procedures

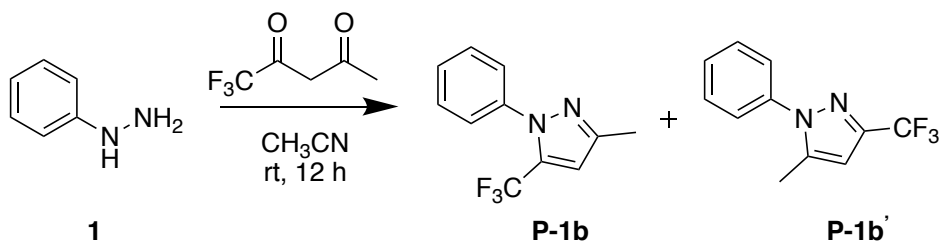
3.6.1 Synthesis of P-1a



Scheme 3.22. Synthesis of **P-1a**.^{151, 155}

Hydrazine **1** (300 mg, 2.8 mmol) and diketone **a** (550 mg, 5.6 mmol) were mixed in 5 ml CH₃CN and stirred at room temperature for 12 hours. The solvent was removed under reduced pressure and column chromatography was performed with 5% ethyl acetate in hexanes to afford **P-1a** as light-yellow liquid (406 mg; 85%). **H-1a** was not observed. ¹H NMR (400 MHz, CDCl₃) δ 7.37-7.35 (4H, m), 7.35-7.34 (1H, m), 6.01 (1H, s), 2.32 (3H, s), 2.32 (3H, s). ¹³C NMR (400 MHz NMR) δ 149.0, 140.0, 139.4, 129.0, 127.2, 124.8, 106.9, 13.5, 12.4. MS (ESI/Q-TOF) m/z: [M+H]⁺ Calcd for C₁₁H₁₂N₂ 172.10; Found 173.01.

3.6.2 Synthesis of P-1b

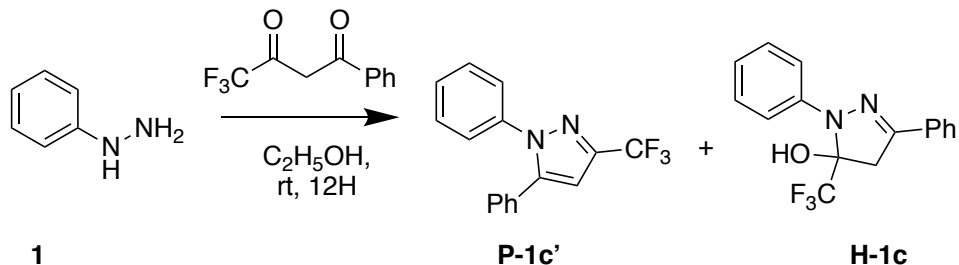


Scheme 3.23. Synthesis of **P-1b** and **P-1b'**.^{151, 155}

Hydrazine **1** (245 mg, 2.3 mmol) and diketone **b** (385 mg, 2.5 mmol) were dissolved in 4 ml of CH₃CN and stirred at room temperature for 12 hours. The solvent was removed under reduced pressure and chromatography was performed with 5% ethyl acetate in hexanes to afford a mixture of **P-1b** and **P-1b'** as slightly yellow liquid (247 mg, 48%). **H-1b** was not observed.

When hydrazine **1** (100 mg, 0.93 mmol) and diketone **b** (154 mg, 1.0 mmol) mixed in 4 ml of absolute ethanol along with 0.5 ml concentrated HCl. Upon purification only **P-1b** (112 mg, 54%) was obtained. **P-1b** and **P-1b'**. ¹H NMR (400 MHz, CDCl₃) δ 7.48-7.46 (5H, m), 6.21 & 6.49 (1H, s), 2.38-2.38 (3H, s). ¹³C NMR (400 MHz CDCl₃) δ 149.0, 143.6-142.5 (q, ²J_{C-F} = 33.4 Hz), 139.2, 138.9, 133.6-132.5 (²J_{C-F} = 33.4 Hz), 129.3, 129.0, 129.03, 128.7, 125.6, 125.3, 126.5-118.5 (q, ¹J_{C-F} = 288.1 Hz), 125.4-117.4, (q, ¹J_{C-F} = 288.1 Hz), 104.8, 13.3, 12.3. MS (ESI/Q-TOF) m/z: [M+H]⁺ Calcd for C₁₁H₉F₃N₂ 226.07; Found 226.98.

3.6.3 Synthesis of H-1c and P-1c'

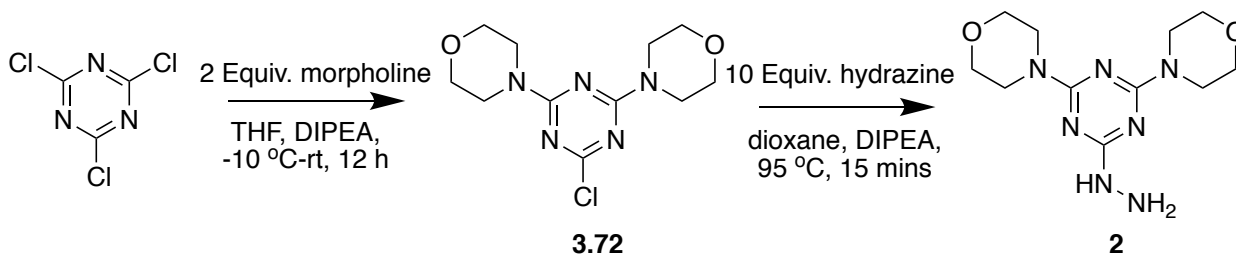


Scheme 3.24. Synthesis of **H-1c** and **P-1c'**.^{157, 158}

Hydrazine **1** (200 mg, 1.85 mmol) and diketone **c** (600 mg, 2.77 mmol) were dissolved in 5 ml of CH₃CN and stirred at room temperature for 12 hours. After evaporation of the solvent, column chromatography using 5% ethyl acetate in hexanes afford two products; **H-1c** (255 mg, 45%) as a slightly yellow solid (mp 79-80 °C) and **P-1c'** (23 mg, 4%) as a slightly yellow solid (mp 52-54 °C). **H-1c**. ¹H NMR (400 MHz, CDCl₃) δ 7.73-7.71 (2H, m), 7.46-7.40 (7H, m), 7.25-7.23 (1H, m), 3.74-3.48 (2H, dd, ²J_{H-H} = 17.99 Hz), 3.25 (1H, s). ¹³C NMR (400 MHz NMR CDCl₃) δ 148.7, 140.8, 131.3, 129.6, 128.9, 128.7, 126.1, 126.0, 124.6, 127.3-119.3 (q, ¹J_{C-F} = 271.0 Hz), 94.1-93.1 (q, ²J_{C-F} = 31.7 Hz), 44.2. MS (ESI/Q-TOF) m/z: [M+H]⁺ Calcd for C₁₆H₁₃F₃N₂O 306.10; Found 306.98. **P-1c'**. ¹H NMR (400 MHz, CDCl₃) δ 7.38-7.35 (8H, m), 7.28-7.26 (2H, m), 6.81 (1H, s). ¹³C NMR (400 MHz CDCl₃) δ 144.8, 143.8-142.7 (²J_{C-F} = 33.4 Hz), 139.3, 129.2, 129.1, 129.0, 128.8, 128.7, 128.5, 125.5, 125.9-117.4, (q, ¹J_{C-F} = 288.1 Hz), 105.6. MS (ESI/Q-TOF) m/z: [M+H]⁺ Calcd for C₁₆H₁₁F₃N₂ 288.09; Found 289.04.

vacuum, the residue re-dissolved in dichloromethane, washed with water, and dried over Na₂SO₄. Column chromatography was performed using 10% ethyl acetate in hexane to afford **P-1d** (20mg, 5%) and **H-1d** (80mg, 21%) as pale-yellow liquids in the mass ratio of 1:4 respectively. Addition of catalytic HCl in a solution of **H-1d** formed **P-1d** after 2 hours. **H-1d**. ¹H NMR (400 MHz, CDCl₃) δ 7.41-7.37 (5H, m), 3.35 (1H, s), 3.60-3.29 (2H, dd, ¹J_{H-H} = 19.1 Hz). ¹³C NMR (400 MHz CDCl₃) δ 138.8-137.9 (q, ²J_{C-F} = 40.3 Hz), 129.1, 127.5, 125.3, 124.0, 124.5--116.4 (q, ¹J_{C-F} = 269.5 Hz), 124.7-116.0 (q, ¹J_{C-F} = 287.1 Hz), 95.0-94.0 (q, ²J_{C-F} = 39.6 Hz), 41.5. MS (ESI/Q-TOF) m/z: [M+H]⁺ Calcd for C₁₁H₈F₆N₂O 298.05; Found 299.20. **P-1d**. ¹H NMR (400 MHz, CDCl₃) δ 7.41-7.37 (5H, m), 7.10 (1H, s). ¹³C NMR (400 MHz CDCl₃) δ 143.3-142.3.9 (q, ²J_{C-F} = 40.3 Hz), 138.2, 134.8-133.8 (q, ²J_{C-F} = 39.6 Hz), 130.3, 129.3, 125.7, 124.7-116.2 (q, ¹J_{C-F} = 288.0 Hz), 122.5-115.8 (q, ¹J_{C-F} = 269.1 Hz), 107.1. MS (ESI/Q-TOF) m/z: [M+H]⁺ Calcd for C₁₁H₆F₆N₂ 280.04; Found 281.07.

3.6.6 Synthesis of hydrazine 2



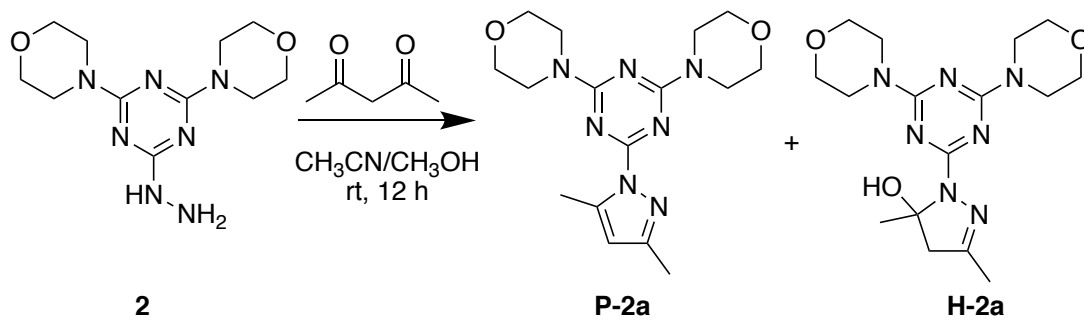
Scheme 3.27. Synthesis of hydrazine 2.

In a three neck round bottom flask purged with argon, cyanuric chloride (4.01 g, 21.8 mmol) was dissolved in 80 ml of tetrahydrofuran and the solution was chilled to -10 °C. A solution of morpholine (3.79 g, 43.5 mmol) and diisopropylethylamine (5.7 g, 44 mmol) of DIPEA in 30 ml THF were added dropwise. The reaction mixture was warmed to room temperature and stirred overnight at room temperature. The reaction mixture was filtered to remove salts before the

solvent was removed under vacuum. After dissolving the residue in 30 ml dichloromethane (x2) and washing the organic phase with 20 ml water, the organic layer was dried over MgSO₄. Upon removal of the solvent, column chromatography using 5% methanol in dichloromethane afforded dimorpholinomono-chlorotriazine intermediate **3.72** (5.90 g, 95%, mp 170-171 °C) as a white solid. ¹H NMR (400 MHz, CDCl₃) δ ¹H NMR 3.81-3.72 (16H, m). ¹³C NMR (400 MHz, CDCl₃) δ 169.7, 164.5, 66.7, 43.9. MS (ESI/Q-TOF) m/z: [M+H]⁺ Calcd for C₁₁H₁₉N₇O₂: 285.10, found: 286.04.

Subsequently, intermediate **3.72** (2.00 g, 7.00 mmol), diisopropylethylamine (1.00 g, 3.5 g) and hydrazine monohydrate (70 mmol, 10 equivalents) were dissolved in 5 ml of dioxane and the solution was subjected to microwave irradiation at 95 °C for 15 minutes. The solvent was removed under vacuum. The residues were dissolved in 25 ml dichloromethane (x2) and washed with 15 ml water. The organic layer was dried over MgSO₄ and the solvent was removed under vacuum. Crude product was further purified by column chromatography using 10:1 hexanes: ethyl acetate to afford **2** (1.8 g, 91%, mp 184-185 °C) as a white solid. ¹H NMR (400 MHz, CDCl₃) δ 6.09 (1H, s), 3.91 (2H, s), 3.79-3.71 (16H, m). ¹³C NMR (400 MHz, CDCl₃) δ 168.8, 165.1, 66.8, 43.6. MS (ESI/Q-TOF) m/z: [M+H]⁺ Calcd for C₁₁H₁₉N₇O₂ 281.16; Found 282.07.

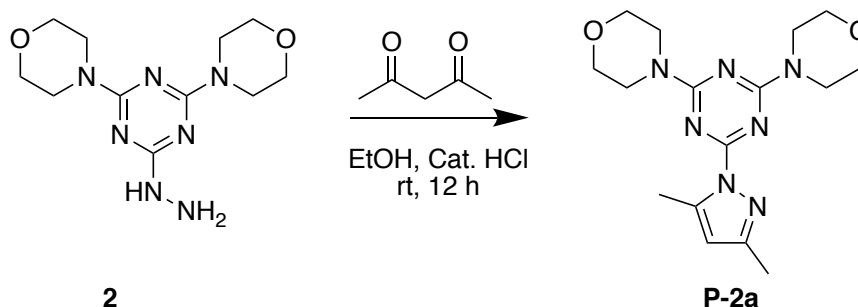
3.6.7 Synthesis of H-2a and P-2a



Scheme 3.28. Synthesis of hydrazine **H-2a** and **P-2a**.

Hydrazine **2** (88 mg, 0.31 mmol) and diketone **a** (63 mg, 0.62 mmol) of **a** were dissolved in 3 ml CH₃CN and 0.5 ml CH₃OH and stirred at room temperature for 12 hours. The solvent was removed under reduced pressure and purified by column chromatography using equal volumes of ethyl acetate and hexane to afford a white solid comprising an inseparable mixture of **P-2a** : **H-2a** (108 mg, 98%) in 1.6:1 ratio respectively. **H-2a**. ¹H NMR (400 MHz, CDCl₃) δ 5.90 (1H, s), 3.87-3.73 (16H, m), 3.13-3.09 (1H, d, ²J_{H-H}: 18.0 Hz), 2.86-2.81 (1H, d, ²J_{H-H}: 18.0 Hz), 2.10 (3H, s), 1.87 (3H, s). ¹³C NMR (400 MHz, CDCl₃) δ 164.5, 162.4, 153.8, 92.1, 66.7, 43.7, 27.5, 16.5. MS (ESI/Q-TOF) m/z: [M+H]⁺ Calcd for C₁₆H₂₅N₇O₃ 363.30; Found 364.26. **P-2a**. ¹H NMR (400 MHz, CDCl₃) δ 6.01 (1H, s), 3.87-3.73 (16H, m), 2.62 (3H, s), 2.32 (3H, s). ¹³C NMR (400 MHz, CDCl₃) δ 165.4, 163.3, 151.4, 143.1, 110.4, 66.8, 43.9, 16.1, 14.1. MS (ESI/Q-TOF) m/z: [M+H]⁺ Calcd for C₁₆H₂₃N₇O₂ 345.19; Found 346.13.

3.6.8 Synthesis of P-2a

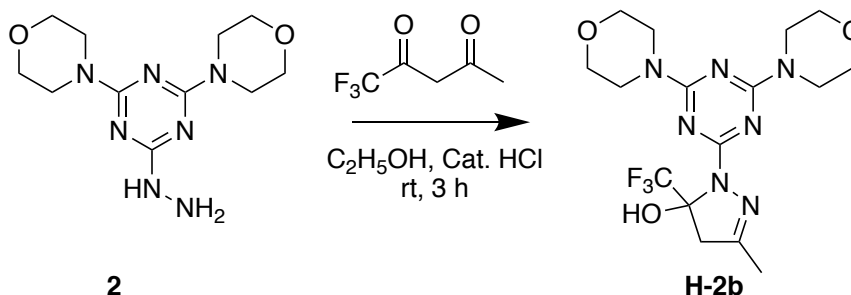


Scheme 3.29. Synthesis of hydrazine **P-2a**.

Hydrazine **2** (100 mg, 0.36 mmol) and diketone **a** (71 mg, 0.71 mmol) were dissolved in 4 ml of absolute ethanol and 1 ml of 1 M HCl was added before stirring the solution overnight at room temperature. After removing the excess solvent under vacuum, the residue was dissolved in 10 ml dichloromethane (x2) and washed with 10 ml water. Excess solvent was removed under reduced pressure and further purified by column chromatography using 15:1 DCM:MeOH to

afford **P-2a** (97 mg, 78%, mp 169-170 °C) as a white solid. ¹H NMR (400 MHz, CDCl₃) δ 6.01 (1H, s), 3.87-3.75 (16H, m), 2.64 (3H, s), 2.32 (3H, s). ¹³C NMR (400 MHz, CDCl₃) δ 165.4, 163.3, 151.4, 143.2, 110.5, 66.8, 43.9, 16.1, 14.1. MS (ESI/Q-TOF) m/z: [M+H]⁺ Calcd for C₁₆H₂₃N₇O₂ 345.19; Found 346.13.

3.6.9 Synthesis of H-2b

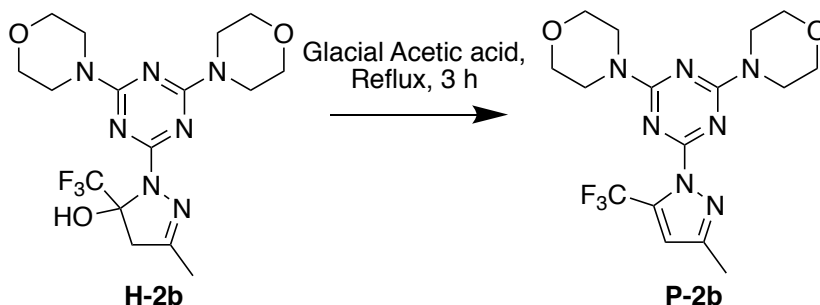


Scheme 3.30. Synthesis of hemiaminal **H-2b**.

Hydrazine **2** (110 mg, 0.39 mmol) and diketone **b** (121 mg, 0.78 mmol) were dissolved in 5 ml of C₂H₅OH and 0.3 ml of 1M HCl and stirred at room temperature for 12 hours. After the solvent was removed under vacuum, column chromatography using 2% methanol in dichloromethane afforded **H-2b** (113 mg, 69%, mp 178-179 °C) as a white solid.

Under neutral conditions, hydrazine **2** (74 mg, 0.26 mmol) and diketone **b** (150 mg, 0.97 mmol) were mixed in 2 ml absolute ethanol and 1 ml acetonitrile. Resulting solution was left to stir at room temperature for 12 hours. Excess solvent was removed and crude product was purified by column chromatography using 2% methanol in dichloromethane to afford **H-2b** (85 mg, 77%) as white solid. ¹H NMR (400 MHz NMR) δ 8.16 (1H, s), 3.76-3.74 (16H, m), 3.33-3.28 (1H, d, ²J_{H-H}; 18.9 Hz), 3.20-3.15 (1H, d, ²J_{H-H}; 18.9 Hz), 2.12 (3H, s). ¹³C NMR (400 MHz NMR) δ 164.0, 163.6, 153.6, 128.1-119.5 (q, ¹J_{C-F} = 288.1 Hz), 92.4-91.3 (q, ²J_{C-F} = 33.6 Hz), 66.7, 47.5, 43.7, 16.0. MS (ESI/Q-TOF) m/z: [M+H]⁺ Calcd for C₁₆H₂₂F₃N₇O₃ 417.17; Found 418.08.

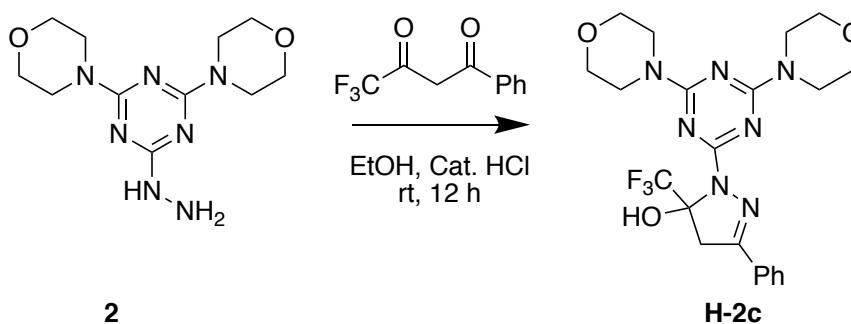
3.6.10 Synthesis of P-2b



Scheme 3.31. Synthesis of pyrazole **P-2b** from hemiaminal **H-2b**.

H-2b (23 mg, 0.055 mmol) of was refluxed in 3 ml of glacial acetic acid. After removal of the solvent, **P-2b** (22 mg, 100 %, mp 163-164°C) was obtained without further purification as a white solid. ^1H NMR (400 MHz, CDCl_3) δ 6.70 (1H, s), 3.89-3.75 (16H, m), 2.40 (3H, s). ^{13}C NMR (400 MHz NMR) δ 165.3, 162.1, 150.6, 134.5-133.5 (q, $^2J_{\text{C-F}} = 33.6$ Hz), 123.9-115.9 (q, $^1J_{\text{C-F}} = 288.1$ Hz), 112.9, 66.8, 43.9, 13.8. MS (ESI/Q-TOF) m/z : $[\text{M}+\text{H}]^+$ Calcd for $\text{C}_{16}\text{H}_{20}\text{F}_3\text{N}_7\text{O}_2$ 399.16; Found 400.09.

3.6.11 Synthesis of H-2c



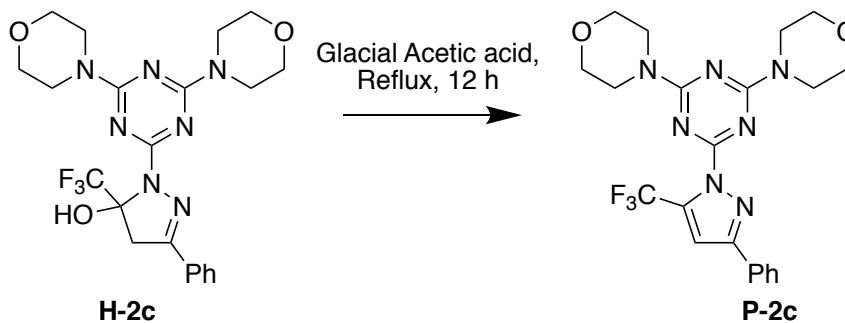
Scheme 3.32. Synthesis of hemiaminal **H-2c**.

Hydrazine **2** (100 mg, 0.36 mmol) and diketone **c** (154 mg, 0.71 mmol) were dissolved in 5 ml of $\text{C}_2\text{H}_5\text{OH}$ and 0.5 ml of 1M HCl (or in glacial acetic acid) and stirred at room temperature

for 12 hours. After removal of the solvent under reduced pressure, column chromatography using a 3:1 ratio of hexanes:ethyl acetate afforded **H-2c** (160 mg, 94%, mp 231-234 °C) as a white solid.

Alternatively, when hydrazine **2** (73 mg, 0.26 mmol) and diketone **c** (100 mg, 0.46 mmol) were mixed in absolute ethanol in the absence of acid, **H-2c** (109 mg 87%) as white solid was recovered after chromatography purifications using a 3:1 ratio of hexanes:ethyl acetate. ¹H NMR (400 MHz, CDCl₃) δ 8.20 (1H, s), 7.80-7.77 (2H, m), 7.45 (3H, m), 3.80-3.73 (17H, m), 3.65-3.60 (1H, d, ²J_{H-H} = 17.9 Hz). ¹³C NMR (400 MHz NMR) δ 163.9, 163.7, 152.1, 128.1-119.5 (q, ¹J_{C-F} = 288.7 Hz), 92.9-91.9 (q, ²J_{C-F} = 33.4 Hz), 66.7, 44.4, 43.7. MS (ESI/Q-TOF) m/z: [M+H]⁺ Calcd for C₂₁H₂₄F₃N₇O₃ 479.19; Found 480.08.

3.6.12 Synthesis of P-2c



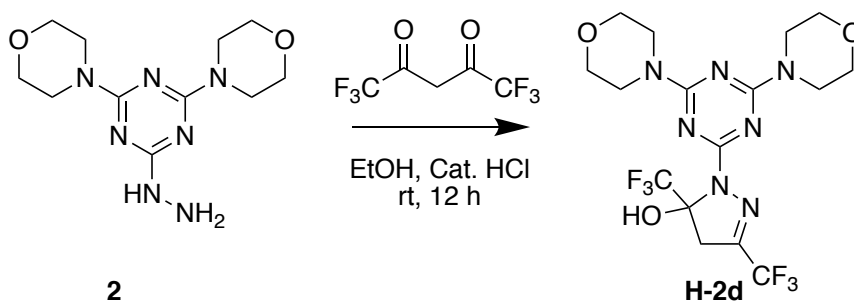
Scheme 3.33. Synthesis of pyrazole **P-2c** from hemiaminal **H-2c**.

H-2c (10 mg, 0.021 mmol) was dissolved in 2 ml glacial acetic acid and refluxed for 12 hours to obtain **P-2c** (9.5 mg, 100%, mp 161-162 °C) after removing of the solvent under vacuum.

Alternatively, hydrazine **2** (100 mg, 0.36 mmol) and diketone **c** (154 mg, 0.71 mmol) were dissolved in 3 ml of glacial acetic acid and refluxed for 12 hours. After removal of the solvent, column chromatography using 5% of methanol in dichloromethane afforded **P-2c** (132 mg, 80%) as a white solid. ¹H NMR (400 MHz, CDCl₃) δ 7.94-7.92 (2H, m), 7.48-7.41 (3H, m), 7.22 (1H, s), 3.95-3.78 (16H, m). ¹³C NMR (400 MHz NMR) δ 165.3, 162.3, 152.1, 135.2-134.0 (q, ²J_{C-F}=

40.5 Hz), 131.2, 129.7, 129.2, 128.7, 126.3, 128.1-119.5 (q, $^1J_{C-F} = 268.5$ Hz), 110.1, 66.7, 43.9.
MS (ESI/Q-TOF) m/z: $[M+H]^+$ Calcd for $C_{21}H_{22}F_3N_7O_2$ 461.18; Found 462.08.

3.6.13 Synthesis of H-2d

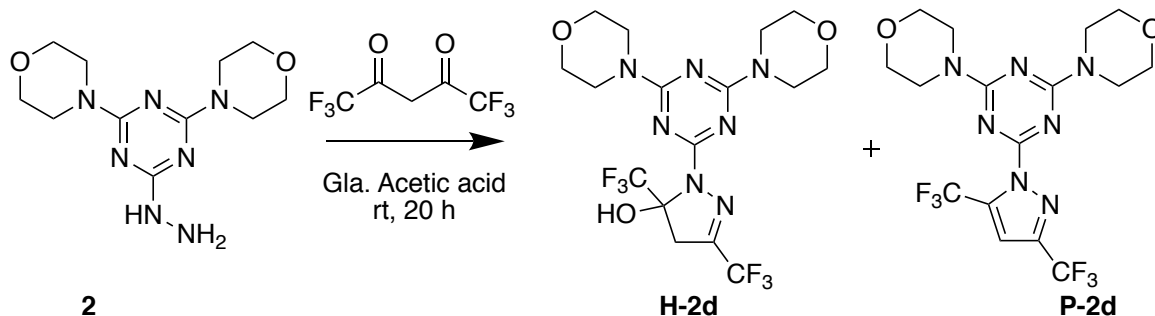


Scheme 3.34. Synthesis of hemiaminal **H-2d**.

Hydrazine **2** (93 mg, 0.33 mmol) was dissolved in 3 ml of absolute ethanol before diketone **d** (71 mg, 0.34 mmol) and 0.5 ml 1M HCl were added. After stirring at room temperature overnight, the solvent was removed under vacuum. The residue was dissolved in 5 ml dichloromethane (x2) and washed with 5 ml water. After drying the organic phase with $MgSO_4$ and evaporating the solvent, column chromatography using 2:1 hexanes:ethyl acetate afforded **H-2d** (112 mg, 72%, mp 155-158 °C) as a white solid.

Hydrazine **2** (100 mg, 0.36 mmol) and diketone **d** (150 mg, 0.72 mmol) were mixed in absolute ethanol and solution was left to stir at room temperature for 12 hours. After chromatographic purifications using 2:1 hexanes:ethyl acetate, **H-2d** (126 mg 75%) was recovered as white solid. 1H NMR (400 MHz, $CDCl_3$) δ 7.95 (1H, s), 3.75-3.70 (16H, m), 3.58-3.37 (2H, dd, $^2J_{H-H} = 18.2$ Hz). ^{13}C NMR (400 MHz NMR) δ 163.8, 142.7-141.5 (q, $^2J_{C-F} = 39.4$ Hz), 127.4-118.9 (q, $^1J_{C-F} = 287.7$ Hz), 123.6-115.5 (q, $^1J_{C-F} = 270.8$ Hz), 93.4-92.4 (q, $^2J_{C-F} = 34.3$ Hz), 66.6, 43.9, 41.8. MS (ESI/Q-TOF) m/z: $[M+H]^+$ Calcd for $C_{16}H_{19}F_6N_7O_3$ 471.15; Found 472.27.

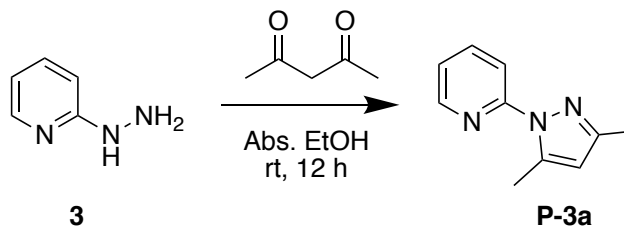
3.6.14 Synthesis of H-2d and P-2d.



Scheme 3.35. Synthesis of hemiaminal **H-2c** and **P-2c**.

Hydrazine **2** (142 mg, 0.505 mmol) and diketone **d** (95 mg, 0.45 mmol) were dissolved in 5 ml glacial acetic acid and refluxed for 20 hours. After removing the excess solvent, the residue was dissolved in 10 ml dichloromethane (x2) and washed with 5 ml water. After evaporating the organic layer, chromatographic purification using 20:1 hexanes:ethyl acetate afforded a 5.9:1 mixture of **P-2d** (45%):**H-2d** (7%) (108 mg). **P-2d**: $^1\text{H NMR}$ (400 MHz, CDCl_3) δ 7.11 (1H, s), 3.75-3.70 (16H, m). $^{13}\text{C NMR}$ (400 MHz NMR) δ 163.8, 144.0-143.0 (q, $^2J_{\text{C-F}} = 39.4$ Hz), 134.0-133.0 (q, $^2J_{\text{C-F}} = 34.3$ Hz), 127.4-118.9 (q, $^1J_{\text{C-F}} = 287.7$ Hz), 123.6-115.5 (q, $^1J_{\text{C-F}} = 270.8$ Hz), 66.6, 43.9. MS (ESI/Q-TOF) m/z : $[\text{M}+\text{H}]^+$ Calcd for $\text{C}_{16}\text{H}_{17}\text{F}_6\text{N}_7\text{O}_2$ 453.01; Found 454.27.

3.6.15 Synthesis of P-3a

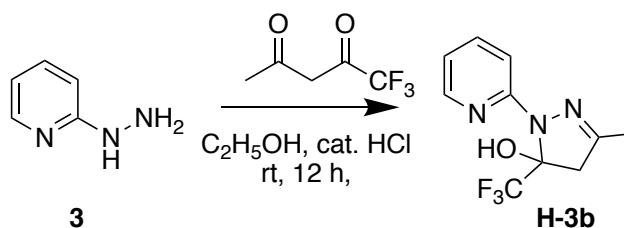


Scheme 3.36. Synthesis of pyrazole **P-3a**.

Hydrazine **3** (227 mg, 2.08 mmol) was dissolved in 4 ml absolute ethanol before diketone **a** (212 mg, 2.12 mmol) was added. After stirring at room temperature for 12 hours, the solvent

was removed under reduced pressure. The residues were dissolved in 15 ml dichloromethane (x2), washed with 10 ml water, and dried over MgSO₄. The crude product was further purified by column chromatography using 2:1 hexanes:ethyl acetate to afford **P-3a** (345 mg, 96%) as a clear oil. ¹H NMR (400 MHz, CDCl₃) δ 8.41 (1H, s), 7.85-7.77 (1H, m), 7.75-7.72 (1H, m), 7.13-7.10 (1H, m), 5.99 (1H, s), 2.63 (3H, s), 2.30 (3H, s). ¹³C NMR (400 MHz CDCl₃) δ 153.6, 149.8, 147.5, 141.5, 138.1, 120.7, 115.7, 109.0, 14.4, 13.6. MS (ESI/Q-TOF) m/z: [M+H]⁺ Calcd for C₁₀H₁₁N₃ 173.10; Found 174.10.

3.6.16 Synthesis of H-3b



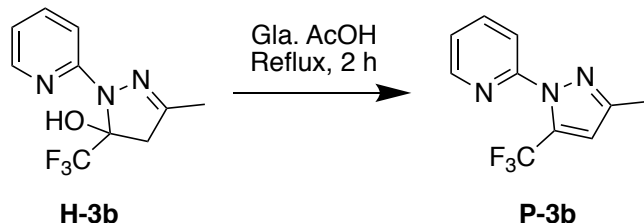
Scheme 3.37. Synthesis of hemiaminal **H-3b**.

Hydrazine **3** (265 mg, 2.43 mmol) and diketone **b** (140 mg, 0.9 mmol) were dissolved in 5 ml absolute ethanol before 0.5 ml 1M HCl was added. After stirring the reaction mixture at room temperature for 12 hours, solvent was removed under reduced pressure. Upon dissolving the residues in 15 ml dichloromethane (x2), the organic layer was washed with 10 ml water, and dried over Na₂SO₄. Excess solvent was removed under vacuum, crude product was purified by column chromatography using 2:1 hexanes:ethyl acetate to afford **H-3b** (201 mg, 91%) as clear liquid.

Under neutral conditions, hydrazine **3** (220 mg, 2.0 mmol) and diketone **b** (146 mg, 0.948 mmol) were mixed in 3 ml absolute ethanol and the resulting solution was left to stir at room temperature for 12 hours. Excess solvent was removed under reduced pressure and crude product

was purified using chromatographic purifications by using a 2:1 mixture of hexanes:ethyl acetate to recover **H-3b** (185 mg 80%) as clear liquid. ^1H NMR (400 MHz, CDCl_3) δ 8.75 (1H, s), 8.08-8.06 (1H, m), 7.64-7.60 (1H, m), 7.35-7.32 (1H, m), 6.83-6.80 (1H, m), 3.36-3.13 (2H, dd, $^2J_{\text{H-H}}$: 18.7 Hz), 2.09 (3H, s). ^{13}C NMR (400 MHz CDCl_3) δ 157.0, 151.0, 145.3, 138.4, 128.2-119.7 (q, $^1J_{\text{C-F}}$: 287.2 Hz), 115.7, 111.9, 93.3-92.3 (q, $^2J_{\text{C-F}}$: 33.1 Hz), 47.9, 15.6. MS (ESI/Q-TOF) m/z : $[\text{M}+\text{H}]^+$ Calcd for $\text{C}_{10}\text{H}_{10}\text{F}_3\text{N}_3\text{O}$ 248.08; Found 247.07.

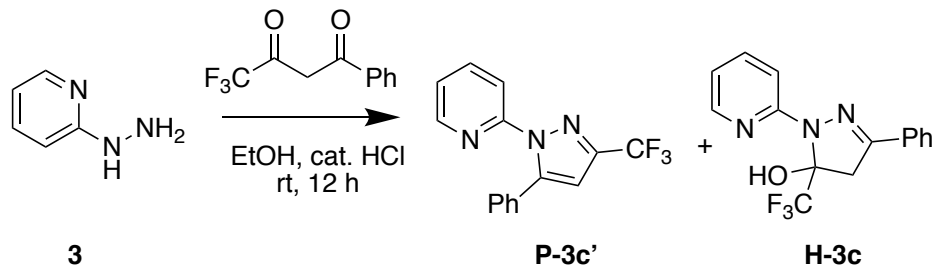
3.6.17 Synthesis of P-3b



Scheme 3.38. Synthesis of pyrazole **P-3b** from **H-3b**.

H-3b (130 mg, 0.56 mmol) was dissolved in 4 ml glacial acetic acid and refluxed for 2 hours. After removing the excess solvent under vacuum, the residue was dissolved in 15 ml dichloromethane (x2), washed with 10 ml water, and dried over MgSO_4 . After removing the solvent under vacuum **P-3b** (113 mg, 89 %) was recovered as clear oil. ^1H NMR (400 MHz, CDCl_3) δ 8.51 (1H, s), 7.87-7.83 (1H, m), 7.78-7.76 (1H, m), 7.32-7.29 (1H, m), 6.97-6.77 (1H, m), 6.69 (1H, s), 2.39 (3H, s). ^{13}C NMR (400 MHz NMR) δ 151.4, 149.7, 148.1, 138.5, 134.7-131.1 (q, $^2J_{\text{C-F}}$: 33.0 Hz), 122.9, 128.2-119.7 (q, $^1J_{\text{C-F}}$: 287.0 Hz), 116.5, 111.0, 13.5. MS (ESI/Q-TOF) m/z : $[\text{M}+\text{H}]^+$ Calcd for $\text{C}_{10}\text{H}_8\text{F}_3\text{N}_3$ 227.07; Found 228.13.

3.6.18 Synthesis of H-3c and P-3c'



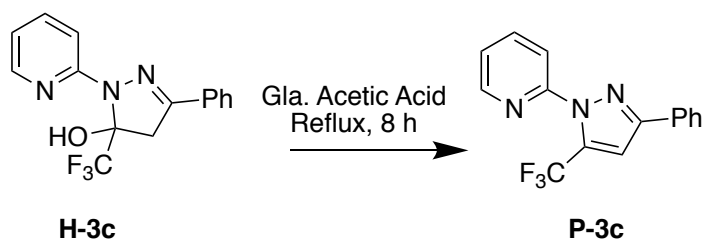
Scheme 3.39. Synthesis of hemiaminal **H-3c** and pyrazole **P-3c'**.¹⁵⁸

Hydrazine **3** (350 mg, 3.20 mmol) and diketone **c** (900 mg, 3.84 mmol) were dissolved in 3 ml 200 proof ethanol followed by the addition of 0.5 ml 1M HCl. After stirring at room temperature for 12 hours, excess solvent was removed under vacuum, extracted and collected in 10 ml DCM (x2). The organic layer was dried over Na₂SO₄ and crude product was further purified using 2:1 hexanes:ethyl acetate to afford two separate products **H-3c** (630 mg, 64%, mp 62-64 °C) and **P-3c'** (24 mg, 3%, mp 72-74 °C) as white solids.

Alternatively, when hydrazine **3** (200 mg, 1.45 mmol) and diketone **c** (102 mg, 0.47 mmol) were mixed in absolute ethanol in the absence of acid, **H-3c** (132 mg 91%) as white solid was recovered after stirring for 12 hours followed by chromatographic purifications using 2:1 hexanes:ethyl acetate. ¹H NMR (400 MHz, CDCl₃) δ 8.73 (1H, s), 8.14-8.12 (1H, m), 7.74-7.67 (3H, m), 7.54-7.44 (4H, m), 6.90-6.87 (1H, m), 3.79-3.58 (2H, dd, ²J_{H-H}: 18.3 Hz). ¹³C NMR (400 MHz NMR CDCl₃) δ 156.7, 149.8, 145.5, 138.5, 131.1, 130.0, 128.8, 126.1, 128.2-119.7 (q, ¹J_{C-F}: 288.4 Hz), 116.3, 111.9, 93.3-92.7 (q, ²J_{C-F}: 33.1 Hz), 44.1. MS (ESI/Q-TOF) m/z: [M+H]⁺ Calcd for C₁₅H₁₂F₃N₃O 307.09; Found 308.10. **P-3c'**. ¹H NMR (400 MHz, CDCl₃) δ 8.14-8.13 (1H, m), 7.98-7.97 (2H, m), 7.74-7.71 (1H, m), 7.56-7.45 (4H, m), 6.96-6.94 (1H, m), 5.35 (1H, s). ¹³C NMR (400 MHz NMR) δ 156.8, 152.1, 145.5, 138.5, 131.1, 130.0, 128.8, 126.9, 128.2-

119.7 (q, $^1J_{C-F}$: 279.3 Hz), 117.1, 112.0, 91.3-89.7 (q, $^2J_{C-F}$: 38.7 Hz). MS (ESI/Q-TOF) m/z: $[M+H]^+$ Calcd for $C_{15}H_{10}F_3N_3$ 289.09; Found 290.08.

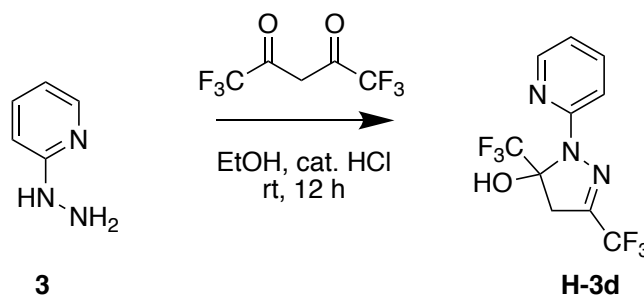
3.6.19 Synthesis of P-3c



Scheme 3.40. Synthesis of pyrazole **P-3c** from hemiaminal **H-3c**.¹⁵⁸

H-3c (164 mg, 0.53 mmol) was refluxed in 4 ml glacial acetic acid for 8 hours. Excess solvent was removed under vacuum and residue was dissolved in 10 ml DCM. The organic layer was washed with 10 ml water and dried over $MgSO_4$. Excess solvent was removed under reduced pressure to recover **P-3c** (132 mg, 86%, mp 66-68°C) as white solid. 1H NMR (400 MHz, $CDCl_3$) δ 8.55-8.54 (1H, m), 7.97-7.87 (4H, m), 7.51-7.43 (3H, m), 7.33-7.31 (1H, m), 7.23 (1H, s). ^{13}C NMR (400 MHz NMR) δ 151.9, 151.5, 148.0, 138.6, 134.2-133.0 (q, $^1J_{C-F}$: 40.8 Hz), 131.6, 128.9, 126.0, 122.9, 124.0-116.0 (q, $^2J_{C-F}$: 268.6 Hz), 116.4, 108.61, 108.58. MS (ESI/Q-TOF) m/z: $[M+H]^+$ Calcd for $C_{15}H_{10}F_3N_3$ 289.09; Found 290.08.

3.6.20 Synthesis of H-3d



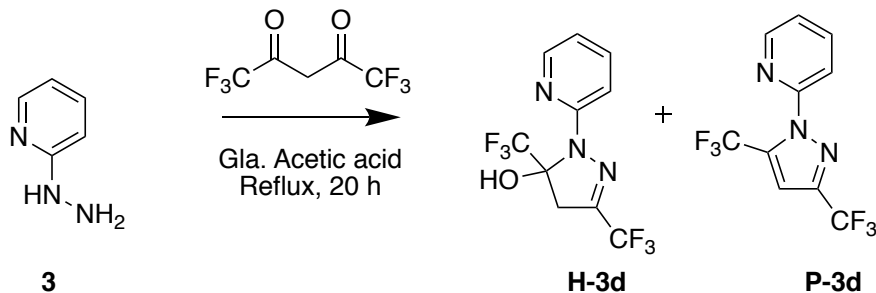
Scheme 3.41. Synthesis of hemiaminal **H-3d**

Hydrazine **3** (115 mg, 1.06 mmol) and diketone **d** (110 mg, 0.52 mmol) were dissolved in 4 ml 200 proof ethanol and 0.5 ml 1M HCl was added. The resulting reaction mixture was left to stir at room temperature for 12 hours. Excess solvent was removed under vacuum, residue was dissolved in 10 ml DCM (x2), washed with 10 ml water, and dried over Na₂SO₄. Crude product was further purified by column chromatography using 2:1 hexanes:ethyl acetate to afford **H-3d** (65 mg, 40%) as light yellow liquid.

Alternatively, when hydrazine **3** (135 mg, 1.23 mmol) and diketone **d** (200 mg, 0.96 mmol) were mixed in absolute ethanol in the absence of acid. After chromatographic purifications using 2:1 hexanes:ethyl acetate, **H-3d** (160 mg 56 %) was recovered as slightly yellow liquid.

A Bis-hemiaminal along with hemiaminal was observed in the NMR spectrum of crude product made from **3** and **d** under neutral conditions. However, during chromatographic purification the bis-hemiaminal was converted to hemiaminal **H-3d**. ¹H NMR (400 MHz, CDCl₃) δ 8.47 (1H, s), 8.17-8.15 (1H, m), 7.75-7.73 (1H, m), 7.43-7.41 (1H, m), 7.01-7.00 (1H, m), 3.61-3.38 (2H, dd, ²J_{H-H} = 19.2 Hz). ¹³C NMR (400 MHz NMR) δ 155.7, 145.6, 140.4-139.3 (q, ¹J_{C-F}: 39.3 Hz), 139.0, 127.5-119.0 (q, ¹J_{C-F}: 287.5 Hz), 123.8-115.7 (q, ¹J_{C-F}: 270.1 Hz), 118.4, 112.5, 94.8-93.8 (q, ²J_{C-F}: 33.9 Hz), 41.9. MS (ESI/Q-TOF) m/z: [M+H]⁺ Calcd for C₁₀H₇F₆N₃O 299.05; Found 300.03.

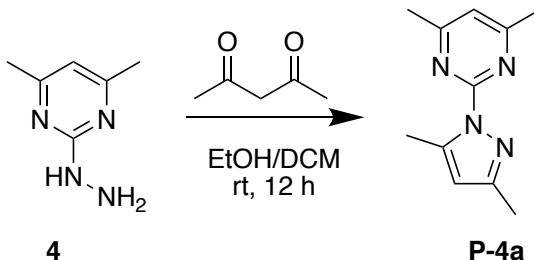
3.6.21 Synthesis of mixture of H-3d and P-3d



Scheme 3.42. Synthesis of hemiaminal **H-3d** and **P-3d**.

Hydrazine **3** (150 mg, 1.3 mmol) and diketone **d** (150 mg, 0.7 mmol) were dissolved in 5 ml glacial acetic acid. After refluxing the resulting solution for 20 hours, the mixture was dissolved in 10 ml DCM (x2), washed with 10 ml water, and further purified by column chromatography using 9:1 hexane: ethyl acetate to afford an inseparable mixture (65 mg) of **P-3d** (23%) and **H-3d** (8%) as light yellow liquid in the ratio of 2.7 to 1 in favor of **P-3d**. **H-3d**: $^1\text{H NMR}$ (400 MHz, CDCl_3) δ 8.17-8.15 (0.36H, m), 7.72-7.71 (0.36H, m), 7.43-7.41 (0.36H, m), 7.00-6.98 (0.35H, m), 3.61-3.37 (0.74H, dd, $^2J_{\text{H-H}} = 19.2$ Hz). $^{13}\text{C NMR}$ (400 MHz NMR) δ 155.7, 145.6, 140.4-139.3 (q, $^1J_{\text{C-F}}: 39.3$ Hz), 139.0, 127.5-119.0 (q, $^1J_{\text{C-F}}: 287.5$ Hz), 123.8-115.7 (q, $^1J_{\text{C-F}}: 270.1$ Hz), 118.4, 116.4, 112.5, 94.8-93.8 (q, $^2J_{\text{C-F}}: 33.9$ Hz), 41.9. MS (ESI/Q-TOF) m/z : $[\text{M}+\text{H}]^+$ Calcd for $\text{C}_{10}\text{H}_7\text{F}_6\text{N}_3\text{O}$ 299.05; Found 300.03. **P-3d**: $^1\text{H NMR}$ (400 MHz, CDCl_3) δ 8.52 (1H, m), 7.92-7.85 (2H, m), 7.43-7.41 (1H, m), 7.14 (1H, s). $^{13}\text{C NMR}$ (400 MHz NMR) δ 151.1, 148.6, 143.7-142.5 (q, $^2J_{\text{C-F}}: 39.3$ Hz), 138.7, 127.5-119.0 (q, $^1J_{\text{C-F}}: 287.5$ Hz), 124.1, 123.8-115.7 (q, $^1J_{\text{C-F}}: 270.1$ Hz), 118.4, 116.4, 112.5, 134.7-133.4 (q, $^2J_{\text{C-F}}: 33.9$ Hz), 108.9. MS (ESI/Q-TOF) m/z : $[\text{M}+\text{H}]^+$ Calcd for $\text{C}_{10}\text{H}_5\text{F}_6\text{N}_3$ 281.04; Found 282.00.

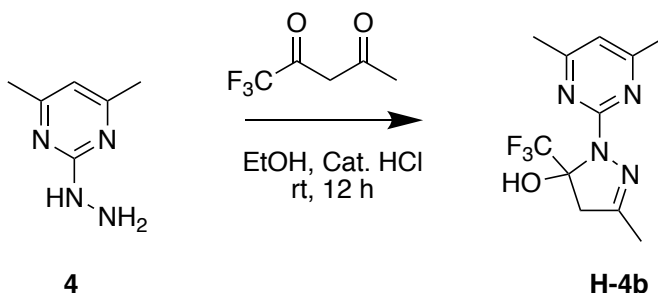
3.6.22 Synthesis of P-4a



Scheme 3.43. Synthesis of pyrazole **P-4a**.

Hydrazine **4** (143 mg, 1.03 mmol) and diketone **a** (106 mg, 1.06 mmol) were dissolved in total of 4 ml of equal volumes of 200 proof ethanol and dichloromethane. After stirring the resulting solution at room temperature for 12 hours, excess solvent was removed under vacuum. The residue was dissolved in 10 ml DCM (x2), washed with water, dried over Na₂SO₄, and further purified by column chromatography using 9:1 hexanes: ethyl acetate to afford **P-4a** (199 mg, 96%, mp 57-58°C) as light yellow solid. ¹H NMR (400 MHz, CDCl₃) δ 6.74 (1H, s), 5.88 (1H, s), 2.51 (3H, s), 2.39 (6H, s), 2.21 (3H, s). ¹³C NMR (400 MHz CDCl₃) δ 168.4, 157.0, 150.7, 142.6, 116.8, 109.8, 23.9, 15.2, 13.8. MS (ESI/Q-TOF) m/z: [M+H]⁺ Calcd for C₁₁H₁₄N₄ 202.12; Found 203.13.

3.6.23 Synthesis of H-4b



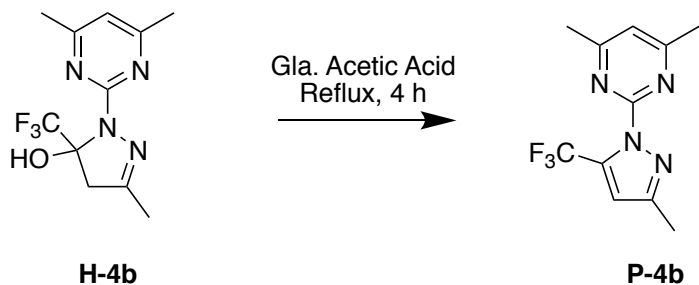
Scheme 3.44. Synthesis of hemiaminal **H-4b**.¹⁶¹

Hydrazine **4** (150 mg, 1.08 mmol) and diketone **b** (139 mg, 0.90 mmol) were dissolved in 4 ml 200 proof ethanol and 0.5 ml 1M HCl. After stirring resulting solution at room temperature

for 12 hours, excess solvent was removed under vacuum. The crude product was dissolved in 10 ml DCM (x2), washed with 5 ml water, and dried over Na₂SO₄. Crude product was further purified by column chromatography using 9:1 hexane: ethyl acetate to afford **H-4b** (217 mg, 88%, mp 123-124 °C) as white solid.

Alternatively, when hydrazine **4** (42 mg, 0.18 mmol) and diketone **b** (100 mg, 0.65 mmol) were mixed in absolute ethanol in the absence of acid. After stirring the resulting solutions for 12 hours, **H-4b** (42 mg, 82%) was recovered as white solid after chromatography purifications using 9:1 hexane: ethyl acetate. ¹H NMR (400 MHz, CDCl₃) δ 8.19 (1H, s), 6.44 (1H, s), 3.22-3.03 (2H, dd, ¹J_{H-H} = 18.8 Hz), 2.26 (6H, s), 1.99 (3H, s). ¹³C NMR (400 MHz CDCl₃) δ 167.6, 159.0, 152.9, 128.0-119.3 (q, ²J_{C-F} = 288.4 Hz), 112.9, 92.3-91.3 (q, ²J_{C-F} = 33.2 Hz), 47.3, 23.8, 15.6. MS (ESI/Q-TOF) m/z: [M+H]⁺ Calcd for C₁₁H₁₃F₃N₄O 274.10; Found 275.07.

3.6.24 Synthesis of P-4b

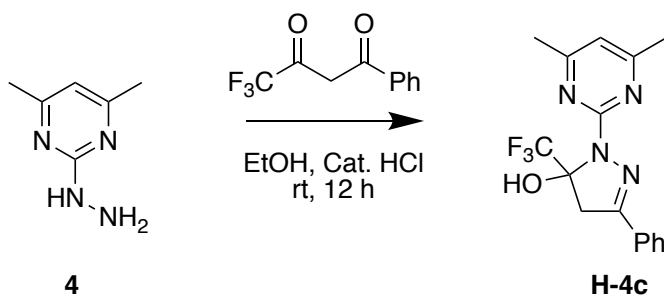


Scheme 3.45. Synthesis of pyrazole **P-4b** from hemiaminal **H-4b**.¹⁶¹

H-4b (85 mg, 0.31 mmol) was dissolved in 4 ml of glacial acetic acid and resulting reaction mixture was refluxed for 4 hours. Crude product was dissolved in 10 ml DCM, washed with 10 ml water, and dried over Na₂SO₄. Excess solvent was removed to afford **P-4b** (77 mg, 97%, mp 58-60 °C) as white solid. ¹H NMR (400 MHz, CDCl₃) δ 6.97 (1H, s), 6.68 (1H, s), 2.53 (6H, s), 2.39 (3H, s). ¹³C NMR (400 MHz CDCl₃) δ 169.1, 155.3, 150.7, 134.7-133.3 (q, ²J_{C-F} =

33.2 Hz), 121.2, 123.9-115.9 (q, $^2J_{C-F} = 288.4$ Hz), 112.3, 23.8, 13.7. MS (ESI/Q-TOF) m/z: $[M+H]^+$ Calcd for $C_{11}H_{11}F_3N_4$ 256.09; Found 257.13.

3.6.25 Synthesis of H-4c

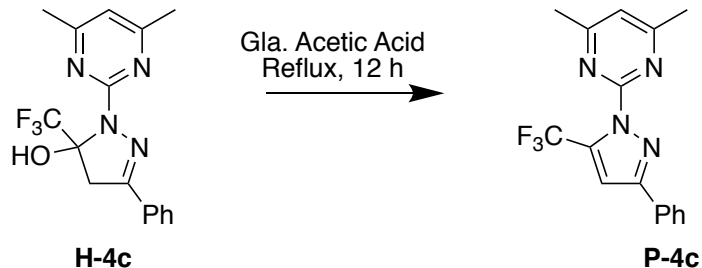


Scheme 3.46. Synthesis of hemiaminal **H-4c**.¹⁶¹

Hydrazine **4** (115 mg, 0.833 mmol) and diketone **c** (163 mg, 0.757 mmol) and 0.5 ml of 1 M HCl were mixed with 4 ml 200 proof ethanol. After stirring the resulting solution at room temperature for 12 hours, excess solvent was removed under vacuum. The residues were dissolved in 15 ml DCM (x2), washed with 10 ml water, dried over Na_2SO_4 , and further purified by column chromatography using 2:1 hexanes:ethyl acetate to recover **H-4c** (123 mg, 48%, mp 158-160 °C) as white solid.

Alternatively, hydrazine **4** (25 mg, 0.18 mmol) and diketone **c** (33 mg, 0.15 mmol) were left to stir at room temperature in absolute ethanol for 12 hours. **H-4c** (39 mg, 78%) was recovered as white solid after chromatographic purifications using 2:1 hexanes:ethyl acetate. 1H NMR (400 MHz, $CDCl_3$) δ 8.48 (1H, s), 7.84-7.81 (2H, m), 7.44-7.43 (3H, m), 6.66 (1H, s), 3.82-3.64 (2H, dd, $^2J_{H-H} = 18.35$ Hz), 2.47 (6H, s). ^{13}C NMR (400 MHz $CDCl_3$) δ 167.8, 159.2, 151.5, 130.6, 130.3, 128.6, 126.7, 128.2-119.6 (q, $^1J_{C-F} = 288.4$ Hz), 113.6, 92.7-91.7 (q, $^2J_{C-F} = 33.2$ Hz), 44.02, 24.1. MS (ESI/Q-TOF) m/z: $[M+H]^+$ Calcd for $C_{16}H_{15}F_3N_4O$ 336.12; Found 337.07.

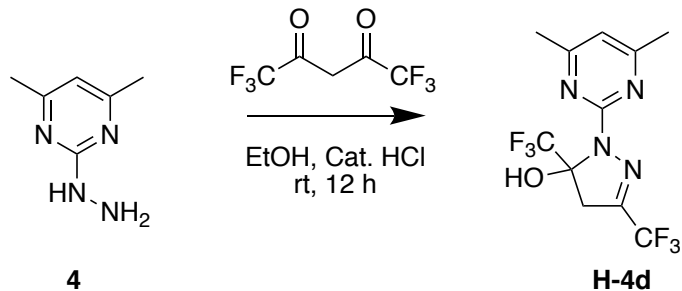
3.6.26 Synthesis of P-4c



Scheme 3.47. Synthesis of pyrazole **P-4c** from hemiaminal **H-4c**.¹⁶¹

H-4c (60 mg, 0.18 mmol) was dissolved in 4 ml glacial acetic acid and the solution mixture was refluxed for 12 hours. Reaction mixture was dissolved in 10 ml DCM, washed with 10 ml water, and dried over Na₂SO₄. Excess solvent was removed to afford **P-4c** (55 mg, 98%, mp 109-112 °C) as white solid. ¹H NMR (400 MHz, CDCl₃) δ 7.94-7.92 (2H, m), 7.45-7.39 (3H, m), 7.23 (1H, s), 7.07 (1H, s), 3.82-3.64, 2.60 (6H, s). ¹³C NMR (400 MHz CDCl₃) δ 169.3, 155.6, 152.8, 134.7-133.3 (q, ²J_{C-F} = 33.2 Hz), 131.2, 129.1, 128.7, 126.3, 131.1-123.1 (q, ¹J_{C-F} = 288.4 Hz), 119.1, 109.5, 22.7. MS (ESI/Q-TOF) m/z: [M+H]⁺ Calcd for C₁₆H₁₃F₃N₄ 318.11; Found 319.08.

3.6.27 Synthesis of H-4d



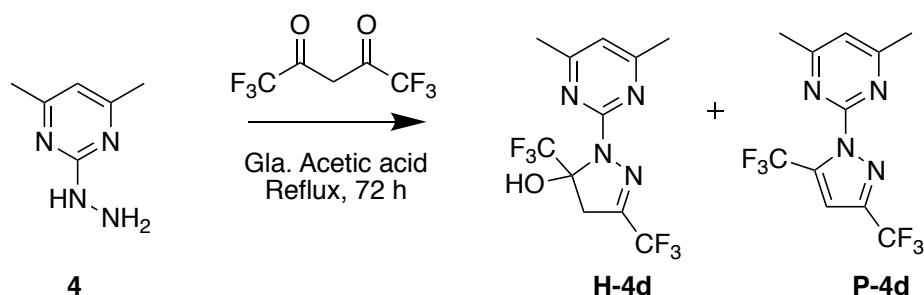
Scheme 3.48. Synthesis of hemiaminal **H-4d**.¹⁶¹

Hydrazine **4** (150 mg, 1.09 mmol) and diketone **d** (187 mg, 0.90 mmol) were dissolved in 4 ml 200 proof ethanol and 0.5 ml of 1M HCl was added. After stirring the reaction mixture overnight at room temperature, excess solvent was removed under vacuum. The residue was

dissolved in 10 ml DCM (x2), washed in 10 ml water, dried over Na₂SO₄, and further purified by column chromatography using 2:1 hexanes:ethyl acetate to afford **H-4d** (70 mg, 25%, mp 57-59 °C) as a white solid.

Under neutral conditions, hydrazine **4** (19 mg, 0.14 mmol) and diketone **d** (50 mg, 0.24 mmol) were mixed in 2 ml absolute ethanol and left to stir overnight at room temperature. **H-4d** (31 mg 69%) was recovered as white solid after chromatographic purifications using 2:1 hexanes:ethyl acetate. ¹H NMR (400 MHz, CDCl₃) δ 8.16 (1H, s), 6.76 (1H, s), 3.62-3.40 (2H, dd, ²J_{H-H} = 19.29 Hz), 2.46 (6H, s). ¹³C NMR (400 MHz CDCl₃) δ 168.3, 158.6, 142.0-140.8 (q, ²J_{C-F} = 39.2 Hz), 127.4-118.3 (q, ¹J_{C-F} = 270.4 Hz), 124.9-115.3 (q, ¹J_{C-F} = 288.4 Hz), 115.6, 94.0-93.0 (q, ²J_{C-F} = 33.2 Hz), 41.8, 23.9. MS (ESI/Q-TOF) m/z: [M+H]⁺ Calcd for C₁₁H₁₀F₆N₄O 328.08; Found 329.13.

3.6.28 Synthesis of mixture of H-4d and P-4d



Scheme 3.49. Synthesis of pyrazole **P-4c** from hemiaminal **H-4c**.¹⁶¹

Hydrazine **4** (110 mg, 0.79 mmol) and diketone **d** (140 mg, 0.67 mmol) were dissolved in 5 ml glacial acetic acid and resulting reaction mixture was refluxed for 72 hours. Excess solvent was removed under vacuum, the residue was dissolved in 10 ml DCM (x2), washed with 10 ml water, dried over Na₂SO₄, and further purified by column chromatography using 9:1 hexanes:ethyl acetate to afford isolable mixture of **H-4d** and **P-4d** (175 mg, 84%) in the ratio of 2.7:1 in favor of

P-4d. P-4d: ^1H NMR (400 MHz, CDCl_3) δ 7.15 (2H, m), 2.61 (6H, s). ^{13}C NMR (400 MHz CDCl_3) δ 169.7, 155.0, 144.3-143.2 (q, $^2J_{\text{C-F}} = 33.2$ Hz), 135.7-134.4 (q, $^2J_{\text{C-F}} = 39.2$ Hz), 127.4-118.3 (q, $^1J_{\text{C-F}} = 270.4$ Hz), 124.9-115.3 (q, $^1J_{\text{C-F}} = 288.4$ Hz), 109.4, 115.0, 23.9. MS (ESI/Q-TOF) m/z : $[\text{M}+\text{H}]^+$ Calcd for $\text{C}_{11}\text{H}_7\text{F}_6\text{N}_4$ 310.08; Found 311.13.

Chapter 4: Efficient synthesis of macrocycles of sizes ranging 22 to 28

4.1 Introduction of macrocycles

A compound is considered a macrocycle when it contains a cyclic framework of at least twelve atoms. Various macrocycles with sizes up to 50+ atoms have been naturally found. However, macrocycles with 14, 16, and 18 members frameworks are the most common.¹⁸¹ Over the years, numerous macrocycles have been isolated from natural sources or/and synthesized.¹⁸² Some useful natural macrocycles are erythromycin, nisin, rapamycin, vancomycin, cyclosporin, and epothilone.¹⁸³⁻¹⁸⁶

Erythromycin **4.1**, the first natural macrolide ever discovered, is widely prescribed in patients allergic to penicillin (Figure 4.1). Some other widely used derivatives of this macrolide are azithromycin, clarithromycin, clindamycin, and roxithromycin.¹⁸⁷⁻¹⁹⁰ Azithromycin and clarithromycin are derived (Figure 4.1) from erythromycin to improve the absorption of the drug in the body and decrease side effects.¹⁹¹⁻¹⁹²

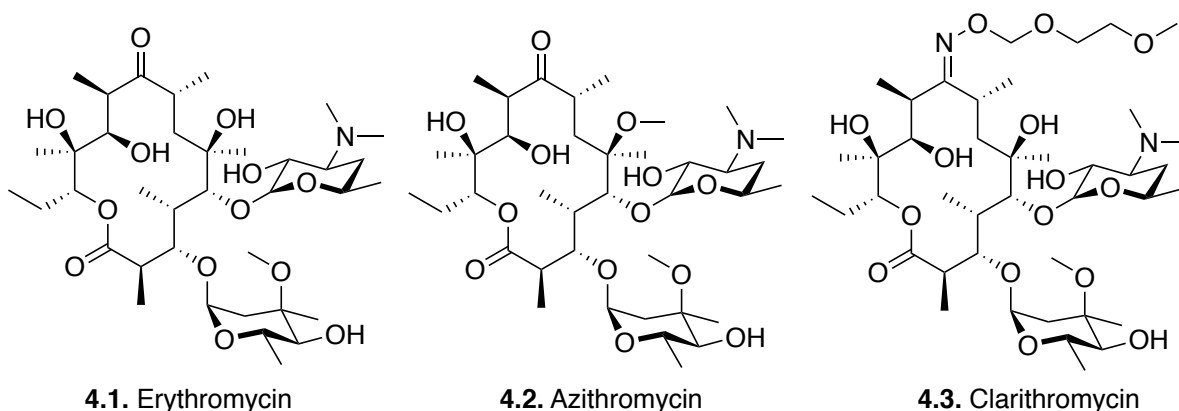


Figure 4.1. Structures of common macrolides.

Biological activity is not limited to these compounds. The 16 membered macrolide antibiotics e.g. tylosin A, spiramycin, and josamycin have similar antibacterial profiles and

activities against different genotypes of erythromycin-susceptible and erythromycin-resistant bacteria.¹⁹³⁻¹⁹⁴ Another category of macrolides that are used to treat respiratory tract infection are called ketolides. Telithromycin, cethromycin, and solithromycin are some of the known ketolides. Telithromycin, sold under the brand name Ketek, is also a semi-synthetic derivative of erythromycin and the first and only FDA-approved ketolide.¹⁹⁵⁻¹⁹⁶

Macrocycles with bigger ring sizes such as daptomycin (30 atoms), polymyxin (20 atoms), and bacitracin (25 atoms) are also used as antimicrobial drugs.¹⁹⁷⁻²⁰⁰ A well-known naturally food preservative nisin is produced by *Lactococcus lactis* through bacterial expression. It contains five macrocycles of various sizes (13, 16, and 22 atoms) and has shown biological activity against various microbes including vancomycin-resistant bacteria.²⁰¹⁻²⁰²

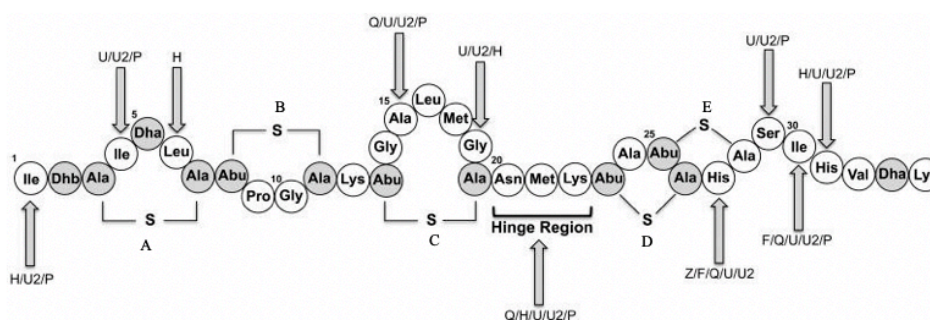


Figure 4.2. Different variants of nisin.

In addition, some macrocycles are used as cancer chemotherapeutic agents. Examples include naturally isolated dactinomycin (Figure 4.3) which contains two rings of 16 atoms each and a chemically synthesized epothilone with ring size of 16 atoms.²⁰³⁻²⁰⁵ The natural product cyclosporine (Figure 4.3) is a 33 membered macrocycles that lowers the activity of T-cells and has been approved to be used as immunosuppressant. It has also been approved in the US for rheumatoid arthritis psoriasis. It is used as eye drops for treating dry eyes caused by Sjogren's syndrome and meibomian gland dysfunction.²⁰⁶⁻²⁰⁷

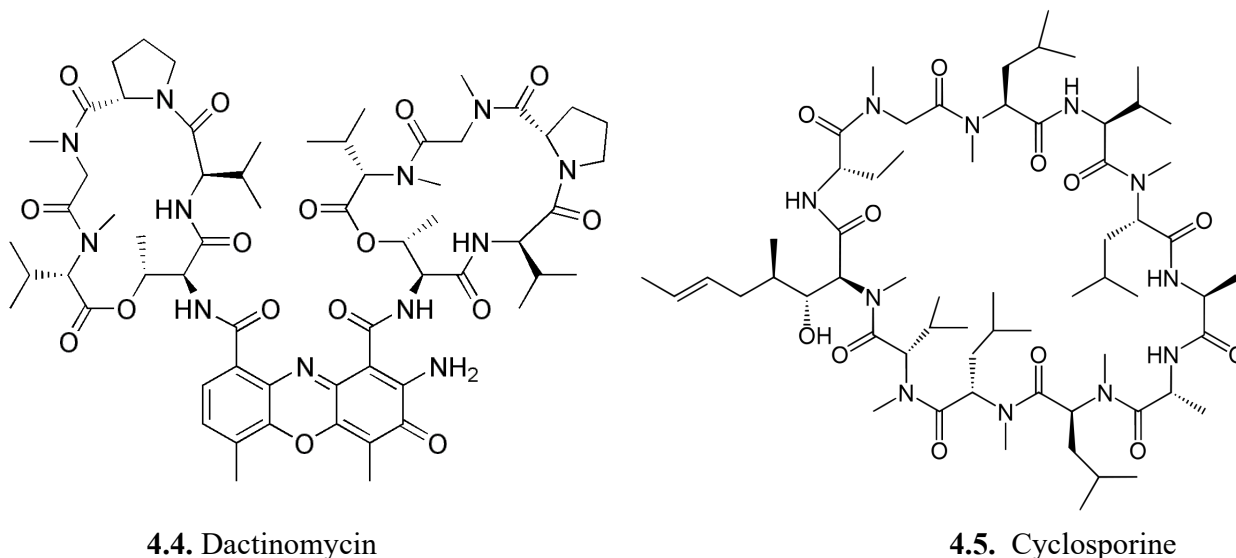


Figure 4.3. Structures of chemotherapeutic and immunosuppressant agents.

4.2 Synthetic methodologies of macrocycles

Developing general strategies for the synthesis of macrocycles is limited and challenging. Ring closure of the linear precursor relies on end groups with complementary reactivity including esterification, amidation, disulfide bond formation, or the formation of imines²⁰⁸⁻²¹⁰. While macrocycles of all sizes have fallen to synthetic conquest, general routes to their synthesis remain an attractive pursuit. Multiple methodologies have been employed to these ends including reversible/dynamic assembly.²¹¹⁻²¹⁴ Macrocyclization usually faces the most difficult challenge as reactions do not favor the formation of large rings. Instead, oligomers or polymers are usually formed. Polymer formation can be avoided and intramolecular reactions can be favored by running these reactions at high dilution. The rate of ring formation (intramolecular/intermolecular) for different types of reactions such as formation of lactones, monoethers, diethers, cyclic ammonium ions, and Szwarc reaction (polymerization of styrene with an alkali metal) is shown in Figure 4.4.²¹⁵⁻²¹⁶

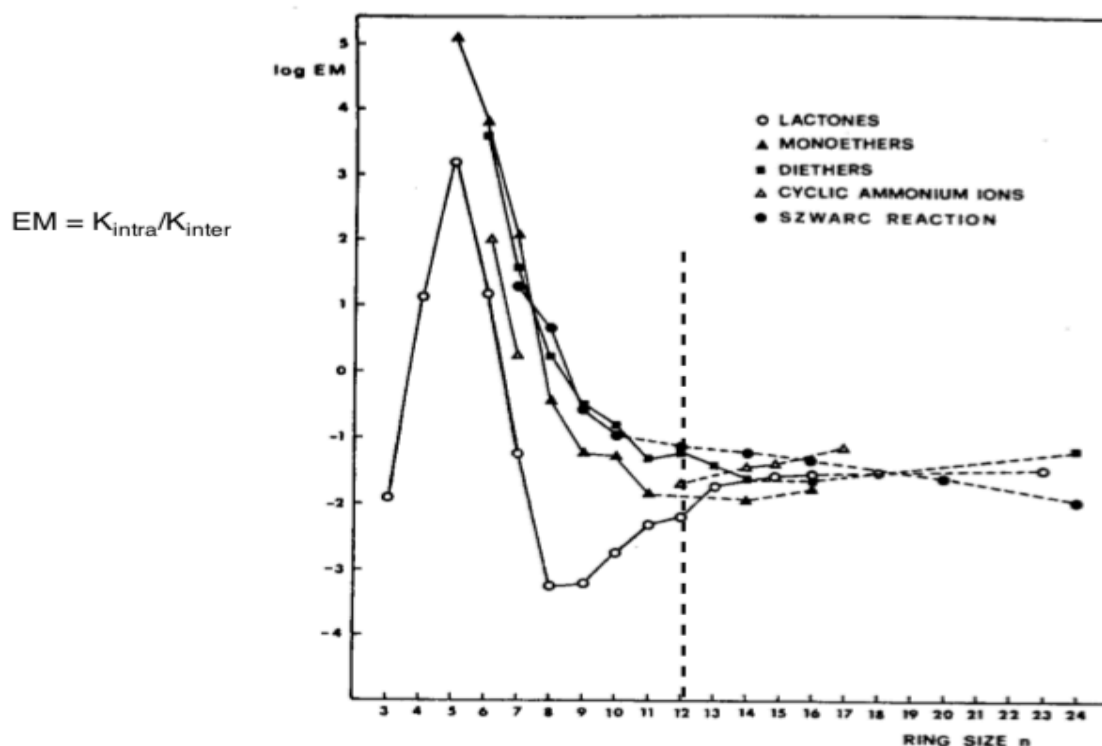


Figure 4.4. EM profiles vs. ring size for different cyclization reaction series.^{adapted from 215-216}

Peptide macrocycles are popular targets. Cyclic peptides restrict peptide conformation, reduce polarity, increase proteolytic stability, and improved efficacy.²¹⁷⁻²²¹ A wide variety of coupling reagents are available to do macrolactamization.²²²⁻²²³ These reagents can be used on solid or in solution phase. To complement these methods, S_N2 and S_NAr reactions are also used for the synthesis of simple and complex macrocyclic structures.²²⁴⁻²²⁵

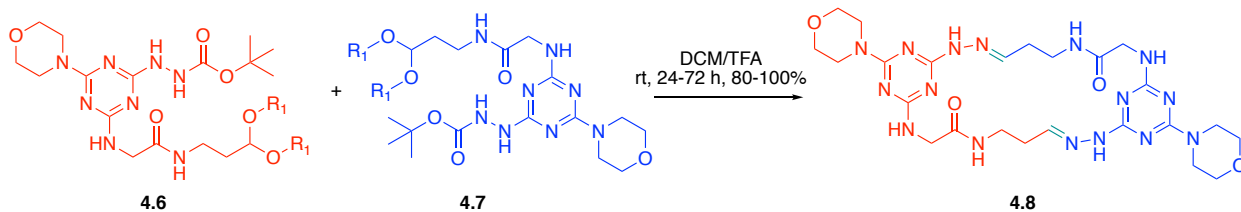
Olefin metathesis has been explored. Second generation of ruthenium Grubbs' catalyst has emerged as a popular choice for ring-closing metathesis for the synthesis of macrocyclic structures.²²⁶⁻²²⁸ This versatile method has high tolerance toward other chemical functionalities and employs mild reaction conditions. Multiple catalysts of varying reactivity and selectivity of this methods are readily available and adaptable to many ring sizes. Limitations of this methods include the production of mixtures of products, unreliable yields, and difficulty in removing Grubb's catalyst.

“Click chemistry” is another method for making macrocycles. Cycloaddition reactions between alkynes and azides have been used to synthesize many different macrocyclic structures including peptidomimetics, β -turn mimics and some non-peptide.²²⁶ However, this method can yield dimers, oligomers, and unreacted monomers. Numerous bioactive macrocyclic structures have been made using click chemistry.²²⁶ Click chemistry has also been shown to be tolerant to variety of functional groups.

The template approach developed by Sauvage and coworkers is highly effective at making catenanes, rotaxanes and knots.²²⁷ Cu(I) coordinates with the ligands of precursor holding them in a specific orientation to direct the macrocyclization and/or stoppering reactions to afford interlocked systems.²²⁷ Ions, molecules, and surfaces can act as templates to binds and pre-organize molecules to favor the formation of particular size rings. For example, the crown ethers cyclize in the presence of alkali metal cations.²²⁸

4.3 Previous work

Our studies rely on the dimerization of a monomer containing a triazine ring displaying both a tethered acetal and BOC-protected hydrazine group. Akop Yepremyan was able to synthesize macrocycles with rings containing 24 atoms, through self-assembly of two units through two hydrazone bond formation.²²⁹ The process involves the condensation of two triazine substituted monomer units **4.6** and **4.7** to yield macrocycle **4.8** in equal volumes of dichloromethane (DCM) and trifluoroacetic acid (TFA) as shown in Scheme 4.1.



Scheme 4.1. Self-assembly of two monomer units.

A total of three macrocycles (two homodimers and one heterodimer) were synthesized (Figure 4.5).²¹² All three macrocycles consist of rings with 24 atoms. An isopropyl group and benzyl group was used to alkylate boc-hydrazide (Figure 4.5). Upon mixing equal moles of monomer units containing isopropyl and benzyl group, heterodimer was also observed.

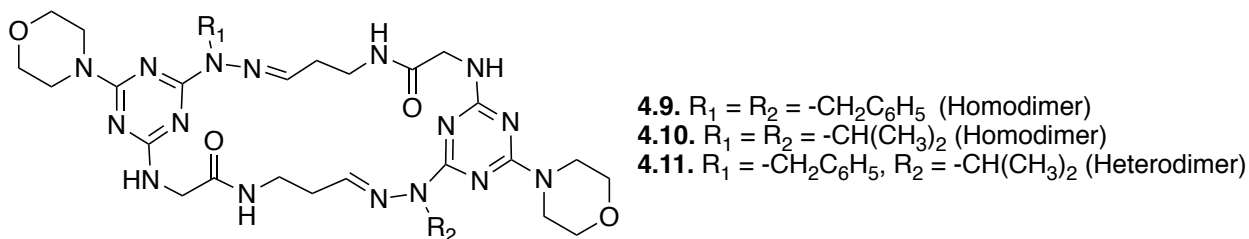


Figure 4.5. Structure of homodimers and heterodimer synthesized.

To explore the generality of this result, macrocycles with ring cycles of 22 to 28 atoms were designed and synthesized. The size of macrocycles is manipulated by varying the amino acid and amino acetal. Even numbered macrocycles are derived from homodimerization of same monomer units. Odd number rings are derived from heterodimerization of two different monomer units. In this case, the reaction mixture is a mixture of three macrocycles. Two different amino acids (β -alanine and glycine) and various length acetal linkers including the 2-carbon aminoethyl acetal, the 3-carbon aminopropyl acetal, and the 4-carbon aminobutyl acetal are used to increase the ring sizes of macrocycles (Chart 4.1).

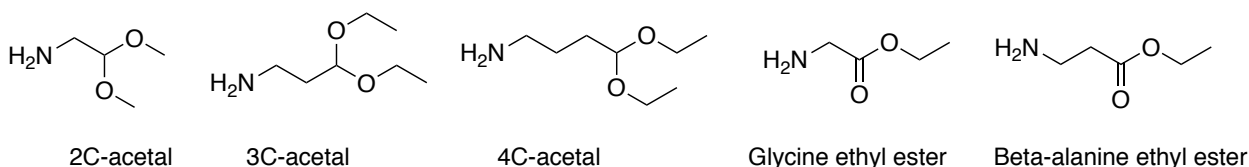


Chart 4.1. Various acetal linkers and amino acids used.

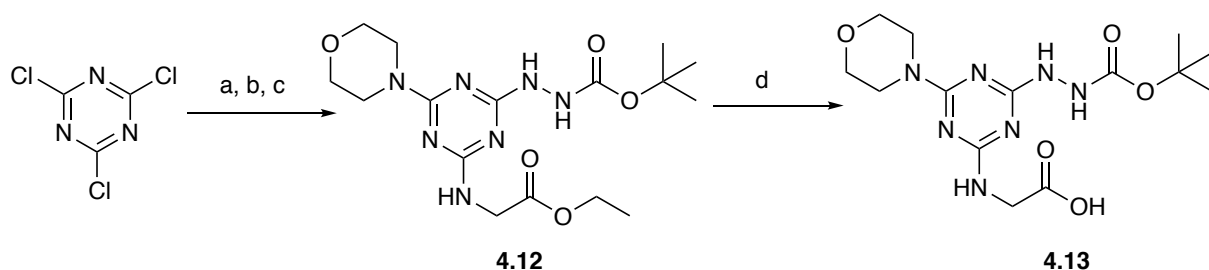
4.4 Results and discussions

4.4.1 Nomenclature

A total of six monomers **M(1-6)** were synthesized. The homodimeric macrocycle made from monomer **1** is called **1•1**, from monomer **2** is called **2•2** and so on. Heterodimeric macrocycle made from monomers **1** and **2** is called **1•2** and so on. In addition, model macrocycle **7•7** is made from monomer **M7** that is similar in size as that of **4•4** but has methyl group at the nitrogen atom (=N-NCH₃) of the hydrazine group.

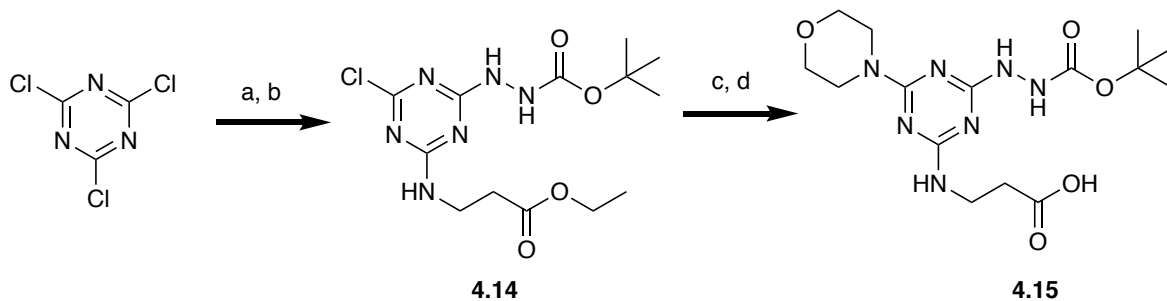
4.4.2 General synthetic routes

The monomers are readily accessible synthetically by stepwise substitution of chlorine atoms on the triazine ring. The general route relies on the addition of the glycine ethyl ester acid at 0 °C followed by the addition of BocNHNH₂ at room temperature and finally morpholine at elevated temperature to yield **4.12**. Saponification of **4.12** followed by acid-work up yields **4.13**.



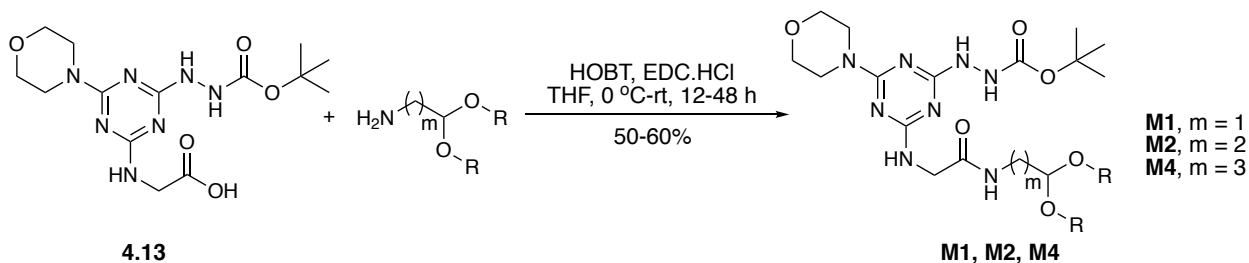
Scheme 4.2. Synthesis of **4.13**. a) Glycine ethyl ester. HCl, DIPEA, THF, 0 °C-RT, 12h. b) BocNHNH₂, DIPEA 0 °C-RT, 12h. c) Morpholine, DIPEA, reflux, 20 minutes (72%). d) MeOH/5% NaOH, 60 °C, 2 h, acid work-up (98%).

The use of beta-alanine ethyl ester instead of glycine ethyl ester with similar steps yields acid **4.15** (Scheme 4.3).



Scheme 4.3. Synthesis of **4.15**. a) beta-alanine ethyl ester. HCl, DIPEA, THF, 0 °C-RT, 12 h. b) BocNHNH₂, DIPEA 0 °C-RT, 12 h, (94%). c) Morpholine, DIPEA, reflux, 20 mins. d) MeOH/5% NaOH, 60 °C, 2 h, acid work-up (92%).

Compound **4.13** is then coupled with different acetal linkers to create monomers **M1**, **M2**, and **M4** with the help of coupling reagent HOBT and additive EDC.HCl (Scheme 4.4)



Scheme 4.4. General synthesis of monomers **M1**, **M2**, and **M4** from **4.13**.

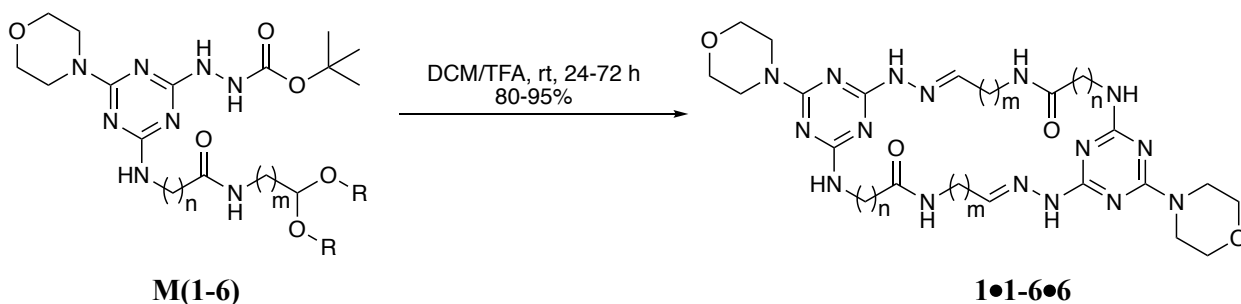
Similarly, compound **4.15** is used to create monomer units **M3**, **M5**, and **M6** using 2-carbon, 3-carbon, and 4-carbon linkers, respectively. The summary of all the monomers synthesized is provided in Table 4.1.

Table 4.1. Summary of monomers synthesized by using **4.13** and **4.15**.

Monomers	Starting Compound	Value of m	Percent yield
M1	4.13	1	51%
M2	4.13	2	50%
M4	4.13	3	40%
M3	4.15	1	56%
M5	4.15	2	55%
M6	4.15	3	42%

4.4.3 Synthesis of macrocycles

In general, monomers **M1-M6** with acid labile protecting groups were mixed in equal volume of dichloromethane (DCM) and trifluoroacetic acid (TFA) at room temperature (Scheme 4.5).



Scheme 4.5. General synthetic schemes of six macrocycles. R = methyl or ethyl group. n = 1 and 2. m = 1, 2, and 3.

The concentration of the monomer in equal volume of TFA and DCM varies from 0.005 mg/mL to 0.03 mg/mL. It appears that the formation of dimers is independent of concentration, however. Homodimer formation does not require high dilution conditions. The mixture of DCM and TFA was allowed to evaporate slowly which took anywhere between 24 to 72 hours. After 72

hours, if the reaction mixture was not dried, another 2 ml of DCM was added and the resulting mixture was left to stir and dry at room temperature.

The proton NMR of the crude product shows undesired peaks when solvents were removed under reduced pressure. A mixture of products was observed including possibly unprotected monomers and homodimers. In some cases, the solid crude product was washed with small volume of dichloromethane and methanol to remove the colored impurities. However, the ^1H NMR of the crude product was as good as after washing it with DCM and methanol. In that case, the formation of desired macrocycles appeared to be quantitative. This method led to the synthesis of six homodimers of macrocycles with even numbered atoms ranging from 22 to 28 atoms with yields ranging between 80-95% (Table 4.2). Homodimer macrocycle **7•7** (26 atom) containing a *N*-methyl group at the hydrazine nitrogen atom (=N-NCH₃) was synthesized to distinguish the hydrogen atoms attached to heteroatoms. All the macrocycles were characterized by mass spectrometry, ^1H -NMR and ^{13}C -NMR spectroscopy, and x-ray crystallography.

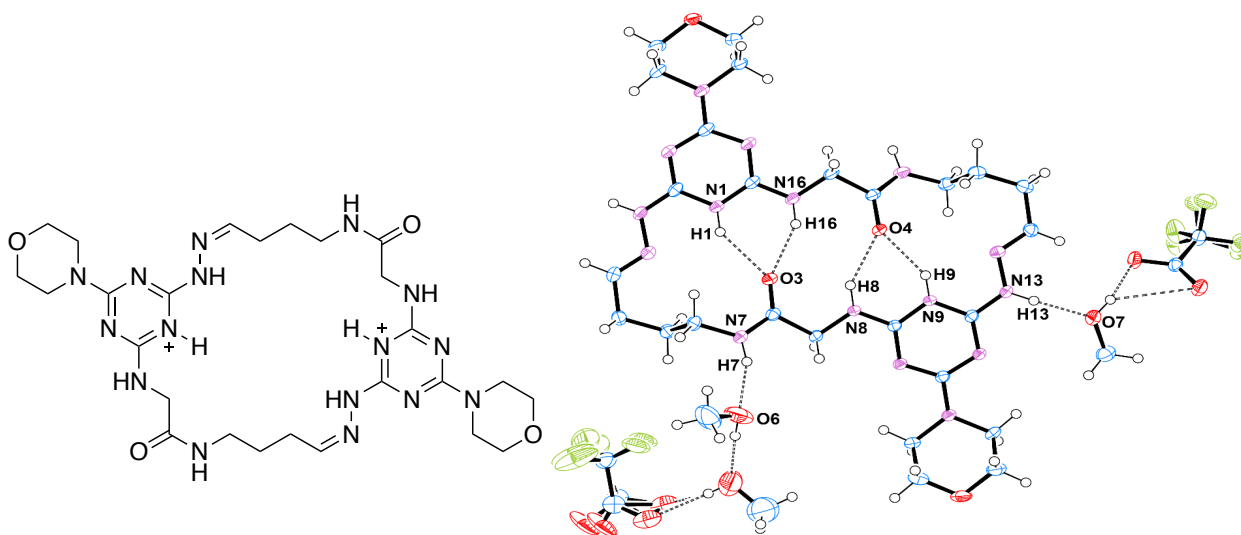
Table 4.2. List of homodimers synthesized.

Macrocycles	n	m	Size	Percent Yield
1•1	1	1	22	93%
2•2	1	2	24	93%
3•3	2	1	24	95%
4•4	1	3	26	80%
5•5	2	2	26	80%
6•6	2	3	28	83%
7•7	1	3	26	88%

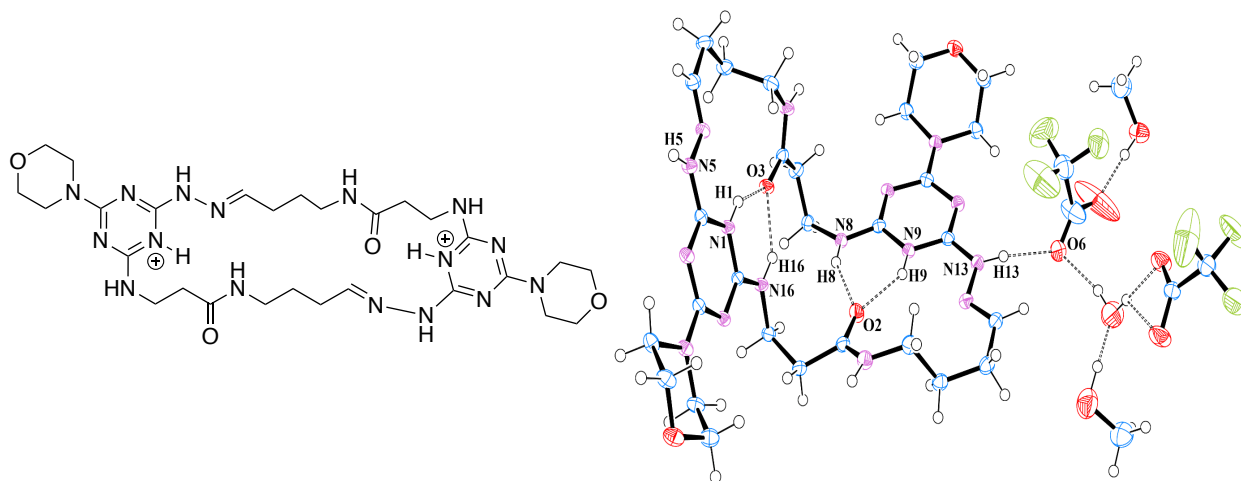
4.4.4 Solid State Structures

X-ray crystal structures were obtained for five out of the six macrocycles. We divide the structures into two different morphologies as shown in Figure 4.6 and 4.7. All the macrocycles co-crystallize with a trifluoroacetate ion and protonates the nitrogen atom of the triazine ring opposite to morpholine ring. This protonated hydrogen atom engages in hydrogen bonding with the counterion (**1•1**, **2•2**, and **3•3**) or carbonyl group of the juxtaposed monomer (**4•4** and **6•6**).

As an example of two different morphologies, the x-ray structure of **4•4** and **6•6** are reminiscent of β -sheets. The x-ray structures of **2•2** and **3•3** are folded in the shape of a taco. The structure of **1•1** appeared to be flat.

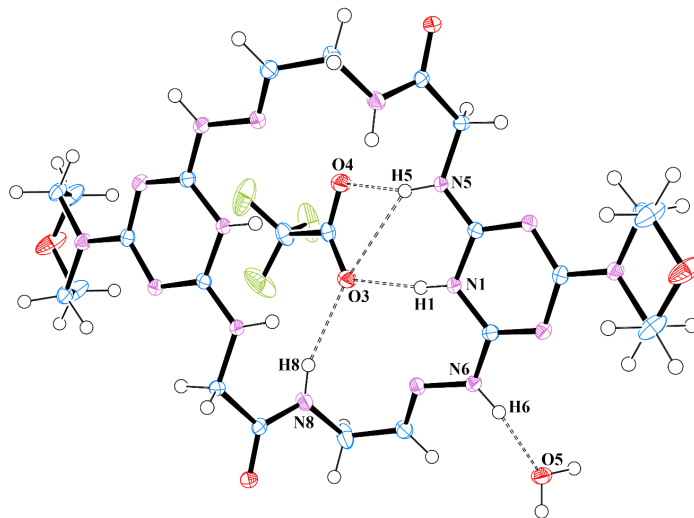
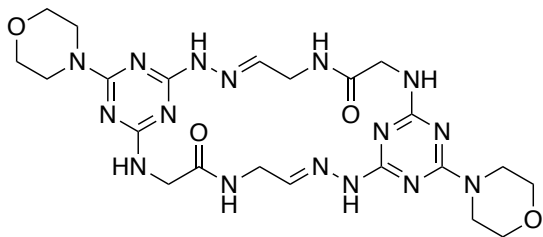


4•4

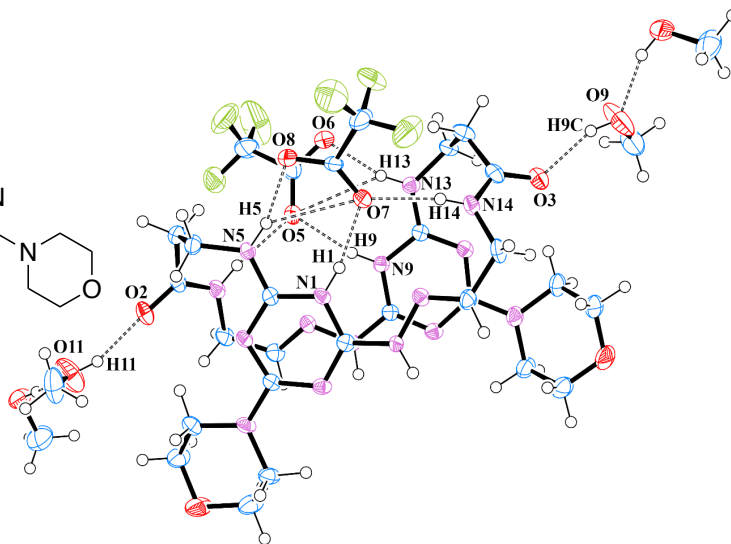
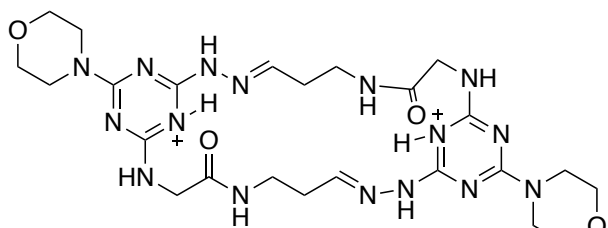


6•6

Figure 4.6. Morphology of bigger macrocycles: x-ray structures of **4•4** comprising 26 atom and **6•6** comprising 28 atoms.



1•1



2•2

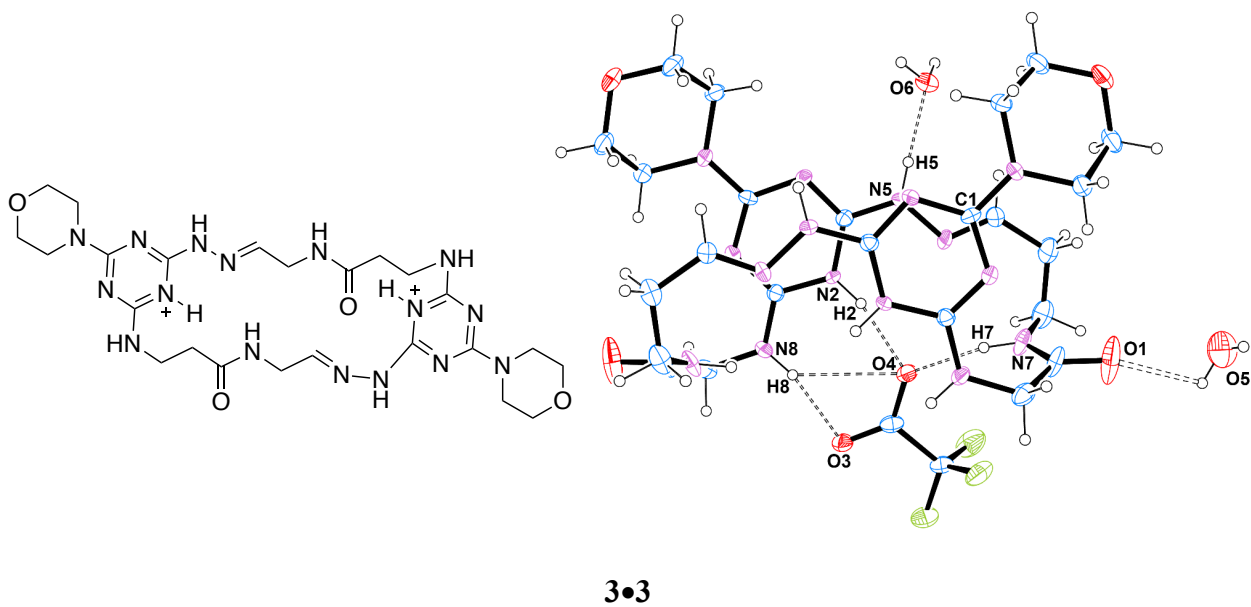


Figure 4.7. Morphology of smaller macrocycles: x-ray structure of **1•1** comprising 22 atoms, **2•2** containing 24 atoms, and **3•3** containing 24 atoms).

4.4.5 One dimensional ^1H NMR of macrocycles

All of the NMR studies were done in $\text{DMSO-}d_6$ and CD_3OD . The summary of the signals is provided in Table 4.3. In $\text{DMSO-}d_6$, the imine protons of **1•1**, **2•2**, **3•3**, **4•4**, **5•5**, and **6•6** appear at 7.63, 7.51, 7.55, 7.62, 7.57, and 7.60 ppm respectively. There appears to be no correlation between the chemical shift of imine proton and the ring size of macrocycles. In the ^1H NMR spectra of all the macrocycles, the four H-bond donor protons are shifted significantly downfield. The proton NMR of all the macrocycles are compared to an open model hydrazones **8** as shown in Figure 4.8.

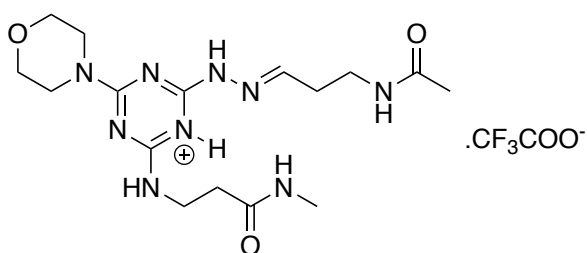


Figure 4.8. Structure of model compound **8**.

As an example, in the ^1H -NMR of **6•6**, H9 and H10 appear at 8.27 and 8.45 ppm, corresponding to the amine proton of beta-alanine and amide proton of the four carbon linker, respectively (Figure 4.9). The triplet at 7.59-7.61 (H8) corresponds to imine proton. The ^1H COSY NMR is used to unambiguously assign the imine (H8), the amino acid (H9), and the amide (H10) protons. When a drop of CD_3OD was added, amide proton appears to be the slowest to exchange, an observation consistent in all the macrocycles. The other two signals at 11.33 ppm (H11) and 12.42 ppm (H12) correspond to protonated nitrogen of triazine ring (Ar-H) and hydrazine proton (N-NH) respectively. The COSY NMR, however, is not helpful in confirming the identity of last two signals at 11.33 ppm and 12.42 ppm as Ar-H or N-NH .

Table 4.3. Selected ^1H data. When $n=1$, glycine. When $n=2$, β -alanine. Ar-H^+ corresponds to the protonated triazine.

#	1•1	2•2	3•3	4•4	5•5	6•6	7•7	8
n	1	1	2	1	2	2	2	2
m	1	2	1	3	2	3	2	2
Size	22	24	24	26	26	28	26	NA
$\underline{\text{HC}}=\text{N}$	7.63	7.51	7.55	7.62	7.57	7.60	7.55	7.60
$=\text{NN}\underline{\text{H}}$	12.37	12.37	12.37	12.58	12.43	12.42	12.36	NA
$\text{Ar-}\underline{\text{H}}^+$	12.15	12.21	12.00	11.45	11.43	11.33	11.55	11.53

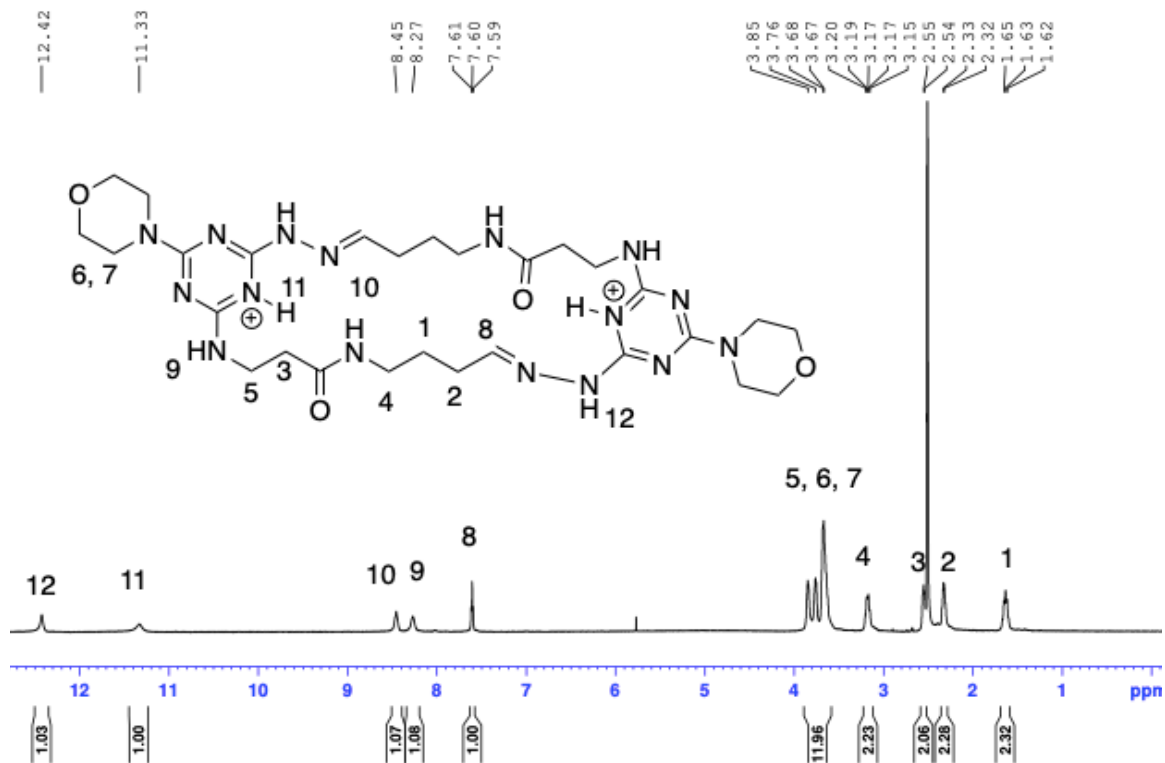


Figure 4.9. $^1\text{H-NMR}$ of **6•6** in $\text{DMSO-}d_6$.

To support the identification of last two signals as the hydrogen atom of protonated triazine ring (Ar-H) or hydrogen of hydrazine ($=\text{N-NH}$), a model macrocycle **7•7** was synthesized. The hydrazine nitrogen atom is methylated ($=\text{N-NCH}_3$) in model macrocycle **7•7** and has the same size as that of macrocycle **4•4**. The last two signals of macrocycle **4•4** (Figure 4.10) at 11.45 ppm and 12.58 ppm represents hydrazine proton ($=\text{NNH}$) and triazine ring proton (Ar-H). When compared to the $^1\text{H-NMR}$ of *N*-methyl substituted macrocycle **7•7**, the signal at 12.58 disappeared (Figure 4.11). The conserved position of peak at 11.53 ppm suggests that it corresponds to the proton on the triazine ring (Ar-H). In addition, the NOESY spectrum of **4•4** also confirmed that the signal at 12.58 ppm corresponds to hydrogen atom of hydrazine group ($=\text{NNH}$) as it shows nOe with imine proton (N=CH). Whereas, *N*-methyl proton ($=\text{NNCH}_3$) of **7•7** show nOe signal with the imine proton (N=CH).

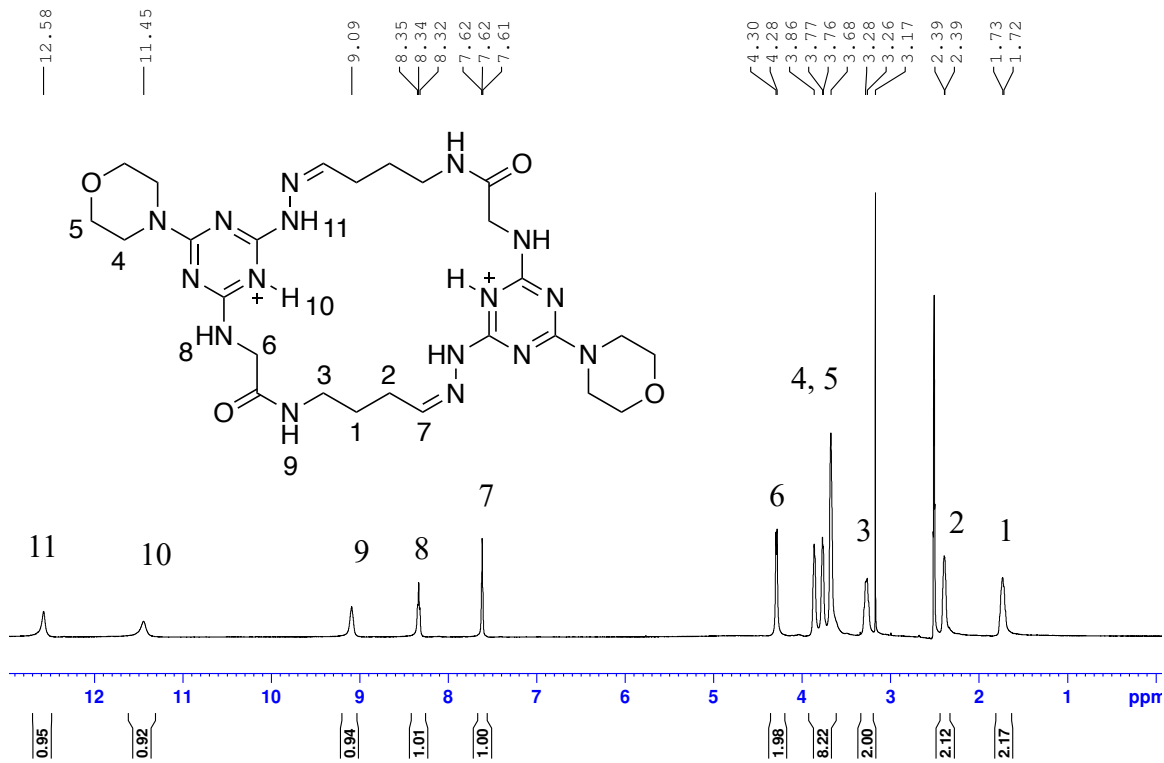


Figure 4.10. $^1\text{H-NMR}$ of **4•4** in $\text{DMSO-}d_6$.

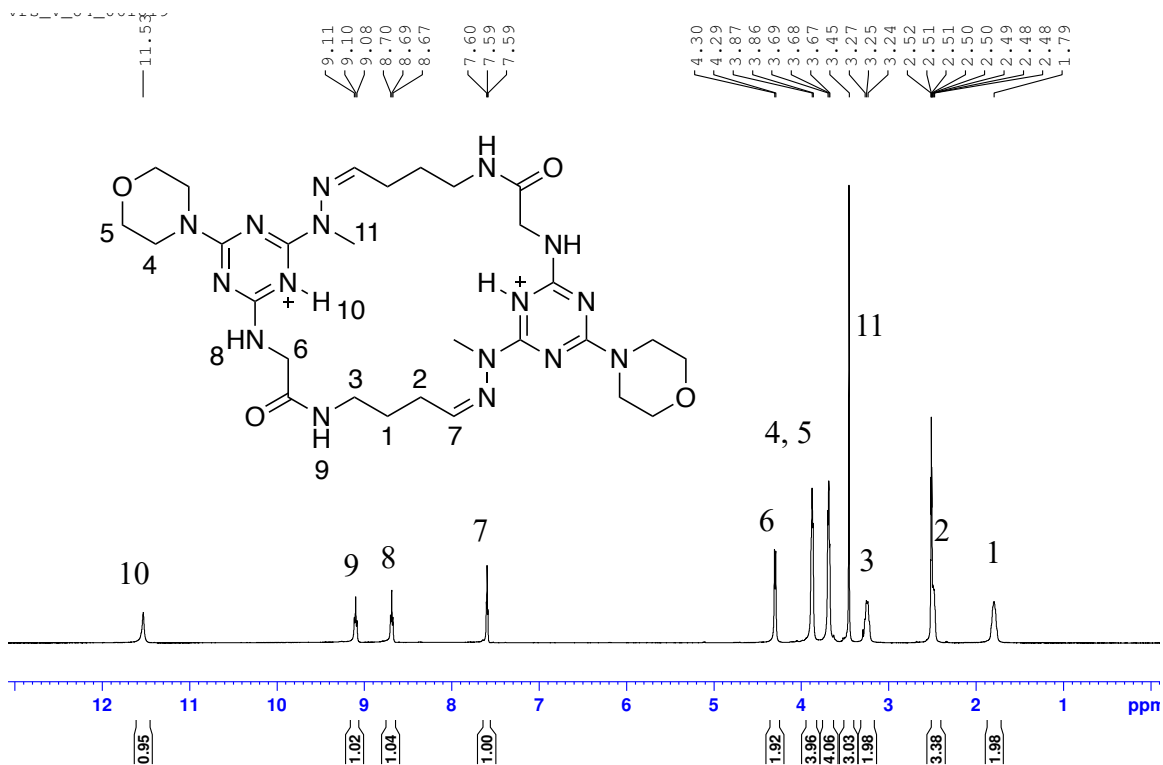


Figure 4.11. $^1\text{H-NMR}$ of **7•7** in $\text{DMSO-}d_6$.

There was no significant difference in the chemical shift of hydrazine proton (=NNH) of all the macrocycles as they appeared in the narrow range between 12.00 to 12.50 ppm. In addition, the chemical shift of amine (-CH₂-NH) proton of amino acid and amide (C-NH) proton do not vary among macrocycles. However, the chemical shift of the protonated nitrogen of triazine ring (Ar-H) appeared in the range of 11.33 to 12.21 ppm. The proton on the nitrogen atom of triazine ring of the smaller macrocycles **1•1** (22), **2•2** (24), and **3•3** (24) appears at 12.15 ppm, 12.21 ppm, and 11.94 ppm, respectively. The same proton of larger macrocycles **4•4** (26), **5•5** (26), and **6•6** (28) appears at 11.45 ppm, 11.43 ppm, and 11.33 ppm, respectively.

4.4.6 One dimensional ¹³C NMR of macrocycles

The ¹³C NMRs show trends that are indicative of formation and conformation of macrocycles. A summary of some of the important signals of ¹³C NMR is shown in Table 4.4.

Table 4.4. Selected ¹³C NMR data. T1-T3 refer to unassigned lines of the ¹³C atoms of the triazine ring. When n=1, glycine. When n=2, β-alanine.

#	1•1	2•2	3•3	4•4	5•5	6•6	7•7	8
n	1	1	2	1	2	2	1	2
m	1	2	1	3	2	3	3	2
Size	22	24	24	26	26	28	26	NA
T1	161.7	161.3	161.3	161.6	161.7	161.7	161.6	161.0
T2	155.0	154.6	155.3	154.5	154.7	154.7	154.7	154.7
T3	154.8	154.0	154.3	154.1	154.6	154.3	154.3	154.2
HC=N	147.5	147.9	146.6	150.5	150.7	150.6	151.8	149.1

The chemical shift of imine ($\text{HC}=\text{N}$) varies with the size of the macrocycles. The imine chemical shifts for smaller macrocycles (**1•1**, **2•2**, and **3•3**) range from 146-148 ppm. For larger macrocycles (**4•4**, **5•5**, and **6•6**), the range spans from 150 to 152 ppm. Some other interesting differences in the ^{13}C -NMR signals of triazine carbon atoms were observed in the macrocycles from their precursors. The carbon atoms of triazine ring with chlorine as substituents usually appear between 168-169 ppm. However, after replacing chlorine atom with nitrogen atom nucleophiles, the chemical shift decreases to between 164-169 ppm. As an example, Figure 4.12 shows the triazine carbon atoms of monomer **M2** with at 164.7, 165.9, and 167.6 ppm

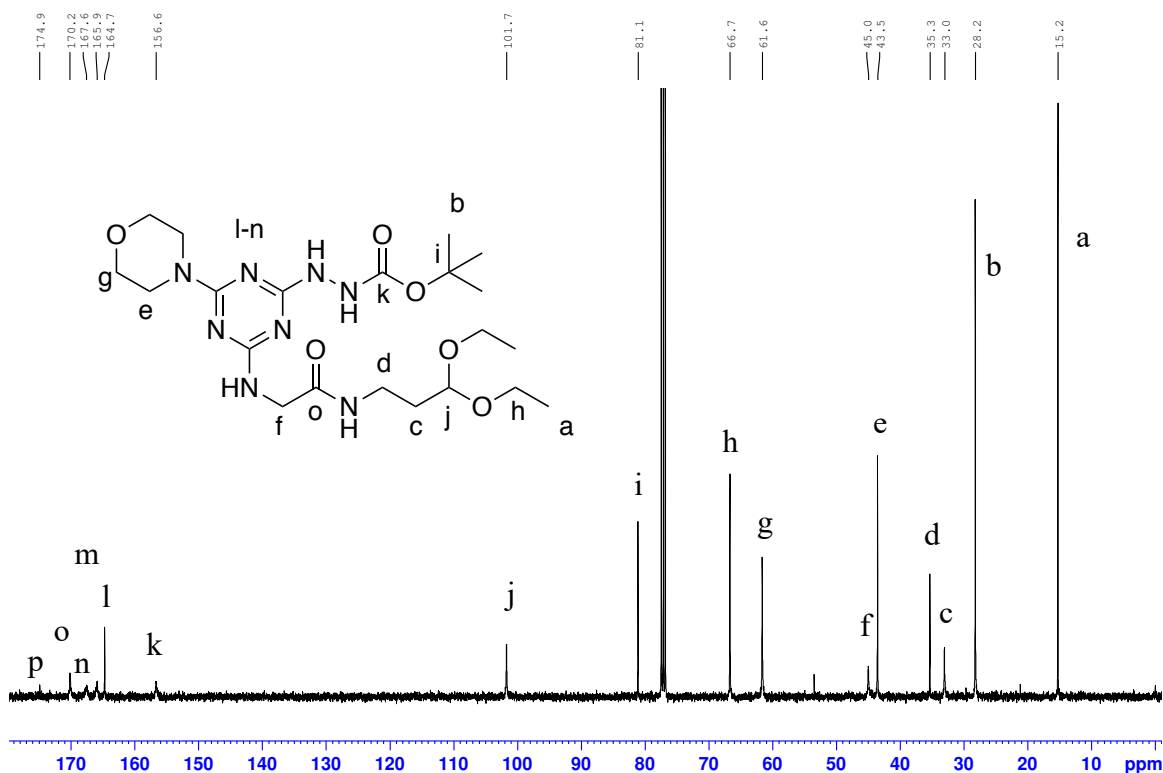


Figure 4.12. ^{13}C -NMR of **M2** in CDCl_3 .

However, the ^{13}C -NMR of the **2•2** macrocycle shows a significant shift of triazine carbon atoms to 161.3, 154.6, and 154.0 ppm (Figure 4.13). Two of the triazine carbon atoms show a shift of more than 10 ppm. ^1H -NMR and crystal structure showed that nitrogen atom opposite to the morpholine of the triazine ring is protonated and as a result has positive charge on it. A positive

charge on the nitrogen should make nearby carbon atoms more deshielded and as a result, shift further downfield. However, they show upfield chemical shift. The shift of more than 10 ppm is unusually high for triazine carbon considering they are not directly involved in any sort of bond formation during macrocyclization step. This trend is consistent with the ^{13}C -NMR of all the macrocycles synthesized. One explanation is the stacking of two monomers units on the top of the one another in the macrocycle providing extra electron density. This possibly indicates a specific conformation of the macrocycles that is relatively favored. Stacking of two monomer units has been observed in the X-ray crystal structures of **1•1**, **2•2**, and **3•3**. However, the stacking of triazine rings was not observed in bigger macrocycles such as **4•4** and **6•6**.

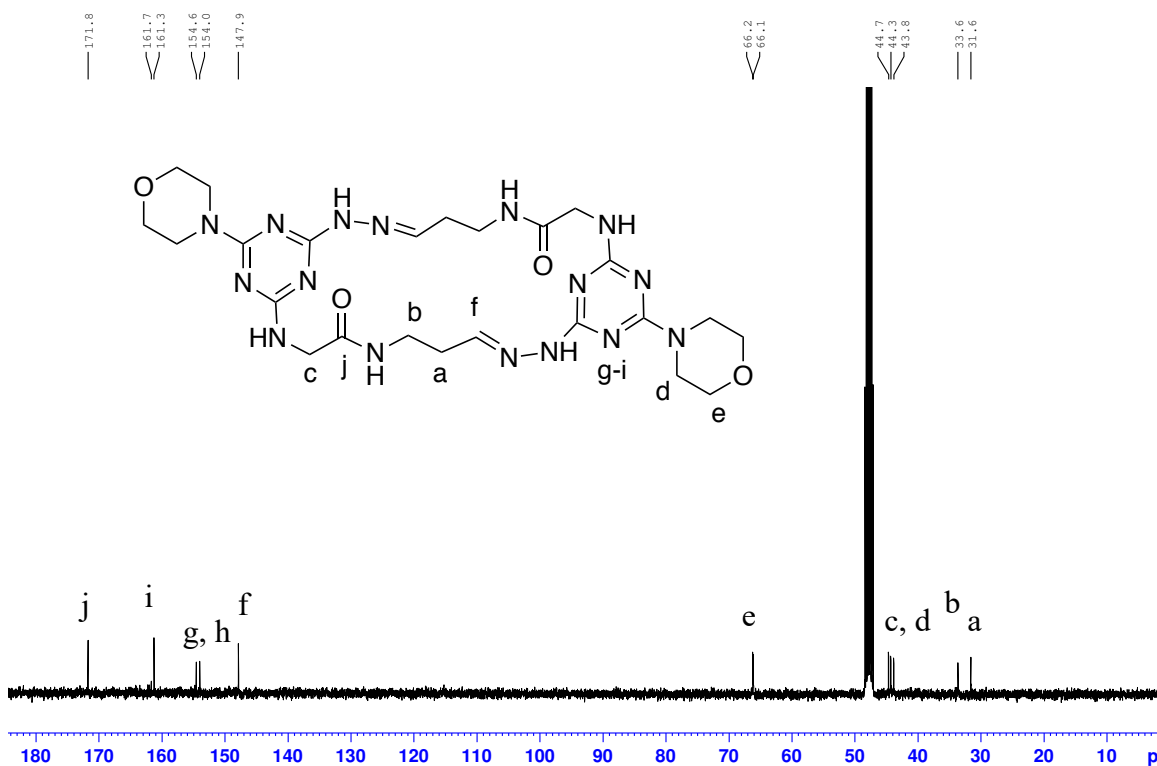


Figure 4.13. ^{13}C -NMR of **2•2** in CD_3OD .

To test the hypothesis of stacking of two monomer units to justify the drop in the chemical shift in ^{13}C NMR, a model compound **8** was prepared by mixing equal moles of compounds **4.16** and **4.17** in DCM and TFA (Scheme 4.6). The ^1H and ^{13}C NMR of **8** was taken without any

arrow. In conformation **III**, the amine proton of amino acid (C-NH) does not show any nOe signal with protonated triazine ring (Ar-H). Two other noe signals are seen, however. Conformation **IV** shows only one nOe signal between hydrazine proton (=N-NH) and imine proton (-N=CH).

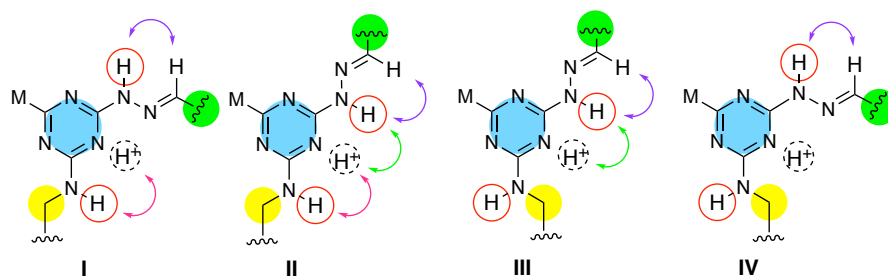


Figure 4.14. Possible rotational isomers of the macrocycles. ‘M’ represents morpholine substituent. Different color arrows show potential noe signals.

NOESY spectra of all the macrocycles shows an signal between the hydrazine proton (=N-NH) and imine proton (-N=CH) indicated by purple arrow. As an example, the COSY (Figure 4.15) and NOESY (Figure 4.16) NMR spectra of **4•4** can be compared to study the nOe patterns. The NOESY spectrum of **4•4** shows all three signals indicated by conformation **II**. Two other bigger macrocycles **5•5** and **6•6** do not show the nOe signal indicated by red arrow. As a result, these two macrocycles appear to have the conformation of **III** in solution. However, solid state structures of **4•4** (Figure 4.6) and **6•6** (Figure 4.6) do not seem to form conformation **III** suggesting that multiple conformations are possible.

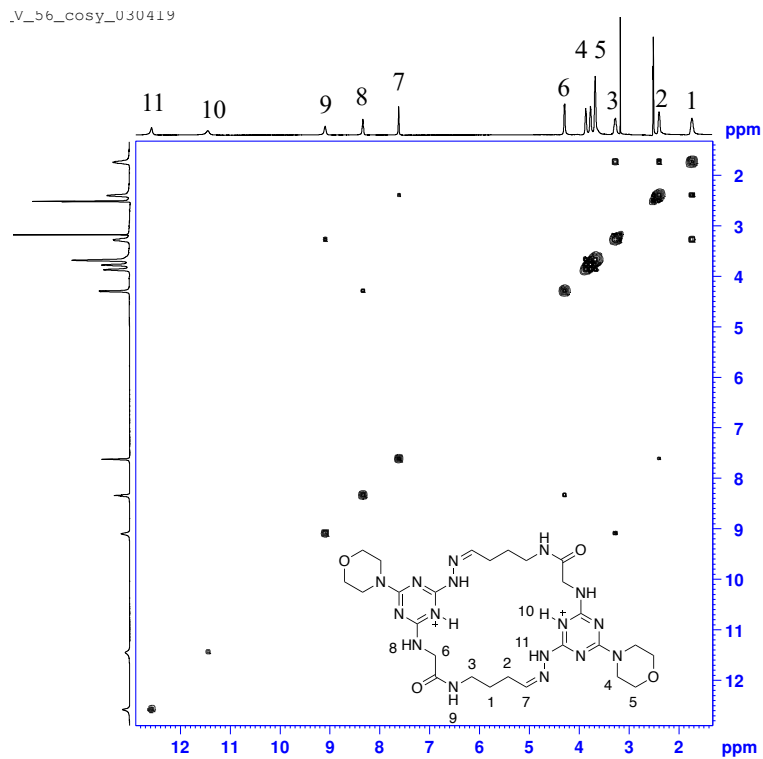


Figure 4.15. ^1H COSY of **4•4** in $\text{DMSO-}d_6$.

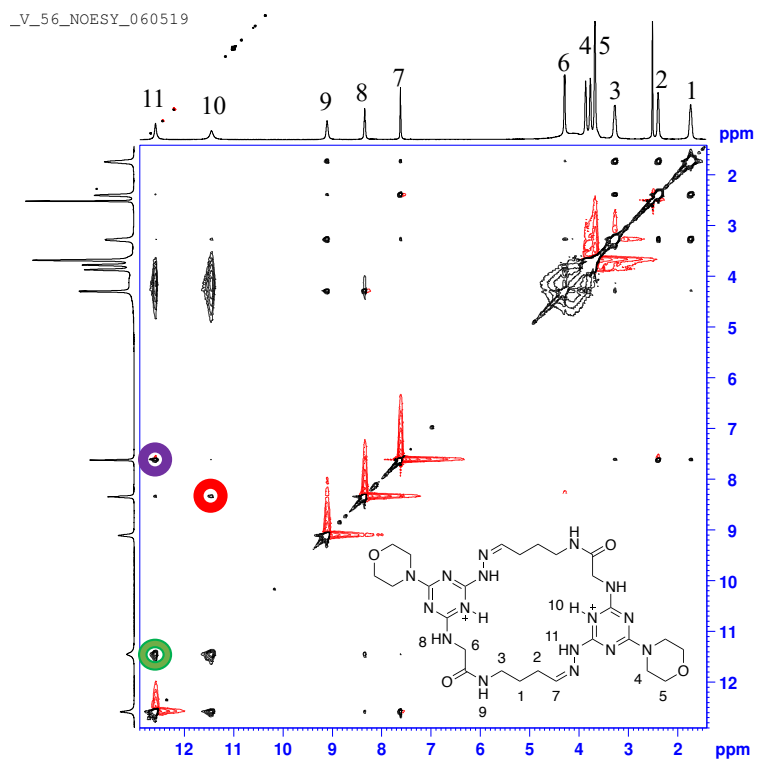


Figure 4.16. ^1H NOESY of **4•4** in $\text{DMSO-}d_6$.

Small macrocycles **1•1**, **2•2**, and **3•3** do not show noe between the triazine proton (Ar-H) and the hydrazine proton (=N-NH). In addition, **1•1** and **3•3** do not show nOe signals between the triazine proton (Ar-H) and the amino acid proton (C-NH) which suggests that **1•1** and **3•3** adopt conformation **IV** while **2•2** adopts conformation **I**. Crystal structures of smaller macrocycles shown in Figure 4.3 (A-C) suggest that macrocycles **1•1**, **2•2**, and **3•3** adopt conformation **I**. We conclude that multiple conformations can be adopted by these macrocycles. Table 4.5 summarizes the nOe signals seen in NOESY NMR and those expected from the x-ray structure

Table 4.5. Comparison of solution state and expected solid state nOe signals.

	Solution structure		Solid state	
	nOe	Conf.	Exp. nOe	Conf.
1•1	Purple	IV	Purple, Red	I
2•2	Purple, Red	I	Purple, Red	I
3•3	Purple	IV	Purple, Red	I
4•4	Purple, Red, Green	II	Purple, Red	I
5•5	Purple, Green	III	NA	NA
6•6	Purple, Green	III	Purple, Red	I
7•7	Purple(<u>CH</u> ₃ - N= <u>CH</u> =), Red	I	NA	NA

4.4.8 Assessing the purity of macrocycles with HPLC

The purity of macrocycles was established using HPLC. An Agilent 1200 series HPLC with column Eclipse XDB-C18, 5 μm , 4.6 x 150 mm was used for all detection analysis. The macrocycles were dissolved in an aqueous solution of methanol and were diluted to 0.5 mM. The eluting solvents were A 60:40 ratio of water:acetonitrile mixture with 0.1% TFA dissolved. was used as mobile system. The gradient flow rate of 0.5 ml/min for the first 12 minutes was used before it was increased to 1.0 ml/min.

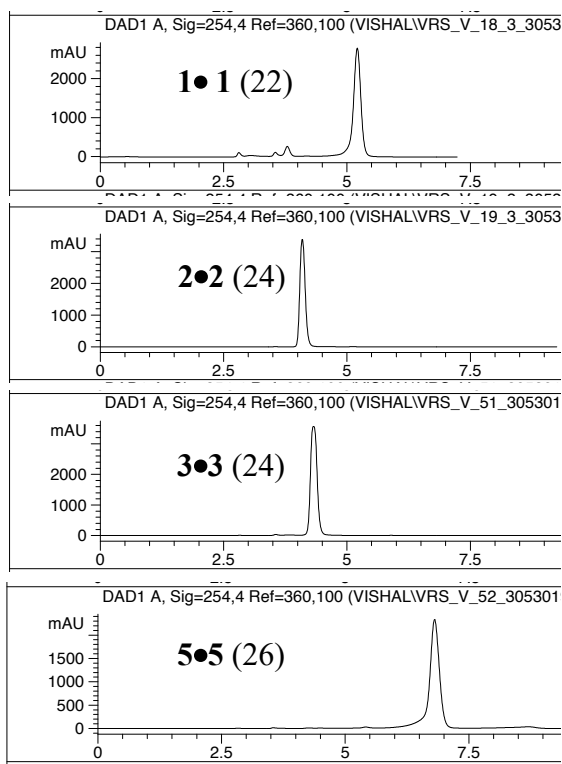


Figure 4.17. HPLC chromatograms of **1•1**, **2•2**, **3•3**, and **5•5**.

The elution times of the macrocycles fall roughly into two categories (short and long) which correlates with the incorporation of the 4-carbon acetal ($m=3$). That is, macrocycles **1•1** (5.01 min), **2•2** (4.03 min), **3•3** (4.42 min) and **5•5** (6.44 min) elution times are markedly shorter (Figure 4.17) than the elution times of macrocycles **4•4** (16.9 min) and **6•6** (each at 16.1 min) as shown in Figure 4.18. This suggests that four carbon linker makes the macrocycles relatively more

non-polar than two and three carbon linkers. The chain of glycine or β -alanine appeared to have little effect on the overall elution time of the macrocycles. Although not as pronounced, unexpectedly **1•1** elutes slightly later than **2•2**. However, **3•3** ($m=1$) elute rapidly then **5•5** ($m=2$).

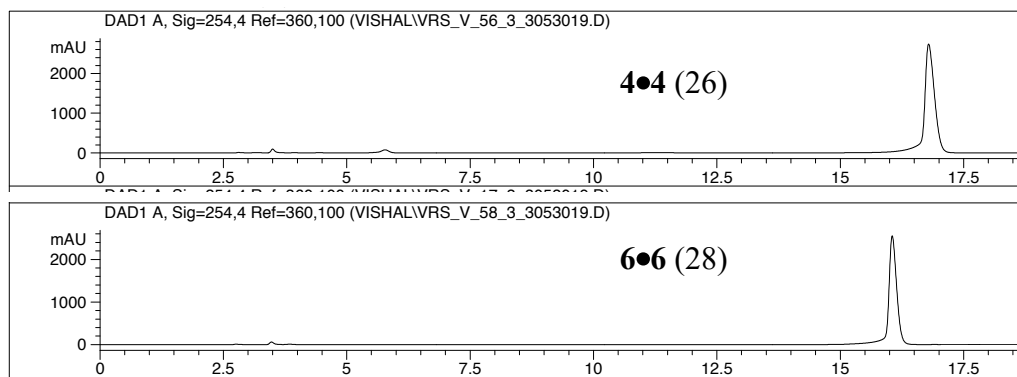


Figure 4.18. HPLC chromatograms of **4•4** and **6•6**.

4.4.9 HPLC studies of heterodimers

We further investigated the selective pairing of some of the macrocycles by mixing equal mole ratios of different monomers. When equal moles of compounds **1** and **2** were mixed, HPLC shows the formation of three macrocycles **1•1**, **1•2**, and **2•2** in the ratio of 0.29:0.35:0.37 respectively (Figure 4.19). The formation of three macrocycles **1•1**, **1•2**, and **2•2** was also confirmed by mass spectroscopy with molar masses of 583.5 a.m.u., 597.5 a.m.u., and 612 a.m.u., respectively (Figure 4.20). In addition, when equal mole ratio of monomers **3** and **5** were mixed, three macrocycles **3•3**, **3•5**, and **5•5** were made (Figure 4.21). However, in either case, the macrocycles made could not be separated using regular column chromatography.

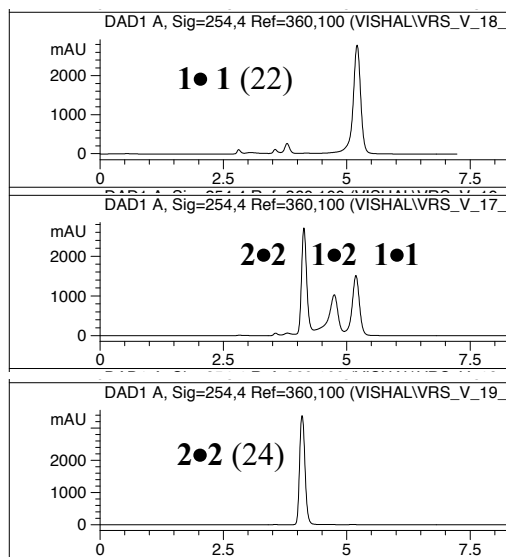


Figure 4.19. HPLC chromatograms of **1•1**, **1•2**, and **2•2**.

vrs_V_17 #1 RT: 0.01 AV: 1 NL: 5.66E6
 T: + c ESI Full ms [250.00-1000.00]

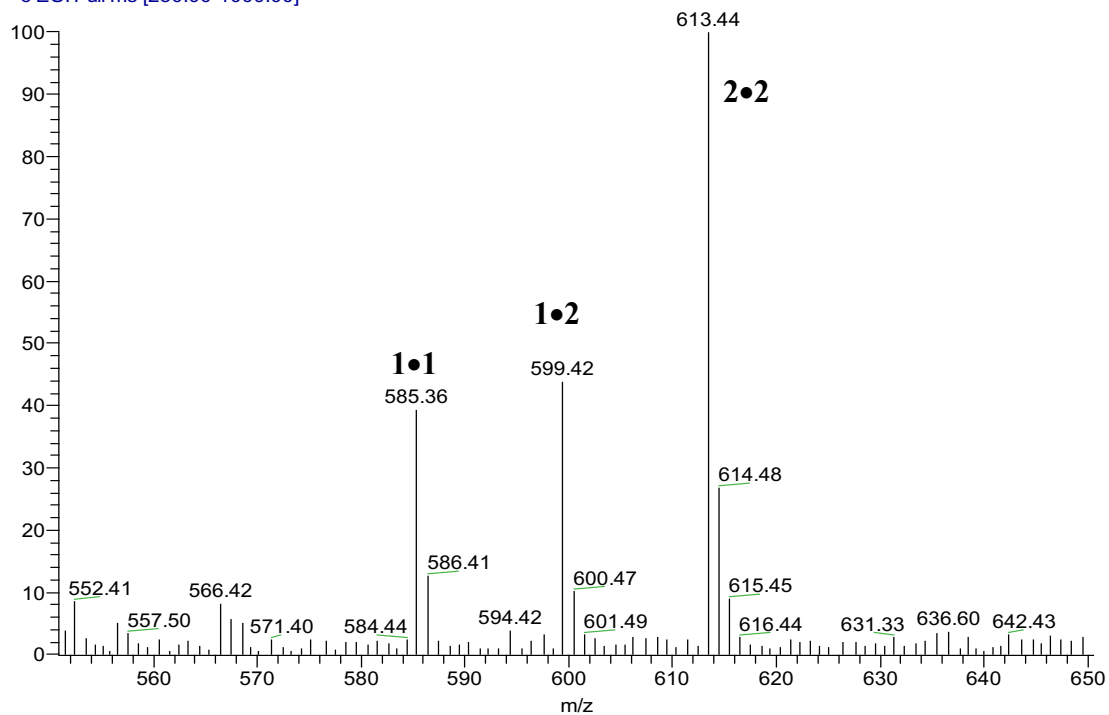


Figure 4.20. Mass spectrum of mixture of **1•1**, **1•2**, and **2•2**.

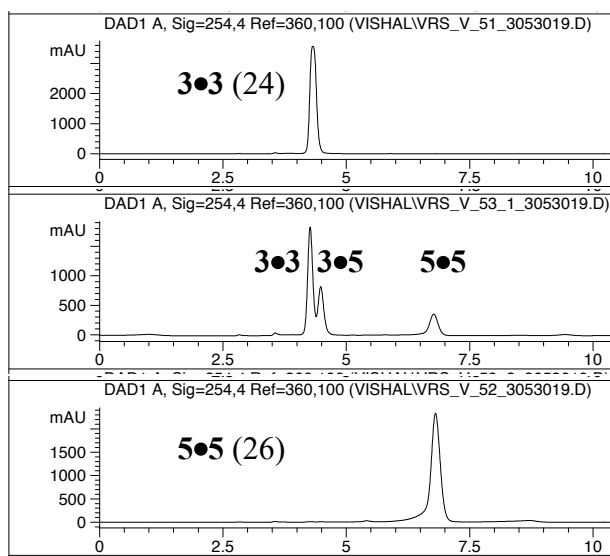


Figure 4.21. HPLC chromatograms of **3•3**, **3•5**, and **5•5**.

Other equimolar combination of monomers were also mixed to form heterodimers. A summary of products observed when equimolar amounts of different monomers were mixed is shown in Table 4.6.

Table 4.6. Products observed based on HPLC after mixing equal mole of precursors.

Reactants	Macrocycles observed		
1 + 2	1•1 (29%)	1•2 (35%)	2•2 (37%)
1 + 4	1•1 (25%)	1•4 (29%)	4•4 (45%)
1 + 5	1•1 (11%)	1•5 (26%)	5•5 (47%)
1 + 6	1•1 (25%)	1•6 (47%)	6•6 (18%)
2 + 6	2•2 (31%)	2•6 (30%)	6•6 (33%)
3 + 5	3•3 (52%)	3•5 (27%)	5•5 (21%)

After mixing equal moles of all the compounds (**1-6**) in equal volume of DCM and TFA, at least fourteen out of theoretically possible twenty one macrocycles (**1*1**, **1*2**, **1*3**, **1*4**, **1*5**,

1•6, 2•2, 2•3...) were observed using liquid chromatography-mass spectrometry (LC-MS) as shown in Figure 4.22.

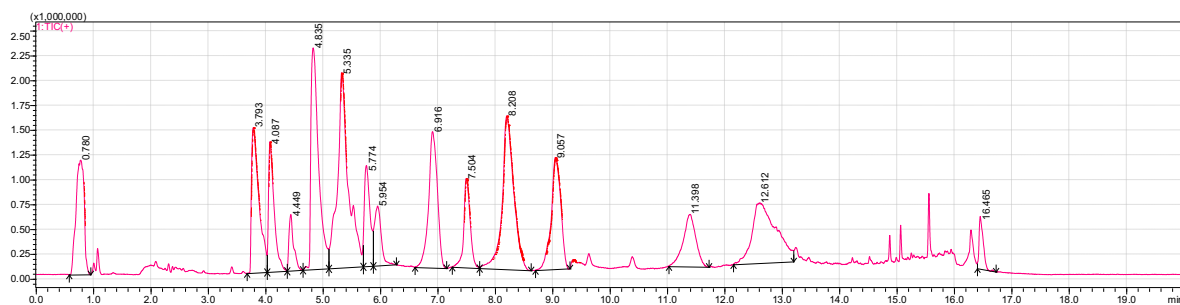


Figure 4.22. LC-MS of mixture of possible 21 macrocycles. Mixture obtained after mixing equal moles of compounds **1-6**. Data collected at Shimadzu Center of UTA.

Many combinations of macrocycles share a common molecular mass making an unambiguous assignment difficult. However, the appearance of at least 14 different species with molecular weights corresponding to dimeric products is satisfying. Macrocycles **1•1** and **6•6** with molecular masses 583 and 669 a.m.u. respectively are the only two out of twenty one macrocycles with unique molecular masses and, interestingly enough, appear to be absent in the mixture of products. They also represent the smallest (22-atoms) and largest (28-atoms) macrocycles respectively. The absence of **1•1** and **6•6** and possibly some other species is suggestive that selective pairing may be occurring. Some of the macrocycles on the LC-MS were identified and their summary is provided in Table 4.7.

Table 4.7. LC-MS molar mass of mixture of possible 21 products.

Elution Time	Molar Mass	Possible Macrocycle
3.8	613.3	4•4
4.1	613.3	1•3, 1•5, 2•4
4.5		1•2
4.8	613.3 627.3	2•2 4•5
5.3	613.3	1•3, 1•5, 2•4
5.6	627.3	1•6, 2•5, 2•3, 3•4
5.8	641.3	2•6, 3•6, 4•6
6.9	641.3	5•5
7.5	627.3	1•6, 2•5, 2•3, 3•4
8.2	655.3	5•6
9.1	641.3	2•6, 3•5, 4•6
11.4	655.3	3•6
12.6	641.3	3•3

4.4.10 Solubility of macrocycles

All of the macrocycles are insoluble in dichloromethane, chloroform, and other non-polar organic solvents. Macrocycles dissolve in DMSO. All of the macrocycles dissolve in mixture of methanol and water. Macrocycles **1•1** and **4•4** are completely insoluble in water. Solubility of all the macrocycles was determined qualitatively by dissolving about 1 mg of each macrocycle in increasing volumes of water, methanol, and dichloromethane (Table 4.8). To increase the solubility of macrocycles in future, the morpholine substituent of the triazine ring could be replaced. Incorporation of dimethyl amine is already under consideration. The solubility results are summarized in Table 4.8.

Table 4.8. Solubility of macrocycles in H₂O, CH₃OH, and CH₂Cl₂. I= insoluble, SS = slightly soluble, S = soluble.

Macrocycles	H ₂ O (ml)		CH ₃ OH (ml)		CH ₂ Cl ₂ (ml)	
	0.2	1.0	0.2	1.0	0.2	1.0
1•1	I	I	I	S	I	I
2•2	SS	S	I	S	I	I
3•3	S		S		I	I
4•4	I	I	S		I	I
5•5	S		S		I	I
6•6	S		S		I	SS

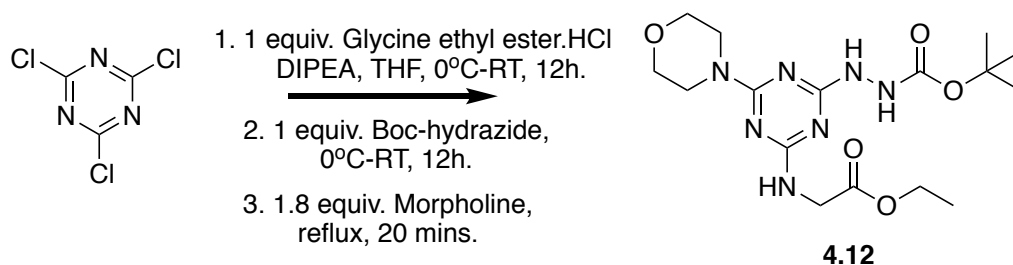
4.5 Conclusion

The work demonstrates the generality of the macrocyclization strategy for the preparation of rings of 22-28 atoms. These targets are synthesized with high yield and purity. The chemistry presented provides rapid access to dimeric products of varied ring sizes in high yields. Solution and solid state structural data suggests a range of morphologies can be adopted. Mixtures of homodimers and heterodimers can be obtained readily by mixing the desired protected monomers to yield odd-membered rings as well. However, the use of methylene groups to increase the size of the macrocycles generate flexibility in the ring. One of the future projects might include the incorporation of the rigidity by replacing the linear aliphatic acetals with cyclohexane, benzene,

and other rings. The self-condensation method of creating macrocycles can be used to create combinatory library of macrocycles containing triazine scaffolds with different ring sizes, amino acids, and *N*-alkyl groups. Incorporation of the more hindered amino acids than glycine is already being pursued.

4.6 Experimental Procedure

4.6.1 Synthesis of compound 4.12 from cyanuric chloride

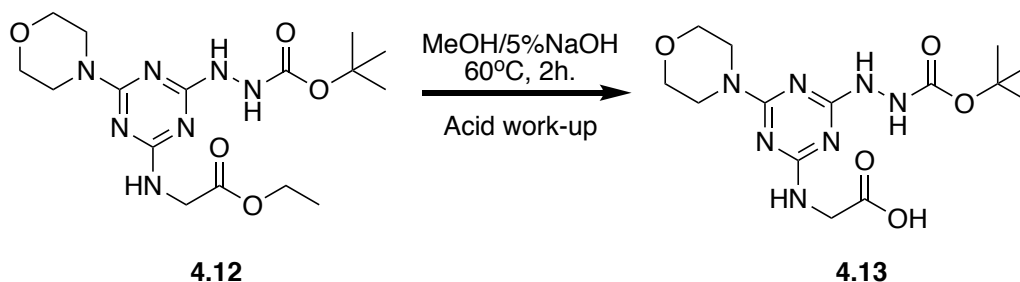


Scheme 4.7. Synthesis of compound **4.12**.

Cyanuric chloride (5.0 g, 0.027 moles) was dissolved in 40 ml dry THF in a three neck round bottom flask equipped with stirring bar and purged with argon. Glycine ethyl ester hydrochloride salt (3.8 g, 0.027 moles) and DIPEA (14 g, 0.10 moles) dissolved in a mixture of 2.0 ml MeOH and 5.0 ml THF were added dropwise at -20 °C. Temperature of the reaction mixture was raised slowly to room temperature and left to stir overnight. The reaction progress was monitored via TLC. Boc-hydrazide (3.6 g, 0.027 moles) was dissolved in 5 ml THF and then added dropwise to the reaction mixture at 0 °C. Resulting solution was warmed slowly to room temperature and left to stir over night. Morpholine (4.3 g, 0.05 moles) was added to the reaction mixture and refluxed for 20 minutes. Excess solvent was removed under vacuum and crude product was dissolved in 30 ml DCM (x2) and washed with H₂O. After removing excess solvent under vacuum, crude product was purified by column chromatography using 1:1 mixture of Hexane and ethyl acetate to afford **4.12** (7.7 g, 72%) as white solid. ¹H-NMR, CDCl₃, δ 4.21 (2H, 2), 4.12-4.06

(2H, q), 3.73-3.65 (8H, m), 1.44 (9H, s), 1.27-1.23 (3H, t). ^{13}C -NMR, CDCl_3 , δ 170.8, 167.8, 165.8, 164.9, 156.5, 81.0, 66.8, 61.1, 43.5, 43.0, 28.2, 14.2.

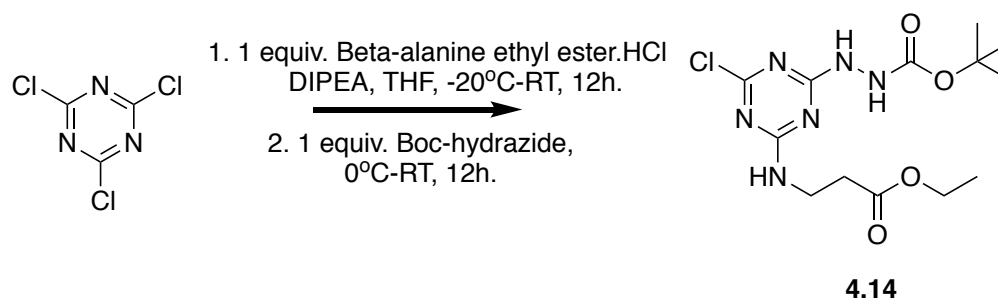
4.6.2 Synthesis of compound 4.13 (ester hydrolysis)



Scheme 4.8. Synthesis of compound 4.13.

Compound **4.12** (6.5 g, 0.016 moles) was dissolved in 20 ml MeOH and 10 ml 5% NaOH. The resulting mixture was stirred at 50 °C for 2 hours. Methanol was removed under vacuum and resulting solution was extracted with 25 ml DCM to retrieve any impurities and unreacted ester in organic layer. Aqueous Layer was acidified using 1 M HCl to pH 4.0-5.0 to precipitate the product. Solution was filtered to retrieve compound **4.13** (5.9 g, 98%) as white solid. ^1H -NMR, CDCl_3 , δ 4.15 (2H, 2), 3.85-3.72 (8H, m), 1.47 (9H, s).

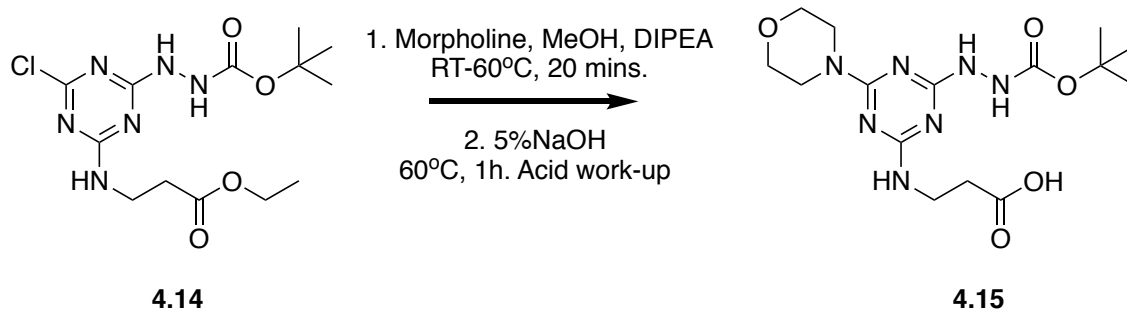
4.6.3 Synthesis of 4.14 from cyanuric chloride



Scheme 4.9. Synthesis of compound 4.14.

In a three neck round bottom flask equipped with stirring bar and purged with argon, cyanuric chloride (3.0 g, 0.016 moles) and 40 ml dry THF were added. β -alanine ethyl ester hydrochloride salt (2.5 g, 0.016 moles) and DIPEA (4.3 g, 0.03 moles) were dissolved in a mixture of 2 ml MeOH and 5 ml THF. The mixture was then added to flask at -20 °C. Reaction mixture was brought to room temperature slowly and left to stir overnight. The reaction progress was monitored by TLC. Boc-hydrazide (2.1 g, 0.016 moles) dissolved in 5 ml THF was then added to the reaction mixture at 0 °C. The resulting solution was raised slowly to room temperature and left to stir over night. After confirming the completion of reaction via TLC, excess solvent was removed under vacuum, crude product was dissolved in 20 ml DCM, extracted with 20 ml H₂O and collected in DCM (x3). Crude product was further purified by column chromatography using 1:1 mixture of hexanes:ethyl acetate to afford **4.14** (5.4 g, 94%) as white solid. ¹H-NMR, CDCl₃, δ 4.16-4.11 (2H, q), 3.69-3.68 (2H, m), 2.62-2.60 (2H, t), 1.45 (9H, s), 1.27-1.22 (3H, t). ¹³C-NMR, CDCl₃, δ 172.0, 168.4, 167.5, 165.7, 159.5, 81.7, 60.8, 36.6, 33.6, 28.1, 14.2.

4.6.4 Synthesis of 4.15 from 4.14

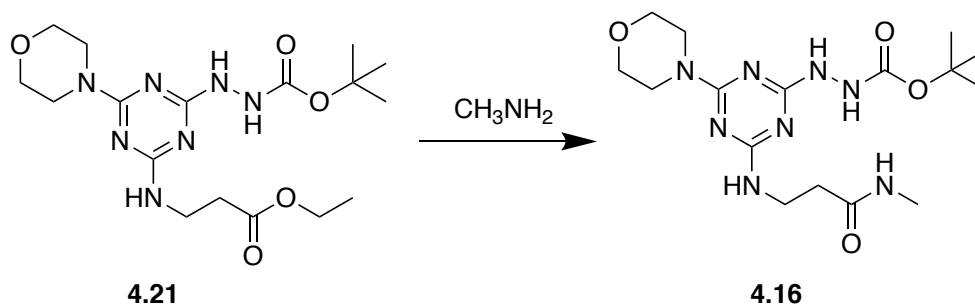


Scheme 4.10. Synthesis of compound **4.15**.

Compound **4.14** (2.8 g, 0.0078 moles) was dissolved in methanol in a small flask equipped with stirring bar. Morpholine (0.81 g, 0.0093 moles) and DIPEA (1.0 g) were added to flask. Reaction mixture was heated to 60 °C and left to stir for 15 minutes. Reaction progress was

monitored via TLC. After the completion of reaction 5 ml of 5% NaOH was added to reaction mixture and stirred for one hour at 60 °C. Methanol was removed under vacuum and crude was extracted with 30 ml DCM to remove any impurities and unreacted ester. Aqueous layer was acidified by adding 1 M HCl until precipitates appeared. Solution was filtered, washed with cold water, and dried under vacuum to retrieve **4.15** (2.75 g, 92%) as white solid. ¹H-NMR, CDCl₃/CD₃OD, δ 3.77-3.57 (10H, m), 2.44 (2H, m), 1.39 (9H, s). ¹³C-NMR, CDCl₃/CD₃OD, δ 179.3, 163.0, 158.0, 155.6, 81.3, 66.5, 43.9, 36.5, 34.7, 28.0.

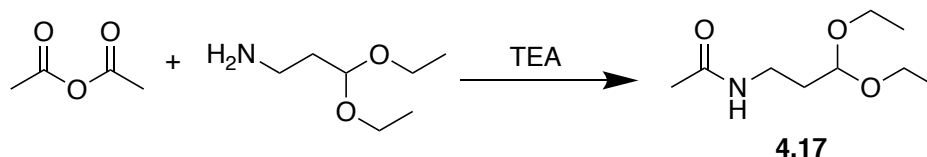
4.6.5 Synthesis of model compound **4.16**



Scheme 4.11. Synthesis of model compound **4.16**.

Compound **4.21** (200 mg, 0.52 mmol) was dissolved in 10 ml methanol in small three neck flask equipped with stirring bar and purged with argon. Methyl amine (40 mg, 1.3 mmol) was added to the reaction flask. Resulting solution was stirred overnight at room temperature for 4 days. Excess solvent was removed, residue was dissolved in 5 ml DCM (x2), and washed with 5 ml water. Crude product was further purified by column chromatography using dichloromethane and methanol (25:1) to recover compound **4.16** (128 mg, 62%) as white solid. ¹H-NMR, CDCl₃; δ 3.85-3.69 (10H, m), 3.33 (3H, s), 2.55 (2H, m), 1.46 (9H, s).

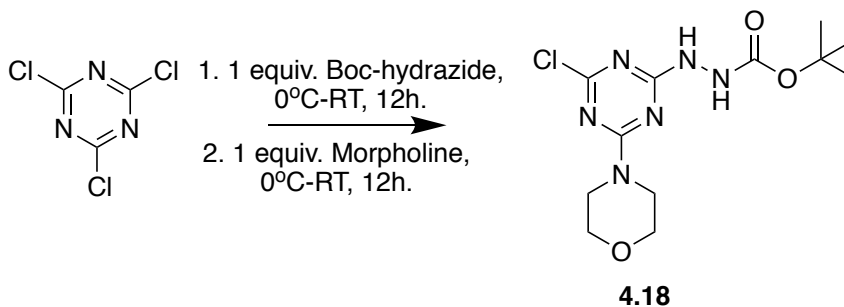
4.6.6 Synthesis of model compound 4.17



Scheme 4.12. Synthesis of model compound 4.17.

Acetic anhydride (10 ml) and amino propionaldehyde diethyl acetal (1.1 g, 7.4 mmol) was mixed in a small flask equipped with stirring bar. Triethylamine(0.5 ml) was added to the flask and resulting solution was stirred at room temperature for 12 hours. Reaction progress was measured by TLC. 5 ml of 10% NaOH was added to the reaction mixture and refluxed for 30 minutes. Reaction mixture was extracted using 15 ml ethyl acetate (x2) and 5 ml water. Product was recovered in ethyl acetate and purified by column chromatography using 2:1 hexanes:ethyl acetate to afford **4.17** (1.26 g, 89%) as slightly yellow liquid. ¹H-NMR, CDCl₃; δ 6.23 (1H, s), 4.59-4.57 (2H, q), 3.73-3.67 (2H, d), 3.66-3.50 (2H, m), 3.38-3.35 (2H, t), 2.08 (3H, s), 1.97-1.85 (2H, q), 1.25-1.22 (6H, t). ¹³C-NMR, CDCl₃; δ 170.0, 102.6, 62.0, 35.7, 32.7, 23.3, 20.8, 15.4

4.6.7 Synthesis of 4.18 from cyanuric chloride

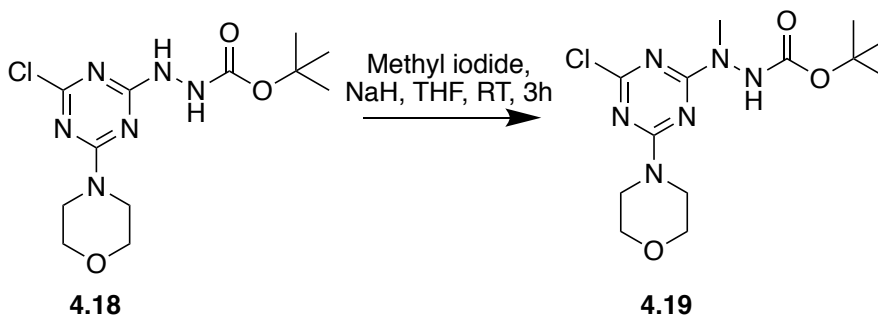


Scheme 4.13. Synthesis of compound 4.18.

In a small three neck flask equipped with stirring bar and purged with argon, cyanuric chloride (1.0 g, 5.4 mmol) and 30 ml THF were added. Two equivalent DIPEA (1.40 g, 10.8 mmol)

was added to the solution. One equivalent *tert*-butyl carbazate (0.72 g, 5.4 mmol) dissolved in 10 ml THF was added to reaction mixture at 0 °C. The resulting solution was brought to room temperature slowly and left to stir overnight at room temperature. Reaction progress was monitored by TLC. Once the reaction was complete, one equivalent morpholine (0.473 g, 5.4 mmol) dissolved in 10 ml was added dropwise to reaction solution at -30 °C. Resulting solution was brought to room temperature and left to stir overnight. Excess solvent was removed under vacuum, re-dissolved in 20 ml DCM (x2), washed with 10 ml water, dried over brine, and finally chromatographic purifications were done using 2:1 hexane: ethyl acetate solution to afford **4.18** (1.61 g, 91%) as white solid. ¹H-NMR, CDCl₃; δ 7.97 (1H, s), 6.55 (1H, s), 3.82-3.71 (8H, m), 1.47 (9H, s). ¹³C-NMR, CDCl₃; 169.3, 167.3, 155.4, 81.6, 66.5, 44.0, 39.2, 28.2.

4.6.8 Synthesis of 4.19 from 4.18

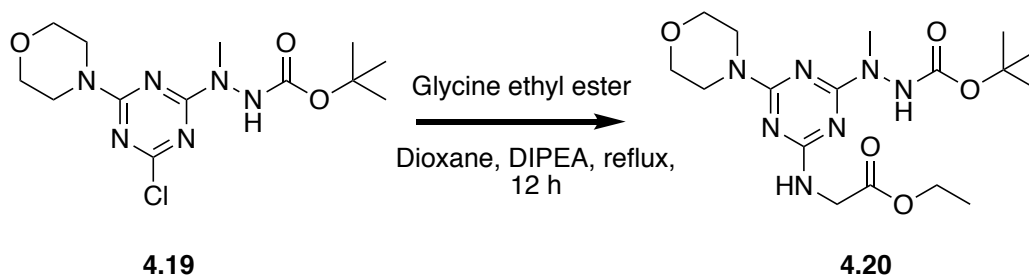


Scheme 4.14. Synthesis of compound **4.19**.

In a small round bottom flask purged with nitrogen, compound **4.18** (50 mg, 0.15 mmol) was dissolved in dry THF. One equivalent sodium hydride (3.7 mg, 0.15 mmol) was added to flask at 0 °C. After about 10 minutes, methyl iodide (43 mg, 0.30 mmol) was added to the solution. Reaction mixture was brought to room temperature and left to stir for 2 hours. Excess solvent was removed, the residue was dissolved in 5 ml DCM (x2), washed with 5 ml water, and further purified by column chromatography using 2:1 hexanes:ethyl acetate solvent system to afford **4.19**

(31 mg, 60%) as white solid. $^1\text{H-NMR}$, CDCl_3 ; δ 3.82-3.71 (8H, m), 3.40-3.36 (3H, s), 1.47 (9H, s). $^{13}\text{C-NMR}$, CDCl_3 ; δ 164.5, 81.9, 66.6, 43.9, 38.1, 28.2.

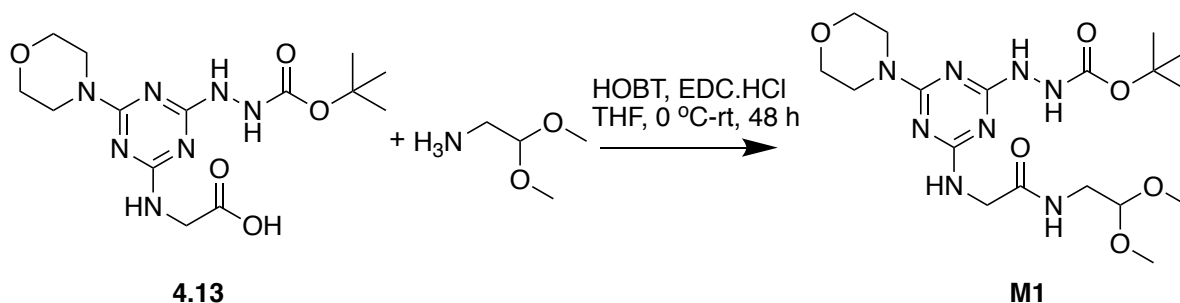
4.6.9 Synthesis of 4.20 from 4.19



Scheme 4.15. Synthesis of compound 4.20.

Compound **4.19** (30 mg, 0.087 mmol) was dissolved in 2 ml dioxane in a 5 ml round bottom flask. DIPEA (0.5 ml) and glycine ethyl ester (24 mg, 0.17 mmol) were added to reaction mixture and was refluxed for 12 hours. Excess solvent was removed under vacuum and purified by column chromatography using 1:1 hexanes:ethyl acetate solution mixture to yield **4.20** (26 mg, 74%) as white solid. $^1\text{H-NMR}$, CDCl_3 ; δ 5.51 (1H, m), 4.23-4.18 (2H, q), 4.13-4.10 (2H, d), 3.74-3.67 (8H, m), 3.30 (3H, s), 1.47 (9H, s), 1.29-1.26 (3H, t). $^{13}\text{C-NMR}$, CDCl_3 ; 170.7, 167.2, 166.0, 165.0, 156.2, 81.0, 66.8, 61.1, 43.5, 43.0, 37.5, 28.2, 14.2.

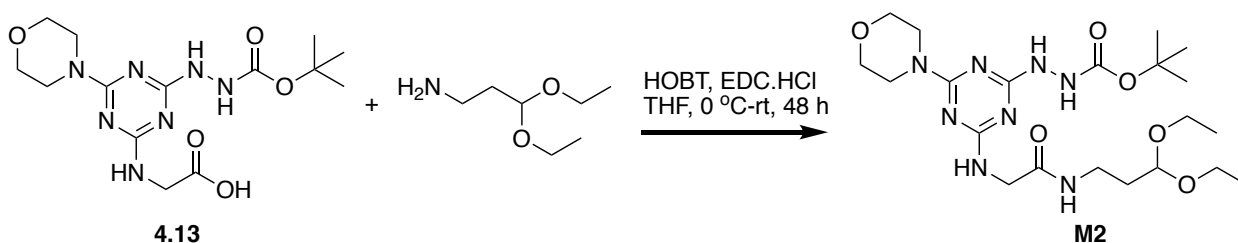
4.6.10 Coupling of 4.13 with amino acetaldehyde dimethyl acetal, synthesis of M1



Scheme 4.16. Synthesis of compound M1.

Compound **4.13** (1.0 g, 2.7 mmol) was dissolved in a mixture of 10 ml DCM and 5 ml dry DMF in a two-neck flask equipped with stirring bar and purged with Argon. HOBT (0.54 g, 3.5 mmol) and EDC.HCl (0.65 g, 3.6 mmol) were dissolved in 5 ml DMF and added to flask dropwise at 0 °C. After stirring the reaction mixture for 10 minutes, 0.35 g of DIPEA was added slowly. After 10 minutes, amino acetaldehyde dimethyl acetal (3.5 mmol, 0.37 g) of was added dropwise to flask. Resulting solution was brought to room temperature and left to stir for 48 hours at room temperature. Excess solvent was removed under vacuum and reaction mixture was washed with 10 ml water and collected in 15 ml DCM (x3). Crude product was further purified using column chromatography with 1:1 solvent ratio of Hexanes:ethyl acetate to remove the side product of HOBT and then 25:1 solvent ratio of DCM:MeOH to afford **M1** (610 mg, 51%) as white solid. ¹H-NMR, CDCl₃; δ 4.15 (2H, 2), 3.98 (2H, s), 3.85-3.72 (8H, m), 3.35 (6H, s), 1.47 (9H, s). ¹³C-NMR, CDCl₃; 170.7, 167.8, 166.2, 164.9, 156.5, 102.5, 81.3, 66.7, 54.3, 45.1, 43.6, 40.8, 28.2. MS (ESI/Q-TOF) m/z: [M+H]⁺ Calcd for C₁₈H₃₂N₈O₆ 456.24; Found 457.15.

4.6.11 Coupling of 4.13 with amino propionaldehyde diethyl acetal, synthesis of M2

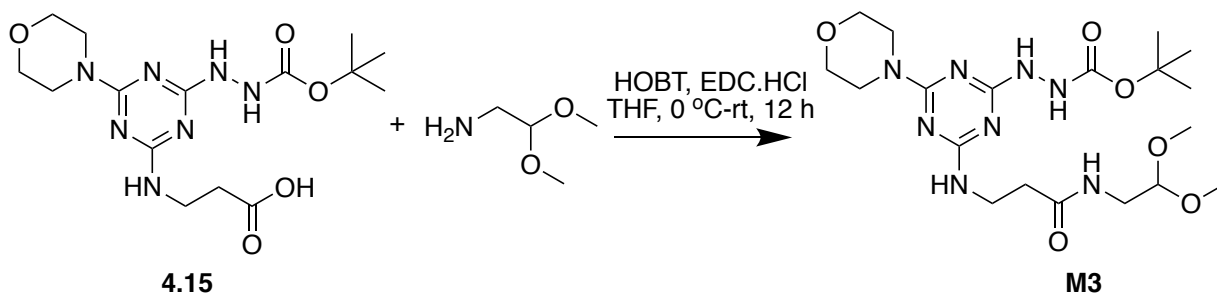


Scheme 4.17. Synthesis of compound **M2**.

Compound **8** (1.0 g, 2.7 mmol) was dissolved in a mixture of 10 ml DCM and 5 ml dry THF in a two-neck flask equipped with stirring bar and purged with Argon. HOBT (0.54 g, 3.5 mmol) and EDC.HCl (0.65 g, 3.6 mmol) dissolved in 5 ml DMF were added to flask dropwise at 0 °C. Reaction mixture was left to stir for 10 minutes and 0.35 g of DIPEA was added slowly.

After 5 minutes, amino propionaldehyde diethyl acetal (0.52 g, 3.5 mmol) was added dropwise to flask. Resulting solution was brought to room temperature and left to stir for 48 hours at room temperature. Excess solvent was removed under vacuum and reaction mixture was washed with water and crude product collected in DCM (x3). Crude product was further purified using column chromatography with 1:1 solvent ratio of Hexane: ethyl acetate to remove the side product made by HOBT and then 25:1 solvent ratio of DCM:MeOH to retrieve 650 mg (50%) of **P-2** as white solid. ¹H-NMR, CDCl₃; δ 4.48 (2H, s), 3.92-3.91 (2H, d), 3.41-3.70 (10H, m), 3.35 (6H, s), 3.32-3.39 (2H, q), 3.27-3.32 (2H, q), 1.75-1.78 (2H, m), 1.42 (9H, s), 1.12-1.16 (3H, t). ¹³C-NMR, CDCl₃; δ 170.2, 167.6, 165.9, 164.7, 156.5, 101.7, 81.3, 66.7, 61.6, 45.0, 43.5, 35.3, 33.0, 28.2, 15.2. MS (ESI/Q-TOF) m/z: [M+H]⁺ Calcd for C₂₁H₃₄N₈O₆ 498.29; Found 499.11.

4.6.12 Coupling of acid, **4.15**, with amino acetaldehyde dimethyl acetal, synthesis of **M3**

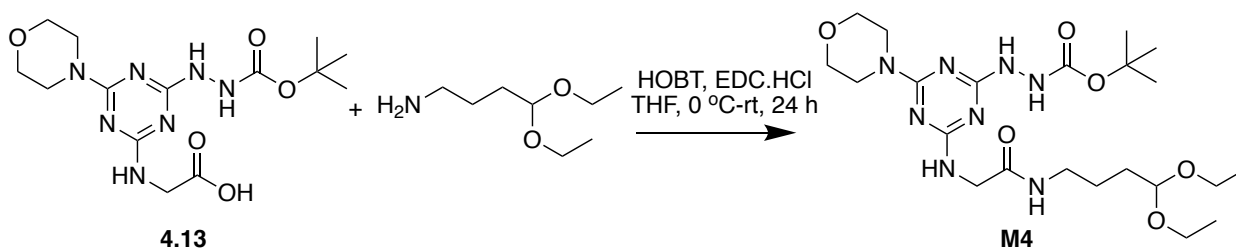


Scheme 4.18. Synthesis of compound **M3**.

Compound **4.15** (1.0 g, 2.6 mmol) was dissolved in a mixture of 5 ml DCM and 10 ml dry THF in a two-neck flask equipped with stirring bar and purged with Argon. HOBT (0.52 g, 3.4 mmol) was added to flask dropwise at 0 °C. Reaction mixture was left to stir for 10 minutes and EDC.HCl (0.65, 3.4 mmol) was added. After stirring for 10 minutes, amino acetaldehyde dimethyl acetal (0.33 g, 3.1 mmol) was added dropwise to flask at 0 °C. Resulting solution was brought to room temperature slowly and stirred for 36 hours. Excess solvent was removed under vacuum and

reaction mixture was washed with 15 ml 0.5 M acetic acid and crude product was collected in 20 ml DCM (x3). Organic layer was washed with 10 ml saturated NaHCO₃ to remove any acid. Crude product was further purified using column chromatography with 1:1 solvent ratio of Hexanes:ethyl acetate to remove the side products and then with 25:1 solvent ratio of DCM:MeOH to afford **M3** (580 mg, 56%) as white solid. ¹H-NMR, CDCl₃; δ 4.38 (1H, t), 3.72-3.68 (10H, m), 3.39 (8H, m), 2.50-2.47 (2H, t), 1.47 (9H, s). ¹³C-NMR, CDCl₃; 171.8, 165.0, 156.5, 102.7, 81.1, 66.8, 54.4, 43.5, 40.9, 36.9, 28.2. MS (ESI/Q-TOF) m/z: [M+H]⁺ Calcd for C₁₉H₃₄N₈O₆ 470.26; Found 471.18.

4.6.13 Coupling of 4.13, with 1-amino-4,4-diethoxybutane, synthesis of M4

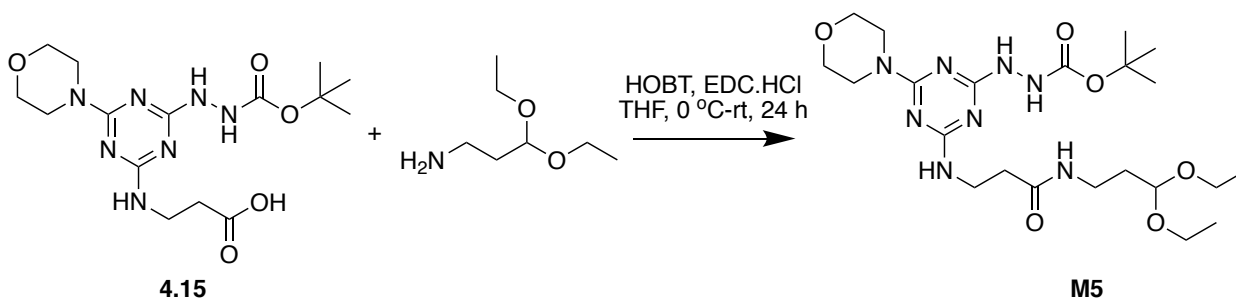


Scheme 4.19. Synthesis of compound **M4**.

Compound **4.13** (1.0 g, 2.7 mmol) was dissolved in a mixture of 5 ml DCM and 5 ml dry THF in a two-neck flask equipped with stirring bar and purged with Argon. HOBT (0.54 g, 3.5 mmol) and EDC.HCl (0.65 g, 3.6 mmol) were dissolved in 5 ml DMF and added to flask dropwise at 0 °C. Reaction mixture was stirred for 10 minutes and DIPEA (0.35 g) was added slowly. After stirring the mixture for 10 minutes, amino propionaldehyde diethyl acetal (0.52 g, 3.5 mmol) was added dropwise. Resulting solution was warmed to room temperature and stirred for 30 hours. Excess solvent was removed under vacuum, dissolved in 15 ml DCM, washed with 10 ml 0.5 M acetic acid, and collected in DCM (x3). Organic layer was washed with 10 ml saturated NaHCO₃. Crude product was further purified using column chromatography with 1:1 Hexanes:ethyl acetate

to remove the side product and then with 25:1 DCM:MeOH to retrieve **M4** (550 mg, 40%) as white solid. ¹H-NMR, CDCl₃; δ 4.46-4.43 (1H, t), 3.72-3.56 (10H, m), 3.59-3.43 (2H, m), 3.24-3.21 (2H, q), 1.57-1.53 (4H, m), 1.43 (9H, s), 1.18-1.15 (3H, t). ¹³C-NMR, CDCl₃; δ 170.2, 167.6, 166.1, 164.8, 156.8, 102.5, 81.2, 66.7, 61.2, 46.0, 45.0, 39.0, 30.9, 28.2, 24.7, 24.7, 15.3. MS (ESI/Q-TOF) m/z: [M+H]⁺ Calcd for C₂₂H₄₀N₈O₆ 512.31; Found 513.15.

4.6.14 Coupling of acid, **4.15**, with amino propionaldehyde diethyl acetal, synthesis of **M5**

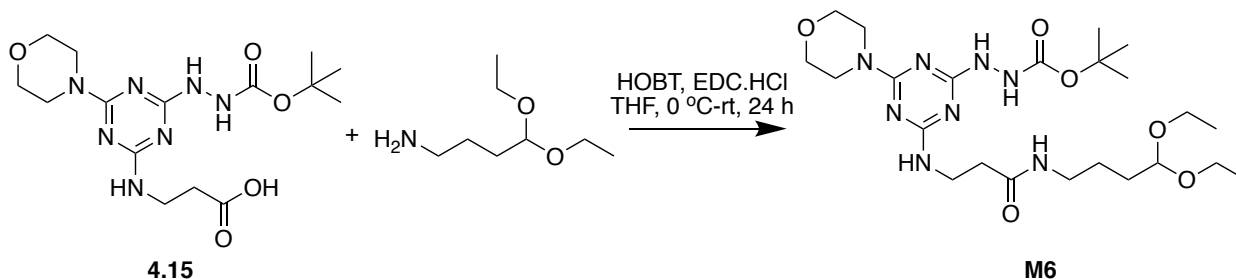


Scheme 4.20. Synthesis of compound **M5**.

Compound **4.15** (700 mg, 1.8 mmol) was dissolved in a mixture of 4 ml DCM and 8 ml dry THF in a two-neck flask equipped with stirring bar and purged with Argon. HOBT (0.29 g, 1.9 mmol) was added to flask dropwise at 0 °C. Reaction mixture was left to stir for 10 minutes and EDC.HCl (0.36 g, 1.9 mmol) was added. After 10 minutes, amino propionaldehyde diethyl acetal (0.18g, 1.9 mmol) dissolved in 3 ml THF was added dropwise to flask at 0 °C. Resulting solution was warmed to room temperature slowly and stirred for 24 hours. Excess solvent was removed under vacuum, reaction mixture was washed with 10 ml 0.5 M acetic acid and crude product was collected in 20 ml DCM (x3). Organic layer was washed with 10 ml saturated NaHCO₃ to remove acid. Crude product was further purified by column chromatography using 1:1 hexanes:ethyl acetate to remove the side product and then with 25:1 DCM:MeOH to retrieve **M5** (510 mg, 55%) as white solid. ¹H-NMR, CDCl₃; δ 4.55 (1H, t), 3.76-3.63 (12H, m), 3.51-3.48 (2H,

q), 3.34-3.31 (2H, q), 2.45-2.42 (2H, t), 1.81-1.80 (2H, q), 1.46 (9H, s), 1.22-1.19 (3H, t). ¹³C-NMR, CDCl₃; 171.3, 165.0, 156.6, 102.2, 81.0, 66.8, 61.8, 43.5, 37.0, 36.3, 35.5, 32.8, 28.2, 15.3. MS (ESI/Q-TOF) m/z: [M+H]⁺ Calcd for C₂₂H₄₀N₈O₆ 512.31; Found 513.17.

4.6.15 Coupling of acid, 4.15, with 1-amino-4,4-diethoxybutane, synthesis of M6

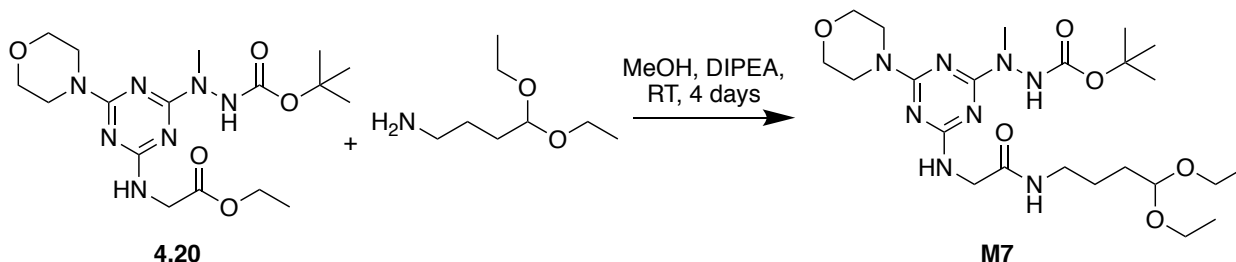


Scheme 4.21. Synthesis of compound M6.

Compound **4.15** (920 mg, 2.4 mmol) was dissolved in a mixture of 5 ml DCM and 5 ml dry THF in a two-neck flask equipped with stirring bar and purged with Argon. HOBT (0.44 g, 2.8 mmol) was added to flask dropwise at 0 °C and resulting reaction mixture was stirred for 10 minutes. EDC.HCl (2.8 mmol, 0.55 g) was added. After 10 minutes, amino butanaldehyde diethyl acetal (2.8 mmol, 0.47 g) dissolved in 2 ml THF was added dropwise to flask. Resulting solution was warmed to room temperature slowly and left to stir for 24 hours at room temperature. Excess solvent was removed under vacuum and reaction mixture was washed with 0.5 M acetic acid and crude product collected in DCM (x3). Crude product was then further washed with saturated NaHCO₃ to remove any acid. Crude product was further purified using column chromatography with 1:1 hexanes:ethyl acetate to remove the side product made by HOBT and then with 25:1 DCM:MeOH to retrieve **M6** (520 mg, 42%) as white solid. ¹H-NMR, CDCl₃; δ 4.48-4.45 (1H, t), 3.76-3.60 (12H, m), 3.50-3.44 (2H, m), 3.21-3.20 (2H, q), 2.44-2.41 (2H, t), 1.61-1.59 (2H, m), 1.56-1.54 (2H, m), 1.45 (9H, s), 1.21-1.18 (3H, t). ¹³C-NMR, CDCl₃; 171.7, 167.6, 166.6, 165.7,

164.9, 156.7, 102.6, 80.8, 66.8, 61.2, 43.5, 39.2, 37.0, 36.3, 31.0, 28.2, 24.5, 15.3. MS (ESI/Q-TOF) m/z: [M+H]⁺ Calcd for C₂₃H₄₂N₈O₆ 526.31; Found 527.17.

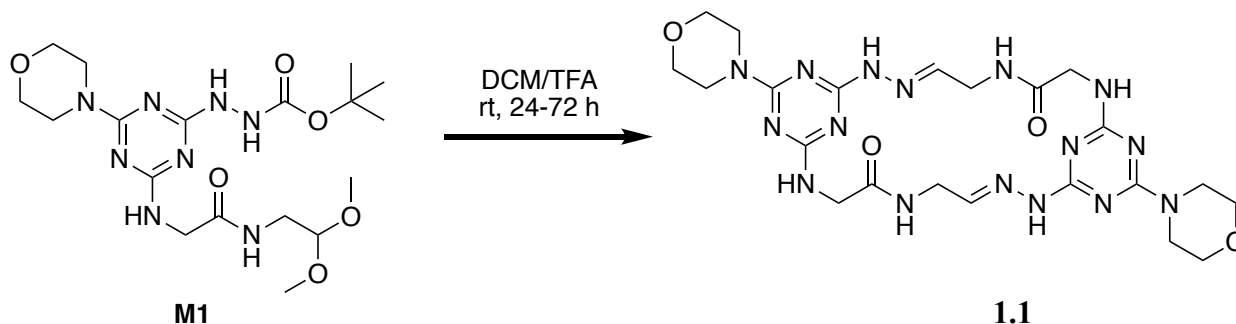
4.6.16 Synthesis of monomer **M7** from **4.20** by direct amidation of ester



Scheme 4.22. Synthesis of monomer **M7**.

In a small flask equipped with stirring bar and purged with argon, compound **4.20** (21 mg, 0.051 mmol) was dissolved in 2 ml methanol. DIPEA (0.5 ml) and amino butanal diethyl acetal (17 mg, 0.12 mmol) were added to reaction mixture. The resulting solution was left to stir at room temperature for 4 days. Product formation was determined by the TLC. After the completion of the reaction, excess solvent was removed, and the crude product was further purified by column chromatography using 25:1 solvent ratio of DCM:MeOH to retrieve **7** (20 mg, 74%) as white solid. Compound **M7** was used to make macrocycle **7.7** without further characterization. R_f value of **M7** was lower than that of **4.20** and taken as the evidence of product formation.

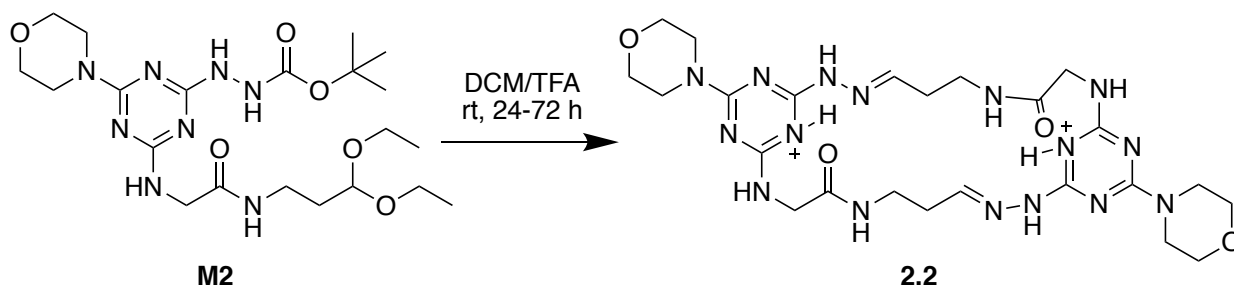
4.6.17 Synthesis of Macrocycle **1•1** from **M1**



Scheme 4.23. Synthesis of macrocycle **1•1**.

Compound **M1** (220 mg, 0.35 mmol) was dissolved in a 3 ml DCM and 3ml TFA in a small flask equipped with stirring bar. The resulting solution was left to stir at room temperature for 48 hours. Crude product was then washed with 1 ml DCM (x2) and filtered. The precipitates were washed with 0.5 ml MeOH. Excess MeOH should be avoided as macrocycle is slightly soluble in MeOH at room temperature. Precipitates were dried under vacuum to afford macrocycle **1•1** (130 mg, 93%) as white solid. All the NH proton disappeared quickly when a drop of CD₃OD was added to NMR tube. Protons of Protonated nitrogen of triazine ring and the hydrazine disappeared faster than the protons of nitrogen of glycine and amide linker. ¹H-NMR, DMSO; δ 12.62 (1H, s), 8.44-8.42 (1H, t), 8.24-8.22 (1H, t), 7.63 (1H, s), 4.21-4.20 (H, d), 4.13-4.12 (2H, d), 3.84-3.66 (8H, m). ¹³C-NMR DMSO-*d*₆; 168.3, 161.7, 155.0, 154.0, 147.5, 66.2, 44.6, 44.5, 41.0. MS (ESI/Q-TOF) m/z: [M+H]⁺ Calcd for C₂₂H₃₂N₁₆O₄ 584.28; Found 585.29.

4.6.18 Synthesis of **2•2** from **M2**

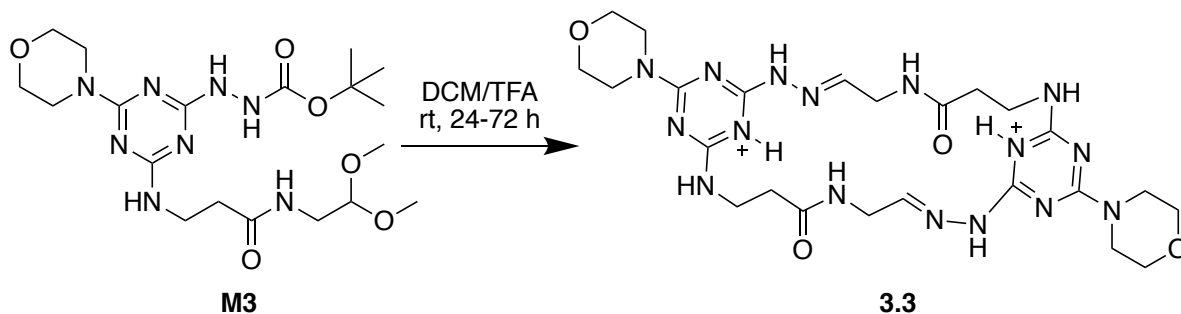


Scheme 4.24. Synthesis of macrocycle **2•2**.

In a small flask equipped with stirring bar, monomer **M2** (350 mg, 0.70 mmol) was dissolved in a 3 ml DCM and 3 ml TFA. Resulting solution was left to stir at room temperature for 48 hours. Crude product was then washed with 2 ml DCM and filtered. The precipitates were washed with 0.5 ml MeOH (x2). Precipitates were dried under vacuum to afford **2•2** (201 mg, 93%) as white solid. ¹H-NMR, DMSO; δ 12.37 (1H, s), 9.04 (1H, s), 8.91 (1H, s), 7.51 (1H, s),

3.89-3.88 (2H, d), 3.71-3.49 (10H, m), 2.56 (2H, m). ^{13}C -NMR, CD_3OD ; δ 171.8, 161.3, 154.6, 154.0, 147.9, 66.2, 44.7, 43.8, 33.6, 31.6. MS (ESI/Q-TOF) m/z : $[\text{M}+\text{H}]^+$ Calcd for $\text{C}_{24}\text{H}_{36}\text{N}_{16}\text{O}_4$ 612.31; Found 613.32.

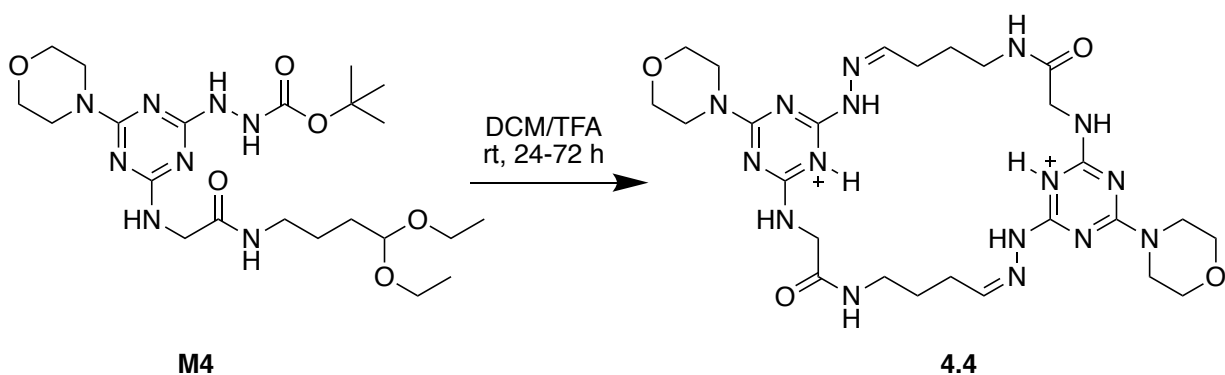
4.6.19 Synthesis of **3•3** from **M3**



Scheme 4.25. Synthesis of macrocycle **3•3**

Compound **M3** (90 mg, 0.19 mmol) was dissolved in a mixture of 2 ml DCM and 2 ml TFA in a small flask equipped with stirring bar. Reaction mixture and resulting solution was left to stir at room temperature for 48 hours. Crude product was then washed with 2 ml DCM and filtered. The precipitates were then washed with 0.5 ml MeOH. Precipitates were air dried to afford **3•3** (55 mg, 95%) as white solid. ^1H -NMR, DMSO; δ 12.62 (1H, s), 11.45 (1H, s), 9.09 (1H, t), 8.35-8.32 (1H, t), 7.62-7.61 (1H, t), 4.30-4.28 (2H, d), 3.86-3.68 (8H, m), 3.28-3.26 (2H, m), 2.39 (2H, m), 1.73-1.72 (2H, m). ^{13}C -NMR, CD_3OD ; δ 172.6, 161.3, 155.3, 154.3, 146.6, 66.4, 44.3, 40.0, 37.7, 37.3. M/Z: MS (ESI/Q-TOF) m/z : $[\text{M}+\text{H}]^+$ Calcd for $\text{C}_{24}\text{H}_{36}\text{N}_{16}\text{O}_4$ 612.31; Found 613.37.

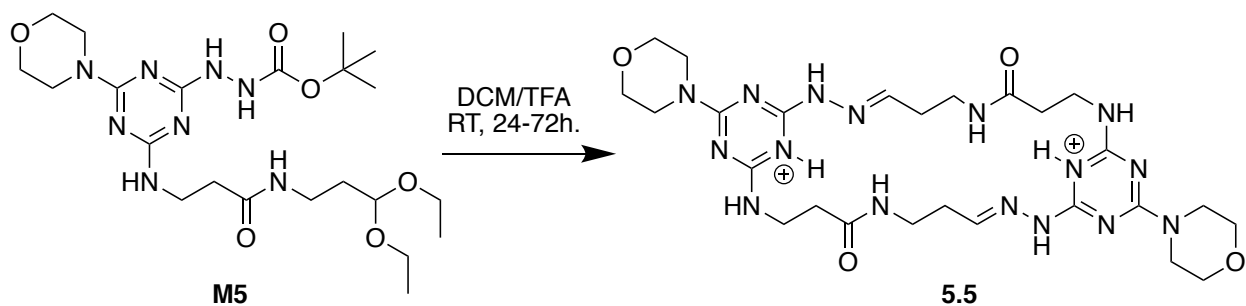
4.6.20 Synthesis of macrocycle 4•4 from M4



Scheme 4.26. Synthesis of macrocycle 4•4

Compound **M4** (220 mg, 0.39 mmol) was dissolved in a mixture of 3 ml DCM and 3 ml TFA in a small flask equipped with stirring bar. Produced solution was left to stir at room temperature for 48 hours. Crude product was then washed with 2 ml DCM (x2) and filtered. The precipitates were then washed with 0.5 ml MeOH. Precipitates were air dried to afford 98 mg (80%) of **4•4** as white solid. ¹H-NMR, DMSO; δ 12.62 (1H, s), 11.45 (1H, s), 9.09 (1H, t), 8.35-8.32 (1H, t), 7.62-7.61 (1H, t), 4.30-4.28 (2H, d), 3.86-3.68 (8H, m), 3.28-3.26 (2H, m), 2.39 (2H, m), 1.73-1.72 (2H, m). ¹³C-NMR, CD₃OD; δ 169.2, 161.6, 154.4, 154.1, 150.5, 66.1, 44.5, 42.6, 37.8, 27.7, 24.5. M/Z: MS (ESI/Q-TOF) m/z: [M+H]⁺ Calcd for C₂₆H₄₂N₁₆O₄ 640.31; Found 641.40.

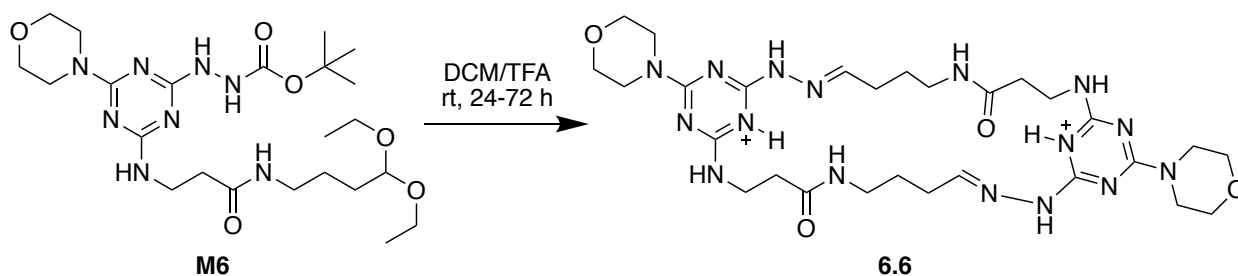
4.6.21 Synthesis of 5•5 from M5



Scheme 4.27. Synthesis of macrocycle **5•5**.

Compound **M5** (20 mg, 0.039 mmol) was dissolved in a mixture of 1 ml DCM and 1 ml TFA in a small flask equipped with stirring bar. The resulting solution was left to stir at room temperature for 48 hours. Crude product was air dried to afford **5•5** (12 mg, 100%) as white solid. No further purification was done, and NMR of crude product was taken. $^1\text{H-NMR}$, DMSO; δ 12.62 (1H, s), 11.45 (1H, s), 9.09 (1H, t), 8.35-8.32 (1H, t), 7.62-7.61 (1H, t), 4.30-4.28 (2H, d), 3.86-3.68 (8H, m), 3.28-3.26 (2H, m), 2.39 (2H, m), 1.73-1.71 (2H, m). $^{13}\text{C-NMR}$, DMSO; δ 171.5, 161.7, 154.7, 154.6, 150.7, 66.2, 44.6, 36.6, 35.9, 34.4, 33.0. M/Z: MS (ESI/Q-TOF) m/z: $[\text{M}+\text{H}]^+$ Calcd for $\text{C}_{26}\text{H}_{40}\text{N}_{16}\text{O}_4$ 640.34; Found 641.37.

4.6.22 Synthesis of **6•6** from **M6**

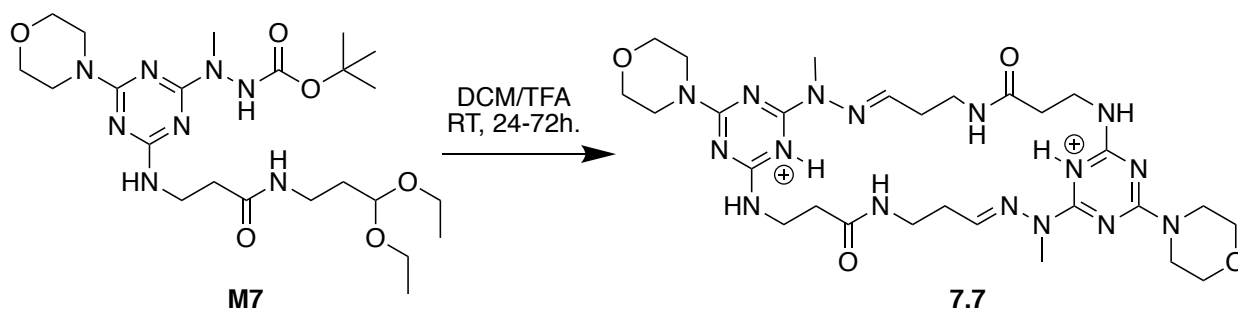


Scheme 4.28. Synthesis of macrocycle **6•6**.

Monomer **M6** (150 mg, 0.29 mmol) was dissolved in a 3 ml DCM and 3 ml TFA in a small flask equipped with stirring bar. Resulting solution was left to stir at room temperature for 48 hours. Crude product was then washed with 2 ml DCM and filtered. The precipitates were washed with 0.3 ml MeOH (x2). Precipitates were air dried to afford of **6•6** (85 mg, 86%) as white solid. $^1\text{H-NMR}$, DMSO- d_6 ; δ 12.62 (1H, s), 11.45 (1H, s), 9.09 (1H, t), 8.35-8.32 (1H, t), 7.62-7.61 (1H, t), 4.30-4.28 (2H, d), 3.86-3.68 (8H, m), 3.28-3.26 (2H, m), 2.39 (2H, m), 1.73-1.72 (2H, m). $^{13}\text{C-}$

NMR, CD₃OD; 172.5, 161.7, 154.7, 154.3, 150.6, 66.1, 44.4, 37.7, 36.4, 33.3, 27.6, 24.5. M/Z:
MS (ESI/Q-TOF) m/z: [M+H]⁺ Calcd for C₂₈H₄₆N₁₆O₄ 668.37; Found 669.46.

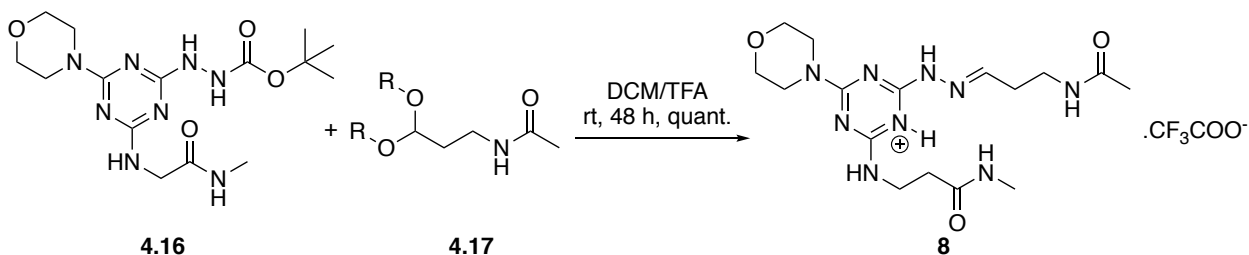
4.6.23 Synthesis of macrocycle **7•7** from **M7**



Scheme 4.29. Synthesis of macrocycle **7•7**.

Compound **M7** (20 mg, 0.038 mmol) was dissolved in a 2 ml DCM and 2 ml TFA in a small flask equipped with stirring bar. Resulting solution was left to stir at room temperature for 48 hours. Crude product was then washed with 1 ml DCM (x2) and filtered. Precipitates were dried under vacuum to afford macrocycle **7•7** (11 mg, 87%) as white solid. ¹H-NMR, DMSO-*d*₆; δ 11.53 (1H, s), 9.11-9.08 (1H, t), 8.70-8.67 (1H, t), 7.60-7.59 (1H, t), 4.30-4.29 (2H, d), 3.87-3.86 (4H, m), 3.69-3.67 (4H, m), 3.45 (3H, s), 3.27-3.24 (2H, m), 2.50-2.48 (2H, m), 1.79 (2H, m). ¹³C-NMR, DMSO-*d*₆; δ 169.6, 161.0, 154.7, 154.2, 149.1, 66.2, 44.8, 43.4, 37.7, 29.9, 28.4, 24.5.

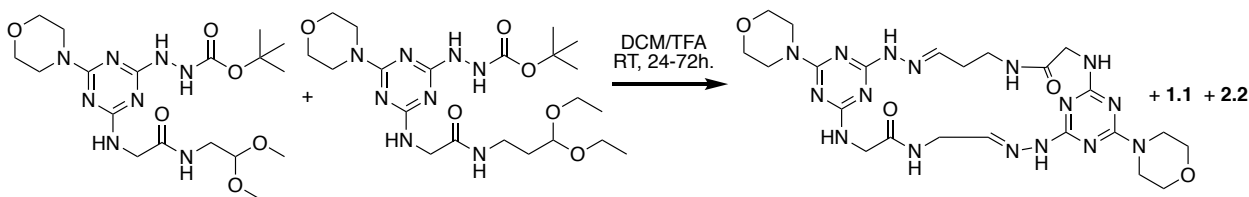
4.6.24 Synthesis of model imine **8** from **4.16** and N-acetyl propionaldehyde acetal (**4.17**)



Scheme 4.30. Synthesis of imine model compound **8**.

Compound **4.16** (20 mg, 0.049 mmol) and **4.17** (9.3 mg, 0.049 mmol) were dissolved in 2 ml DCM and 2 ml TFA. Resulting reaction mixture was left to stir at room temperature for 24 hours. No purification was done and the NMR of the crude product was taken. ¹H-NMR, DMSO-*d*₆; δ 12.36 (1H, s), 11.55 (1H, s), 8.14-8.13 (1H, t), 8.07-8.04 (1H, t), 7.56-7.55 (1H, t), 3.83-3.57 (10H, m), 3.31-3.26 (2H, q), 2.61-2.59 (3H, d), 2.51-2.41 (4H, m), 1.80 (3H, s). ¹³C-NMR, DMSO-*d*₆; δ 171.1, 170.0, 161.6, 154.7, 154.3, 151.8, 66.2, 44.6, 37.0, 36.0, 34.4, 33.2, 25.9, 23.0

4.6.25 Reaction of macrocycles **1•1**, **2•2**, and **1•2**



Scheme 4.31. Synthesis of macrocycles **1•1**, **2•2**, and **1•2**

Compound **M2** (95 mg, 0.19 mmol) and compound **M1** (87 mg, 0.19 mmol) were dissolved in a 3 ml DCM and 3 ml TFA in a small flask equipped with stirring bar. Resulting solution was left to stir at room temperature for 48 hours. Crude product was then washed with 3 ml DCM (x2) and filtered. The precipitates were washed with 0.5 ml MeOH (x2). Precipitates were dried under vacuum to afford 121 mg of mixture of **1•1**, **1•2**, and **2•2** as white solid. M/Z: MS (ESI/Q-TOF) *m/z* (**1.2**): [M+H]⁺ Calcd for C₂₃H₃₄N₁₆O₄ 598.29; Found 599.33.

4.6.26 Synthesis of macrocycles **3•3**, **3•5**, and **5•5**

Compound **M3** (90 mg, 0.192 mmol) and compound **M5** (98 mg, 0.192 mmol) were dissolved in equal mixture of 2 ml of DCM and 2 ml of TFA in a small flask. Solution was left to

stir for 24 hours at room temperature. Mass spectrum of crude product indicate the formation of **3•3**, **3•5**, and **5•5**. In addition, their formation was confirmed by HPLC analysis.

4.6.27 Synthesis of macrocycles 1•1, 1•4, and 4•4

Compound **M1** (8.5 mg, 0.018 mmol) and compound **M4** (9.3 mg, 0.018 mmol) were dissolved in equal mixture of 1 ml of DCM and 1 ml of TFA in a small flask. Solution was left to stir for 24 hours at room temperature. Mass spectrum of crude product confirmed the formation of **1•1**, **1•4**, and **4•4**. In addition, their formation was confirmed by HPLC analysis.

4.6.28 Synthesis of macrocycles 1•1, 1•6, and 6•6

Compound **M1** (10 mg, 0.02 mmol) and compound **M6** (11 mg, 0.02 mmol) were dissolved in equal mixture of 1 ml of DCM and 1 ml of TFA in a small flask. Solution was left to stir for 24 hours at room temperature. Mass spectrum and HPLC analysis of crude product indicated the formation of **1•1**, **1•6**, and **6•6**.

4.6.29 Synthesis of macrocycles 1•1, 1•5, and 5•5

Compound **M1** (9 mg, 0.019 mmol) and compound **M5** (9.8 mg, 0.019 mmol) were dissolved in equal mixture of 1 ml of DCM and 1 ml of TFA in a small flask. Solution was left to stir for 24 hours at room temperature. After slow evaporation of solvents, HPLC and mass spectrum was taken without further purifications. Mass spectrum of crude product indicate the formation of **1•1**, **1•5**, and **5•5**. In addition, their formation was confirmed by HPLC analysis

4.6.30 Synthesis of macrocycles **2•2**, **2•6**, and **6•6**

Compound **M2** (22.7 mg, 0.05 mmol) and compound **M5** (23.3 mg, 0.05 mmol) were dissolved in equal mixture of 2 ml of DCM and 2 ml of TFA in a small flask. Solution was left to stir for 24 hours at room temperature. After slow evaporation of solvents, HPLC and mass spectrum was taken without further purifications. Mass spectrum of crude product indicate the formation of **2•2**, **2•6**, and **6•6**. In addition, their formation was also confirmed by HPLC analysis.

4.6.31 Synthesis of mixture of 14-21 macrocycles

Compounds **M(1-6)** in equal moles of **M1** (40 mg, 0.09 mmol), **M2** (43.7 mg), **M3** (41.2 mg), **M4** (45 mg), **M5** (45 mg), and **M6** (46.1 mg)) were dissolved in 5 ml DCM and 5 ml TFA. The resulting solution was left to stir at room temperature for more than 48 hours. No purification was done and HPLC was run of the crude sample. HPLC chromatogram shows the formation of at least 14 products. In addition, LC-MS also shows the formation of at least 14 macrocycles based on the number of peaks and molar masses of macrocycles. However, identification of the peaks is an undergoing investigation.

Chapter 5: Conclusions and future work

Triazinyl hydrazones: Triazinyl hydrazones have been found to be more stable at low pH compare to acyl hydrazones. Hydrazones have been used in drug delivery. However, 1,3-diketones could not be used as they make stable pyrazole or hemiaminal ring. Our designs *N*-substituted triazinyl hydrazines preclude the formation of pyrazole or hemiaminal rings. The reaction of *N*-substituted triazinyl hydrazine with 1,3- diketone formed open chain hydrazone that contains enol functional group.

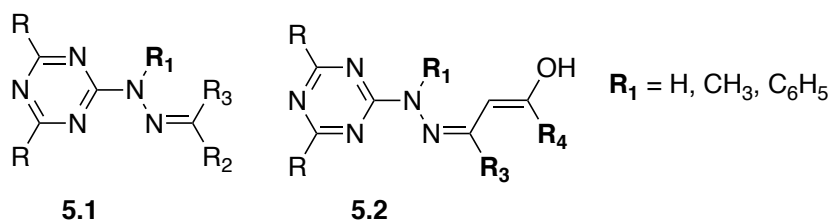


Figure 5.1. General structure of triazinyl hydrazones synthesized.

The analogy of creating an open chain hydrazone with enol functional group can be used in future for delivering drugs that contain 1,3-diketones.

Hemiaminal: Literature reports various examples of hemiaminals. Here, we used triazine chloride as core to create stable cyclic hemiaminals in ethanol under acidic conditions. This observation underscores the influence of adopting both a strong electron withdrawing group and a hydrogen bond acceptor as design criteria. We conclude the presence of both a hydrogen bond and a strong electron withdrawing group produce a stable hemiaminal. Absence of any one of two requirements will not produce a stable hemiaminal.

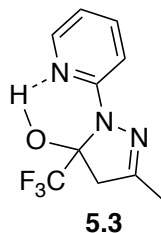
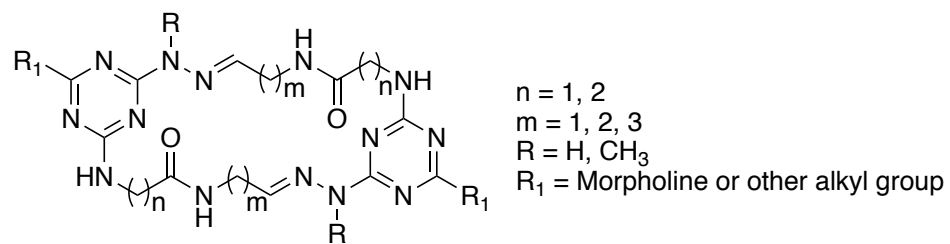


Figure 5.2. General structure of stable hemiaminals synthesized.

Hemiaminals were found to be stable at room temperature in acidic ethanolic solutions (HCl, glacial acetic acid, *p*TSA, and H₂SO₄). Refluxing for three hours hemiaminals in solutions of diisopropylethylamine or pyridine led to no change. However, the hemiaminals containing hydrogen-bond acceptor and CF₃ required acid and elevated temperature to convert to respective pyrazole derivatives.

The experimental findings are in agreement with computational data recorded by Arshad Mehmood of Dr. Janesko group. Stability at room temperature across a range of pH values as well as in neat glacial acetic acid suggests that these structures might have general utility in a range of applications.

Macrocycles: We designs a synthetic method using triazine chemistry to form macrocycles of various ring sizes in high yields and purity. Self-assembly of two triazine monomer units containing an amine and aldehyde functional group promotes the formation of the large macrocycles of rings 22-28 atoms. Two hydrazone groups are used to connected two monomer units. The synthesis of macrocycles appears to be independent of the concentration of starting material.



5.4

Figure 5.3. General structure of macrocycles synthesized. $R_1 = H, CH_3$, or other alkyl groups.

Macrocycles made in this project are rather flexible and do not necessarily translate the size of the core of ring. Flexibility of these macrocycles also makes it challenging to determine the solution conformation. Macrocycles can be made rigid by incorporating the use of aliphatic and aromatic rings as linkers.

References:

1. Schiff, H. *Justus Liebigs Ann. Chem.* **1864**, *131*, 118–119.
2. Patai, S. *The Chemistry of the Carbon-Nitrogen Double Bond*; Wiley: New York, NY, USA, **1970**.
3. Tennant, G. Sutherland, I.O., Ed.; Pergamon: Oxford, UK, **1979**, *2*, 385–590.
4. Whitesell, J.K. In *Comprehensive Organic Synthesis*, Winterfeldt, E., Ed.; Pergamon: Oxford, UK, **1991**, *6*, 703–732.
5. Robertson, G.M.; Katritzky, A.R.; Meth-Cohn, O.; Rees, C.W. *Elsevier: Amsterdam, The Netherlands*, **1995**, *3*, 403–423.
6. Pawlenko, S.; Klamann, D.; Hagemann, H. *Thieme: Stuttgart, Germany*, **1980**, *E14b*, 222–281.
7. Holm, R.H.; Everett, J.G.W.; Chakravorty, *Prog. Inorg. Chem.* **1966**, *7*, 83–214.
8. Vigato, P.A.; Tamburini, S. *Coord. Chem. Rev.* **2004**, *248*, 1717–2128.
9. Schiff, H. *Justus Liebigs Ann. Chem.* **1966**, *140*, 92–137.
10. Schiff, U. *Palermo*, **1867**, *2*, 1–59.
11. Dobbs, A.P.; Rossiter, S.; Alan, R.K.; Taylor, R.J.K. *Elsevier: Oxford, UK*, **2005**, 419–450.
12. Westheimer, F.H.; Taguchi, K. *J. Org. Chem.* **1971**, *36*, 1570–1572.
13. Love, B. E.; Ren, J. *J. Org. Chem.* **1993**, *58*, 5556–5557.
14. Look, G.C.; Murphy, M.M.; Campbell, D.A.; Gallop, M.A. *Tetrahedron Lett.* **1995**, *36*, 2937–2940.
15. Billman, J.H.; Tai, K.M. *J. Org. Chem.* **1958**, *23*, 535–539.
16. White, W. A.; Weingarten, H. *J. Org. Chem.* **1967**, *32*, 213–214.

17. Liu, G.; Cogan, D. A.; Owens, T. D.; Tang, T. P.; Ellman, J. A. *J. Org. Chem.* **1999**, *64*, 1278–1284.
18. Chakraborti, A. K.; Bhagat, S.; Rudrawar, S. *Tetrahedron Lett.* **2004**, *45*, 7641–7644.
19. Panneerselvam, P.; Nair, R.R.; Vijayalakshmi, G.; Subramanian, E.H.; Sridhar, S.K. *Eur. J. Med. Chem.* **2005**, *40*, 225–229.
20. Dalpozzo, R.; de Nino, A.; Nardi, M.; Russo, B.; Procopio, A. *Synthesis* **2006**, *7*, 1127–1132.
21. Naeimi, H.; Salimi, F.; Rabiei, K. *J. Mol. Catal.* **2006**, *260*, 100–104.
22. Branchaud, B. P. *J. Org. Chem.* **1983**, *48(20)*, 3531–8.
23. Shiraishi, Y.; Ikeda, M.; Tsukamoto, D.; Tanaka, S.; Hirai, T. *Chem. Commun.* **2011**, *47*, 4811–4813.
24. Jiang, L.; Jin, L.; Tian, H.; Yuan, X.; Yu, X.; Xu, Q. *Chem. Commun.* **2011**, *47*, 10833–10835.
25. Huang, B.; Tian, H.; Lin, S.; Xie, M.; Yu, X.; Xu, Q. *Tetrahedron Lett.* **2013**, *54*, 2861–2864.
26. Soule, J.-F.; Miyamura, H.; Kobayashi, S. *Chem. Commun.* **2013**, *49*, 355–357.
27. Shen, Y. F.; Zenger, R. P.; DeGuzman, R. N.; Suib, S. L.; McCurdy, L.; Potter, D. I.; O'Young, C. L. *Science*, **1993**, *260*, 511–515.
28. Cui, W.; Zhaorigetu, B.; Jia, M.; Ao, W.; Zhu, H. *RSC Adv.*, **2014**, *4*, 2601–2604.
29. Lan, Y.-S.; Liao, B.-S.; Liu, Y.-H.; Peng, S.-M.; Liu, S.-T. *Eur. J. Org. Chem.* **2013**, *2013*, 5160–5164.
30. Pickard, P.L.; Young, C.W. Ketimines. III.. *JACS.* **1951**, *73*, 42–43.
31. Pickard, P.L.; Tolbert, T.L. *J. Org. Chem.* **1961**, *26*, 4886–4888.
32. Porai-Koshits, B.A.; Remizov, A.L. *Chem. Abst.* **1956**, *50*, 16686.

33. Hoesch, K. *Chem. Ges.* **1915**, *48*, 1122–1133.
34. Hoesch, K. *Chem. Ges.* **1917**, *50*, 462–468.
35. Houben, J.; Fischer, W. *J. Prakt. Chem.* **1929**, *123*, 262–313.
36. Claisen, L. *Chem. Ges.* **1896**, *29*, 2931–2933.
37. Reddelien, G. *Chem. Ges.* **1920**, *53*, 355–358.
38. Boyer, J.H.; Canter, F.C. *Chem. Rev.* **1954**, *54*, 1–57.
39. Langheld, K. *Chem. Ges.* **1909**, *42*, 2360–2374.
40. Varma, R. S.; Dahiya, R.; Kumar, S. *Tetrahedron Lett.* **1997**, *38*(12), 2039–42.
41. Schmeyers, J.; Toda, F.; Boy, J.; Kaupp, G. *J Chem Soc Perkin Trans*, **1998**, *2*, 989–93.
42. Vass, A.; Duda's, J.; Varma, R. S. *Tetrahedron Lett.* **1999**, *40*(27), 4951–4.
43. Tanaka, K.; Shiraishi, R. *Green Chem* **2000**, *2*(6), 272–3.
44. Andrade, C. Z.; Takada, S. C.; Alves, L. M.; Rodrigues, J. P.; Suarez, P.; Brandã, R. F. *Syn. Let.* **2004**, *12*, 2135–8.
45. Vázquez, M. A.; Landa, M.; Reyes, L.; Miranda, R.; Tamariz, J.; Delgado, F. *Synth. Commun.* **2004**, *34*(15), 2705–18.
46. Gopalakrishnan, M.; Sureshkumar, P.; Kanagarajan, V.; Thanusu, J.; Govindaraju, R. *J. Chem. Res.* **2005**, *5*, 299–303.
47. Gopalakrishnan, M.; Sureshkumar, P.; Kanagarajan, V. *J. Res. Chem. Intermed*, **2007**, *33*(6), 541–8.
48. Guzen, K.P.; Guarezemini, A. S.; Ó rfa, O.; Cella, R.; Pereira, C. P.; Stefani, H. A. *Tetrahedron Lett.* **2007**, *48*(10), 1845–8.
49. Jencks, W. P. *J. Am. Chem. Soc.* **1959**, *81*, 475 – 481.
50. Anderson, B. M.; Jencks, W. P. *J. Am. Chem. Soc.* **1960**, *82*, 1773 – 1777.
51. Wolfenden, R.; Jencks, W. P. *J. Am. Chem. Soc.* **1961**, *83*, 2763 – 2768.

52. Cordes, E. H.; Jencks, W. P. *J. Am. Chem. Soc.* **1962**, *84*, 826 – 831.
53. Cordes, E. H.; Jencks, W. P. *J. Am. Chem. Soc.* **1962**, *84*, 832 – 837.
54. Cordes, E. H.; Jencks, W. P. *J. Am. Chem. Soc.* **1962**, *84*, 4319 – 4328.
55. Sander, E. G.; Jencks, W. P. *J. Am. Chem. Soc.* **1968**, *90*, 6154 – 6162.
56. Sayer, J. M.; Peskin, M.; Jencks, W. P. *J. Am. Chem. Soc.* **1973**, *95*, 4277 – 4287.
57. Cordes, E. H.; Jencks, W. P. *J. Am. Chem. Soc.* **1963**, *85*, 2843 – 2848.
58. Jencks, W. P. *Prog. Phys. Org. Chem.* **1964**, *2*, 63 – 128.
59. Carey, F. A.; Sundberg, R. J. *Advanced Organic Chemistry*, Vol. A, 5th ed. Springer, New York, **2008**, 650 – 651.
60. Kalia, J.; Raines, R. T. *Chem., Int. Ed.* **2008**, *47*, 7523–7526.
61. Wiberg, K. B.; Glaser, R. *J. Am. Chem. Soc.* **1992**, *114*, 841 – 850.
62. Yoon, T.P.; Jacobsen, E.N. *Science* **2003**, *299*, 1691–1693.
63. Cozzi, P.G. *Chem. Soc. Rev.* **2004**, *33*, 410–421.
64. Katsuki, T. *Chem. Soc. Rev.* **2004**, *33*, 437–444.
65. Matsunaga, S.; Shibasaki, M. *Synthesis*, **2013**, *45*, 421–437.
66. Whiteoak, C. J.; Salassa, G.; Kleij, A.W. *Chem. Soc. Rev.* **2012**, *41*, 622–631.
67. Dalla Cort, A.; de Bernardin, P.; Forte, G.; Mihan, F.Y. *Chem. Soc. Rev.* **2010**, *39*, 3863–3874.
68. Szumna, A. *Chem. Soc. Rev.* **2010**, *39*, 4274–4285.
69. Das, M.C.; Xiang, S.C.; Zhang, Z.J.; Chen, B.L. *Chem. Int. Ed.* **2011**, *50*, 10510–10520.
70. Dhanaraj, C.J.; Johnson, J.; Joseph, J.; Joseyphus, R.S. *J. Coord. Chem.* **2013**, *66*, 1416–1450.
71. Drozdak, R.; Allaert, B.; Ledoux, N.; Dragutan, I.; Dragutan, V.; Verpoort, F. *Adv. Synth. Catal.* **2005**, *347*, 1721–1743.

72. Frischmann, P. D.; MacLachlan, M. J. *Chem. Soc. Rev.* **2013**, *42*, 871–890.
73. Gupta, K. C.; Sutar, A. K. *Coord. Chem. Rev.* **2008**, *252*, 1420–1450.
74. Kumar, S.; Dhar, D.N.; Saxena, P.N. *J. Sci. Ind. Res. India*, **2009**, *68*, 181–187.
75. Lim, S.; Choi, B.; Min, Y. S.; Kim, D.; Yoon, I.; Lee, S. S.; Lee, I. M. *J. Organomet. Chem.* **2004**, *689*, 224–237.
76. Dhar, D. N.; Taploo, C. L. *J. Sci. Ind. Res.* **1982**, *41(8)*, 501–6.
77. Przybylski, P.; Huczynski, A.; Pyta, K.; Brzezinski, B.; Bartl, F.; *Curr. Org. Chem.* **2009**, *13(2)*, 124–48.
78. Bringmann, G.; Dreyer, M.; Faber, J. H.; Dalsgaard, P. W.; Staerk, D.; Jaroszewski, J. W. *J. Nat. Prod.* **2004**, *67(5)*, 743–8.
79. De Souza, A. O.; Galetti, F. C. S.; Silva, C. L.; Bicalho, B.; Parma, M. M.; Fonseca, S. F. *Quim Nova* **2007**, *30(7)*, 1563–6.
80. Guo, Z.; Xing, R.; Liu, S.; Zhong, Z.; Ji, X.; Wang, L. *Carbohydr. Res.* **2007**, *342(10)*, 1329–32.
81. Bohach, G. A.; Fast, D. J.; Nelson, R. D.; Schlievert, P. M.; Rodes, J.; Benhamou, J. P.; Blei, A.; Reichen, J.; Rizzetto, M. Oxford (UK): *Wiley Blackwell*; **2007**. 1029–34.
82. Kayser, O.; Kiderlen, A. F.; Croft, S. L. *Parasitol. Res.* **2003** *90(2)*, 55–62.
83. Rathelot, P.; Vanelle, P.; Gasquet, M.; Delmas, F.; Crozet, M. P.; Timon-David, P. *Eur. J. Med. Chem.* **1995**, *30(6)*, 503–8.
84. Baquero, F. J. *Antimicrob. Chem.* **1997**, *39*, 1–6.
85. Alekshun, M. N.; Levy, S. B. *Cell* **2007**, *128(6)*, 1037–50.
86. Rice, L. B. *Biochem. Pharmacol.* **2006**, *71(7)*, 991–5.
87. Shi, L.; Ge, H. M.; Tan, S. H.; Li, H. Q.; Song, Y. C.; Zhu, H. L. *Eur. J. Med. Chem.* **2007**, *42(4)*, 558–64.

88. Panneerselvam, P.; Nair, R. R.; Vijayalakshmi, G.; Subramanian, E. H.; Sridhar, S. K. *Eur J. Med. Chem.* **2005**, *40*(2), 225-9.
89. Sundriyal, S.; Sharma, R. K.; Jain, R. *Curr. Med. Chem.* **2006**, *13*(11), 1321–35.
90. Nucci, M.; Marr, K. A. *Clin. Infect. Dis.* **2005**, *41*(4), 521–6.
91. Guo, Z.; Xing, R.; Liu, S.; Zhong, Z.; Ji, X.; Wang, L. *Carbohydr. Res.* **2007**, *342*, 1329–1332.
92. Karthikeyan, M. S.; Prasad, D. J.; Poojary, B.; Bhat, K. S.; Holla, B. S.; Kumari, N. S. *Bioorg. Med. Chem.* **2006**, *14*(22), 7482–9.
93. Echevarria, A.; Nascimento, M. G.; Geroñimo, V.; Miller, J.; Giesbrecht, A. *J. Braz. Chem. Soc.* **1999**, *10*(1), 60–4.
94. Clercq, de. *Nat. Rev. Drug Discov.* **2002**, *1*, 13–25.
95. Sriram, D.; Yogeewari, P.; Myneedu, N. S.; Saraswat, V. *Bioorg. Med. Chem. Lett.* **2006**, *16*(8), 2127–9.
96. Richard, J. P.; Amyes, T. L.; Crugeiras, J.; Rios, A. *Biochem biophys acta.* **2011**, *1814*(11), 1419-1425
97. Takagi, T.; Ramachandran, C.; Bermejo, M.; Yamashita, S.; Yu, L.X.; Amidon, G.L. *Mol. Pharm.* **2006**, *3*, 631-643.
98. Rautio, J.; Kumpulainen, H.; Heimbach, T.; Oliyai, R.; Oh, D.; Järvinen, T.; Savolainen, J. *Nat. Rev. Drug Discov.* **2008**, *7*, 255–270.
99. Huttunen, K.; Raunio, H.; Rautio, J. *Pharmacol. Rev.* **2011**, *63*, 750–771.
100. Stella, V.J.; Nti-Addae, K.W. *Adv. Drug Deliv. Rev.* **2007**, *59*, 677–694.
101. Rijcken, C. J. F.; Soga, O.; Hennink, W. E.; van Nostrum C F *Journal of Controlled Release*, **2007**, *120*, 131–148
102. Redasani, V.K.; Bari, S.B. 1st ed. Academic Press: London, UK, **2015**.

103. Zovko, M.; Zorc, B.; Novak, P.; Tepeš, P.; Cetina, C.; Horvat, M. *Int. J. Pharm.* **2004**, *285*, 35–41
104. Gillies, E. R.; Frechet, J. M. J. *Bioconjugate Chem.* **2005**, *16*, 361–368
105. Gillies, E. R.; Frechet, J. M. J. *Chem. Commun.* **2003**, *14*, 1640–1641.
106. Gillies, E. R.; Frechet, J. M. J. *Pure Appl. Chem.* **2004**, *76*, 1295–1307.
107. Beaumont, K.; Webster, R.; Gardner, I.; Dack, K. *Curr. Drug Metab.* **2003**, *4*, 461–485.
108. Testa, B. *Curr. Opin. Chem. Biol.* **2009**, *13*, 338–344.
109. Tatum, L. A.; Su, X.; *Ivan Acc. Chem. Research*, **2014**, *47*, 2141-2149.
110. Thol, F. *Web of Sci.* **2015**, *38*, 195.
111. Murdoch, L. *J. World Trade*, **2013**, *29*, 8-9.
112. Zhang, X.; Achazi, K.; Steinhilber, D.; Kratz, F.; Dervedde, J.; Haag, R. *J. Control Release*, **2014**, *174*, 209-216
113. Kruger, H. R.; Schutz, I.; Justies, A.; Licha, K.; Welker, P.; Haucke, V.; Calderon, M. *J. Control. Release*, **2014**, *194*, 189-196
114. Hamann, P. R.; Hinman, L. M.; Beyer, C. F.; Lindh, D.; Upešlaciš, J.; Flowers, D. A.; Bernstein, I. *Bioconjugate Chem.* **2002**, *13*, 40-46
115. Alani, A. W. G.; Bae, Y.; Rao, D. A.; Kwon, G. S. *Biomaterials*, **2010**, *31*, 1765-1772
116. Sawant, R. R.; Torchilin, V. P. *Int. J. Pharm.* **2009**, *374*, 114-118
117. Hami, Z.; Amini, M.; Ghazi-Khansari, M.; Rezayat, S. M.; Gilani, K. *Colloids Surf. Biointerfaces*, **2014**, *116*, 309-317
118. Kostkova, H.; Etrych, T.; Rihova, B.; Kostka, L.; Starovoytova, L.; Kovar, M. *Macromol. Biosci.* **2013**, *13*, 1648-1660
119. Howard, M. D.; Ponta, A.; Eckman, A.; Jay, M.; Bae, Y. *Pharm. Res.* **2011**, *28*, 2435-2446

120. Dhar, S.; Gu, F. X.; Langer, R.; Farokhza, O. C.; Lippard, S. J. *Proc. Natl. Acad. Sci. USA*, **2008**, *105*, 17356-17361
121. Ji, K.; Chung Suk, L.; Janesko, B.; Simanek, E. *Mol. Pharm.* **2015**, *12*, 2924-2927.
122. (a) Corbett, P. T.; Leclaire, J.; Vial, L.; West, K. R.; Wietor, J.-L.; Sanders, J. K. M.; Otto, S. *Dynamic Combinatorial Chemistry. Chem. Rev.* **2006**, *106*, 3652–3711. (b) Li, J.; Nowak, P.; Otto, S. *J. Am. Chem. Soc.* **2013**, *135*, 9222–9239. (c) Lehn, J.-M.; Ramström, O. *Nat. Rev. Drug Discovery*, **2002**, *1*, 26–36. (d) Dirksen, A.; Dirksen, S.; Hackeng, T. M.; Dawson, P. E. *J. Am. Chem. Soc.* **2006**, *128*, 15602–15603.
123. Lazny, R.; Nodzevska, A. *Chem. Rev.* **2010**, *110*, 1386–1434.
124. Levrand, B.; Fieber, W.; Lehn, J.-M.; Herrmann, A. *Helv. Chim. Acta.* **2007**, *90*, 2281-2314.
125. Rollas, S.; Kucukguzel, S. G. *Molecules*, **2007**, *12*, 1910–1939.
126. Hamann, P. R.; Hinman, L. M.; Beyer, C. F.; Lindh, D.; Upešlacis, J.; Flowers, D. A.; Bernstein, I. *Choice of Linker. Bioconjugate Chem.* **2002**, *13*, 40–46.
127. Zhang, X.; Achazi, K.; Steinhilber, D.; Kratz, F.; Dervede, J.; Haag, R. *J. Control. Release.* **2014**, *174*, 209–216.
128. Kruger, H. R.; Schutz, I.; Justies, A.; Licha, K.; Welker, P.; Haucke, V.; Calderon, M. *J. Controlled Release.* **2014**, *194*, 189–196.
129. Sharma, A.; Jad, Y.; Mohammed, R. H.; Siddiqui, B. G.; Fernando, A.; Ayman, E. F. *J. Chem.* **2017**, *10*.
130. Lee, J.; Brune, M. E.; Warner, R. B. *Pharmacology*, **1993**, *47(3)*, 176–187
131. Grams, F.; Brandstetter, H.; D’Alo, S.; Geppert, D.; Krell, H.; Leinert, H.; Livi, V.; Menta, E.; Oliva, A.; Zimmerman, G. Hans-Willi, K.; *Biol. Chem.* **2001**, *382*, 1277-1285
132. Kempter, C.; Karst, U. *Analyst*, **2000**, *125*, 433-438.

133. Amir, M.; Hassan, M.; *Arch. Pharm.* **2014**, *347*, 958-968
134. Vaupel, P.; Kallinowski, F.; Okunieff, P. *Cancer res.* **1989**, *49*, 6449-6465
135. Engin, K.; Leeper, D. B.; Cater, J. R.; Thistlethwaite, A. J.; Tupchong, L.; McFarlane, J. D. *Int. J. Hyperthermia.* **1995**, *11*, 211-216
136. Baymak, M.S.; Zuman, P. *Tetrahedron lett.* **2007**, *63*, 5450–5454.
137. Namli, H.; Turhan, O. *Vib. Spectrosc.* **2007**, *43*, 274–283.
138. Evans, D.A.; Borg, G.; Scheidt, K.A. *Angew. Chem. Int. Ed.* **2002**, *41*, 3188–3191.
139. Hooley, R.J.; Iwasawa, T.; Rebek, J. *J. Am. Chem. Soc.* **2007**, *129*, 15330–15339.
140. Iwasawa, T.; Hooley, R.J.; Rebek, J. *Science* **2007**, *317*, 493–496.
141. Xu, L.; Hua, S.; Li, S. *Chem. Commun.* **2013**, *49*, 1542–1544.
142. Kawamichi, T.; Haneda, T.; Kawano, M.; Fujita, M. *Nature* **2009**, *461*, 633–635.
143. Morris, W.; Doonan, C. J.; Yaghi, O. M. *Inorg. Chem.* **2011**, *50*, 6853–6855.
144. Dolotko, O.; Wiench, J.W.; Dennis, K.W.; Pecharsky, V.K.; Balema, V.P. *New J. Chem.* **2010**, *34*, 25–28.
145. Yufit, D. S.; Howard, J. A. K. *J. Mol. Struct.* **2010**, *984*, 182–185.
146. Suni, V.; Kurup, M. R. P.; Nethaji, M. *J. Mol. Struct.* **2005**, *749*, 177–182.
147. Barys, M.; Ciunik, Z.; Drabent, K., Kwiecień, A. *New J. Chem.* **2010**, *34*, 2605–2611.
148. Sayer, J. M.; Jencks, W. P. *J. Am. Chem. Soc.* **1977**, *99*, 464–474.
149. Kwiecien, A.; Ciunik, Z. *Molecules*, **2015**, *20*, 14365-14376.
150. Zelenin, K.; Alekseyev, A.; Tygysheva, A. *Tetrahedron Lett.* **1995**, *51*, 11251-11256.
151. Lyga, J.; Patera, R. *J. heterocyc. chem.* **1990**, *27*, 919-920.
152. Threadgill, M.; Heer, A.; Jones, B. *J. Fluorine Chem.* **1993**, *65*, 21-23.
153. Bonacorso, H.; Porte, L.; Paim, G.; Luz, F.; Martins, M, Zanatta, N. *Tetrahedron. Lett.* **2010**, *51*, 3759-3761.

154. Martins, M. A. P.; Cunico, W.; Pereira, C.; Sinhorin, A. *Org. Syn.* **2004**, *4*, 391-403
155. Martins, M. A. P.; Beck, P.; Cunico, W.; Pereira, C. *Tetrahedron Lett.* **2002**, *43*(39), 7005-7008
156. Perrone, M.; Vitale, P.; Malerba, P.; Altomare, A.; Giovani, C.; Lavecchia, A.; Scilimati, A. *Chemmedchem.* **2012**, *7*, 629-641.
157. Fustero, S. et. al *J. Org. Chem.* **2008**, *73*(9), 3523-3529.
158. Hsieh, M.; Kuo, S.; Lin, H. *Adv. Syn. Catal.* **2015**, *357*, 683-689.
159. Singh, S.; Kumar, D.; Jones, B.; Threadgill, M. *J Fluor. Chem.* **1999**, *94*, 199-203.
160. Singh, S.; Kumar, V.; Aggarwal, R. *J. Heterocyclic Chem.* **2006**, *43*, 1003-1014.
161. Aggarwal, R. et. al. *Eur. J. Med. Chem.* **2013**, *70*, 350-357.
162. Bonaccorso, H. G. et. al *Synthesis*, **2001**, *10*, 1505-1508.
163. Flores, A. F. C.; Piovesan, L. A.; Flores, D.; Pizzuti, D.; Malavolta, J.; Martins, M. P. J. *Heterocyc. Chem.* **2013**, *51*, 733-750.
164. Bouffard, F.A.; Hammond, M.L.; Arison, B.H. *Tetrahedron Lett.* **1995**, *36*, 1405-1408.
165. Lal, B.; Gund, V. G. *Bioorg. Med. Chem. Lett.* **2004**, *14*, 1123-1128.
166. LaLonde, R. T.; Wong, C. J. *Org. Chem.* **1976**, *41*, 291-294.
167. Graff von Stosch, A. *Biochemistry*, **1996**, *35*, 15260-15268.
168. Salvà, A.; Donoso, J.; Frau, J.; Muñoz, F. *J. Mol. Struc.-Theochem.* **2002**, *577*, 229-238.
169. Erdtman, E.; Bushnell, E. A. C.; Gauld, J. W.; Eriksson, L. A. *Comp. Theor. Chem.* **2011**, *963*, 479-489.
170. Allen, F.H. *Acta. Crystallogr.* **2002**, *B58*, 380-388.
171. Liu, X.; Banister, S. D.; Christie, M. J.; Banati, R.; Meikle, S.; Coster, M. J.; Kassiou, M. *Eur. J. Pharmacol.* **2007**, *555*, 37-42.

172. Prins, L. H. A.; deVries, A.; Caira, M. R.; Oliver, D. W.; vanDyk, S.; Malan, S. F. *J. Chem. Crystallogr.* **2008**, *38*, 705–709.
173. Prins, L. H. A.; du Preez, J. L.; van Dyk, S.; Malan, S. F. *Eur. J. Med. Chem.* **2009**, *44*, 2577–2582.
174. Wilkes, D.K.; de Vries, A.; Oliver, D.W.; Malan, S.F. *Arch. Pharm. Chem. Life Sci.* **2009**, *342*, 73–79.
175. Banister, S. D.; Moussa, I. A.; Jordan, M. J. T.; Coster, M. J.; Kassiou, M. *Bioorg. Med. Chem. Lett.* **2010**, *20*, 145–148.
176. Banister, S. D.; Manoli, M.; Doddareddy, M. R.; Hibbs, D. E.; Kassiou, M. *Bioorg. Med. Chem. Lett.* **2012**, *22*, 6053–6058.
177. Al-bogami, A. S.; Saleh, T. S.; Mekky, A. M.; Shaaban, M. R. *J. Mol. Structure.* **2016**, *1121*, 167-179.
178. Frank, A. T.; Farina, N. S.; Sawwan, N.; Wauchope, O. R.; Qi, M.; Brzostowska, E. M.; Chan, W. Grasso, F. W.; Haberhold, P.; Greer, A. *Mol. Diversity*, **2007**, *11*, 115–118.
179. Schaefer, T.; Marat, K.; Peeling, J.; Veregin, R. *Can. J. Chem.* **1983**, *61(12)*, 2779-2784
180. Wessjohann, L. A.; Ruijter, E.; Garcia-Rivera, D.; Brandt, W. *Mol. Diversity*, **2005**, *9*, 171–186.
181. Driggers, E. M.; Hale, S. P.; Lee, J.; Terrett, N. K. *Nat. Rev. Drug Discovery*, **2008**, *7*, 608–624.
182. Butler, M. S. *Nat. Prod. Rep.* **2005**, *22*, 162–195.
183. Hsu, S.; Breukink, E.; Tischenko, E.; Lutters, M.; Kruijff, B.; Kaptein, R.; Bonvin, W.; Nuland, N. *Nat. Struct. Mol. Biol.* **2004**, *11*, 963-967.
184. Siegers, K.; Heinzmann, S.; Entain, K. D. *J. Biol. Chem.* **1996**, *271*, 12294-12301.
185. Bahal, N., Nahata, M. C. *Ann pharmacotherapy*, **1992**, *26(1)*, 46-55

186. McDaneil, R.; Welch, M.; Hutchinson, C. R. *Int. Chem. Rev.* **2005**, *105*, 543-558.
187. Zuckerman, J. M.; Qamar, F.; Bono, B. R. *Med. Clin. N. Am.* **2011**, *95*, 761-791.
188. Alvarez-Elcoro, S.; Enzler M. J. *Mayo Clin. Proc.* **1999**, *74*, 613-634.
189. Hamill, R. L.; Haney, M. E.; Stamper, M.; Wiley, P. F. *Antibiot. Chem.* **1961**, *11*, 328-334.
190. Mazzariol, A.; Raffaella, K.; Vitali, L. A.; Cornaglia, G. J. *Antimicrob. Chemther.* **2007**, *59*, 1171-1176.
191. Giordanetto, F.; Kihlberg, J. *J. Med. Chem.* **2014**, *57*(2), 278-295.
192. Jones, R. N.; Barry, A. L. *Antimicrob. Agents Chemother.* **1987**, *31*, 625-629.
193. Johnson, B. A.; Anker, H.; Meleney, F. L. *Science*, **1945**, *102*, 376-377.
194. Zhanel, G. G.; Walters, M.; Noreddin, A.; Vercaigne, L. M.; Wierzbowski, A.; Gin, A. S.; Douthwaite, S.; Hoban, D. J. *Drugs*, **2002**, *62*(12), 1771-1804.
195. Zhanel, G. G.; Dueck, M.; Hoban, D. J. *Drugs*, **2001**, *61*, 443-498.
196. Lexi-Comp Online. Lexi-Comp, Inc.: Hudson, OH, USA, **2013**.
197. Hollstein, U. *Chem. Rev.* **1974**, *74*, 625-652.
198. Ho, S.; Clipstone, N.; Timmermann, L.; Northrop, J; Graef, I.; Fiorentino, D.; Nourse, J.; Crabtree, G. R. *Clin. Immunol. Immunopathol.* **1996**, *80*, S40-S45
199. Matsuda, S.; Koyasu, S. *Immunopharmacology.* **2000**, *47*, 119-25.
200. Watts, R.; Clunie, G.; Hall, F.; Marshall, T. *Rheumatology.* Oxford University Press. **2009**, page. 558.
201. Atcher, J.; Sola, J.; Alfonso, I. *Org. Biomol. Chem.* **2017**, *15*, 213-219.
202. He, Z.; Ye, W.; Juang, W. *Chem. Eur. J.* **2015**, *21*, 3005-3012.
203. Beeren, S. R.; Sanders, J. K. M. *Chem. Sci.* **2011**, *2*, 1560-1566.
204. Jin, Y.; Yu, C.; Denman, R. J.; Zhang, W. *Chem. Soc. Rev.* **2013**, *42*, 6634-6654.

205. Adessi, C.; Soto, C. *Curr. Med. Chem.* **2002**, *9*, 963–978.
206. Gilon, C.; Halle, D.; Chorev, M.; Selinger, Z.; Byk, G. *Backbone cyclization: Biopolymers*, **1991**, *31*, 745–750.
207. Borchardt, R. T.; Jeffrey, A.; Siahaan, T. J.; Gangwar, S.; Pauletti, G. M. *Adv. Drug Delivery Rev.* **1997**, *27*, 235–256.
208. Burton, P. S.; Conradi, R. A.; Ho, N. F.; Hilgers, A. R.; Borchardt, R. T. *J. Pharm. Sci.* **1996**, *85*, 1336–1340.
209. McGeary, R. P.; Fairlie, D. P. *Curr. Opin. Drug Discovery Dev.* **1998**, *1*, 208–217.
210. Parenty, A.; Moreau, X.; Campagne, J. M. *Chem. Rev.* **2006**, *106*, 911–939.
211. Nshimyumukize, P.; Delest, B.; Mijatovic, T.; Kiss, R.; Marchand-Brynaert, J.; Robiette, R. *Tetrahedron Lett.* **2010**, *66*, 4515–4520.
212. Davies, J. S. *J. Pept. Sci.* **2003**, *9*, 471–501.
213. Han, S. Y.; Kim, Y. A. *Tetrahedron Lett.* **2004**, *60*, 2447–2467.
214. Albericio, F. *Curr. Opin. Chem. Biol.* **2004**, *8*, 211–221.
215. Illuminati, G. *J. Am. Chem. Soc.* **1997**, *99*, 6308–6312
216. Galli, C.; Mandolini, L. *J. Org. Chem.* **1981**, *46*, 3127–3128
217. Burgess, K.; Lim, D.; Bois-Choussy, M.; Zhi, J. *Tetrahedron Lett.* **1997**, *38*, 3345–3348.
218. Fotsch, C.; Kumaravel, G.; Sharma, S. K.; Wu, A. D.; Gounarides, J. S.; Nirmala, N. R.; Petter, R. C. *Bioorg. Med. Chem. Lett.* **1999**, *9*, 2125–2130.
219. Gradillas, A.; Perez-Castells, J. *Angew. Chem., Int. Ed.* **2006**, *45*, 6086–6101.
220. Tsantrizos, Y. S. *Curr. Opin. Invest. Drugs*, **2009**, *10*, 871–881.
221. Van de Weghe, P.; Eustache, J. *Curr. Top. Med. Chem.* **2005**, *5*, 1495–1519.
222. Martin, W. H.; Blechert, S. *Curr. Top. Med. Chem.* **2005**, *5*, 1521–1540.
223. Holub, J. M.; Kirshenbaum, K. *Chem. Soc. Rev.* **2010**, *39*, 1325–1337.

224. Angell, Y.; Burgess, K. *J. Org. Chem.* **2005**, *70*, 9595–9598.
225. Looper, R. E.; Pizzirani, D.; Schreiber, S. L. *Org. Lett.* **2006**, *8*, 2063–2066.
226. Tron, G. C.; Pirali, T.; Billington, R. A.; Canonico, P. L.; Sorba, G.; Genazzani, A. *Med. Res. Rev.* **2008**, *28*, 278–308.
227. Megiatto J. D.; Schuster, D. *J. Am. Chem. Soc.* **2008**, *130*, 12872-12873
228. Krakowiak, K. E.; Bradshaw, J. S.; Krakowiak, D. J. *Chem. rev.* **1989**, *89(4)*, 929-972
229. Yepremyan, A.; Mehmood, A.; Asgari, P.; Janesko, B.; Simanek, E. E. *ChemBioChem* **2019**, *20*, 241-246.

VITA

Vishal Rajat Sharma was born on October 11th, 1986, in Himachal Pradesh, India. He arrived in the United States of America at the age of 19 on September 25th, 2005. In January 2006, he started his college education at Collin College and transferred to Southern Methodist University in Spring 2007. He received his Bachelor of Science degree with a major in Chemistry from Southern Methodist University, Dallas, in 2010.

In August 2012, he started his graduate studies at Texas Woman's University, where he earned his Master of Science degree in Chemistry in 2014. During this time, he worked as a Graduate Teaching Assistant for four semesters.

In August 2015, he joined the PhD program at Texas Christian University in Fort Worth, Texas. During his graduate career, he served as a Teaching Assistant for four semesters.

He has been working as an adjunct instructor of Chemistry at Mountain View College since Fall 2014, at Tarrant County College, Northeast Campus, since Fall 2018, and at Collin College, Spring Creek Campus, since Summer 2019. He has taught multiple chemistry courses including Introductory Chemistry, General Chemistry I and II, and Organic Chemistry I.

He is married to Reena Devi, from India, who earned her Master of Science in Chemistry from Himachal Pradesh University, Shimla, in 2014.

Synthesis of Novel Architectures from Triazinyl Hydrazines and Various Carbonyl Compounds

Abstract

The pH labile nature of hydrazones has made them useful in various fields from material to medical science.¹ Here, explorations of triazinyl hydrazones are reported. Three different projects will be described; the hydrolysis of novel triazinyl hydrazones, the synthesis of remarkably stable hemiaminals, and the creation of macrocycles derived from hydrazone dimers.

Novel triazinyl hydrazones. Elaborating on previous work,² the role of *N*-alkylation on hydrazone hydrolysis was studied using ArNHNH_2 , $\text{ArN}(\text{CH}_3)\text{NH}_2$ and $\text{ArN}(\text{Ph})\text{NH}_2$ wherein Ar is a triazine ring. The study relied on four different carbonyl donors. The use of diketones affords an opportunity to study the effects of intramolecular hydrogen bonding when *N*-alkylhydrazines (which preclude pyrazole formation) are employed. Hydrolysis rates were measured by high performance liquid chromatography (HPLC) using an established competitive exchange reaction relying the presence of an excess of formaldehyde.³ The studies show that the presence of methyl group increases hydrolysis rates when compared to phenyl (which is similar) and to unalkylated hydrazones which proceed most slowly.

Stable hemiaminals. During the synthesis of hydrazones, stable cyclic hemiaminals were observed. Cyclic hemiaminals are obtained from acidic conditions using an aromatic ring containing hydrogen bond acceptor and diketones with strong electron withdrawing groups.⁴⁻⁷ Triazine ring provides three hydrogen bond acceptors and, hence, used to create stable cyclic hemiaminals under acidic conditions. By surveying a range of 1,3-diketones, stability is attributed to the effect of hydrogen bonding and the presence of a strong electron withdrawing group (trifluoromethyl). Using resistance to dehydration as a surrogate for stability, these hemiaminals survives in ambient, neat glacial acetic acid for long periods of time and requiring reflux for

conversion to the corresponding pyrazole. DFT calculations corroborate design criteria that are crucial for the stability.

Macrocycles. Finally, an earlier report from the Simanek group identified three macrocycles that derive from dimerization of a protected triazinyl hydrazine bearing an acetal when exposed to acid.⁸ The resulting bishydrazone presented 24 atoms in a ring. The simplicity of monomer preparation and the nearly quantitative yields of product led to the question of whether rings of varying sizes could be prepared. Ring size is readily manipulated by changing the tether between the acetal and triazine ring which contains an amino acid and an amino acetal. For these studies, 6 monomers were prepared using glycine and β -alanine along with acetals including the 2-carbon aminoethyl acetal, the 3-carbon aminopropyl acetal, and the 4-carbon aminobutyl acetal. Treatment with trifluoroacetic acid and slow evaporation of solvent yielded macrocycles that are characterized by x-ray diffraction, ¹H and ¹³C NMR spectroscopy, mass spectrometry and HPLC. Macrocylic homodimers of ring sizes of 22-28 atoms were obtained in high yield. In addition, when a 1:1 mole ratio of different monomers were mixed, heterodimeric macrocycles with odd-numbered ring sizes (23-27 atoms) were also made. Solid state structures and solution state NMR studies suggest that these macrocycles form networks of hydrogen bonds and might be templated by protonation.

References:

1. Rollas, S.; Kucukguzel, S. G. *Mol.* **2007**, *12*, 1910-1939.
2. Ji, K.; Chung suk, L.; Janesko, B.; Simanek, E. *Mol. Pharm.* **2015**, *12*, 2924-2927.
3. Kalia, J.; Raines, R. T. *Angew. Chem., Int. Ed.* **2008**, *47*, 7523-7526.
4. Fustero, S. et. al *J. Org. Chem.* **2008**, *73*(9), 3523-3529.
5. Hsieh, M.; Kuo, S.; Lin, H. *Adv. Syn. Catal.* **2015**, *357*, 683-689.
6. Singh, S.; Kumar, D.; Jones, B.; Threadgill, M. *J Fluor. Chem.* **1999**, *94*, 199-203.
7. Aggarwal, R. et. al. *Eur. J. Med. Chem.* **2013**, *70*, 350-357.
8. Yepremyan, A.; Mehmood, A.; Asgari, P.; Janesko, B.; Simanek, E. *ChemBioChem.* **2018**, *20*, 241-246.

